Study of the connection between components of the circadian clock and lipid metabolism in Arabidopsis thaliana

Salim Makni

Par **Salim MAKNI**

Study of the connection between components of the circadian clock and lipid metabolism in Arabidopsis thaliana

Thèse présentée
pour l'obtention du grade
de Docteur de l'UTC

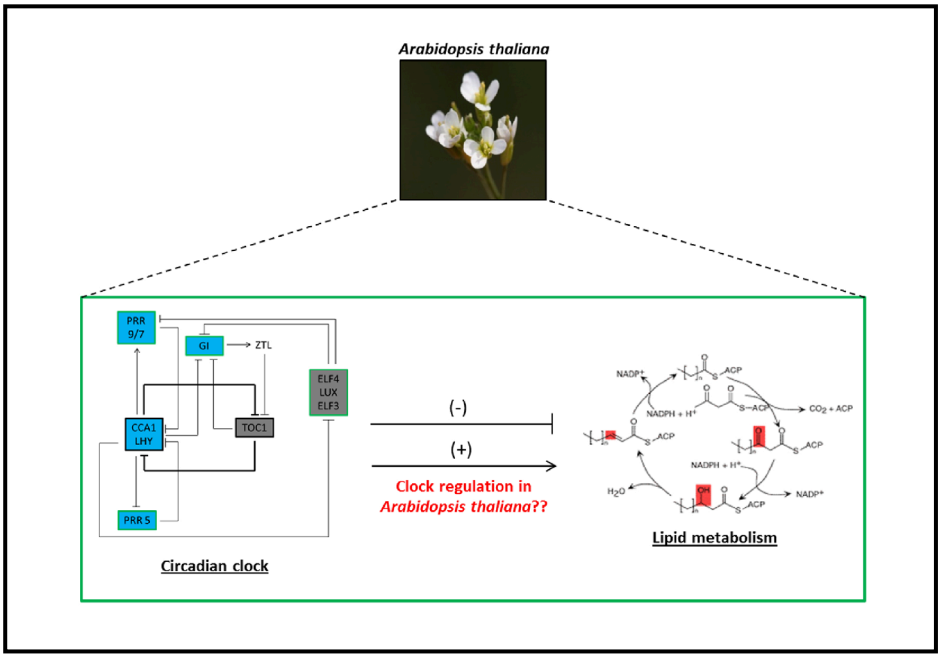

Soutenue le 25 novembre 2022
Spécialité : Biotechnologie : Unité de recherche Génie Enzymatique et Cellulaire - GEC (UMR-7025)
D2714

UNIVERSITE de TECHNOLOGIE de COMPIEGNE

Doctoral school “Science pour l’ingénieur”

Génie Enzymatique et Cellulaire unit research, CNRS UMR 7025

PhD

In order to obtain the degree of

DOCTOR OF THE UNIVERSITY OF TECHNOLOGY OF COMPIEGNE

Spécialité : Biotechnologie

Salim MAKNI

Study of the connection between components of the circadian clock and lipid metabolism in Arabidopsis thaliana

Soutenue le 25 novembre 2022 devant le jury composé de :

Mme	Y. PERRIN (Présidente)
M.	S. ACKET (Directeur de thèse)
M.	A. TRONCOSO-PONCE (Directeur de thèse)
M.	D. ROLIN (Rapporteur)
M.	O. VAN WUYTSWINKEL (Rapporteur)
Mme	S. PLANCHAIS
Mme	A. REPELLIN

Acknowledgement

My gratitude goes to Pr. Olivier VAN WUYTSWINKEL, Pr. Dominique ROLIN, Dr. Séverine PLANCHAIS, Pr. Anne REPELLIN and Pr. Yolande PERRIN for judging my research work.

I acknowledge the “Ministère de l’Enseignement Supérieur et de la Recherche et de l’Innovation”, “Région Hauts-de-France” and “Fonds Européen de Développement Régional” for their contribution in the funding of this research project.

I am grateful to Pr. Karsten Haupt, the director of the “Génie Enzymatic et Cellulaire” (GEC, UMR CNRS 7025) unit research, who welcomed me in the laboratory in order to perform all the experiments related to this research work.

I would like to address all my gratitude to my dear supervisors, Dr. Adrian Troncoso-Ponce and Dr. Sébastien Acket, for their good moods and all their advices to achieve this research work. They gave me the opportunity to be trained in several approaches (FA analysis, RT-qPCR, lipidomic approaches, etc) which have been helpful for the generation of results during this PhD project. They also taught me to develop critical thinking skills, which is crucial for the advancement of the scientific research. I would like to introduce a special thanking mention for Dr. Adrian Troncoso-Ponce who encouraged me to supervise a total of eight students during their internship and to perform teaching, which allowed me to transmit my scientific skills to students during their experimental work class session.

I would like to thank Laurent Gutierrez who welcomed me in the CRRBM platform to perform qPCR experiments, as well as Stéphanie Guénin, Maxime Sommer and Sana Afensiss who helped me for the generation of RT-qPCR results related to this research work.

I would like to thank all the intern, PhD students and post-doctoral researchers with whom we spent a lot of good time together outside the laboratory. I would never forget to thank my parents (Sihem Hamza and Mohamed Makni), my sister (Nourhène Makni), my sister’s husband (Badr Rezgui) and my lovely niece (Baya Rezgui) for all the support. I would like to dedicate this thesis to them and to my grandparents (Fadhila, Wassila, Ameur and Mahmoud), my “Shrimp” aunt (Faiza Hamza) and my dear cousins (Hamed and Salima Chaabouni).

ENJOY THE READING

Abstract

Plants, as sessile organisms, are constantly exposed to rhythmic environmental fluctuations, which can affect their own development and survival. Plants cope with these fluctuations by the presence of an internal timekeeper, known as the circadian clock. The role of the circadian clock is anticipating these rhythmic environmental fluctuations in order to adjust several physiological processes to external conditions. During the development of this PhD program, the role exerted by molecular components of the circadian clock on fatty acid and glycerolipid metabolism within seed was studied using the model plant *Arabidopsis thaliana*. The composition of fatty acids and glycerolipids were characterized in mature seeds collected from circadian clock mutant plants (*toc1-1*, *toc1-2*, TOC1-ox, *prr5-1*, *prr7-3*, *prr9-1* and *cca1-11 lhy*-21) and compared to their respective wild-type (C24, Col-0 and Ws). Modifications in the mole percents of six fatty acids (C18:0, C18:1, C18:2, C18:3, C20:0 and C20:1) observed between both *toc1* mutants and their respective wild-type mature seeds reached up to 5 % in contrast to the other circadian clock mutants (TOC1-ox, *prr5-1*, *prr7-3*, *prr9-1* and *cca1-11 lhy*-21) where differences with their respective WT were lower than 2 %. Both *toc1* mutants were, therefore, selected in order to study the potential role of TOC1 in the regulation of fatty acid metabolism during seed maturation. The qualitative analyses of fatty acids showed that the mole percents of C18:0, C18:3, C20:0 and C20:1 were significantly increased in both *toc1-1* and *toc1-2* mutant mature seeds. The percentages of C18:0, C18:3, C20:0 and C20:1 moieties glycerolipids were also significantly increased in both *toc1* mutant mature seeds. The quantitative analyses showed that the total amount of fatty acids was increased in both *toc1* mutant mature seeds. Results showed that fatty acid and glycerolipid profiles observed in both *toc1* mutant mature seeds were specifically associated to seed maturation. RT-qPCR analyses revealed that the expression of fatty acid desaturase 2 (*FAD2*, AT3G12120), fatty acid desaturase 3 (*FAD3*, AT2G29980), fatty acid elongase (*FAE1*, AT4G34520) and the transcription factor *bZIP67* (AT3G44460) and *WRINKLED1* (*WRI1*, AT3G54320) were increased in *toc1-1* developing seeds. Collectively, all these results point to the participation of TOC1 in the control of fatty acid synthesis in developing *Arabidopsis thaliana* seeds.

Keywords: Glycerolipid and fatty acid metabolism, molecular components of the circadian clock, circadian clock mutants, seed maturation, *Arabidopsis thaliana.*

Résumé

En tant qu'organismes sessiles, les plantes sont constamment exposées à des fluctuations rhythmiques environnementales qui peuvent affecter leurs propres développements et leurs survies. Les plantes font face à ces fluctuations grâce à la présence d'une horloge biologique interne, également appelée l'horloge circadienne. Le rôle de l'horloge circadienne est d'anticiper ces fluctuations rythmiques environnementales afin d'ajuster les processus physiologiques des plantes aux conditions externes. Au cours de cette thèse, le rôle exercé par des composants moléculaires de l'horloge biologique sur le métabolisme des acides gras et des glycérolipides dans les graines a été étudié en utilisant la plante modèle *Arabidopsis thaliana*. La composition des acides gras et des glycérolipides a été caractérisée dans des graines matures collectées à partir de plantes mutantes de l'horloge circadienne (*toc1-1*, *toc1-2*, TOC1-ox, *prr5-1*, *prr7-3*, *prr9-1* et *cca1-11 lhy-21*) et comparée à leurs graines sauvages respectives (C24, Col-0 et Ws). Les modifications dans le pourcentage molaires de six acides gras observées entre les deux mutants *toc1* et leurs graines matures sauvages ont atteint jusqu'à 5 % contrairement aux autres mutants de l'horloge circadienne où les différences avec leurs graines sauvages étaient inférieures à 2 %. Les deux mutants *toc1* ont donc été sélectionnés afin d'étudier le rôle potentiel de TOC1 dans la régulation du métabolisme des acides gras au cours de la maturation des graines. Les analyses qualitatives ont montré une augmentation dans le pourcentage molaire de C18:0, C18:3, C20:0 et C20:1 dans les graines matures mutantes *toc1-1* et *toc1-2*. Le pourcentage molaire des glycérolipides contenant les acides gras C18:0, C18:3, C20:0 et C20:1 est augmenté dans les graines matures *toc1*. Les analyses quantitatives des acides gras ont montré que la quantité totale des acides gras est augmentée dans les graines matures *toc1*. Les profils en acides gras et en glycérolipides observés dans les graines matures *toc1* sont spécifiquement associés au processus de maturation des graines. Les résultats de RT-qPCR ont révélé que l'expression de *FAD2* (AT3G12120), *FAD3* (AT2G29980), *FAE1* (AT4G34520), *bZIP67* (AT3G44460) et *WRI1*, AT3G54320), étaient augmentées dans les graines en développement *toc1-1*. Ces résultats conduisent à la conclusion que TOC1 participe au contrôle du métabolisme des acides gras au cours du développement des graines d'*Arabidopsis thaliana*.

Mots clés : Métabolisme des acides gras et des glycérolipides, composants de l'horloge circadienne, mutants de l'horloge circadienne, maturation des graines, *Arabidopsis thaliana.*

List of Abbreviations

*	<=>	low significance (p-value < 0.05)
**	<=>	medium significance (p-value < 0.01)
***	<=>	high significance (p-value < 0.001)
°C	<=>	Celsius degree
%	<=>	percent
2D projection	<=>	two dimensions projection
5'UTR	<=>	5' Untranslated Transcribed Region
$[M+FA-H]^-$	<=>	Negative adducts: addition of formic acid and loss of proton
$[M+H]^+$	<=>	Positive adducts: ionization of by the addition of proton
$[M-H]^-$	<=>	Negative adducts: ionization by loss of proton
$[M-H_2O-H]^-$	<=>	Negative adducts: ionization by loss of water and proton
$[M+Hac-H]^-$	<=>	Negative adducts: ionization by acetic acid and loss of proton
$[M+Na]^+$	<=>	Positive adducts: ionization of molecules by sodium
$[M+NH_4]^+$	<=>	Positive adducts: ionization of molecules by ammonium
A260	<=>	Absorbance at 260 nm
A280	<=>	Absorbance at 280 nm
AAD	<=>	Δ9 acyl-ACP desaturases
AAPT2	<=>	gene encoding for the aminoalcohol aminophosphotransferase
ABI3	<=>	ABSCISIC ACID INSENSITIVE 3
AC	<=>	antipodal cells
ACC	<=>	acetyl-CoA carboxylase
ACC1	<=>	cytosolic acetyl-CoA carboxylase
ACP	<=>	acyl carrier protein
ACS	<=>	acetyl-CoA synthetase
ACX	<=>	acyl-CoA oxidase
ADP	<=>	Adenosine diphosphate
ADP-glucose	<=>	glucose esterified to ADP
ALDO	<=>	aldolase
a.m.	<=>	ante meridiem
AP2	<=>	APETALA2
ATP	<=>	Adenosine triphosphate
ATP-CL	<=>	ATP citrate lyase
AW-box	<=>	ASML1/WRI1-box
BADC	<=>	BIOTIN ATTACHMENT DOMAIN-CONTAINING protein
BC	<=>	biotin carboxylase
BCCP	<=>	biotin carboxyl carrier protein
BE-PSS	<=>	Base-exchange-type phosphatidylserine synthase
BHT	<=>	butylated hydroxytoluene
bp	<=>	base pair
BPM	<=>	BTB/POZ-MATH
bZIP67	<=>	basic LEUCINE ZIPPER TRANSCRIPTION FACTOR 67
c	<=>	chalaza
C14:0	<=>	myristic acid
C15:0	<=>	pentadecanoic acid

C16:0	<=>	palmitic acid
C16:1	<=>	palmitoleic acid
C16:2	<=>	hexadecadienoic acid
C16:3	<=>	hexadecatrienoic acid
C17:0	<=>	heptadecanoic acid
C18:0	<=>	stearic acid
C18:1	<=>	oleic acid
C18:2	<=>	linoleic acid
C18:3	<=>	linolenic acid
C20:0	<=>	arachidic acid
C20:1	<=>	eicosenoic acid
C20:2	<=>	eicosadienoic acid
C22:0	<=>	docosanoic acid
C22:1	<=>	docosenoic acid
C24:0	<=>	tetracosanoic acid
C4:0-ACP	<=>	butyryl-ACP
C6:0-ACP	<=>	hexanoyl-ACP
C8:0-ACP	<=>	octanoyl-ACP
CC	<=>	central cell
CCA1	<=>	CIRCADIAN CLOCK ASSOCIATED 1
cca1-11	<=>	loss-of-function in which *CCA1* was altered
cca1-11 lhy-21	<=>	double mutants in which *CCA1* and *LHY* were altered
CCT	<=>	CTP: phosphorylcholine cytidyltransferase
cDNA	<=>	complementary DNA
CDP-DAG	<=>	diacylglycerol esterified to cytidine diphosphate
CDP-DAGS	<=>	CDP-DAG synthase
CDS1,4	<=>	gene encoding for the CDP-DAG synthase
CDP-choline	<=>	Choline esterified to CDP
CDP-ethanolamine	<=>	Ethanolamine esterified to CDP
CK	<=>	Choline kinase
CK5	<=>	gene encoding for the choline kinase
cl	<=>	columella
CNRS	<=>	Centre national de la recherche scientifique
CO_2	<=>	carbon dioxide
CoA	<=>	coenzyme-A
Col-0	<=>	Columbia-0
cpt	<=>	chalazal proliferating tissue
CRRBM	<=>	Centre de Ressources Régionales en Biologie Moléculaire
CRY	<=>	cryptochrome
CSH	<=>	Charged Surface Hybrid
ct	<=>	cuticle
CT	<=>	carboxyltransferase
Ct	<=>	cycle threshold
CTI	<=>	CARBOXYLTRANSFERASE INTERACTOR
CTP	<=>	Cytidine triphosphate
CTS	<=>	COMATOSE

CUL3	<=>	CULLIN3-based E3 ligase
CV	<=>	central vacuole
Da	<=>	Dalton
DAF	<=>	days after flowering
DAG	<=>	diacylglycerol
DAG-CPT	<=>	CDP-choline: DAG cholinephosphotransferase
DAG-EPT	<=>	CDP-ethanolamine: DAG ethanolamine phosphotransferase
DGAT	<=>	acyl-CoA: DAG acyltransferase
dgat1-1	<=>	Loss-of-function mutant in which *DGAT1* is altered
DGAT1	<=>	Gene encoding for the acyl-CoA: DAG acyltransferase
DGD1	<=>	Gene encoding for the digalactosyldiacylglycerol synthase
DGDG	<=>	digalactosyldiacylglycerol
DGDGS	<=>	DGDG synthase
DHAP	<=>	dihydroxyacetone phosphate
DNA	<=>	desoxyribonucleic acid
dNTP	<=>	desoxyribonucleotide
Dr.	<=>	Doctor
EC	<=>	egg cell (Abbreviation used only in Figure 3)
EC	<=>	evening complex (Abbreviation only used in Figure 16)
EC	<=>	enzyme code (indicated in the text as followed: EC X.X.X.X)
ECL	<=>	Equivalent chain length
ECM	<=>	extracellular matrix
ECR	<=>	enoyl-CoA reductase
EDTA	<=>	ethylenediaminetetraacetic acid
EF1α	<=>	elongation factor 1α
eFP	<=>	Electronic Fluorescent Pictograph
EK	<=>	ethanolamine kinase
ela1	<=>	*enhanced linolenate accumulation 1*
ELF3	<=>	EARLY FLOWERING 3
ELF4	<=>	EARLY FLOWERING 4
ENO	<=>	enolase
EPI	<=>	epimerase
ER	<=>	endoplasmic reticulum (abbreviation used in text)
ER	<=>	enoyl-ACP reductase (abbreviation only used in Figure 9 and 14)
ESI	<=>	electrospray ionization source
ESI+	<=>	Ionization of molecules by ESI in positive mode
ESI-	<=>	Ionization of molecules by ESI in negative mode
eV	<=>	electronvolt
F6P	<=>	fructose-6-phosphate
FA	<=>	Fatty acids
FAB2	<=>	fatty acid biosynthesis 2
FAD	<=>	fatty acid desaturase
FAE complex	<=>	fatty acid elongation complex
FAE1	<=>	fatty acid elongase 1
FAME	<=>	fatty acid methyl ester
FAO	<=>	Food and Agricultural Organization

FAS	<=>	fatty acid synthase
FFA	<=>	free fatty acids
FID1	<=>	Flame ionization detector
FRK	<=>	fructokinase
FUS3	<=>	FUSCA 3
g, mg, µg, ng	<=>	gram, milligram, microgram, nanogram
G1P	<=>	glucose-1-phosphate
G3P	<=>	glycerol-3-phosphate
G6P	<=>	glucose-6-phosphate
G6PDH	<=>	glucose-6-phosphate dehydrogenase
G6PI	<=>	glucose-6-phosphate isomerase
GAPDH	<=>	glyceraldehyde-3-phosphate dehydrogenase
GC	<=>	Gas chromatography
GC-FID	<=>	Gas Chromatography with Flame-Ionization Detector
GC-MS	<=>	Gas Chromatography coupled with mass spectrometer
GEC	<=>	Génie Enzymatique et Cellulaire
GI	<=>	GIGANTEA
GPAT	<=>	glycerol-3-phosphate acyltransferase
h	<=>	hyaline layer (abbreviation only used in Figure 7)
h	<=>	hours (e.g.: 12h light/12h dark for 12 hours light/12 hours dark)
H_2	<=>	dihydrogen
H_2O	<=>	water
H_2SO_4	<=>	sulfuric acid
HACD	<=>	β-hydroxyacyl-CoA dehydratase
HAD	<=>	hydroxyacyl-ACP dehydratase
HAF	<=>	hours after flowering
HPLC	<=>	high-performance liquid chromatograph
HPLC-QTOF	<=>	liquid chromatography coupled with a quadrupole time-of-flight
HRMS	<=>	high resolution mass spectrometer
HXK	<=>	hexokinase
ii1, ii1’ and ii2	<=>	inner layer of integument
INV	<=>	invertase
ISO	<=>	isomerase
KAR	<=>	3-ketoacyl-ACP reductase
KAS	<=>	3-ketoacyl-ACP synthase
KAT	<=>	3-ketoacyl-CoA thiolase
kb	<=>	kilobase
KCR	<=>	β-ketoacyl-CoA reductase
KCS	<=>	β-ketoacyl-CoA synthase
KIN10	<=>	protein kinase 10
KOH	<=>	potassium hydroxide
kPa	<=>	kilopascal
L, mL, µL	<=>	Litre, millilitre, microlitre
L1L	<=>	LEAFY COTYLEDON 1-like
LACS	<=>	long-chain acyl-CoA synthetase
LAFL	<=>	LEC1, ABI3, FUS3 and LEC2

Late M.	<=>	late-maturation
LD	<=>	long-day
LEC1	<=>	LEAFY COTYLEDON 1
LEC2	<=>	LEAFY COTYLEDON 2
LHY	<=>	LATE ELONGATED HYPOCOTYL
lhy-21	<=>	loss-of-function mutant in which *LHY* was altered
LiCl	<=>	lithium chloride
LL	<=>	continuous light
LPA	<=>	lysophosphatidic acid
LPAAT	<=>	2-lysophosphatidic acid acyltransferase
LPAT5	<=>	gene encoding for the LPA acyltransferase (LPAAT)
LPC	<=>	lyso-phosphatidylcholine (lyso-PC)
LPCAT	<=>	lysophosphatidylcholine acyltransferase
LUX	<=>	LUX ARRHYTHMO
m, cm, mm, µm, nm	<=>	metre, centimetre, millimetre, micrometre, nanometre
M, mM, µM	<=>	Molar, millimolar, micromolar
m/z	<=>	mass-to-charge ratio
MAG	<=>	monoacylglycerol
MCMT	<=>	malonyl-CoA: ACP transacylase
MDH	<=>	malate dehydrogenase
MFP	<=>	multifunctional protein
MGDG	<=>	monogalactosyldiacylglycerol
MGDGS	<=>	MGDG synthase
min	<=>	minute or minutes
MIPS	<=>	myo-inositol-3-phosphate synthase
MLS	<=>	malate synthase
mol%	<=>	molar percentage
MS	<=>	mass spectrometer/mass spectrometry
MS medium	<=>	Murashige and Skoog medium
MS1, MS2 (MS/MS)	<=>	mass spectra
MTBE	<=>	methyl tert-butyl ether
mu	<=>	mucilage
MYB	<=>	Myeloblastosis
N	<=>	the number of cDNA after n cycle of amplification
n	<=>	number of replicates
NaCl	<=>	sodium chloride
NAD^+	<=>	oxidized form of the Nicotinamide adenine dinucleotide
NADH	<=>	reduced form of the Nicotinamide adenine dinucleotide
$NADP^+$	<=>	oxidized form of the Nicotinamide adenine dinucleotide phosphate
NADPH	<=>	reduced form of the Nicotinamide adenine dinucleotide phosphate
n cycle	<=>	n number of amplification cycle
NF-YA	<=>	NUCLEAR FACTOR Y-SUBUNIT A
NF-YB	<=>	NUCLEAR FACTOR Y-SUBUNIT B
NF-YC	<=>	NUCLEAR FACTOR Y-SUBUNIT C
No	<=>	the initial number of cDNA in the sample before the amplification
N.S.	<=>	not specified

NS	<=>	non-significant (p-value > 0.05)
NTC	<=>	No Template Control
O_2	<=>	dioxygen
OAA	<=>	Oxaloacetate
oi1 and oi2	<=>	outer layer of integument
PA	<=>	phosphatidic acid
PAD	<=>	Δ9 palmitoyl-ACP desaturase
PC	<=>	phosphatidylcholine
PC 1	<=>	Principal Component 1
PC 2	<=>	Principal Component 2
PCA	<=>	Principal component analysis
PCK	<=>	phosphoenolpyruvate carboxikinase
PCR	<=>	polymerase chain reaction
PDAT	<=>	phospholipid: DAG acyltransferase
PDAT1	<=>	gene encoding for phospholipid: DAG acyltransferase
pdat1-1	<=>	loss-of-function mutant in which *PDAT1* is altered
PDHC	<=>	pyruvate dehydrogenase complex
PDH-E1	<=>	E1 component of pyruvate dehydrogenase complex
pe	<=>	peripheral endosperm
PE	<=>	phosphatidylethanolamine
PEAMT	<=>	phosphoethanolamine N-methyltransferase
PECT	<=>	CTP: phosphorylethanolamine cytidyltransferase
PECT1	<=>	gene encoding for CTP: phosphorylethanolamine cytidyltransferase
PEP	<=>	phosphoenolpyruvate
PFK	<=>	phosphofructokinase
PG	<=>	phosphatidylglycerol
PGD	<=>	6P-gluconate dehydrogenase
PGK	<=>	phosphoglycerate kinase
PGL	<=>	6P-gluconolactonase
PGM	<=>	phosphoglucomutase
PGLYM	<=>	phosphoglycerate mutase
PGP	<=>	phosphatidylglycerol phosphate
PGPP	<=>	phosphatidylglycerol phosphate phosphatase
PGPS	<=>	phosphatidylglycerol phosphate synthase
pH	<=>	potential of hydrogen
PhD	<=>	Philosophiæ doctor
PHY	<=>	phytochrome
PI	<=>	phosphatidylinositol
PIS	<=>	phosphatidylinositol synthase
PK	<=>	pyruvate kinase
pkp1 and *pkp2*	<=>	loss-of-function mutants in which the plastidial PK are altered
PLA2	<=>	Phospholipase A2
PLC	<=>	phospholipase C
PLD	<=>	phospholipase D
p.m.	<=>	post meridiem
PMC	<=>	pollen mother cell

PMI	<=>	pollen mitosis 1
PMII	<=>	pollen mitosis 2
pmol, µmol, nmol	<=>	picomole, micromole, nanomole
PN	<=>	polar nuclei
POS/NEG mode	<=>	positive/negative mode
PP	<=>	phosphatidate phosphatase
PPP	<=>	pentose phosphate pathway
PQ	<=>	plastoquinone
PQH_2	<=>	plastoquinol
PRR	<=>	PSEUDO-RESPONSE REGULATOR
prr9-1, *prr7-3*, *prr5-1*	<=>	loss-of-function mutants in which PRR9, PRR7 and PRR5 were altered
ps	<=>	pigment strand
PS	<=>	phosphatidylserine
PSD	<=>	PS decarboxylase
PSD3	<=>	Gene encoding for the PS decarboxylase
PSI	<=>	photosystem I
psi	<=>	pound per square inch
PSII	<=>	photosystem II
QC	<=>	quality control
qPCR	<=>	quantitative polymerase chain reaction
QTOF	<=>	hybrid quadrupole time of flight
RAM	<=>	root apical meristem
RNA	<=>	ribonucleic acid
rpm	<=>	rotation per minute
rRNA	<=>	ribosomic RNA
RT-qPCR	<=>	reverse transcription quantitative real-time polymerase chain reaction
Rubisco	<=>	ribulose-1,5-bisphosphate carboxylase/oxygenase
SAD	<=>	Δ9 stearoyl-ACP desaturase
SAM	<=>	shoot apical meristem
SC	<=>	synergid cells
SD	<=>	short-day
SDS	<=>	sodium dodecylsulfate
sec	<=>	second or seconds (unit of time)
SEN	<=>	secondary endosperm nucleus
SGR	<=>	STAY-GREEN
SLS	<=>	sulfolipid synthase
sn-1, *sn-2* and *sn-3*	<=>	first, second and third positions of the glycerol backbone
SQDG	<=>	sulfoquinovosyldiacylglycerol
T6P	<=>	trehalose-6-phosphate
TAE	<=>	Tris, Acetic acid and EDTA
TAG	<=>	Triacylglycerol
TCP4	<=>	TEOSINTE BRANCHED1/CYCLOIDEA/PROLIFERATING CELL FACTOR 4
T-DNA	<=>	transfer DNA
Tm	<=>	melting temperature
TOC1	<=>	TIMING OF CAB EXPRESSION 1
toc1-1 and *toc1-2*	<=>	loss-of-function mutants in which TOC1 was altered

TOC1-ox	<=>	overexpressing TOC1 mutant
TPI	<=>	triose phosphate isomerase
Tris-HCl	<=>	trisaminomethane-hydrochloride
TT	<=>	transmitting tract
TT8	<=>	TRANSPARENT TESTA 8
t-test	<=>	Student test
TTG1	<=>	TRANSPARENT TESTA GLABRA 1
U	<=>	enzyme unit
UDP	<=>	Uridine diphosphate
UDP-glucose	<=>	Glucose esterified to UDP
UDP-sulfoquinovosyl	<=>	Sulfoquinovosyl esterified to UDP
UHD	<=>	Ultra-high definition
UMR	<=>	Unité Mixtes de Recherche
UPJV	<=>	University of Picardie Jules Verne
UPLC	<=>	Ultra-Performance Liquid Chromatography
UTP	<=>	uridine triphosphate
UV	<=>	ultraviolet
v/v	<=>	volume/volume
v/v/v	<=>	volume/volume/volume
V, kV	<=>	Volt, kilovolt
vb	<=>	vascular bundle
VLCFA	<=>	very long chain fatty acids
WRI1	<=>	WRINKLED 1
WRKY	<=>	tryptophan (W)-arginine (R)-lysine (K)-tyrosine (Y)
Ws	<=>	Wassilewskija
WT	<=>	wild-type
w/v	<=>	weight/volume
x g	<=>	relative centrifugal force
ZT	<=>	Zeitgeber time (e.g.: ZT11 => 11h after dawn)
ZT0	<=>	Zeitgeber time 0 (light on or dawn)
ZT12	<=>	Zeitgeber time 12 (light off or 12h after dawn = dusk)
ZTL	<=>	ZEITLUPE

Overview

List of Figures

SECTION 1: INTRODUCTION

SECTION 2: PhD PROJECT

SECTION 3: MATERIALS AND METHODS

SECTION 4: RESULTS AND DISCUSSION

SECTION 5: CONCLUSIONS AND PERSPECTIVES

SUPPLEMENTARY FIGURES

List of Tables

SECTION 3: MATERIALS AND METHODS

SECTION 4: RESULTS AND DISCUSSIONS

SUPPLEMENTARY TABLES

SECTION 1: INTRODUCTION

GENERAL INTRODUCTION

Due to genetic and phenotypic differences, a large diversity of plants is observed throughout the world. Some of them are distinguished by their ability to accumulate large amount of oil either within their mesocarp, like in olive and palm fruits, or within their seeds, like in colza and soybean oilseeds. Despite equipped with similar lipid biosynthetic pathway, the oil content in oilseeds varies from one species to another, as well as between the same species. The percentage of oil ranges from 20 % of seed weight in soybean to 60 % of seed weight in sesame. In *Arabidopsis thaliana*, the oil content is estimated about 35 % of seed weight (Li *et al.,* 2006). These differences in term of oil accumulation are due to different regulatory mechanisms associated to lipid biosynthetic pathways between oilseed plants (Savadi *et al.*, 2017).

Seed storage oil is mainly made of triacylglycerols (TAG), a neutral lipid constituted by the esterification of a glycerol molecule with three fatty acids (FA). TAG physiochemical properties depend on the nature of their FA substituents (number of carbons, the presence of functional group and the level of unsaturation) and their location into the glycerol backbone (*sn-1*, *sn-2* and *sn-3*). The main role of TAG is providing energy and carbon to plants during the early germination stages supporting the development of seedlings before photosynthesis is stablished. During germination, TAG is mobilized by the action of lipases allowing the release of FA. The catabolism of FA by the β-oxidation results in the production of acetyl-CoA and reducing equivalent in form of NADH. The acetyl-CoA produced is the source of carbon for the synthesis of sucrose through the combined action of the glyoxylate cycle and the gluconeogenesis pathway. The enzymatic hydrolysis of sucrose releases glucose. Once released, this hexose is catabolized by glycolysis and pentose phosphate pathway, providing energy, reducing equivalent and carbon necessary for the growth and development of seedlings (Graham, 2008). Moreover, during seedling development, TAG enables the production of membrane lipids that besides their structural functions are also involved in signal transduction, photosynthesis and protection against biotic or abiotic stresses (Kobayashi *et al.*, 2016a).

Although TAG is associated to several biological properties in plants, this molecule, highly concentrated in vegetable oils, can be used for industrial and nutritional applications. Some vegetable oils are a rich source of essential FA, including the omega-3 linolenic (C18:3)

and omega-6 linoleic acids (C18:2) (Glick and Fisher, 2013). In addition, vegetable oils are one of the most important sources of edible calories in the human diet (Zhao *et al*., 2021). Owing to the importance of vegetable oils for food application, one of the challenges in plant oil research thus consists in improving the nutritional quality of plant fats (Zafar *et al.*, 2019). Another important aspect of vegetable oils relies on the structural similarity of FA with long-chain fossil hydrocarbon. Vegetable oils, mainly containing highly reduced TAG molecules, are combined with petroleum-derived products for obtaining biodiesel (Durrett *et al.*, 2008). The simultaneous use of edible vegetable oils for nutritional and industrial purpose, however, leads to the depletion and increase of the price of these oils as source of food, especially in developing countries. In order to avoid depletion and cost issues, the use of non-edible or waste edible oils is preferred for the production of biodiesel (Gui *et al.*, 2008).

Ukraine and Russia are the first producers of sunflowers, both countries representing more than 50 % of the total sunflower oil world's production[1]. Indeed, 70 % of Ukrainian territories are arable land, representing nearly 43 million hectares. The war between Russia and Ukraine, also causing geopolitical tension, has heavy impact on the international sunflower oil market. The production and exportation of this vegetable oil is considerably affected, increasing its price from 640 to 1000 euros per ton between February and May 2022. The current rise of sunflower oil price and the depletion of this vegetable oil in the market lead to the use of other edible oils for industrial and food purposes, including olive and palm oils. The decrease in the exportation of sunflower oil and its replacement by other vegetable oils would also increase the price of these other oilseeds in the market[1]. The use of palm oil especially for nutritional applications has consequences on human health since it can, for instance, increase cardio-vascular risks and other damages (Brown *et al.*, 2005). The consumption of palm oil is also associated to ecological issues, including the deforestation, habitat destruction and water pollution (Brown *et al.*, 2005). In addition, it is well known that the demand in vegetable oils is constantly increasing with the rise of the world's population (Harwood *et al.,* 2013). Another challenge in plant oil research lies in enhancing the yield of several oilseed crops, including sunflower oilseed crops. The increase of the size and number of seeds in plants, as well as the accumulation of oil within seeds, are strategies for the

[1] FAO, Information Note - The Importance of Ukraine and the Russian Federation for Global Agricultural Markets and the Risks Associated with the Current Conflict. FAO Headquarters, Rome, 1-47 March. 2022.

improvement of oilseed crop yield (Bhat, 2010).

The reduction and redistribution of arable land due to demographic and climate change is another critical aspect affecting vegetable oil production. The increase in the World's population combined with the negative effect of the climate changes can lead to the reduction of the arable land across the world[2]. The negative effect of climate changes is more pronounced in low latitude countries since these regions were already subjected to high temperatures (Smith and Hitz, 2002). This requires the redistribution of arable land preferentially in higher latitude regions (Cramer and Solomon, 1993). However, the redistribution of arable land negatively affects the development and survival of plants since these sessile organisms will be exposed to new rhythmic environmental fluctuations (e.g.: rhythmic fluctuation of light). The presence of an internal timekeeper, the circadian clock, in plants helps to cope with these rhythmic environmental fluctuations. Plants can anticipate external changes by synchronizing their internal circadian clock with the external environment (Mas, 2005; Oakenfull *et al*., 2017). Once synchronized, the internal timekeeper is helpful in maintaining the plant physiology and promoting plant development. The circadian clock is involved in the regulation of many physiological processes (Dodd *et al*., 2005; Pan *et al.*, 2015), however, the connection between the circadian clock and the synthesis of vegetable oils has been sparsely studied (Hsiao *et al.*, 2014). Understanding the role of the circadian clock in the regulation of glycerolipid synthesis could help adapting oilseed crops plants to new rhythmic environmental fluctuations and fostering their cultivation over new latitudes. The aim of this PhD project is studying the potential regulation exerted by molecular components of the circadian system on seed lipid metabolism in the model plant *Arabidopsis thaliana*.

[2] FAO, World agriculture towards 2030/2050. FAO Headquarters, Rome, 1-147 June. 2012.

INTRODUCTION

1. Physiology of Arabidopsis seed development

Arabidopsis thaliana, also known as thale cress or mouse-ear cress, is an annual plant widely represented especially in Europe, Asia and Africa. The angiosperm phylogeny group established by Chase *et al.* (2016) shows that plants from the Brassicales order belongs to angiosperms, eudicots and rosids clades **(Figure 1)**. Angiosperm clade encompasses 400,000 flowering plant species. In these species, seeds are produced and enclosed within fruits, also known as siliques in *Arabidopsis thaliana* (Sun *et al.*, 2020). Eudicot clade regroups a total of 190,000 plant species. In these species, seed germination results in the formation of seedlings composed of two immature leaves referred as cotyledons (Simpson, 2019). Rosids clade encompasses plants containing flowers with separated petals (Citerne *et al.*, 2010). Rosids constitute a large part of the eudicot clade since the number of species in this phylogeny group is comprised between 90,000 and 120,000 (Sun *et al.*, 2020). Among rosids, a total of 4,700 species belongs to the Brassicales order. This order is divided into 17 families, including the family of the model plant *Arabidopsis thaliana* referred as Brassicaceae (Franzke *et al.*, 2016).

Arabidopsis thaliana has a short life cycle of approximately 3 or 4 months. The reproductive cycle consists of five developmental stages. In the hermaphrodite *Arabidopsis thaliana* plant, flowers are composed of male and female reproductive systems. The first stage of the reproductive cycle consists in the meiosis of diploid mother cells contained within male and female reproductive systems. This result in the production of male and female haploid reproductive cells referred as spores. Male and female spores are known as microspores and megaspores, respectively. Successive mitoses are then involved in the development of spores into male and female gametophytes. Male and female gametophytes are called pollen grain and embryo sac, respectively (Olsen, 2004; Boavida *et al.*, 2005). Each pollen grain contains two male gametes known as sperm cells, while the embryo sac contains a female gamete called egg cell. The second stage of the reproductive cycle involves the double fertilization between the embryo sac and the pollen grain (Hamamura *et al.*, 2011). Fertilization is followed by the seed development.

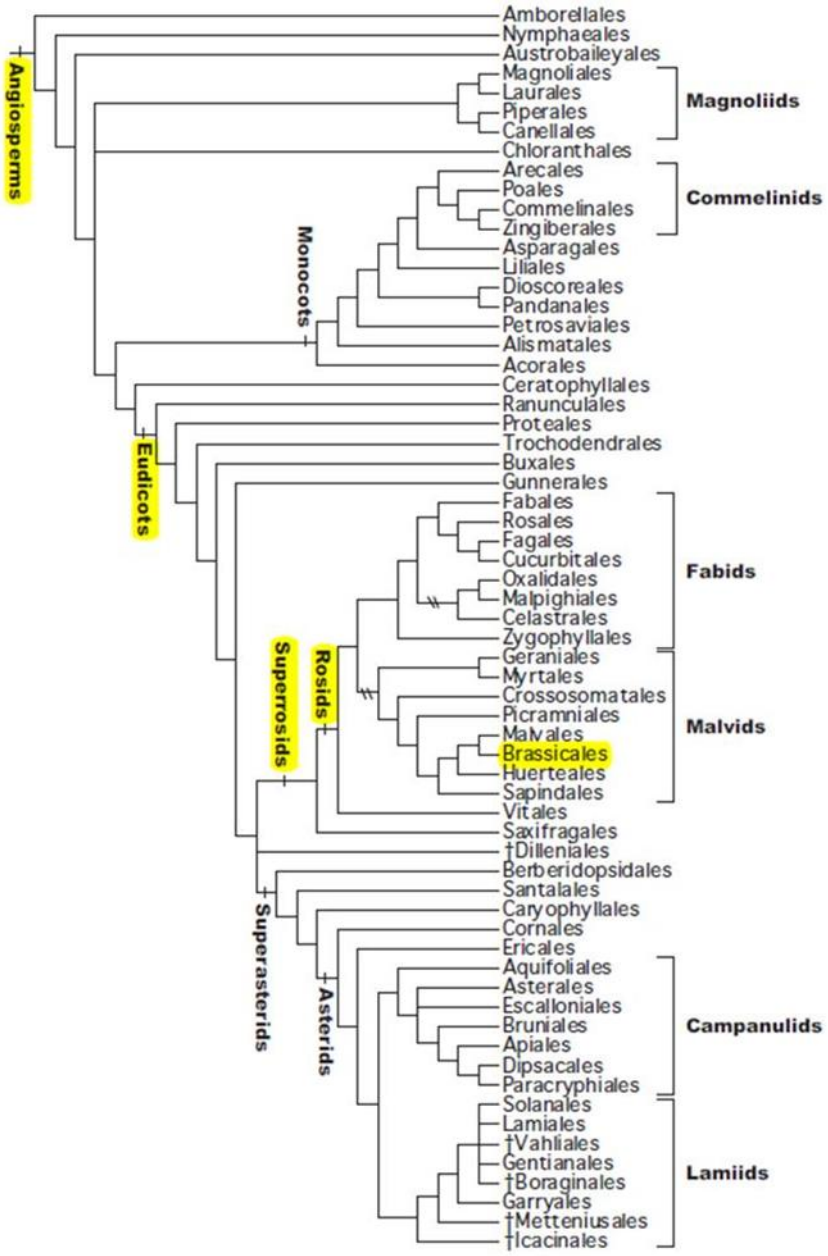

Figure 1. The phylogeny of *Arabidopsis thaliana*. *Highlighted in yellow represents the phylogeny of plants belonging to the Brassicales order, including Arabidopsis thaliana. Adapted from the publication by Chase et al. (2016).*

The third stage is divided into embryo morphogenesis and seed maturation **(Figure 2)**. This stage is carried out within siliques that are formed from the development of the female reproductive system. Embryo morphogenesis consists in a set of physiological processes leading to the formation of the embryo from the egg cell. The endosperm and the seed coat are formed simultaneously to the embryo morphogenesis. The endosperm is produced from the embryo sac. The seed coat is formed from a maternal tissue known as the integument, itself derived from the female reproductive system **(Figure 2)**. Seed coat has crucial roles in seed dormancy and protection of the embryo (Bewley, 1997). The role of the endosperm is

providing nutrients to the embryo in order to ensure its growth during seed development (Yan *et al.,* 2014). The embryo, occupying a large part of the Arabidopsis seed volume, is formed by the root apical meristem, hypocotyl, shoot apical meristem and two cotyledons. These four embryo tissues have fundamental roles for promoting the development of the future plant. The role of cotyledons consists in the storage of reserve lipids. These lipids are mostly TAG accumulated during seed maturation and mobilized during germination in order to ensure plant growth (Graham, 2008). Root apical meristem and hypocotyl are involved in the formation of root, while the shoot apical meristem allows the formation of the aerial part of plants (Boscá *et al.,* 2011).

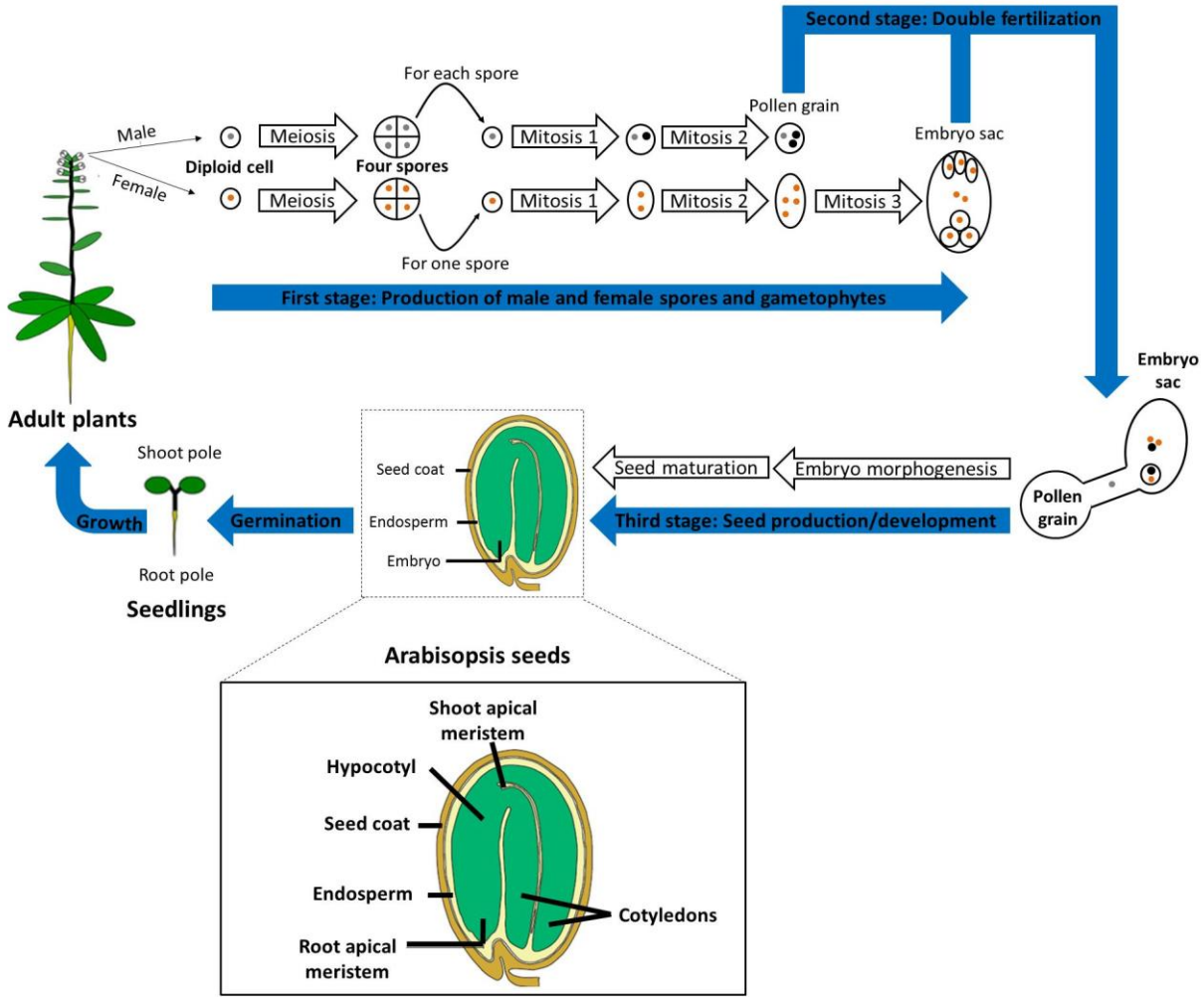

Figure 2. The reproductive cycle of *Arabidopsis thaliana*. *The first stage leads to the formation of male (pollen grain) and female (embryo sac) gametophytes. The second stage consists in the fertilization of the embryo sac nuclei. The development of the fertilized embryo sac into seeds takes place during the third step. Seeds are composed of seed coat, endosperm and embryo. The embryo is itself composed of the shoot apical meristem, cotyledons, hypocotyl and root apical meristem. The two last stages correspond to the germination and growth of the resulting seedlings into adult plants. Adapted from Mayer et al. (2008) and Haughn and Chaudhury (2005).*

The first three stages of the reproductive cycle are then followed by the dissemination of seeds and their growing in soil. Germination consists in the development of the seed embryo into seedlings and represents the fourth developmental stage of the reproductive cycle. During the last stage, the growth of seedlings enables the formation of new adult plants with flowers and siliques. A new set of seeds is thus produced within siliques, closing the reproductive cycle **(Figure 2)**. The first three developmental stages are described in this first chapter.

1.1. Male and female spores and gametophytes

1.1.1. Development of megaspores into the embryo sac

The development of megaspores and the embryo sac takes place in the nucellus, which is a tissue found within the female reproductive system. Diploid cells found in the nucellus first undergo meiosis leading to the formation of four haploid megaspores (**Figure 3A**). The degeneration of three haploid megaspores is followed by three successive nucleus divisions of the surviving female reproductive cell **(Figure 3A)**. This results in the formation of the embryo sac containing eight haploid nuclei **(Figure 3A)** (Olsen, 2004). The eight nuclei are split into two groups located at different poles of the embryo sac (**Figure 3A**) (Drews *et al.*, 1998). This step is followed by the migration of a single haploid nucleus from each pole allowing their fusion at the central position of the embryo sac, producing a diploid nucleus known as the secondary endosperm nucleus (SEN; **Figure 3A**). This nucleus is involved in the production of the endosperm after the realization of the double fertilization (Christensen *et al.*, 1997). Membranes are then formed around each of the six other nuclei, resulting in the development of the embryo sac composed of six small cells and a large central cell that contains the secondary endosperm nucleus **(Figure 3A)** (Drew *et al.*, 1998). In Arabidopsis, three of the six small cells degenerate resulting in an embryo sac containing a larger central cell and three small cells **(Figure 3A)**. These three small cells then differentiate into one egg cell and two synergid cells **(Figure 3A)** (Russell, 1993). The egg cell is involved in the formation of the embryo after the double fertilization, while synergid cells help achieving the fertilization of the embryo sac (Hamamura *et al.,* 2012). Once produced, the embryo sac is surrounded by five layers of cells derived from the female reproductive system known as the integuments **(Figure 3A)**.

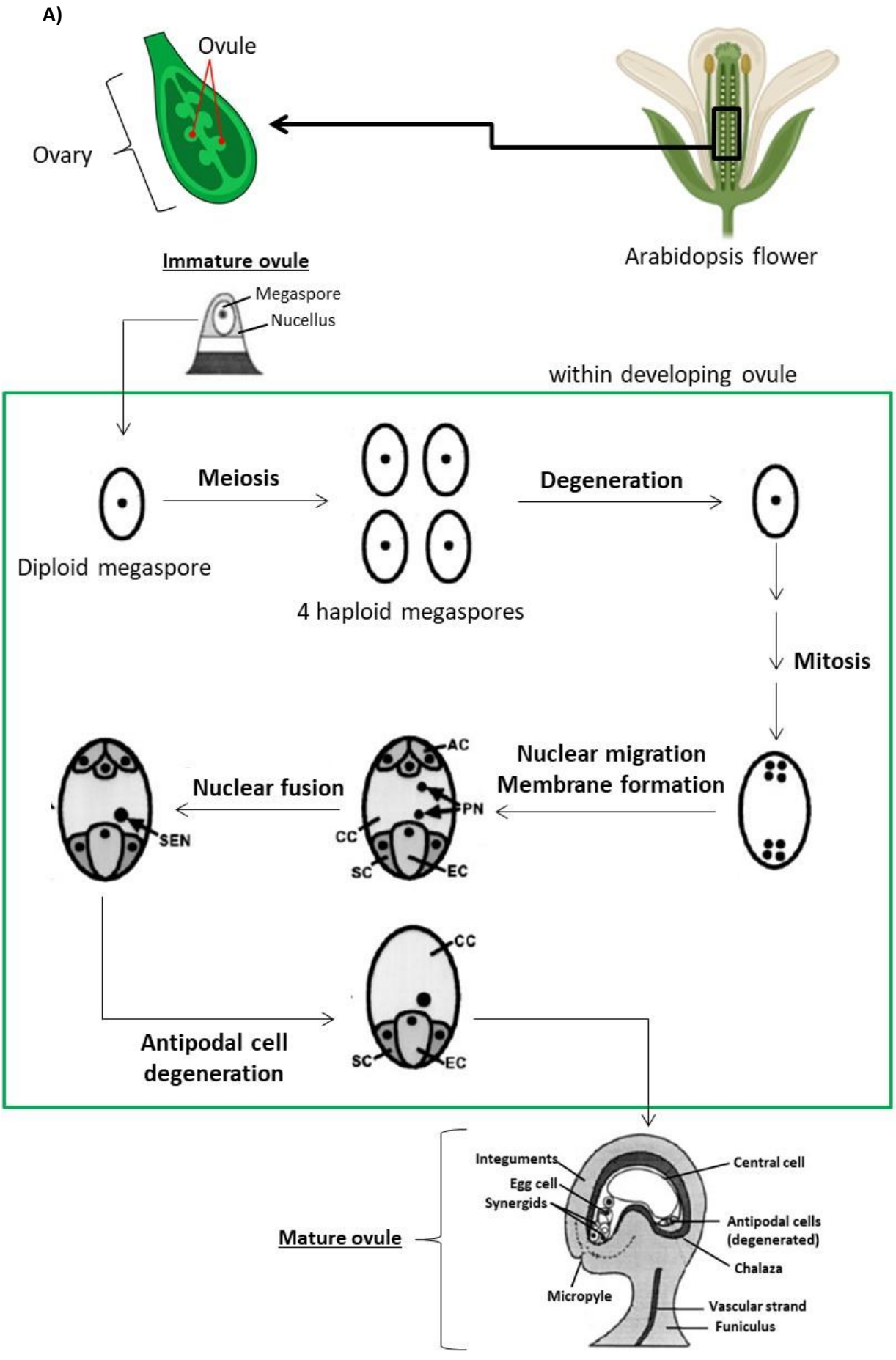
A)
Ovule
Ovary
Arabidopsis flower
Immature ovule
Megaspore
Nucellus
within developing ovule
Meiosis
Degeneration
Diploid megaspore
4 haploid megaspores
Mitosis
Nuclear migration
Membrane formation
Nuclear fusion
AC
PN
CC
SC
EC
SEN
Antipodal cell
degeneration
Mature ovule
Integuments
Egg cell
Synergids
Central cell
Antipodal cells
(degenerated)
Chalaza
Micropyle
Vascular strand
Funiculus

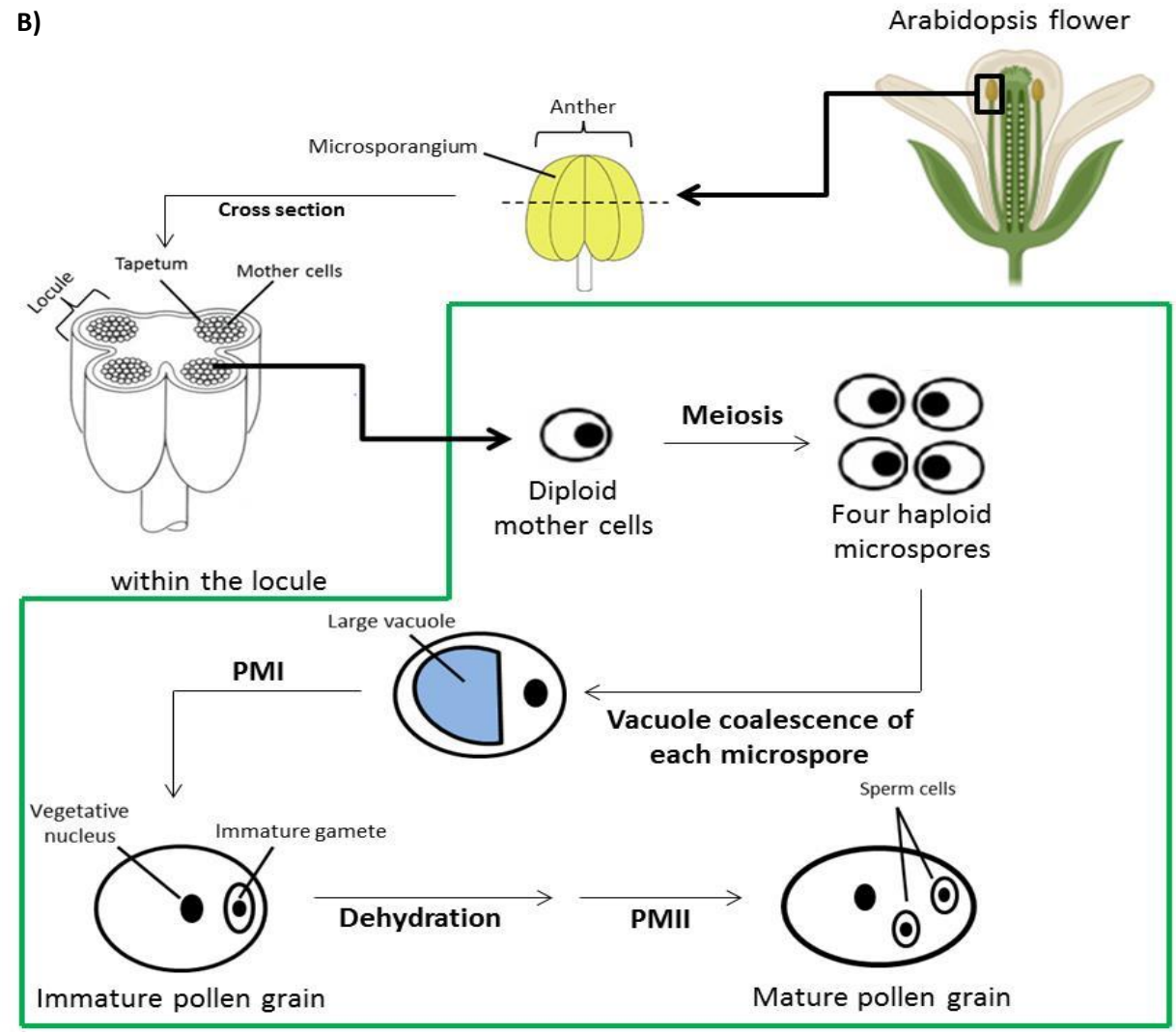

Figure 3. Male and female gametophyte in *Arabidopsis thaliana*. *A) This figure shows the different steps toward the formation of the embryo sac within the developing ovule. Abbreviations: AC, antipodal cells; PN, polar nuclei; CC, central cell; SC, synergid cells; EC, egg cell; SEN, secondary endosperm nucleus. This figure is adapted from Drew et al. (1998). B) This figure illustrates steps leading to the production of pollen grain within the anther. Abbreviations: PMI, pollen mitosis 1; PMII, pollen mitosis 2. This figure is adapted from Boavida et al. (2005).*

1.1.2. Development of microspores and pollen grain

The pollen mother cell (PMC), which is a diploid cell produced within the male reproductive system, undergoes meiosis resulting in the formation of four haploid microspores (Boavida *et al.*, 2005). A single large vacuole is then formed within each haploid microspore. The nucleus migrates toward the membrane of the haploid microspore (Zonia *et al.*, 1999). The polarization of the nucleus allows the realization of an asymmetric division, known as pollen mitosis 1 (PMI), resulting in the formation of the precursor of the male gametes within the pollen grain (Horvitz and Herskowitz, 1992; Eady *et al.*, 1995). The pollen grain is dehydrated in order to prevent a decrease in the viability of this male gametophyte

during its expulsion from the male reproductive system. The precursor of the male gamete then undergoes a second division, known as the pollen mitosis 2 (PMII). This division enables the formation of two sperm cells, which are mature gametes necessary to the future fertilization of the embryo sac **(Figure 3B)**.

1.2. The double fertilization

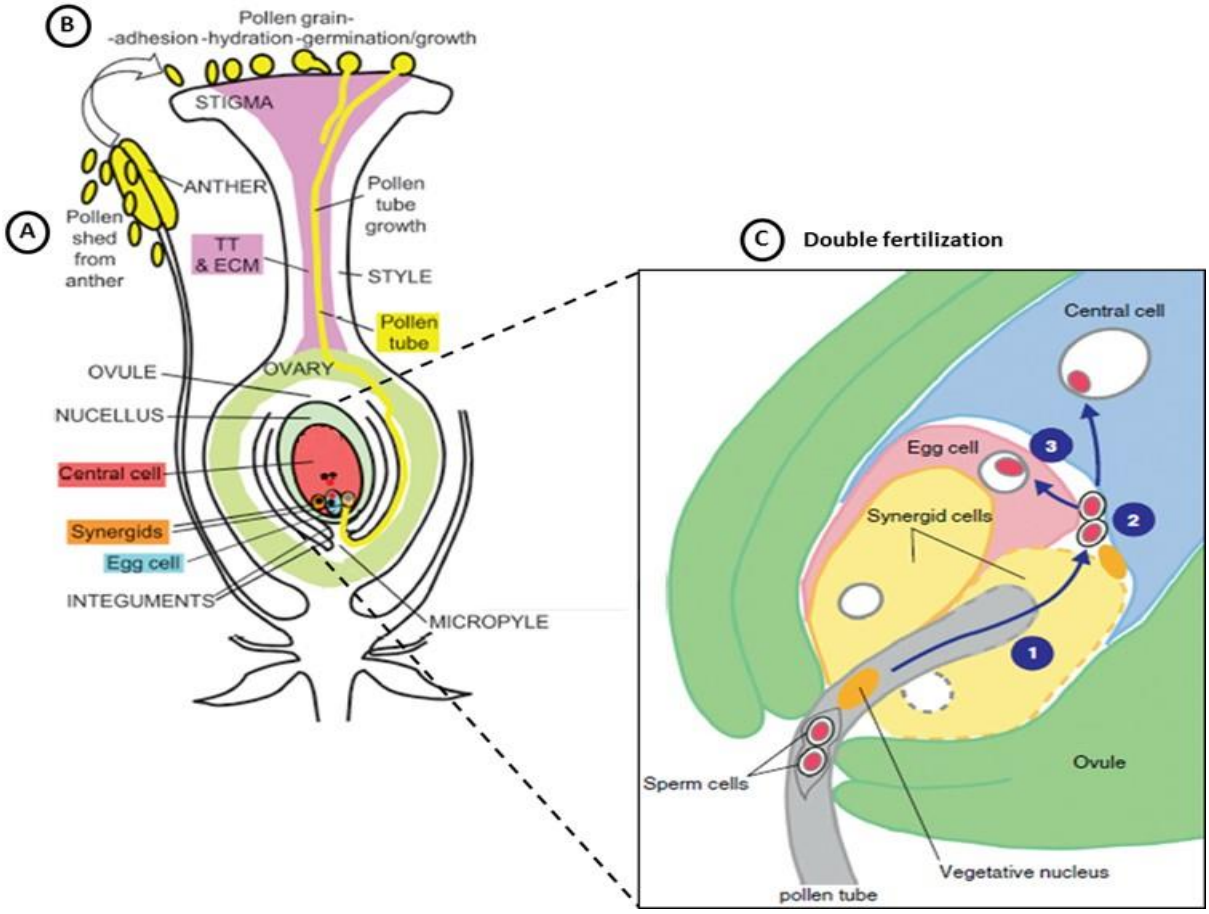

Figure 4. Main events leading to the double fertilization. *Double fertilization (C) is preceded by A: the release of dehydrated pollen grain from the male reproductive system (anther) and B: the interaction of the pollen grain with the stigma resulting in its rehydration and the formation of a cytoplasmic expansion called the pollen tube. C: The double fertilization is itself divided into three main steps, 1: the release of the sperm cells from the pollen tube within a degenerated synergid cell, 2: the immobilization of both sperm cells in a space between the egg and the central cells and 3: the fusion of both sperm cells with nuclei of egg and central cells. Abbreviation: TT, transmitting tract; ECM, extracellular matrix. Adapted from Dresselhaus et al. (2013) and Hamamura et al. (2012).*

The pollen grain is expulsed from the male reproductive system and interacts with the surface of the stigma allowing its hydration (Zinkl *et al.,* 1999; Dresselhaus and Franklin-Tong, 2013). The cytoplasmic expansion of the pollen grain then enables the formation of the pollen tube. The growth of the pollen tube, occurring within the female reproductive system, and its guidance toward the embryo sac allows the non-motile sperm cells to reach the female

gametophyte (Franklin-Tong, 2002; Lora *et al.,* 2018). The degeneration of the synergid cell helps releasing both sperm cells within the embryo sac between egg and central cells (Hamamura *et al.,* 2012). One of the haploid sperm cells fuses with the diploid nucleus of the central cell creating a triploid nucleus whose role consists in producing the endosperm. The second sperm cell fertilizes the egg cell, resulting in the formation of a diploid zygote that will develop into the seed embryo (Hamamura *et al.,* 2012) **(Figure 4 and 5)**.

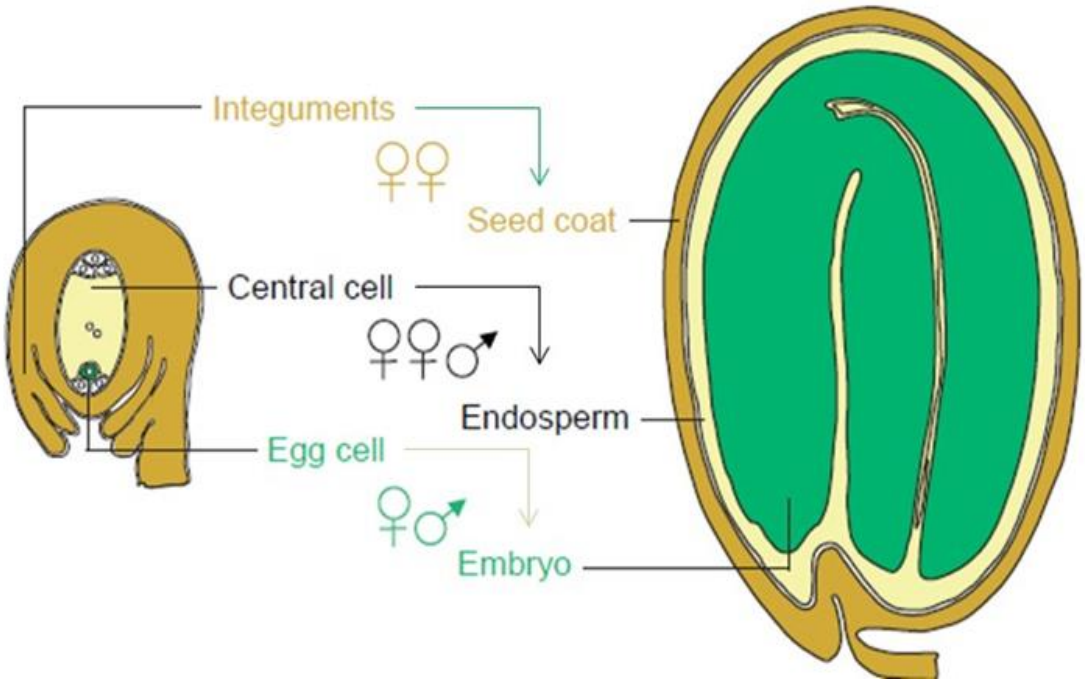

Figure 5. Fate of the embryo sac and integuments after double fertilization. *On the left it is represented the structure of mature ovule in which the embryo sac is surrounded by the ovular integument. On the right it is illustrated the structure of mature Arabidopsis seeds. The integument, which is a mother-derived structure, is involved in the formation of the seed coat. After fertilization, the central cell and the egg cell will the origin of the endosperm and the embryo, respectively. Adapted from Haughn and Chaudhury (2005).*

1.3. Development of Arabidopsis seeds

Seed development includes two crucial physiological processes: seed morphogenesis and seed maturation. Seed morphogenesis consists in the development of the fertilized egg, the central cells and the integuments into the embryo, the endosperm and the seed coat, respectively **(Figure 5)** (Haughn and Chaudhury, 2005). Seed maturation consists in the establishment of the seed dormancy and its preparation for later germination. Seed morphogenesis and maturation take place within siliques, which are derived from the female reproductive system.

1.3.1. Seed morphogenesis (from 4 HAF to 7 DAF)

1.3.1.1. Embryogenesis: formation of the embryo from the fertilized egg cell

Embryogenesis, also known as the embryo morphogenesis, is divided into seven embryonic stages, corresponding to 1-cell, 2-cell, 4-cell, octant, dermatogen, globular and heart stages. Each developmental stage takes place several hours or days after the double fertilization, therefore, they are expressed in hour or day after flowering (HAF or DAF) since the double fertilization is performed simultaneously to the flowering processes (Mansfield *et al.*, 1991).

Embryogenesis consists in the elongation of the fertilized egg cell followed by a transversal asymmetric division of the zygote that occurs between four and eight hours after flowering (HAF). This results in the formation of two cells: an upper spherical cell and a lower vacuolated cell **(Figure 6)**. The vacuolated cell is known as the basal cell due to its role in the formation of structures found in the root (basal) pole of developing seedlings. The spherical cell is referred as the apical cell since its function is producing structures located close to the shoot (apical) pole of developing seedlings (Scheres *et al.*, 1999). Each of the seven embryonic stage is named according to the number of apical cells constituting the embryo, the tissue composing the embryo or the shape of the embryo. The embryo is, therefore, in a 1-cell embryonic stage after the division of the zygote. After several divisions, the apical cell enables the formation of three embryo tissues, including cotyledons, shoot apical meristem and hypocotyl. The basal cell is involved in the formation of the root apical meristem, as well as the extra embryonic structure known as the suspensor **(Figure 6)**. The suspensor allows transferring nutrients from the developing endosperm to the embryo at the early stage of the embryogenesis before its degeneration at 5 or 6 days after flowering (DAF) (Mansfield and Briarty, 1991). The apical cell undergoes one transversal division and two longitudinal divisions. This results in the production of the octant, in which cells are distributed into upper and lower tiers **(Figure 6)** (Capron *et al.,* 2009; Ten Hove *et al.,* 2015). Divisions of the octant cells then result in the formation of 16-cell embryonic structure that is composed of outer and inner cells. This embryonic structure is known as the dermatogen since the outer and inner cells are, in part, involved in the synthesis of epidermal and endodermal precursors in a later embryonic developmental stage **(Figure 6)** (Ten Hove *et al.,* 2015).

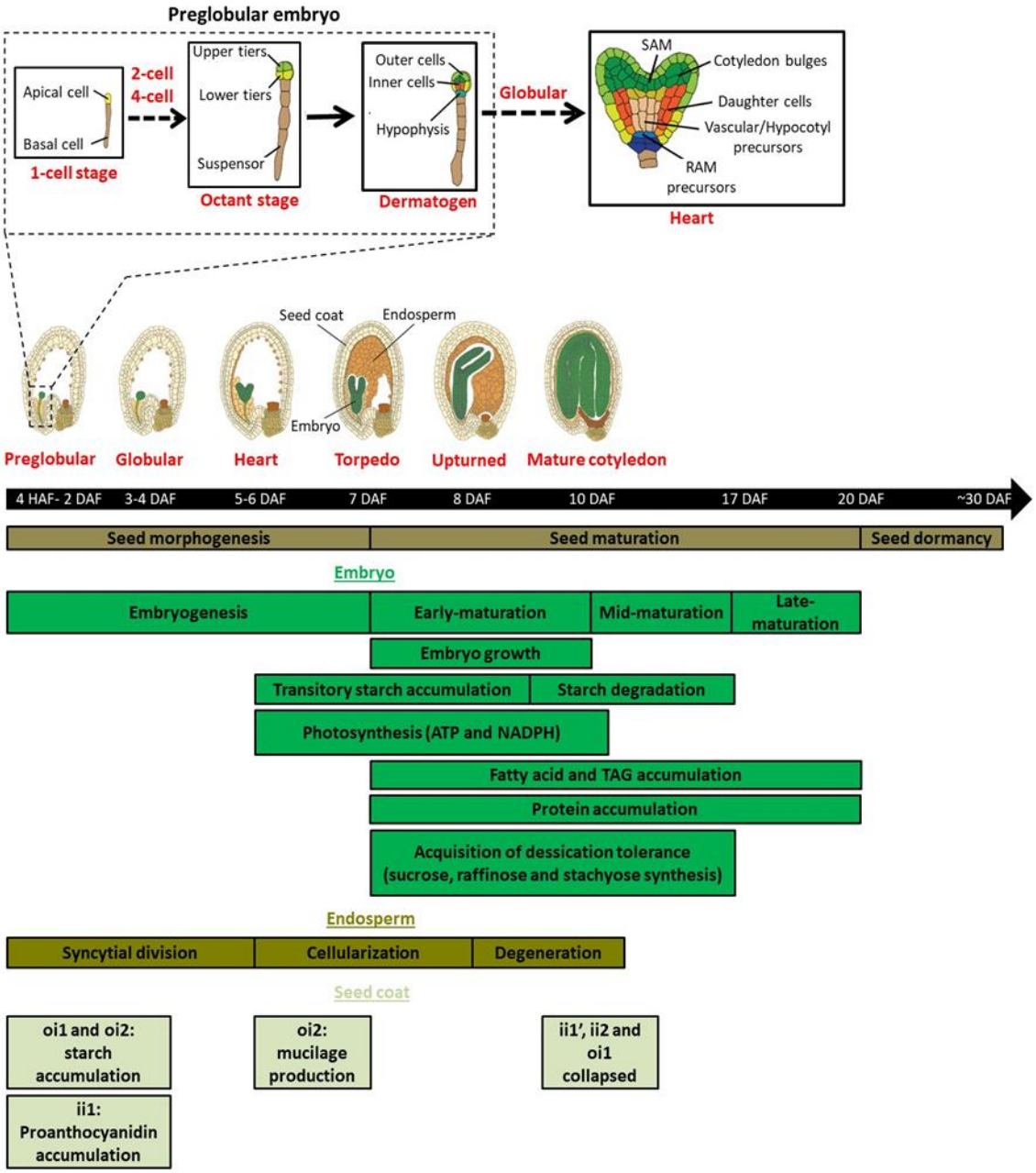

Figure 6. Development of seeds in *Arabidopsis thaliana*. *Physiological processes involved in the development of the embryo, the seed coat and the endosperm are indicated in this figure. These physiological processes are performed several hours (HAF) or days after flowering (DAF). The upper part of the figure shows the different embryonic stages. The first five embryonic stages, including 1-cell, 2-cell, 4-cell, octant and dermatogen, are referred as preglobular. Abbreviations: SAM, shoot apical meristem; RAM, root apical meristem. This figure is adapted from Ten Hove et al. (2015) and Jo et al. (2019).*

The outer and inner cells undergo successive divisions, resulting in the formation of the globular embryonic structure (4 DAF) **(Figure 6)**. The division of the outer cells is involved in the formation of the epidermis precursor, also referred as the protoderm. The division of the inner cells enables the formation of hypocotyl, ground tissue and root vascular precursors. Precursors of the cortex layer and endodermis, known as daughter cells, are formed from the division of the inner cells. In addition, the globular embryonic stage is

characterized by the establishment of the shoot apical meristem and the formation of the cotyledon primordia (Boscá *et al.,* 2011; Ten Hove *et al.,* 2015). The division of cells contained within the globular-shaped embryo results in the formation of the heart embryonic structure (5-6 DAF). The heart stage is characterized by the apparition of two bulges of cotyledon. During the heart stage, the shoot apical meristem becomes visible between cotyledons (Boscá *et al.,* 2011).

1.3.1.2. Development of the endosperm from the fertilized central cell

In *Arabidopsis thaliana*, the role of the endosperm is contributing to the development and growth of the embryo by providing nutrients. The endosperm is derived from the triploid central cell. The development of the endosperm begins with the coenocytic stage, consisting in eight successive syncytial divisions involved in the formation of a large multinucleate cell. These eight divisions are performed from the zygote to the end of the globular embryonic stage. At the end of the coenocytic stage, nuclei are organized in a single layer surrounding a large central vacuole **(Figure 6)** (Brown *et al.*, 1999). Nuclei found within the multinucleate cell are then distributed into several uninucleate cells. This physiological process is known as the cellularization **(Figure 6).** The single nuclei layer is first concerned by the cellularization processes. Membrane is formed around each nucleus, producing a single layer of cells surrounding the central vacuole **(Figure 6)**. Thereafter, successive divisions allow a complete cellularization of the central vacuole between 6 and 8 DAF **(Figure 6)** (Brown *et al.*, 1999; Sorensen *et al.,* 2002). In Arabidopsis, the growth of the embryo from 7 to 10 DAF results in the degeneration of the endosperm in a single and thin layer **(Figure 6)** (Sorensen *et al*., 2002; Olsen, 2004).

1.3.1.3. Development of the integument into seed coat

The development of the integument into seed coat takes place few days after the double fertilization and begins by the growth of the five layers of integument (Haughn and Chaudhury, 2005). The three inner layers of integument are named ii1, ii1' and ii2, while the two outer layers are known as oi1 and oi2 **(Figure 7)**. The expansion of the five layers is then followed by their differentiation, except for ii1' and ii2, resulting in the formation of the seed coat. The differentiation of ii1 enables the accumulation of polyphenol in form of proanthocyanidin. The oxidation of this molecule is responsible in the brown color of mature

seeds (Debeaujon *et al.*, 2003). The ii1 layer is covered by a protective hydrophobic lipid cell wall known as the cuticle. The role of the cuticle consists in promoting seed viability (Beeckman *et al.*, 2000; Ingram and Nawrath, 2017).

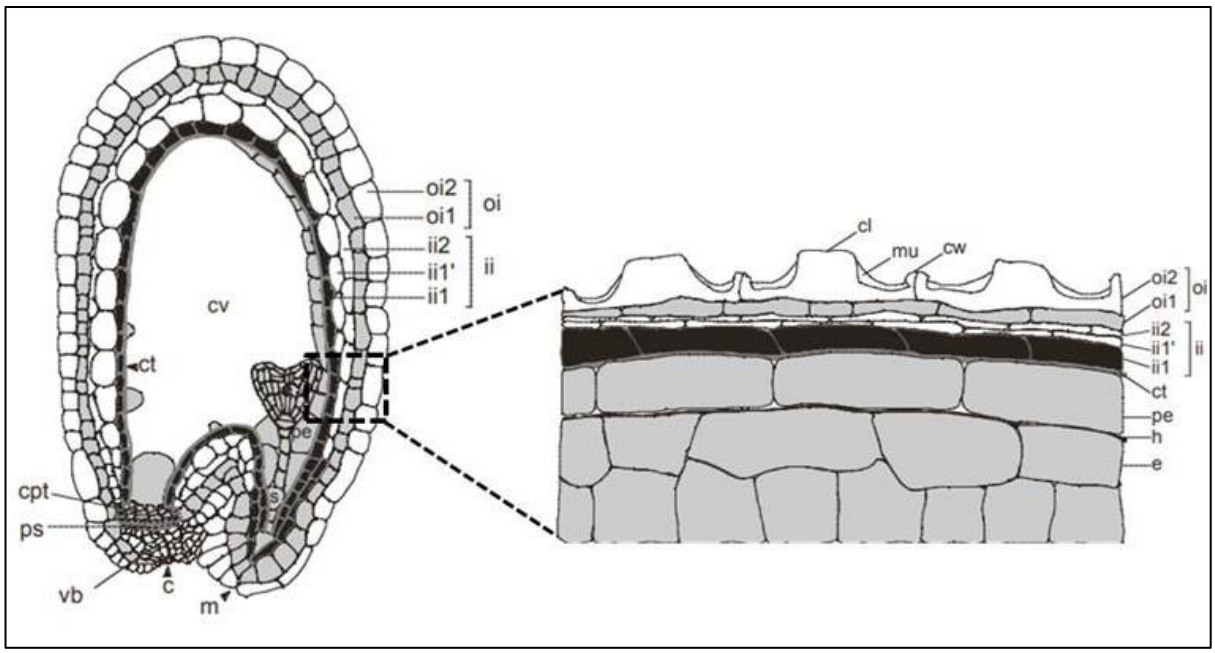

Figure 7. Structure of the seed coat in *Arabidopsis thaliana*. *On the left is represented developing Arabidopsis seed containing embryo with heart shape. In this figure, embryo (e) is connected to the micropylar pole (m) by the suspensor (s). On the right is a zoom of the seed coat structure. Seed coat is composed of three inner (ii1, ii1' and ii2) and two outer layers (oi1 and oi2). Abbreviations: ps, pigment strand; c, chalaza; cpt, chalazal proliferating tissue; vb, vascular bundle; CV, central vacuole; h, hyaline layer; pe, peripheral endosperm; ct, cuticle; cl, columella; mu, mucillage. These figures are adapted from the publication by Debeaujon et al. (2007).*

1.3.2. Seed maturation (from 7 to 30 DAF)

Seed maturation encompasses a set of physiological processes leading to the accumulation of reserve molecules, mainly carbohydrates, proteins and lipids, for germination. This step is also characterized by the establishment of seed dormancy that allows the interruption of the plant life cycle.

Arabidopsis seed maturation is divided into three stages: early- (from 7 to 10 DAF), mid- (from 11 to 16 DAF) and late-maturation (Late M.: from 17 to 20 DAF) **(Figure 6)**. During the early-maturation, embryo grows within seeds. The growth of the embryo is divided into three stages: the torpedo, the upturned-U and the mature cotyledon stages. The torpedo stage (7 DAF) is characterized by the increase in the size of the embryo, which is explained by the growth of the hypocotyl and the two bulges of cotyledon (Mansfield and Briarty, 1991).

During the upturned-U stage (8 DAF), the embryo bends in order to fill the whole

volume of the seed. The final structure of the embryo is reached at 10 DAF during the mature cotyledon stage **(Figure 6)** (Baud *et al.,* 2002). During the early maturation, chlorophyll content is increased in seed embryo and photosynthesis provides ATP and reducing equivalents (NADPH) for FA synthesis **(Figure 6)** (Baud and Lepiniec, 2010). During this stage, sucrose can be directly produced within photosynthetic seeds and starch is transitorily accumulated (Allen *et al.*, 2015). Sucrose, also synthesized by maternal tissues (e.g.: silique walls), can be transported in the phloem toward developing seeds (Fallahi *et al.*, 2008). Starch and sucrose are the source of carbons and energy for later FA synthesis **(Figure 6)** (Baud *et al.*, 2002).

Mid-maturation stage is characterized by the decrease in the amount of starch, while storage lipids and proteins are accumulated within seed cotyledons **(Figure 6)** (Baud *et al.*, 2002). Proteins are synthesized within the embryo, reaching 9 µg of proteins/seed at 20 DAF in Ws ecotype **(Figure 6)** (Baud *et al.*, 2002). An active accumulation of FA is also observed between 10 and 16 DAF **(Figure 6)**. The total amount of FA increases from 2 µg/seed at 10 DAF to 7 µg/seed at 16 DAF, reaching 9 µg/seed at 18 DAF in Ws ecotype (Baud *et al.*, 2002). FA are stored within the cotyledon of the embryo in form of TAG (Baud *et al.*, 2008). During the mid-maturation stage, seeds also undergo degreening processes leading to the decrease of the chlorophyll content in the embryo and the reduction of the photosynthetic capacity of developing seeds from 13 to 16 DAF (Delmas *et al.*, 2013).

Mid- and late-maturation stages are characterized by a sharp decrease of the seed water content. Sucrose, raffinose and stachyose contents increase within seeds simultaneously to the water content loss since these three saccharides confer seed desiccation tolerance (Baud *et al.*, 2002). Given that the content of sucrose is high in dry seed, this disaccharide can be used as a source of energy for supporting early germination (Baud *et al.*, 2002). The mid- and late-maturation stage consists in the establishment of the seed dormancy. Seeds remain in a quiescent state from 20 DAF until their dissemination and subsequent germination.

2. FA and glycerolipid metabolism in *Arabidopsis thaliana*

FA and glycerolipids compositions vary as a consequence of differences in the regulation of the expression of lipid-related genes according to the plant developmental stage (Baud *et al.*, 2009). For instance, during seed maturation, the content of saturated palmitic (C16:0) and stearic (C18:0) acids decreases within embryo from 7 to 11 DAF, resulting in the accumulation of oleic (C18:1), linoleic (C18:2), linolenic (C18:3) and eicosenoic (C20:1) acids in later developmental stage (Baud *et al.*, 2002). Another example of differences between developmental stages concerns TAG content in developing seeds and seedlings. TAG is accumulated, in form of lipid droplets, within cotyledons of developing seeds and then mobilized into free FA (FFA) during early germination (Baud *et al.*, 2002; Graham, 2008). In order to support early germination, FFA are catabolized by β-oxidation providing molecules of acetyl-CoA and reducing equivalents in form of NADH. The glyoxylate cycle and the gluconeogenesis pathway are then involved in the synthesis of sucrose from the acetyl-CoA generated by β-oxidation **(Figure 8)** (Graham, 2008). Unlike maturing seeds, developing seedlings are rather involved in the synthesis of membrane glycerolipids (phospholipids, galactolipids and sulfolipid) than storage lipids (Ohlrogge and Browse, 1995; Shrestha *et al.*, 2016), leading to a decrease of TAG content and increase of membrane glycerolipids within seedling cotyledons.

The synthesis of storage and membrane glycerolipids **(Step 4, Figure 8)** is preceded by the catabolism of glucose by glycolysis and pentose phosphate pathway **(Step 1, Figure 8)** and the intraplastidial synthesis of the *de novo* FA **(Step 2, Figure 8)**.

Glucose is provided either by the degradation of starch, transiently accumulated at the beginning of seed maturation, or by the catabolism of sucrose, synthesized in maternal tissues (e.g.: silique walls) and transported in the phloem toward seeds or directly produced within seeds by photosynthesis during the early-maturation **(Step 1, Figure 8)** (Baud *et al.*, 2002; Schwender *et al.*, 2003). Glycolysis and pentose phosphate pathways (PPP) take place within plastids and cytosol. These metabolic pathways are distributed between both cell locations and several glycolytic and PPP intermediates are exchanged between cytosol and plastids **(Step 1, Figure 8)** (Schwender *et al.*, 2003; Kruger and Schaewen, 2003). Glycolysis and PPP provide energy (ATP), reducing equivalents (NADH and NADPH) and carbon skeletons necessary for the intraplastidial *de novo* FA synthesis **(Step 2, Figure 8)** (Schwender *et al.*,

2003; Hutching *et al.*, 2004). The main products of this anabolic process are the saturated C16:0 and C18:0 FA esterified to the acyl carrier protein (ACP) (C16:0-ACP and C18:0-ACP). Both saturated FA undergo modifications by the addition of double bonds, resulting in the synthesis of monounsaturated C16:1-ACP and C18:1-ACP. Once synthesized, saturated and monounsaturated FA are esterified to coenzyme-A (CoA) before leaving plastids. Acyl-CoA generated are subsequently exported to the endoplasmic reticulum (ER). An acyl-CoA pool, made of newly synthesized FA, is formed within the ER **(Step 3, Figure 8)**. Acyl-CoA can be further elongated allowing the accumulation of very long chain FA (VLCFA) within the acyl-CoA pool **(Step 3, Figure 8)** (Li-Beisson *et al.*, 2013).

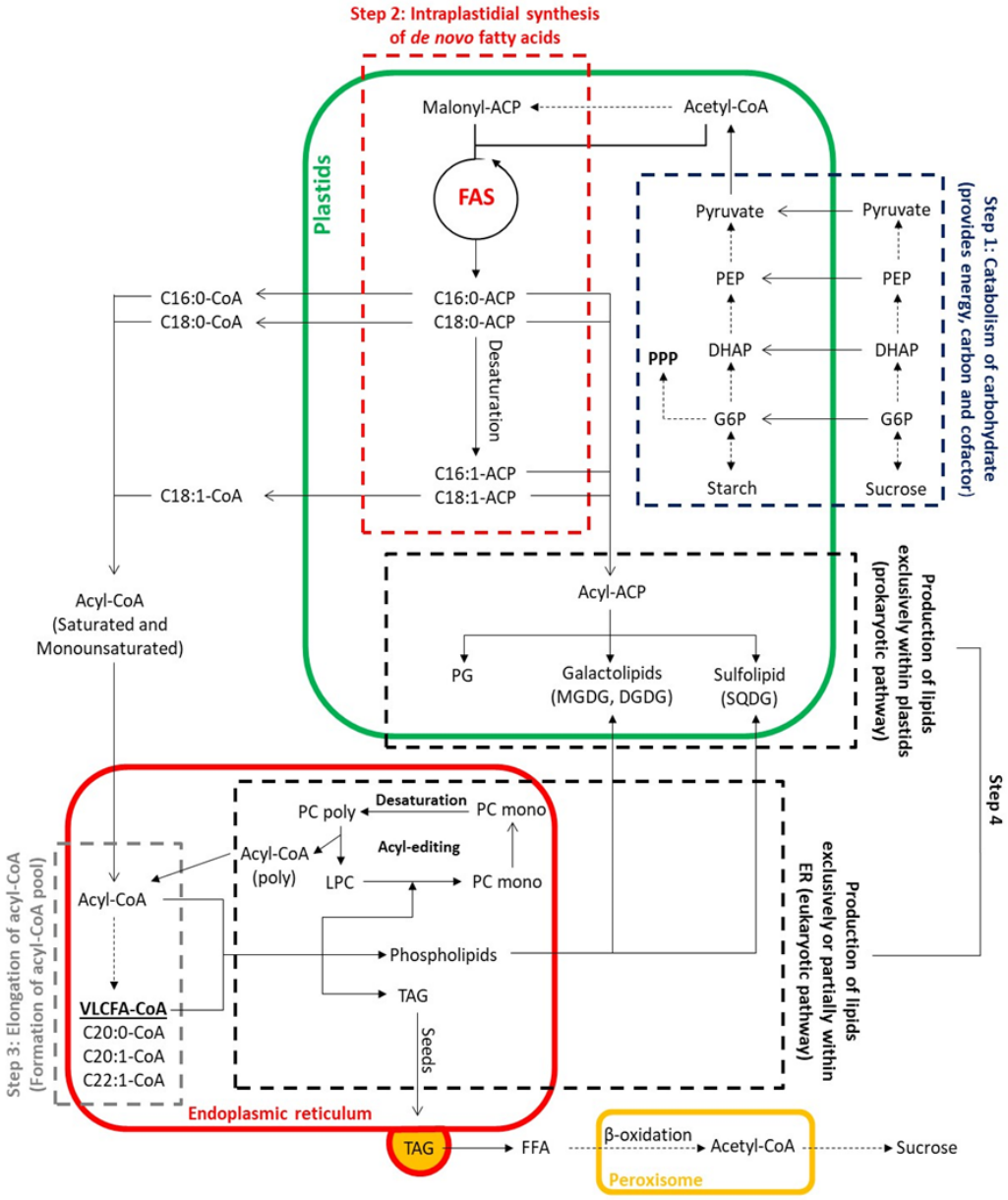

Figure 8. Simplified representation of glycerolipid metabolism in plants. *The synthesis of glycerolipids is divided into four steps. The first step (purple-dotted frame) consists in the catabolism of carbohydrate (glycolysis and pentose phosphate pathway; PPP) within cytosol and plastids for providing energy, reducing equivalents and carbon skeletons. The second step (red-dotted frame) consists in the synthesis of FA within plastids. Step 3 (grey-dotted frame), elongation of FA into very long chain FA (VLCFA-CoA) within the ER. Step 4 (black-dotted frame), synthesis of glycerolipids within the ER by the eukaryotic pathway (phospholipids, triacylglycerol, sulfolipids and galactolipids) or within plastids by the prokaryotic pathway. During germination, acetyl-CoA generated by β-oxidation generates the carbon for sucrose synthesis. Adapted from Li-Beisson et al. (2013).*

The incorporation of FA and VLCFA to glycerol backbones represents the initial step for the *de novo* glycerolipid synthesis in the ER or plastids **(Step 4, Figure 8)**. In the eukaryotic pathway, the synthesis of glycerolipids is located within the ER (Li-Beisson *et al.*, 2013). This pathway encompasses a set of enzymatic reactions involved in the synthesis of TAG (Baud *et al.*, 2002) and membrane phospholipids like phosphatidylinositol (PI), phosphatidylserine (PS), phosphatidylethanolamine (PE) and phosphatidylcholine (PC) (Ohlrogge and Browse, 1995). Most of glycerolipids synthesized by the eukaryotic pathway are characterized by the presence of stearic (C18:0) or oleic (C18:1) acids esterified with the second carbon (*sn-2*) of the glycerol backbone (Li-Beisson *et al.*, 2013). Although the *de novo* FA synthesis together with the FA elongation generate an acyl-CoA pool only made of saturated and mono-unsaturated FA and VLCFA, polyunsaturated FA moieties glycerolipids can also be produced in the ER. The acyl editing is a physiological process that allows the synthesis of polyunsaturated glycerolipids within the ER (Bates *et al.*, 2009). In the eukaryotic pathway, the *de novo* glycerolipid synthesis can be involved in the synthesis of saturated and monounsaturated FA moieties PC. The acyl editing comprises three main enzymatic reactions involving this membrane glycerolipids, including the unsaturation of FA moieties PC, the deacylation of PC into lyso-PC (LPC) and the reacylation of LPC into PC. The first reaction enables the introduction of double bonds, unsaturation, to FA on *sn-2* position of the PC glycerol backbones generating unsaturated FA, including C18:2 and C18:3 (Browse *et al.*, 1993; Okuley *et al.*, 1994). The second and third reactions consists in the deacylation of PC and reacylation of the resulting LPC, allowing the exchange of FA between PC species and the acyl-CoA pool **(Step 4, Figure 8)**. The deacylation of polyunsaturated FA moieties PC into LPC releases polyunsaturated FA in order to be accumulated within the acyl-CoA pool. Polyunsaturated FA accumulated in the acyl-CoA pool is then esterified to glycerol backbones, generating other polyunsaturated glycerolipids, including TAG and membrane glycerolipids. The reacylation of LPC by monounsaturated FA results in the synthesis of monounsaturated FA moieties PC that can undergo unsaturation and deacylation for further accumulation of

polyunsaturated FA in the acyl-CoA pool and production of polyunsaturated FA moieties glycerolipids (Bates *et al.*, 2012; Menard *et al.*, 2018).

Phospholipids synthetized in the ER can be exported to plastids. The chemical structure of these membrane phospholipids can be modified within plastids, leading to the synthesis of other membrane glycerolipids, including sulfolipid (sulfoquinovosyldiacylglycerol; SQDG) and galactolipids (monogalactosyldiacylglycerol; MGDG and digalactosyldiacylglycerol; DGDG) especially within photosynthetic tissues (e.g.: leaves, seedling cotyledons, etc) **(Step 4, Figure 8)**. In plants, the role of galactolipids consists in maintaining the integrity of thylakoid membranes within plastids for the establishment of the photosynthesis (Kobayashi *et al.*, 2016a). In the prokaryotic pathway, phospholipids (phosphatidylglycerol; PG), sulfolipid and galactolipids are synthesized within plastids **(Step 4, Figure 8)**. Glycerolipids produced by the procaryotic pathway are characterized by the presence of palmitic acid (C16:0) esterified to the second carbon of the glycerol backbone (Li-Beisson *et al.*, 2013).

2.1. FA synthesis

2.1.1. Source of carbon and energy for the *de novo* FA synthesis

2.1.1.1. Catabolism of carbohydrate

Glycolysis and PPP regroup a set of enzymatic reactions involved in the catabolism of glucose. Glucose can be provided from the enzymatic hydrolysis of starch and sucrose (**Figure 9**) (Sauter, 2000; Schwender *et al.*, 2003). Starch and sucrose are both carbohydrates produced in autotrophic (e.g.: leaves) and mixotrophic (e.g.: green seeds) tissues by the photosynthesis (Allen *et al.*, 2015).

Photosynthesis is divided into two parts. The first part encompasses reactions dependent to the presence of light (Johnson, 2016). Reactions of the first part are performed through the action of a photosynthetic electron and proton transfer chain associated to the thylakoid membrane and composed of several protein complexes, including two photosystems (PSII and PSI), cytochrome b_6f, plastoquinone (PQ), ferredoxin, ferredoxin-$NADP^+$ reductase and ATP synthase (Johnson, 2016). The first part of the photosynthesis enables the synthesis of energy (ATP) and reducing equivalent (NADPH) required for later FA synthesis or for the conversion of CO_2 into carbohydrate by the Calvin Cycle during the second part of the photosynthesis **(Figure 9)** (Baud and Lepiniec, 2010; Johnson, 2016). The first part

of the photosynthesis begins by the entrance of CO_2 and H_2O within photosynthetic tissues. These molecules can also be produced through diverse metabolic activities. The action of light on the second photosystem of the transfer chain (PSII) allows the reduction of H_2O into O_2 (Johnson, 2016). This reaction is coupled with the transfer of proton in the thylakoid lumen, creating a proton gradient on either side of the thylakoid membrane (Johnson, 2016). Proton is transported from the lumen to the stroma through the ATP synthase, converting ADP into ATP. The reduction of H_2O into O_2 is also coupled to the transport of electron toward the plastoquinone (PQ) cofactor (Johnson, 2016). Electron released by the reduction of H_2O into O_2 is accepted by PQ, reducing this molecule into plastoquinol (PQH_2). Cytochrome b_6f is then involved in the transfer of electron from PQH_2 to a lumen protein referred as the plastocyanin. The action of light on the first photosystem (PSI) enables the transfer of electron from the reduced form of the lumen plastocyanin to the ferredoxin found in the stroma. Ferredoxin is then used by the ferredoxin-$NADP^+$ reductase, catalysing the reduction of $NADP^+$ into NADPH (Johnson, 2016). During the second part of the photosynthesis, ATP and NADPH are used by the Calvin cycle for converting 3 CO_2 into one molecule of glucose. The Calvin cycle can be divided into four phases, including the carbon fixation, the phosphorylation/reduction, the carbohydrate synthesis and the regeneration phases. The first phase, catalysed by the ribulose-1,5-bisphosphate carboxylase/oxygenase (Rubisco; EC 4.1.1.39), enables the fixation of three molecules of CO_2 into three molecules of ribulose-1,5-bisphosphate, generating three unstable six-carbon molecules (Allen *et al.*, 2009; Johnson, 2016). Each of these three unstable molecules is immediately hydrolysed into two molecules of 3-phosphoglycerate. A total of six molecules of 3-phosphoglycerate are produced after this first phase. The second phase uses ATP and NADPH for the conversion of six molecules of 3-phosphoglycerate into six molecules of glyceraldehyde-3-phosphate. The third phase allows the conversion of one molecule of glyceraldehyde-3-phosphate into glucose-6-phosphate (G6P) by the gluconeogenesis, the reverse path of the glycolysis. During the regeneration phase, the five other molecules of glyceraldehyde-3-phosphate are converted into three molecules of ribulose-1,5-bisphosphate through the combined action of PPP and gluconeogenesis enzymes.

Once synthesized, G6P is converted into glucose-1-phosphate (G1P) through the action of the phosphoglucomutase (EC 5.4.2.2). G1P can be converted into ADP-glucose. The synthesis of glucose esterified with ADP is followed by the association of this molecule with

other ADP-glucose generating starch within the embryo of green seeds, as well as in leaves autotrophic cells. Starch is a polysaccharide composed of linear and ramified chains. The linear chain, also known as amylose, is constituted of several molecules of glucose connected together by α-1,4 linkages. Each ramified chain, referred as amylopectin and consisting of α-1,4-linked glucopyranose, are connected to the linear chain by α-1,6 linkage (Martin and Smith, 1995). G1P can be esterified to uridine triphosphate (UTP) into UDP-glucose by UDP-glucose pyrophosphorylase (EC 2.7.7.9). Sucrose phosphate synthase (EC 2.4.1.14) catalyses the association of UDP-glucose with fructose-6-phosphate (F6P) for the synthesis of sucrose phosphate. Sucrose phosphate is finally dephosphorylated by sucrose phosphate phosphatase (EC 3.1.3.24), resulting in the synthesis of sucrose within the embryo of green seeds, including Arabidopsis seeds, and in the autotrophic cells constituting leaves (Granot and Stein, 2019).

Once synthesized by photosynthesis, maternal sucrose can be secreted by the autotrophic cells constituting leaves and transported in the phloem toward sink heterotrophic tissues, including roots. Sucrose synthesized by cells composing silique walls are also transported in the phloem toward heterotrophic or mixotrophic sink tissues of developing seeds. In Arabidopsis seeds, sucrose has thus maternal and embryonic origins. During the early embryogenesis, maternal sucrose undergoes enzymatic hydrolysis in the seed coat, releasing glucose and fructose that can be used as source of carbon and energy for the embryo growth (Fallahi *et al.*, 2008). During seed maturation, maternal sucrose directly enters the embryo in order to be hydrolysed into glucose and fructose, both molecules that can be used as source of carbons and energy for the intraplastidial *de novo* FA synthesis (Fallahi *et al.*, 2008).

The early-maturation stage is characterized by the accumulation of starch within plastids of developing seeds. During the mid-maturation stage, starch is hydrolysed producing glucose-1-phosphate (G1P) by the action of α-amylase (EC 3.2.1.1), debranching enzyme and starch phosphorylase (EC 2.7.1.1) (Sauter, 2000). During the embryogenesis and seed maturation, G1P can be obtained, together with fructose, by the combined action of sucrose synthase (EC 2.4.1.13) and UDP-glucose pyrophosphorylase (EC 2.7.7.9) on sucrose delivered by maternal tissues, therefore converging starch and sucrose hydrolysis in the synthesis of this metabolite (Granot and Stein, 2019). The phosphate group of G1P is transferred from the first to the sixth carbon of the glucose by the phosphoglucomutase (PGM; EC 2.7.5.1), resulting in the production of glucose-6-phosphate (G6P), a precursor interconnecting the glycolysis to

PPP (Schwender *et al.*, 2003). Sucrose can also be hydrolysed by invertase (EC 3.2.1.26), releasing glucose and fructose **(Figure 9)** (Schwender *et al.*, 2003). Glucose is then phosphorylated into G6P by hexokinase (EC 2.7.1.1), the first enzyme of the glycolysis pathway **(Figure 9)** (Karve *et al.*, 2008).

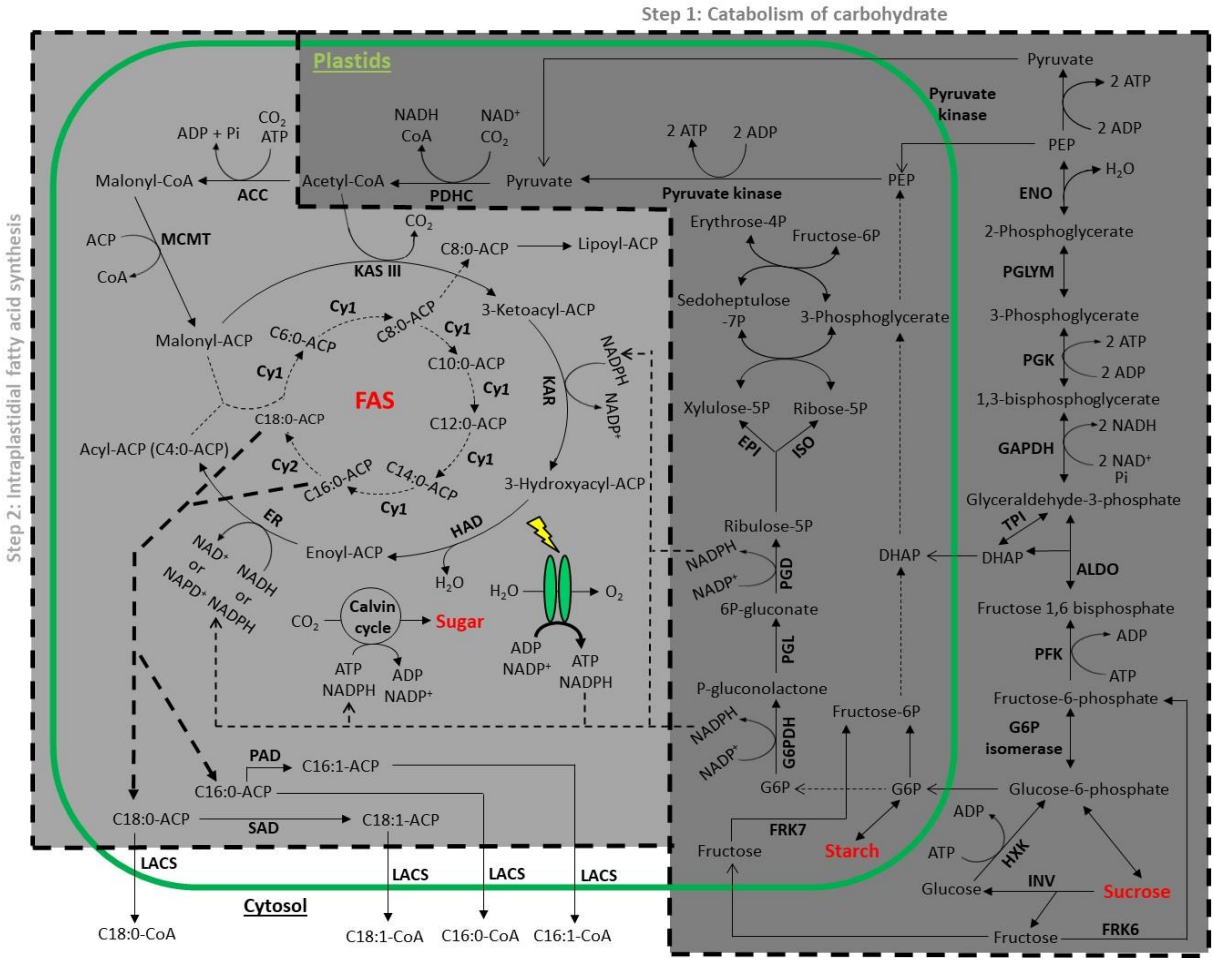

Figure 9. Catabolism of sucrose and intraplastidial synthesis of de novo FA. *Step 1 illustrates the enzymatic hydrolysis of sucrose by invertase (INV), the phosphorylation of fructose by the fructokinase (FRK) and the nine reversible (double arrows) or irreversible (simple arrows) reactions of the glycolysis, catalysed by the hexokinase (HXK), glucose-6-phosphate isomerase (G6PI), phosphofructokinase (PFK), aldolase (ALDO), triose phosphate isomerase (TPI), glyceraldehyde-3-phosphate dehydrogenase (GAPDH), phosphoglycerate kinase (PGK), phosphoglycerate mutase (PGLYM), enolase (ENO) and pyruvate kinase. Pentose phosphate pathway is also represented in step 1 (G6PDH, glucose-6-phosphate dehydrogenase; PGL, 6P-gluconolactonase; PGD, 6P-gluconate dehydrogenase; ISO, isomerase; EPI, epimerase). Glycolysis is followed by the decarboxylation of pyruvate into acetyl-CoA (CoA: coenzyme-A) by the pyruvate dehydrogenase complex (PDHC). Malonyl-CoA is synthesized by the acetyl-CoA carboxylase (ACC) and converted into malonyl-ACP (ACP: acyl carrier protein) by malonyl-CoA: ACP transacylase (MCMT). FA synthase (FAS) complex enables the synthesis of FA by the action of several elongation cycles, involving the 3-ketoacyl-ACP synthase (KAS), 3-ketoacyl-ACP reductase (KAR), hydroxyacyl-ACP dehydratase (HAD) and enoyl-ACP reductase (ER). Cy1 and Cy2 are subsequent elongation cycles in which the first enzymatic reaction is catalysed by KAS I and KAS II, respectively. Once produced, C18:0- and C16:0-ACP are converted into C18:1- and C16:1-ACP by Δ9 stearoyl-ACP desaturase (SAD) and Δ9 palmitoyl-ACP desaturase (PAD), respectively. Acyl-ACP is converted into acyl-CoA by the long-chain acyl-CoA synthetase (LACS). Adapted from Li-Beisson et al. (2013) and Andriotis and Smith (2019).*

In glycolysis, G6P synthesis is followed by nine other glycolytic reactions until the production of the pyruvate **(Figure 9)**. In plants, glycolysis takes place within plastids and cytosol since glycolytic enzymes, including the phosphoglycerate mutase (PGLYM; EC 5.4.2.11), enolase (ENO; EC 4.2.1.11), fructokinase (FRK; EC 2.7.1.4) and pyruvate kinase (PK; EC 2.7.1.40), are found in both cellular locations. The isoform ENO1 is located within plastids, while the isoform ENO2 and ENO3 are found in the cytosol (Prabhakar et *al.*, 2009; Andriotis *et al.*, 2010). The isoform PGLYM1 has been shown to be located within plastids (Andriotis *et al.*, 2010). FRK6 and FRK7 are involved in the phosphorylation of fructose into fructose-6-phosphate (F6P), an intermediate of the glycolysis. FRK6 has a cytosolic location, while FRK7 is found within plastids (Riggs *et al.*, 2017). Several studies have been performed for studying the potential interconnection between the glycolysis and the intraplastidial *de novo* FA synthesis. The alteration of WRINKLED, one of the transcription factors involved in seed maturation, simultaneously decreases seed oil content by 80 % and the activity of five glycolytic enzymes, including FRK, aldolase, PGLYM, ENO and PK (Focks and Benning, 1998). The alteration of the PGM activity, the enzyme involved in the synthesis of the glycolytic intermediate G6P, reduces the seed oil content by 40 % (Periappuram *et al.*, 2000). Glycolytic enzymes, including the FRK, the plastidial phosphoglycerate kinase (PGK, EC 2.7.2.3) and ENO, are upregulated in transgenic sunflower containing high oil seed content (Hajduch *et al.*, 2007). The reduction in the activity of the first and second isoform of the plastidial PK decreases the seed oil content by 60 % in *pkp1* and FA content by 50 and 70 % in *pkp2* and *pkp1 pkp2*, respectively (Andre *et al.*, 2007; Baud *et al.*, 2007a). In addition, the alteration of the plastidial PK results in the modification of the FA composition in seeds (Baud *et al.*, 2007a). The inactivation of the plastidial acetyl-CoA carboxylase, one of the enzymatic complexes involved in the intraplastidial *de novo* FA synthesis, results in the 25 % decrease of the seed oil content and the downregulation of the plastidial glycolytic enzymes, including the plastidial PGM, PGLYM and aldolase (Chen *et al.*, 2009). These findings have shown that the alteration of the glycolytic flux affects FA and oil content in seeds, therefore identifying glycolysis as a metabolic pathway that are interconnected with the intraplastidial *de novo* FA synthesis. The irreversible conversion of the pyruvate into acetyl-CoA allows the interconnection between glycolysis and FA synthesis **(Figure 9)** (Oliver *et al.*, 2009). Although glycolysis is required for the intraplastidial *de novo* FA synthesis, seed oil and FA content has not revealed to be significantly decreased when the expression of the plastidial *ENO1*, *PGLYM1* and *FRK7* is

altered in the *eno1*, *pglym1* and *frk7* simple mutants (Andriotis *et al.*, 2010; Stein *et al.*, 2017). Differences in FA profile was, however, observed in the *frk6 frk7* double mutant (Stein *et al.*, 2017). FA synthesis has been shown to be affected only when the cytosolic and plastidial glycolytic fluxes are both altered in plants. The alteration of the plastidial glycolytic flux due to the decrease in the activity of the plastidial ENO1, PGLYM1 and FRK7 can be rescued through the import by plastids of cytosolic intermediates synthesized downstream of reactions catalyzed by the cytosolic ENO, PGLYM and FRK (Andriotis *et al.*, 2010; Stein *et al.*, 2017). Cytosolic intermediates of the glycolysis, including G6P, dihydroxyacetone phosphate (DHAP), phosphoenolpyruvate (PEP) and pyruvate, can be imported by plastids through the action of transporters, therefore showing an interconnection between the plastidial and cytosolic glycolysis. However, most of the pyruvate required for the FA synthesis has been shown to be rather produced within plastids than imported by plastids (Schwender *et al.*, 2003; Troncoso-Ponce *et al.*, 2011). In plants, the interconnection between cytosolic and plastidial glycolysis is crucial for ensuring the intraplastidial *de novo* FA synthesis since the alteration of both cytosolic and plastidial glycolysis considerably affects the FA profile (Stein *et al.*, 2017).

The synthesis of G6P can be followed by PPP. This metabolic pathway is divided into oxidative and non-oxidative phases. The oxidative PPP, composed of three enzymatic reactions, allows the conversion of G6P into ribulose-5-phosphate. The first and third reactions of the oxidative PPP is coupled with the reduction of $NADP^+$ into NADPH **(Figure 9)** (Andriotis and Smith, 2019). The role of the oxidative part of PPP is providing reducing equivalents (NADPH) required for the intraplastidial *de novo* FA synthesis (Hutching *et al.*, 2005). The non-oxidative part of PPP results in the synthesis of glycolytic intermediates, including fructose-6-phosphate and glyceraldehyde-3-phosphate. The non-oxidative PPP interconnects the oxidative PPP with the glycolysis.

Glycolysis, together with the PPP and photosynthesis, enables the production of energy (ATP), carbon skeletons (pyruvate) and reducing equivalents in form of NADH and NADPH required for the *de novo* FA synthesis **(Figure 9)**. Once synthesized from pyruvate, acetyl-CoA is converted into malonyl-CoA by the plastidial ACC (Salie and Thelen, 2016). The first committed step in the intraplastidial *de novo* FA synthesis catalyzed by the plastidial ACC requires the hydrolysis of the ATP into ADP and inorganic phosphate, therefore providing energy for the conversion of the acetyl-CoA to malonyl-CoA. The malonyl group, once

esterified to the ACP (malonyl-ACP), and the acetyl-CoA are both carbon sources for the intraplastidial FA synthesis. The condensation of one molecule of acetyl-CoA with several molecules of malonyl-ACP results in the synthesis of an oxidized carbon chain, known as the ketoacyl-ACP. The reduction of this carbon chain coupled with the oxidation of NADH or NADPH generates FA (Li-Beisson *et al.*, 2013).

2.1.1.2. Synthesis of acetyl-CoA

Acetyl-CoA is the source of carbon for the *de novo* FA synthesis. This molecule can be produced from acetate by the acetyl-CoA synthetase (ACS; EC 6.2.1.1) or by the oxidative decarboxylation of pyruvate through the activity of the pyruvate dehydrogenase complex (PDHC) (Johnston *et al.*, 1997; Oliver *et al*., 2009). The intraplastidial *de novo* FA synthesis is interconnected with the glycolysis pathway through the action of PDHC, ensuring a rapid and stable supply of acetyl-CoA **(Figure 9)** (Oliver *et al.*, 2009). The PDHC complex is composed of three components: E1, E2 and E3 (Johnston *et al.*, 1997). The component E1, corresponding to the pyruvate dehydrogenase (EC 1.2.4.1), allows the fixation of the pyruvate to a thiamine pyrophosphate cofactor, resulting in the decarboxylation of pyruvate into acetyl group (Johnston *et al.*, 1997). Once produced by E1, the acetyl group is transferred to the oxidized form of the lipoamide cofactor of the E2 component. This component, known as the dihydrolipoamide acetyltransferase (EC 2.3.1.12), enables the esterification of the acetyl group with coenzyme-A (CoA). This results in the formation and release of acetyl-CoA from the E2 component. At this stage, the lipoamide cofactor of the E2 component is found in a reduced state (Lin *et al.*, 2003). The catalytic cycle of the PDHC is completed once the lipoamide cofactor is re-oxidized by the E3 component, known as the dihydrolipoamide dehydrogenase (EC 1.8.1.4) (Drea *et al.*, 2001).

2.1.2. Intraplastidial *de novo* FA synthesis

Once synthesized by the PDHC, the acetyl-CoA is converted into malonyl-CoA by the ACC. This enzymatic complex is divided into two functional enzymes, the biotin carboxylase (BC; EC 6.3.4.14) and the carboxyltransferase (CT; EC 6.4.1.2), and a single protein containing a biotin prosthetic group known as the biotin carboxyl carrier protein (BCCP; EC 6.4.1.2). BC transfers CO_2 from bicarbonate to the biotin prosthetic group of BCCP. Once carboxylated, the biotin prosthetic group of BCCP moves from BC to CT. CT transfers CO_2 from

the carboxylated biotin to the acetyl-CoA, resulting in the carboxylation of the acetyl-CoA into malonyl-CoA (Ohlrogge and Browse, 1995; Harwood, 1996). Two isoforms of the ACC can be distinguished in the nature, including the heteromeric and homomeric forms. In the homomeric form, BCCP and both CT and BC enzymes are located in a single polypeptide. This ACC isoform is involved in the cytosolic *de novo* FA synthesis in animal and fungi cells and the intraplastidial *de novo* FA synthesis in some monocot species (e.g.: graminaceous plants). The homomeric form of the ACC is also found in the cytosol of all plant species. The cytosolic ACC enables the synthesis of malonyl-CoA, therefore providing carbons to FA during its elongation in the ER (Salie and Thelen, 2016). The heteromeric form of the ACC corresponds to a multi-enzymatic complex composed of BCCP, CT and BC subunits. This ACC isoform is found in prokaryotic cells, as well as within plastids of several dicot plant species (Salie and Thelen, 2016). In plants, the first committed step of the intraplastidial *de novo* FA synthesis consists in the carboxylation of the acetyl-CoA through the activity of the plastidial ACC **(Figure 9)** (Thelen *et al.*, 2002). The plastidial ACC is an ATP-dependent enzyme or enzymatic complex that is positively and diurnally regulated by light in a light/dark cycle. Light also enhances the interaction of the CARBOXYLTRANSFERASE INTERACTOR (CTI) with the CT subunit, therefore decreasing the activity of the heteromeric ACC. The dual effect of light on the heteromeric ACC activity is crucial for ensuring a tight control of the intraplastidial *de novo* FA synthesis in many plant species, including *Arabidopsis thaliana* (Ye *et al.*, 2020).

In order to initiate the synthesis of FA by the multi-enzymatic FA synthase (FAS) complex, malonyl-CoA is first converted into malonyl-ACP by the malonyl-CoA: ACP transacylase (MCMT; EC 2.3.1.39) **(Figure 9)** (Lessire and Stumpf, 1983). Several elongation cycles are then performed by the FAS enzymatic complex, resulting in the elongation of acetyl-CoA into palmitic (C16:0) and stearic (C18:0) acids esterified to ACP (C16:0-ACP and C18:0-ACP) (Brown *et al.*, 2006). During the first elongation cycle, acetyl-CoA provides two carbons to malonyl-ACP, generating butyryl-ACP (C4:0-ACP) **(Figure 9)**. Malonyl-ACP then enables the extension of the resulting acyl-ACP by the addition of two more carbons in each subsequent cycle. The second elongation cycle consists in the addition of two carbons to C4:0-ACP in order to produce hexanoyl-ACP (C6:0-ACP), while the third elongation cycle extends C6:0-ACP to octanoyl-ACP (C8:0-ACP) (Li-Beisson *et al.*, 2013). The synthesis of C16:0-ACP and C18:0-ACP is thus performed in a total of seven and eight elongation cycles, respectively **(Figure 9)**. The

octanoyl-ACP, produced after the end of the third elongation cycle, is involved in the synthesis of the lipoic acid co-factor that is associated to the E2 component of PDHC (Wada *et al.*, 1997).

Each elongation cycle is divided into four reactions catalysed by enzymes belonging to the FAS complex. The first reaction involves the 3-ketoacyl-ACP synthase (KAS) (EC 2.3.1.41) **(Figure 9)**. This enzyme catalyses the condensation of malonyl-ACP with acetyl-CoA or with several acyl-ACP molecules containing up to 16 carbons. Three KAS isoforms have been identified in plants. During the first elongation cycle, the isoform KAS III catalyzes the initial condensation of the acetyl-CoA with malonyl-ACP **(Figure 9)** (Jaworski et al, 1989). The second elongation cycle begins with the condensation between malonyl-ACP and C4:0-ACP by the isoform KAS I **(Figure 9)**. The first reaction of each subsequent elongation cycle is also catalysed by KAS I until the production of 16-carbon 3-ketoacyl-ACP (Shimakata and Stumpf, 1982). The first reaction of the eighth elongation cycle is performed by the isoform KAS II **(Figure 9)**. This isoform catalyses the condensation between the malonyl-ACP and C16:0-ACP, yielding 18-carbon 3-ketoacyl-ACP (Pidkowich *et al.*, 2007).

The second reaction of each elongation cycle consists in the reduction of 3-ketoacyl-ACP to 3-hydroxyacyl-ACP coupled to the oxidation of the NADPH produced by PPP and photosynthesis **(Figure 9)**. This reaction is catalysed by the 3-ketoacyl-ACP reductase (KAR; EC 1.1.1.100) (Sheldon *et al.*, 1990). During the third reaction, 3-hydroxyacyl-ACP is dehydrated into enoyl-ACP by the hydroxyacyl-ACP dehydratase (HAD; EC 4.2.1.17) (Olhrogge and Browse, 1995; Brown et al, 2008). The enoyl-ACP reductase (EC 1.3.1.9) catalyses the reduction of the enoyl-ACP into acyl-ACP containing from four (C4:0-ACP) up to 18 (C18:0-ACP) carbons depending on the number of elongation cycles that have been performed by the FAS complex **(Figure 9)** (Mou *et al.*, 2000). The reduction of enoyl-ACP is performed by the transfer of electrons either from NADH or NADPH, produced by the glycolysis, PPP and photosynthesis, to enoyl-ACP (Li-Beisson *et al.*, 2013).

Elongation cycles are followed by the introduction of double bonds at carbon 9 by the Δ^9 acyl-ACP desaturases (AAD) (EC 1.14.99.6). Several AAD have been identified, including Δ^9 stearoyl-ACP desaturase (SAD) and Δ^9 palmitoyl-ACP desaturase (PAD) **(Figure 9)**. SAD activity consists in the addition of double bonds to C18:0-ACP generating ω9 oleoyl-ACP (C18:1-ACP) (Jaworski and Stumpf, 1974). PAD synthetizes ω7 C16:1-ACP (palmitoleic-ACP) mainly in the endosperm although the content remains weak (Troncoso-Ponce *et al.*, 2016).

2.1.3. FA elongation

Once produced, saturated (C16:0 and C18:0) and mono-unsaturated (C16:1 and C18:1) FA can be exported from the plastids to the ER in order to be elongated. The conversion of acyl-ACP (C16:0-ACP, C16:1-ACP, C18:0-ACP and C18:1-ACP) into acyl-CoA (C16:0-CoA, C16:1-CoA, C18:0-CoA and C18:1-CoA) by the long-chain acyl-CoA synthetase (LACS; EC 6.2.1.3) is first required for exporting FA (Shockey *et al.*, 2002). Once exported to the ER, several elongation cycles are performed by enzymes belonging to the FA elongation (FAE) complex, extending C16:0-CoA, C16:1-CoA, C18:0-CoA and C18:1-CoA into C20:0-CoA (eicosanoic-CoA), C20:1-CoA (eicosenoic-CoA), C22:0-CoA (docosanoic-CoA), C22:1-CoA (docosenoic-CoA) and C24:0-CoA (tetracosanoic-CoA) (James *et al.*, 1995; Millar and Kunst, 1997). C20:0-CoA, C20:1-CoA, C22:0-CoA, C22:1-CoA and C24:0-CoA are also referred as very long chain FA (VLCFA). During the maturation of Arabidopsis seeds, the intraplastidial *de novo* FA synthesis following by their elongation within the ER results in the formation of an acyl-CoA pool made of C16:0-CoA, C16:1-CoA, C18:0-CoA, C18:1-CoA, C20:0-CoA, C20:1-CoA, C22:0-CoA, C22:1-CoA and C24:0-CoA **(Figure 10)**. Each elongation cycle enables the addition of two carbons, provided by the malonyl-CoA, to the acyl-CoA. The synthesis of the malonyl-CoA takes places in the cytosol and consists in the carboxylation of the acetyl-CoA by the cytosolic ACC (ACC1; EC 6.4.1.2) (Baud *et al.*, 2003).

Each elongation cycle is divided into four enzymatic reactions, catalysed by enzymes belonging to the FAE complex. The first reaction consists in the condensation between malonyl-CoA and acyl-CoA by the β-ketoacyl-CoA synthase (KCS; EC 2.3.1.120) resulting in the synthesis of β-ketoacyl-CoA (Blacklock *et al.*, 2006). In the second reaction, β-ketoacyl-CoA is reduced to β-hydroxyacyl-CoA by the β-ketoacyl-CoA reductase (KCR) (EC 1.1.1.35) (Li-Beisson *et al.*, 2013). During the third reaction, β-hydroxyacyl-CoA is dehydrated to enoyl-CoA by the β-hydroxyacyl-CoA dehydratase (HACD) (EC 4.2.1.17) (Li-Beisson *et al.*, 2013). The last reaction of each elongation cycle, catalysed by the enoyl-CoA reductase (ECR) (EC 1.3.1.38), consists in the reduction of the enoyl-CoA into acyl-CoA containing at least 18 carbons **(Figure 10)** (Li-Beisson *et al.*, 2013).

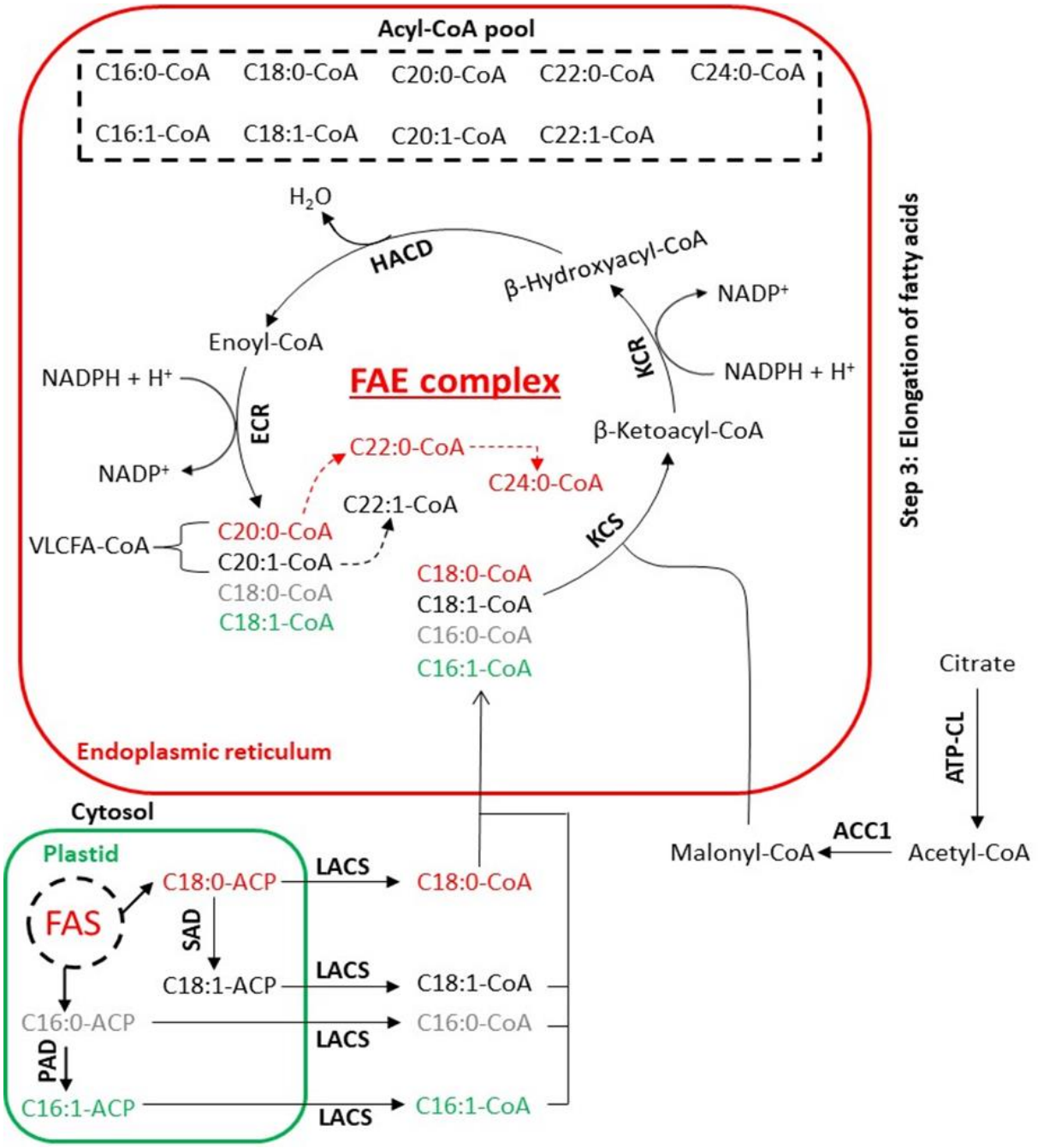

Figure 10. The elongation of FA into very long chain FA (VLCFA). *The elongation of FA is located in the ER. Once produced within plastids, acyl-ACP is converted into acyl-CoA by the long-chain acyl-CoA synthetase (LACS). Acyl-CoA is then exported from plastids to the ER. The elongation of acyl-CoA (C16:0-CoA, C18:0-CoA and C18:1-CoA) into VLCFA-CoA (C20:0-CoA, C20:1-CoA, C22:0-CoA, C22:1-CoA and C24:0-CoA) is catalysed by the FA elongation (FAE) complex, including the β-ketoacyl-CoA synthase (KCS), the β-ketoacyl-CoA reductase (KCR), the β-hydroxyacyl-CoA dehydratase (HACD) and the enoyl-CoA reductase (ECR). These enzymes enable the synthesis of acyl-CoA elongated by two carbons. These two carbons are provided by malonyl-CoA through the action of KCS. Malonyl-CoA is itself synthesized in the cytosol by the carboxylation of the acetyl-CoA through the activity of the cytosolic acetyl-CoA carboxylase (ACC1). Abbreviation: SAD, Δ9 stearoyl-ACP desaturase; PAD, Δ9 stearoyl-ACP desaturase; ATP-CL, ATP citrate lyase; FAS, FA synthase. Adapted from Li-Beisson et al. (2013).*

2.2. Glycerolipid synthesis

2.2.1. Eukaryotic pathway

2.2.1.1. Synthesis of TAG and membrane phospholipids within the ER

The eukaryotic pathway is involved in the synthesis of storage glycerolipids (TAG) and membrane phospholipids (PC, PE, PS and PI) within the ER. Glycerolipids synthesized by the eukaryotic pathway are characterized by the presence of C18:0 or C18:1 esterified to the second position (*sn-2*) of the glycerol backbone.

One of the pathways involved in TAG synthesis corresponds to the glycerol phosphate pathway, also known as the Kennedy pathway. The first two enzymatic reactions of the Kennedy pathway are common to those involved in the synthesis of membrane phospholipids. The first reaction consists in the esterification of acyl-CoA with the first carbon (*sn-1*) of the glycerol-3-phosphate (G3P) resulting in the synthesis of lysophosphatidic acid (LPA) by the glycerol-3-phosphate acyltransferase (GPAT; EC 2.3.1.15). The second reaction allows the conversion of LPA into a precursor of several glycerolipids, known as the phosphatidic acid (PA). This reaction, catalysed by the 2-lysophosphatidic acid acyltransferase (LPAAT; EC 2.3.1.51), consists in the esterification of acyl-CoA, mostly C18:0-CoA or C18:1-CoA, with the second carbon (*sn-2*) of the glycerol backbone (Li-Beisson *et al.*, 2013). The third reaction consists in the synthesis of diacylglycerol (DAG) or DAG esterified to cytidine diphosphate (CDP-DAG). The dephosphorylation of PA into diacylglycerol (DAG) is catalysed by the phosphatidate phosphatase (PP; EC 3.1.3.4). CDP-DAG is synthesized through the action of the CDP-DAG synthase (CDP-DAGS; EC 2.7.7.41) (Li-Beisson *et al.*, 2013; Shrestha *et al.*, 2016). In the eukaryotic pathway, DAG is the precursor of TAG, PC, PE and PS, while CDP-DAG is involved in the synthesis of PI **(Figure 11)** (Li-Beisson *et al.*, 2013). The last reaction of the Kennedy pathway is the acylation of DAG into TAG, a third acyl-CoA is esterified to the third position (*sn-3*) of the glycerol backbone by the acyl-CoA: DAG acyltransferase (DGAT; EC 2.3.1.20) **(Figure 11)** (Li-Beisson *et al.*, 2013).

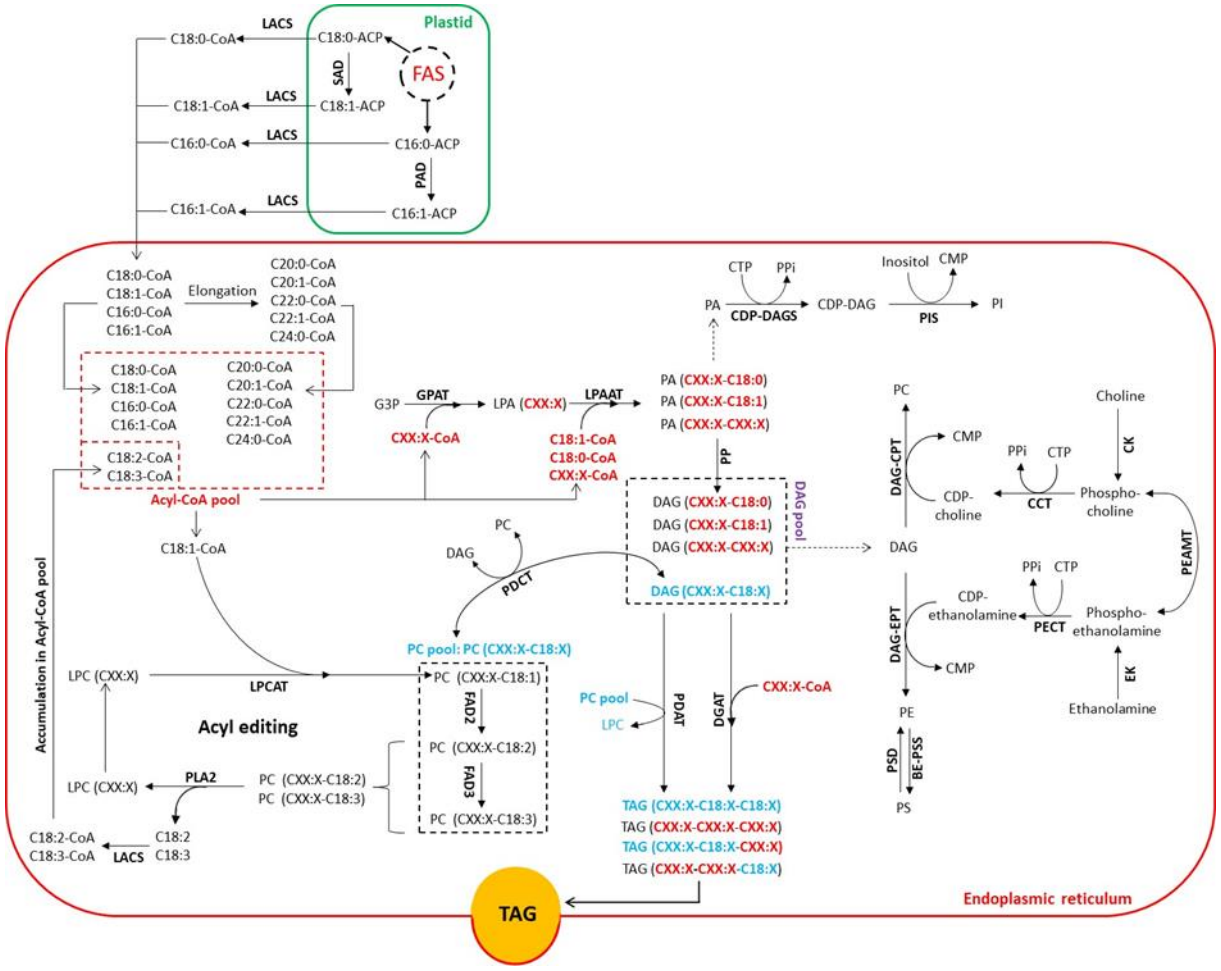

Figure 11. Synthesis of TAG and membrane phospholipids by the eukaryotic pathway. *The eukaryotic pathway takes place within the ER. PA is synthesized by the combined action of the glycerol-3-phosphate acyltransferase (GPAT) and lysophosphatidic acid (LPA) acyltransferase (LPAAT). PA is involved in the synthesis of diacylglycerol (DAG) by the phosphatidate phosphatase (PP) and CDP-DAG by the CDP-DAG synthetase (CDP-DAGS), respectively. CDP-DAG enables the synthesis of phosphatidylinositol (PI) by the PI synthase (PIS). Phosphatidylcholine (PC), phosphatidylethanolamine (PE), phosphatidylserine (PS) and TAG are synthesized from DAG. For the synthesis of PE, ethanolamine kinase (EK) is first involved in the phosphorylation of ethanolamine into phosphoethanolamine, itself transferred to CTP in order to generate CDP-ethanolamine by the CTP: phosphorylethanolamine cytidyltransferase (PECT). CDP-ethanolamine is then esterified to DAG by the CDP-ethanolamine: DAG ethanolamine phosphotransferase (DAG-EPT). Choline kinase (CK), CTP: phosphorylcholine cytidyltransferase (CCT) and CDP-choline: DAG cholinephosphotransferase (DAG-CPT) synthesize PC in a similar enzymatic mechanism than the one described for PE. The interconnection between PC and PE synthesis is ensured by the phosphoethanolamine N-methyltransferase (PEAMT). Base-exchange-type phosphatidylserine synthase (BE-PSS) generates PS from PE, while the PS decarboxylase (PSD) enables the synthesis of PE from PS. TAG can be synthesized from the acylation of DAG by DAG acyltransferase (DGAT). PC can transfer a third FA to DAG, producing TAG by the phospholipid: DAG acyltransferase (PDAT). Phospholipase A2 (PLA2) and LPC acyltransferase (LPCAT) enable the deacylation of PC and acylation of LPC, respectively. Abbreviation: FAD, FA desaturase. Adapted from Li-Beisson et al. (2013).*

Previous studies have been performed in order to identify other potential metabolic pathways involved in the synthesis of TAG in Arabidopsis seeds. Katavic *et al*. (1995) have first suggested that several enzymes, other than DGAT, may be involved in the synthesis of TAG since only a 25 % decrease of the total lipid content has been observed in the loss-of-function Arabidopsis *dgat* mutant seeds. Mhaske *et al*. (2005) have been focused on the

potential role of phospholipid: DAG acyltransferase (PDAT; EC 2.3.1.43) in the synthesis of TAG in Arabidopsis seeds since this enzyme is involved in the accumulation of TAG in yeast and other oil seed plants (Dahlqvist *et al.*, 2000). Mhaske *et al.* (2005) were not able to identify a significant change in the oil content in *PDAT* knockout seeds, suggesting that the alteration of *PDAT* may be compensated by another gene involved in the synthesis of TAG. The suppression of *PDAT1* in *dgat1-1*, as well as the suppression of *DGAT1* in *pdat1-1*, showed a decrease in oil content estimated between 70 and 80 % (Zhang *et al.*, 2009). It was thus revealed that PDAT and DGAT are both associated to the synthesis of TAG and have complementary function since the alteration of one of these two genes does not lead to a sharp decrease of TAG content. PDAT is involved in the synthesis of TAG by the transfer of FA from phospholipids, mostly PC, to DAG **(Figure 11)**. During seed maturation, TAG is accumulated in form of lipid droplets, especially within the cotyledon of seed embryo (Baud *et al.*, 2002), providing energy and carbon to plants during the early germination.

PC is synthesized from DAG within the ER. The CDP-choline pathway is involved in the synthesis of PC by the addition of a choline polar head group to DAG. The first step of this pathway consists in the phosphorylation of the choline by the choline kinase (CK; EC 2.7.1.32). The resulting phosphocholine is then converted into CDP-choline by the CTP: phosphocholine cytidyltransferase (CCT; EC 2.7.7.15). CDP-choline is then esterified to DAG, resulting in the synthesis of PC through the action of the CDP-choline: DAG choline phosphotransferase (DAG-CPT; EC 2.7.8.2) (Goode and Dewey, 1999). Once PC is synthesized, one or two desaturations can be added to monounsaturated FA moieties this membrane glycerolipids. FA desaturase 2 (FAD2; EC 1.14.19.6) introduces desaturation to the monounsaturated C18:1 FA, increasing the content of C18:2 moieties PC **(Figure 11)** (Okuley *et al.*, 1994). FAD3 (EC 1.14.19.25) is involved in the conversion of C18:2 into C18:3, therefore increasing the content of triunsaturated C18:3 FA moieties PC **(Figure 11)** (Browse *et al.*, 1993).

PE is synthesized from DAG by a metabolic pathway known as the CDP-ethanolamine pathway **(Figure 11)**. This pathway is similar to the one described for the synthesis of PC. The first reaction of the CDP-ethanolamine pathway allows the phosphorylation of the ethanolamine into phosphoethanolamine by the ethanolamine kinase (EK; EC 2.7.1.82). The second reaction consists in the transfer of phosphoethanolamine to CTP, generating CDP-ethanolamine through the action of the CTP: phosphoethanolamine

cytidyltransferase (PECT; EC 2.7.7.14) (Mizoi *et al.*, 2006). CDP-ethanolamine is then esterified to DAG, resulting in the synthesis of PE by the CDP-ethanolamine: DAG ethanolamine phosphotransferase (EC 2.7.8.1) (Goode and Dewey, 1999). CDP-ethanolamine and CDP-choline pathways are interconnected since phosphoethanolamine can be methylated into phosphocholine by the S-Adenosyl-L-methionine: phosphoethanolamine N-methyltransferase (PEAMT; EC 2.1.1.103) **(Figure 11)** (Mou *et al.*, 2002). Once synthetized within ER, PE can also be converted into PS by a base-exchange-type PS synthase (BE-PSS; EC 2.7.8.8) (Yamaoka *et al.*, 2011). PS can also be converted into PE by PS decarboxylase (PSD; EC 4.1.1.65) **(Figure 11)** (Nerlich *et al.*, 2007).

PI is synthesized from CDP-DAG by two enzymatic reactions. The first reaction consists in the conversion of the G6P into the inositol-3-phosphate by the myo-inositol-3-phosphate synthase (MIPS; EC 5.5.1.4). The inositol is then transferred to the CDP-DAG, generating PI through the activity of the phosphatidylinositol synthase (PIS; EC 2.7.8.11) **(Figure 11)** (Li-Beisson *et al.*, 2013).

2.2.1.2. Synthesis of polyunsaturated glycerolipids within the ER

In plants, the intraplastidial *de novo* FA synthesis generates saturated and mono-unsaturated FA. In the eukaryotic pathway, these FA are incorporated to glycerol backbones resulting in the synthesis of TAG and phospholipids containing saturated and mono-unsaturated FA (Li-Beisson *et al.*, 2013). However, polyunsaturated FA moieties TAG and phospholipids are also produced by the eukaryotic pathway. The acyl editing is a physiological process allowing the synthesis of polyunsaturated FA moieties TAG and membrane glycerolipids in the ER. During the *de novo* glycerolipid synthesis, one of the phospholipids produced by the eukaryotic pathway corresponds to monounsaturated FA moieties PC. The acyl editing involving this glycerolipids is composed of three main enzymatic reactions, including the unsaturation of FA moieties PC, the deacylation of PC into lyso-PC (LPC) and the reacylation of LPC into PC.

The acyl editing begins by the conversion of PC containing monounsaturated FA into diunsaturated C18:2 and triunsaturated C18:3 FA constituting PC through the action of FAD2 and FAD3, respectively (Browse *et al.*, 1993; Okuley *et al.*, 1994). Phospholipase A2 (PLA2; EC 3.1.1.4) hydrolyses PC into lysophosphatidylcholine (LPC), releasing polyunsaturated

FA esterified to the second position (*sn-2*) of the glycerol backbone **(Figure 11)**. Once released from PC, polyunsaturated FA are esterified to CoA by LACS (EC 6.2.1.3) and incorporated to the acyl-CoA pool already made of saturated and mono-unsaturated FA and VLCFA, including C16:0-CoA, C16:1-CoA, C18:0-CoA, C18:1-CoA, C20:0-CoA, C20:1-CoA, C22:0-CoA, C22:1-CoA and C24:0-CoA **(Figure 11)**. LPC acyltransferase (LPCAT: EC 2.3.1.23) allows the reacylation of LPC by saturated and monounsaturated FA composing the acyl-CoA pool **(Figure 11)**. Once incorporated to PC, monounsaturated FA are converted into di- or tri-unsaturated FA through the action of FAD2 and FAD3. The PC deacylation and LPC reacylation cycle is repeated, therefore, accumulating polyunsaturated FA within the acyl-CoA pool **(Figure 11)** (Bates *et al.*, 2012). At this stage, the acyl-CoA pool is made of C16:0-CoA, C16:1-CoA, C18:0-CoA, C18:1-CoA, C18:2-CoA, C18:3-CoA, C20:0-CoA, C20:1-CoA, C22:0-CoA, C22:1-CoA and C24:0-CoA **(Figure 11)**. Polyunsaturated FA accumulated within the acyl-CoA pool can be esterified to the first and second carbon of the glycerol-3-phosphate by GPAT (EC 2.3.1.15) and LPAAT (EC 2.3.1.51), resulting in the synthesis of polyunsaturated PA. After the dephosphorylation of PA into DAG, polyunsaturated TAG or membrane glycerolipids are synthesized by the esterification of a third acyl-CoA or by the transfer of a polar head group to DAG, respectively **(Figure 11)** (Li-Beisson *et al.*, 2013).

2.2.1.3. Synthesis of galactolipids and sulfolipid by the eukaryotic pathway

The eukaryotic pathway is also characterized by the synthesis of sulfolipid (SQDG) and galactolipids (MGDG and DGDG) within plastids from precursors generated in the ER. MGDG and DGDG are involved in plastid biogenesis (Yu *et al.*, 2015). These glycerolipids are crucial for the establishment of the photosynthesis and thylakoid assembly (Yu and Benning, 2003; Kobayashi *et al.*, 2016a). During phosphate starvation, galactolipids and sulfolipid can replace phospholipids in order to provide endogenous phosphate supply to the plant without affecting the negative charge density of thylakoid membranes (Nakamura, 2013).

In the eukaryotic pathway, PC synthesized in the ER is the precursor of sulfolipid and galactolipids **(Figure 12)**. Once generated within the ER, PC species can be exported from ER to plastids in order to be converted into DAG by the phospholipase C (PLC; EC 3.1.4.3) or by the combined action of the phospholipase D (PLD; EC 3.1.4.4) and the phosphatidate phosphatase (PP; EC 3.1.3.4) (Li-Beisson *et al.*, 2013). Galactolipid and sulfolipid are then synthesized from DAG. The synthesis of galactolipids takes place within the membrane of the

chloroplasts. MGDG synthase (MGDGS; EC 2.4.1.46) is involved in the synthesis of MGDG by the transfer of a galactose moiety to DAG. The transfer of a galactose moiety to MGDG generates DGDG through the activity of the DGDG synthase (DGDGS; EC 2.4.1.241) **(Figure 12)** (Kelly and Dörmann, 2004). SQDG synthesis takes place in the stroma of plastids. In plants, G1P can be synthesized from the enzymatic hydrolysis of starch (Sauter, 2000). The esterification of UTP with G1P generates UDP-glucose through the action of UDP-glucose pyrophosphorylase (EC 2.7.7.9). The transfer of a sulfonate group to UDP-glucose allows the synthesis of UDP-sulfoquinovosyl by the UDP-sulfoquinovose synthase (EC 3.13.1.1) (Sanda *et al.*, 2001). UDP-sulfoquinovosyl is then esterified to DAG by sulfolipid synthase (SLS) in order to synthesize SQDG **(Figure 12)** (Yu *et al.*, 2002).

2.2.2. Prokaryotic pathway

The prokaryotic pathway is involved in the synthesis of phospholipid (PG), sulfolipid (SQDG) and galactolipids (MGDG and DGDG) exclusively within plastids. The synthesis of these glycerolipids begins by the esterification of saturated and monounsaturated FA in form of acyl-ACP to the first carbon (*sn-1*) of the G3P by GPAT, generating LPA (Li-Beisson *et al.*, 2013). LPAAT allows the esterification of C16:0-ACP to the second carbon (*sn-2*) of the glycerol backbone, resulting in the synthesis of PA. This glycerolipid precursor is then converted into DAG or CDP-DAG through the action of PP or CDP-DAGS. In the prokaryotic pathway, DAG is the precursor of sulfolipid and galactolipids, while PG is synthesized from CDP-DAG **(Figure 12)** (Li-Beisson *et al.*, 2013).

The subsequent enzymatic reactions allowing the synthesis of sulfolipid (SQDG) and galactolipid (MGDG and DGDG) by the prokaryotic pathway are similar to those described for the eukaryotic pathway. In the prokaryotic pathway, PG is synthesized from CDP-DAG through the activity of two enzymes, including the phosphatidylglycerol phosphate (PGP) synthase (PGPS; EC 2.7.8.5) and PGP phosphatase (PGPP; EC 3.1.3.27). The first reaction consists in the transfer of G3P to the CDP-DAG, resulting in the synthesis of PGP by the PGPS **(Figure 12)**. During the second reaction, PGP is dephosphorylated into PG by the PGPP **(Figure 12)** (Li-Beisson *et al.*, 2013). PG is an essential component of thylakoid membranes since this phospholipid is involved in the biogenesis of these membranes and the establishment of the photosynthesis (Kobayashi *et al.*, 2016b).

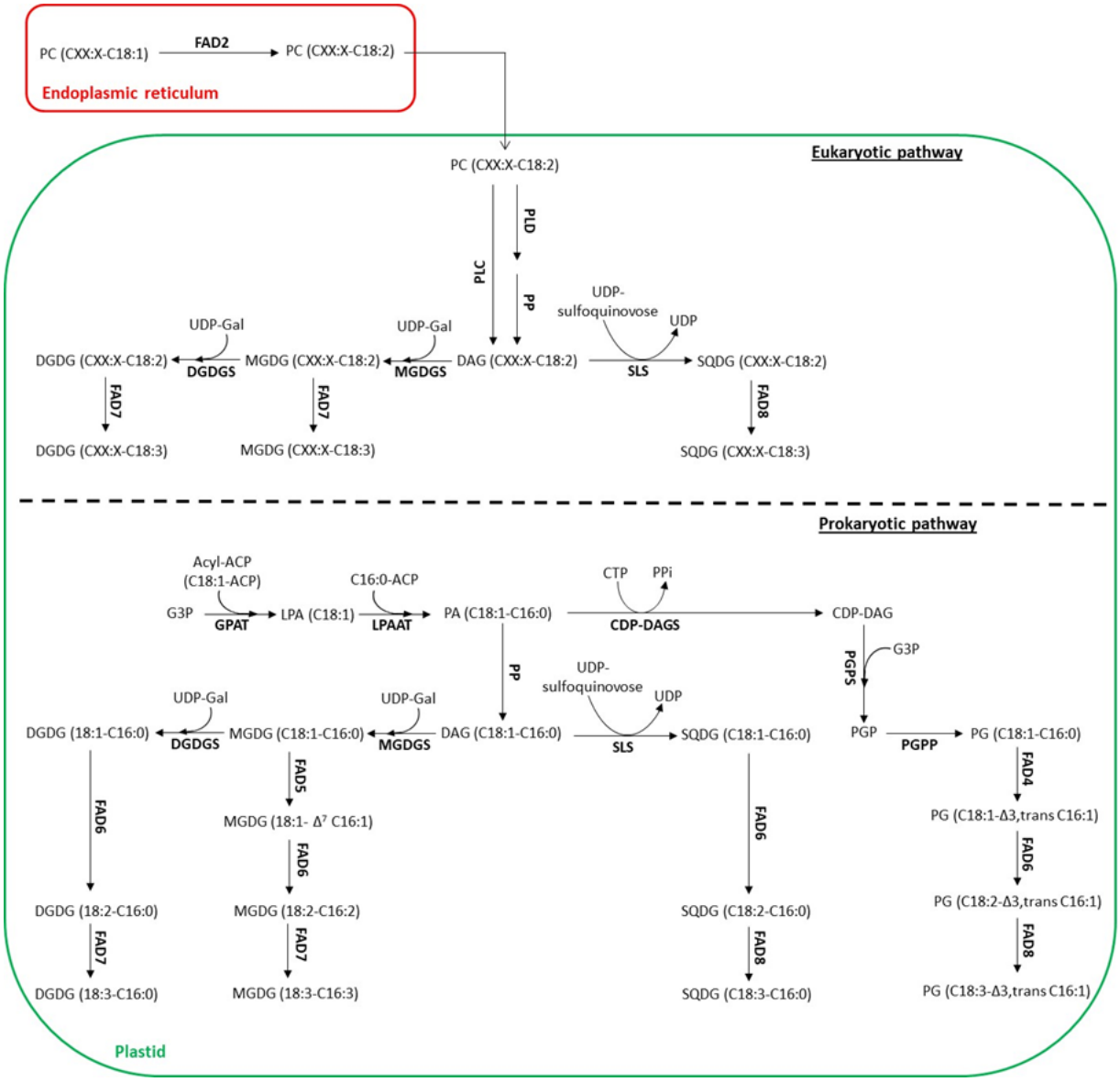

Figure 12. Synthesis of membrane glycerolipids within plastids. *The prokaryotic pathway is involved in the synthesis of galactolipids, sulfolipid and phospholipid. In the prokaryotic pathway, PA is generated by the glycerol-3-phosphate acyltransferase (GPAT) and the lysophosphatidic acid (LPA) acyltransferase (LPAAT). PA is the substrate of both phosphatidate phosphatase (PP) and the CDP-DAG synthetase (CDP-DAGS) generating GAG and CDP-DAG, respectively. Phosphatidylglycerol (PG) is synthesized through the action of the phosphatidylglycerol phosphate synthase (PGPS) and PGP phosphatase (PGPP). DAG is involved in the synthesis of MGDG by the MGDG synthase (MGDGS) and DGDG by the DGDG synthase (DGDGS). SQDG is obtained from DAG by the sulfolipid synthase (SLS). In the prokaryotic pathway, the addition of desaturations to FA is catalysed by FA desaturases (FAD): FAD4, FAD5, FAD6, FAD7 and FAD8. In the eukaryotic pathway, the precursor of galactolipids and sulfolipid is PC. Once synthesized, PC species are exported from ER to plastids. DAG species are generated from PC by the phospholipase C (PLC) or through the action of phospholipase D (PLD) and the phosphatidate phosphatase (PP). Similar enzymatic reactions are performed for the synthesis of sulfolipid and galactolipids by the eukaryotic pathway. Adapted from Li-Beisson et al. (2013).*

The synthesis of MGDG, DGDG, SQDG and PG is followed by the introduction of double bonds to FA moieties of these glycerolipids. FAD4 (EC 1.14.19.43) introduces double bond to palmitic acid (C16:0) esterified to the second position (*sn-2*) of the glycerol backbone of PG, resulting in the synthesis of hexadecenoic acid containing a trans double bond at carbon

3 ($\Delta^{3,trans}$ C16:1) **(Figure 12)** (Gao *et al.*, 2009). FAD5 (EC 1.14.19.42) enables the conversion of C16:0 into Δ^7 C16:1 in MGDG **(Figure 12)** (Heilmann *et al.*, 2004). FAD6 (EC 1.14.19.23) synthesizes the hexadecadienoic (C16:2) and linoleic (C18:2) acids in galactolipids, sulfolipid and PG **(Figure 12)** (Browse *et al.*, 1989). FAD7 (EC 1.14.19.) increases the content of tri-unsaturated FA, including hexadecatrienoic (C16:3) and linolenic (C18:3), preferentially in galactolipids **(Figure 12)** (Browse *et al.*, 1986; Roman *et al.*, 2015). FAD8 (EC 1.14.19.) specifically introduces double bond to C18:2, increasing the content of C18:3 preferentially in sulfolipid and PG **(Figure 12)** (McConn *et al.*, 1994; Roman *et al.*, 2015).

2.3. Catabolism of TAG during the early germination

During seed maturation, TAG is accumulated in form of lipid droplet within the cotyledon of the embryo. During the early germination, this storage lipid is mobilized by the action of lipases, resulting in the release of FFA from their glycerol backbones (Eastmond, 2006). FFA are then catabolized by the β-oxidation, producing acetyl-CoA and reducing equivalents in form of NADH (Penfield et al, 2006; Graham, 2008). The glyoxylate cycle and gluconeogenesis are involved in the production of sucrose from the acetyl-CoA generated by the β-oxidation. Sucrose is one of the sources of carbon and energy required for promoting the growth and the development of seedlings (Graham *et al.*, 2008).

2.3.1. FA β-oxidation

During early germination lipases release FFA from TAG. In Arabidopsis, SUGAR-DEPENDANT 1 (SDP1) has been identified as a lipase involved in the storage lipid breakdown (Eastmond, 2006). FFA are then catabolised by β-oxidation within the peroxisome (Penfield *et al.*, 2006; Graham, 2008). FFA are transported into the peroxisome by transporters, including the PEROXISOMAL ABC TRANSPORTER 1, COMATOSE (CTS) and PEROXISOME DEFICIENT 3 (Zolman *et al.*, 2001; Footitt *et al.*, 2002; Hayashi *et al.*, 2002). The conversion of FFA into acyl-CoA is performed by LACS (EC 6.2.1.3) (Fulda *et al.*, 2004).

Acyl-CoA is then catabolized into several molecules of acetyl-CoA by successive β-oxidation cycles **(Figure 13)**. A total of eight β-oxidation cycles are, for instance, performed for the catabolism of C18:0-CoA into nine molecules of acetyl-CoA. The first β-oxidation cycle consists in the enzymatic cleavage of C18:0-CoA into C16:0-CoA and one molecule of acetyl-CoA, while the second β-oxidation cycle generates C14:0-CoA (myristic-CoA) and one molecule

of acetyl-CoA from the enzymatic cleavage of C16:0-CoA. Each β-oxidation cycle results in the synthesis of acyl-CoA containing two less carbons in comparison to the acyl-CoA generated from the β-oxidation previous cycle. The last β-oxidation cycle is involved in the synthesis of two molecules of acetyl-CoA **(Figure 13)** (Graham, 2008).

Each β-oxidation cycle is divided into four reactions. The acyl-CoA oxidase (ACX) (EC 1.3.3.6), which is the first enzyme involved in the catabolism of acyl-CoA, allows the oxidation of acyl-CoA into 2-trans-enoyl-CoA coupled to the reduction of FAD^+ (Pinfield-Wells *et al.*, 2005; Graham, 2008). The conversion of the 2-trans enoyl-CoA into 3- ketoacyl-CoA is performed through the combined action of two enzymes belonging to the multifunctional protein (MFP), the 2-trans enoyl-CoA hydratase (EC 4.2.1.17) and 1,3-hydroxyacyl-CoA dehydrogenase (EC 1.1.1.35) (Graham, 2008). The last reaction, catalysed by the 3-ketoacyl-CoA thiolase (KAT) (EC 2.3.1.16), consists in the enzymatic cleavage of 3-ketoacyl-CoA into one molecule of acetyl-CoA and acyl-CoA containing two less carbons in comparison to the acyl-CoA generated from the previous cycle (Graham, 2008). The resulting acyl-CoA enters in new cycles, providing other molecules of acetyl-CoA and NADH **(Figure 13)**.

2.3.2. Production of sucrose by the glyoxylate cycle and gluconeogenesis

Once synthesized, acetyl-CoA is used for the synthesis of sucrose by the gluconeogenesis. However, the three-carbon pyruvate is not able to be directly synthesized from the two-carbon acetyl-CoA. The objective of the glyoxylate cycle is thus providing two extra-carbons to the acetyl-CoA in order to form a four-carbon molecule, the malate, before undergoing a decarboxylation into a three-carbon one, the pyruvate (Graham, 2008).

The first enzyme of the glyoxylate cycle, catalysed by the malate synthase (MLS) (EC 2.3.3.9), enables the condensation between acetyl-CoA and another two-carbon molecule known as glyoxylate, resulting in the production of four-carbon malate. Glyoxylate is itself synthetized from the degradation of the isocitrate by the isocitrate lyase (EC 4.1.3.1). Once produced, malate is converted into four-carbon oxaloacetate by the extra-peroxisomal malate dehydrogenase (MDH) (EC 1.1.1.37) (Graham, 2008). Oxaloacetate (OAA) is then involved in the synthesis of the three-carbon PEP by the PEP carboxykinase (PCK) (EC 4.1.1.49) **(Figure 13)**.

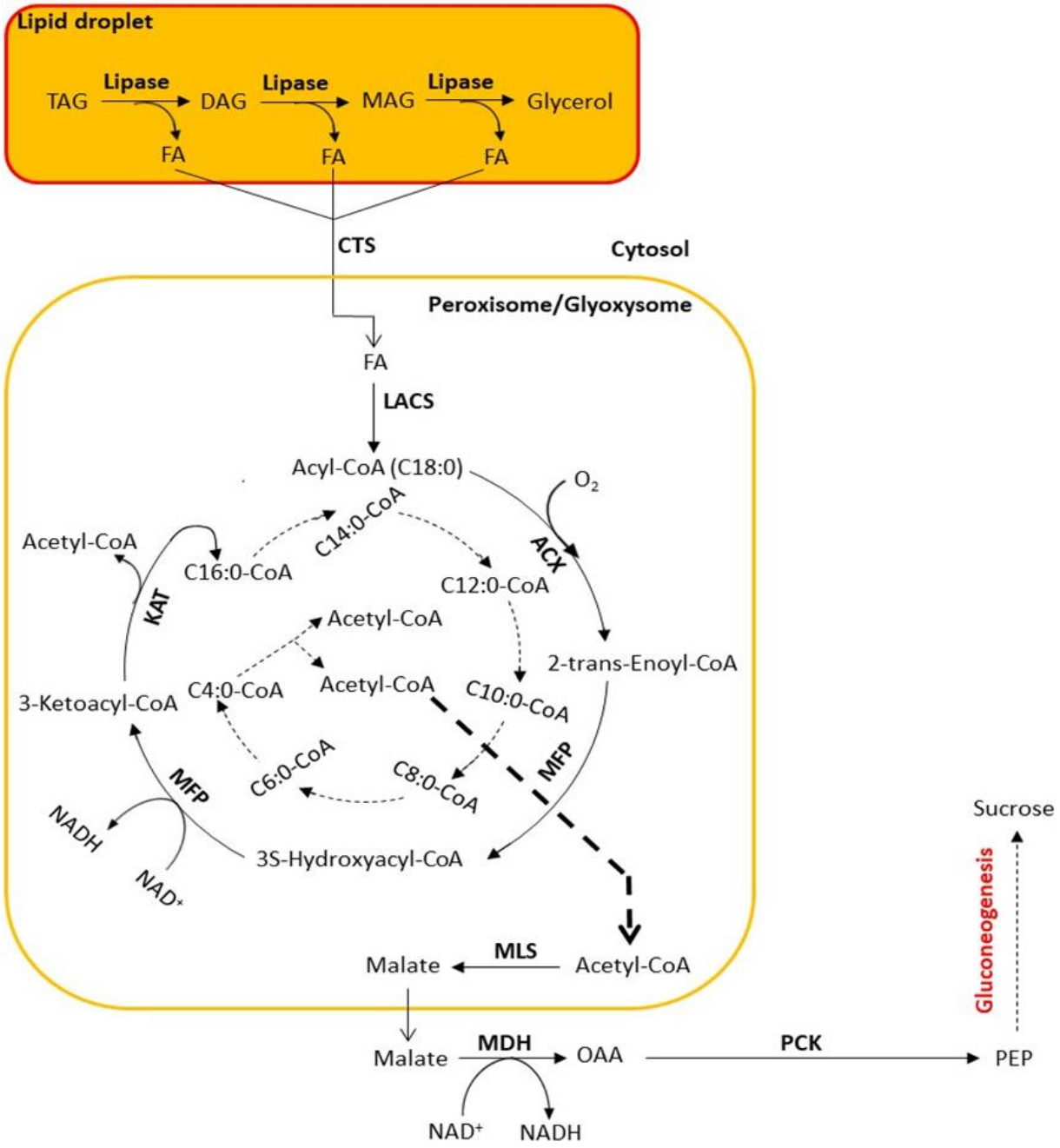

Figure 13. TAG Mobilization, FA catabolism and production of sucrose during the germination. *TAG is first mobilized, resulting in the release of FA. FA are imported within the peroxisome by transporters (CTS, COMATOSE). FA is activated into acyl-CoA by long-chain acyl-CoA synthetase (LACS). Acyl-CoA enters in several two-carbon degradation cycles, which enable the production of several molecules of acetyl-CoA. For the catabolism of saturated FA, acyl-CoA oxidase (ACX), multifunctional protein (MFP) and 3-Ketoacyl-CoA thiolase (KAT) are involved in the production of acetyl-CoA and saturated acyl-CoA with two less carbons or two molecules of acetyl-CoA for the last cycle. Once produced, acetyl-CoA is involved in the realization of the glyoxylate cycle. Malate synthase (MLS), malate dehydrogenase (MDH) and phosphoenolpyruvate (PEP) carboxikinase (PCK) are involved in the synthesis of PEP. Sucrose is then produced by gluconeogenesis. MAG, monoacylglycerol; OAA, oxaloacetate. Adapted from Graham (2008).*

Gluconeogenesis consists in the synthesis of G6P from PEP by carrying out the reverse path of the glycolysis since most of the glycolysis-belonging enzymatic reactions are reversible with the exception of the phosphofructokinase (EC 2.7.1.11), PK, FRK and

hexokinase **(Figure 9)**. The dephosphorylation of the fructose-1,6-bisphosphate into fructose-6-phosphate is performed by the fructose-1,6-bisphosphatase (EC 3.1.3.11) (Daie, 1993). The synthesis of G6P is then followed by the synthesis of sucrose (Stein and Granot, 2019). The phosphate group of the G6P is transferred from the sixth to the first carbon of glucose, resulting in the formation of the G1P by phosphoglucomutase (EC 5.4.2.2). G1P is then converted into UDP-glucose by UDP-glucose pyrophosphorylase (EC 2.7.7.9). Sucrose phosphate synthase (EC 2.4.1.14) catalyses the association of UDP-glucose with fructose-6-phosphate for the synthesis of sucrose phosphate. Sucrose phosphate is finally dephosphorylated by sucrose phosphate phosphatase (EC 3.1.3.24), resulting in the synthesis of sucrose (Stein and Granot, 2019). Sucrose can be transported in the phloem from seedling cotyledon to the radicle. The enzymatic hydrolysis of sucrose releases glucose. Once released, this hexose is catabolized by glycolysis and PPP, providing energy and carbons necessary for the growth and development of cotyledons into leaves and radicle into roots (Graham, 2008).

2.4. Regulation of FA and glycerolipid metabolism in Arabidopsis developing seeds

Several transcription factors are involved in the regulation of FA and glycerolipid metabolism, as well as in the genesis of lipid droplets during seed development. These transcription factors correspond to WRINKLED 1 (WRI1), LEAFY COTYLEDON 1 (LEC1), LEC1-like (L1L), LEAFY COTYLEDON 2 (LEC2), ABSCISIC ACID INSENSITIVE 3 (ABI3) and FUSCA 3 (FUS3). WRI1 is characterized by the presence of two APETALA2 (AP2) protein domains, whereas, ABI3, FUS3 and LEC2 are transcription factors that contain B3 domain and LEC1 belongs to the NUCLEAR FACTOR Y-SUBUNIT B (NF-YB) protein family (Braybrook and Harada, 2008; Santos-Mendoza *et al.,* 2008).

LEC1, ABI3, FUS3 and LEC2, collectively named LAFL, are referred as master regulators since one of their main functions is positively regulating the expression of other transcription factors, including *WRI1* and *L1L*. The expression of *WRI1* is positively modulated by LEC2, ABI3, FUS3 and LEC1 (Baud *et al.*, 2007; Yamamoto *et al.*, 2010), while the expression of *L1L* is regulated by FUS3 **(Figure 14)** (Yamamoto *et al.*, 2010). Each LAFL can also regulate the expression of other master regulators. LEC2 positively modulates the expression of *LEC1*, *FUS3* and *ABI3* (Braybrook *et al.*, 2006). LEC1 positively controls the expression of *LEC2*, *ABI3* and *FUS3* (Mu *et al*., 2008; Pelletier *et al.*, 2017). ABI3 and FUS3 have a positive action on the expression of *FUS3* and *ABI3*, respectively **(Figure 14)** (To *et al.*, 2006).

WRI1 and L1L are known as secondary regulators. Both transcription factors control, downstream to the master regulators, the expression of FA- and glycerolipid-related genes (Kumar *et al.*, 2020). In addition, WRI1 positively regulates the expression of glycolytic genes (Focks and Benning, 1998). In order to ensure a correct seed development and maturation, FA and glycerolipid metabolism is not only positively controlled by master and secondary regulators but also negatively regulated by other transcription factors.

2.4.1. Role of the master regulators (LAFL) during seed maturation

LAFL are essential regulators of seed development (Verma *et al.*, 2022). LEC1 and LEC2 regulate the embryogenesis during seed development (Casson and Lindsey, 2006). LEC1 is also involved in the initiation of seed maturation (Song *et al.*, 2021). LAFL are involved in the development of chloroplasts during the early-maturation stage, conferring green color and photosynthetic capacity to the embryo (O'Neill *et al.*, 2019). ABI3 takes part to seed degreening between 13 and 16 DAF through its positive action on the expression of *STAY-GREEN 1* (*SGR1*) and *SGR2*, both genes promoting chlorophyll breakdown (Delmas *et al.*, 2013).

During seed development, each LAFL controls the expression of FA-related genes and desaturases (*FAD2*, *FAD3* and *FAB2*) during seed maturation **(Figure 14)**. In addition, LEC2 regulates the expression of genes involved in TAG synthesis, like *DGAT*, *LPCAT* and *PDAT* (Kim *et al.*, 2015), and genes encoding for proteins participating in the genesis of lipid droplets, including the oleosin and cruciferin (Santos Mendoza *et al.*, 2005). ABI3 and FUS3 are both involved in the regulation of FA-related genes. ABI3 positively regulates the expression of *FAD3* and the stearoyl-ACP desaturase *FAB2* (Tian *et al.*, 2020). The expression of *FAD3*, *KAS I* and the gene encoding for KCS (FA elongase 1: *FAE1*) can be upregulated by FUS3 (Yamamoto *et al.*, 2010). ABI3 and FUS3 are also involved in the accumulation of storage proteins, like oleosin and cruciferin (To *et al.*, 2006). The synthesis of storage proteins in seeds is rather regulated by ABI3 than FUS3, while lipid content is rather controlled by FUS3 than ABI3 (Roscoe *et al.*, 2015; Baud *et al.*, 2016). Transcription factors containing a B3 domain, including LEC2, ABI3 and FUS3, directly regulates the expression of target genes through its interaction with a DNA sequence referred as a RY element (Baud *et al.*, 2016; Sasnauskas *et al.*, 2018). Unlike LEC2, ABI3 and FUS3, LEC1 is not able to directly bind with target DNA sequences. In order to regulate the expression of target genes, LEC1 interacts with the NUCLEAR FACTOR Y-SUBUNIT A (NF-YA) and NF-YC, allowing the formation of NF-Y complex that binds with the

CCAAT DNA sequence (Baud *et al.*, 2016). LEC1 can also be associated with the NF-YC and bZIP67, generating a trimeric complex that activates the expression of *FAD3* and *CRUCIFERIN* through the interaction of bZIP67 with the G-box DNA sequence of these two genes (Mendes *et al.*, 2013; Pelletier *et al.*, 2017). It was suggested that LEC1 also increases the expression of several FA-related genes, including *BCCP*, *MCMT* and the stearoyl-ACP desaturase *FAB2* (Mu *et al.*, 2008).

2.4.2. Role of WRI1 and L1L in the regulation of FA and glycerolipid metabolism

WRI1 is a transcription factor involved in the regulation of glycolytic enzymes, including FRK, aldolase, PGLYM, ENO and PK (Focks and Benning, 1998). It was also suggested that WRI1 regulates pathways from carbohydrate catabolism to oil accumulation since the overexpression of *WRI1* in seeds led to the increase of the seed oil content (Cernac and Benning, 2004). This hypothesis was supported in a previous study conducted by Ruuska *et al.* (2002) in which differences in the expression of some glycolytic genes and FA-related genes has been revealed between the wild-type and *wri1* developing seeds. The expression of the cytosolic FRK and PGLYM, the plastidial PK, as well as the expression of *FAD2* and several FA-related genes including *BCCP*, *KAS I*, *ENOYL-ACP REDUCTASE* and *PDHC*, has been shown to be potentially under WRI1 control (Ruuska *et al.*, 2002). In Arabidopsis seeds, *WRI1* is highly expressed between 6 and 16 DAF (Baud *et al.*, 2007) and the expression of several FA-related genes is increased from 6 to 12 DAF (Baud *et al.*, 2009a; 2009b), showing a positive correlation between the expression of *WRI1* and FA-related genes. A reduction of the FA content between 45 and 55 % and the decrease of the expression of FA-related genes, including *BCCP* and *PDH-E1*, has been observed in *wri1* seeds (Baud *et al.*, 2007), confirming some of the results generated by Ruuska *et al.* (2002). In addition, WRI1 has been shown to bind to the conserved AW (ASML1/WRI1)-box sequence found in the upstream region of several FA-related genes, including *BCCP2* and *KAS I* (Maeo *et al.*, 2009). WRI1 is a transcription factor that positively regulates the intraplastidial *de novo* FA synthesis during seed maturation.

L1L is a transcription factor that interacts with NF-YC and bZIP67, allowing the formation of a trimeric complex that positively regulates the expression of *FAD3* (Yamamoto et al., 2009). Once expressed, FAD3 increases C18:3 content in seeds (Mendes *et al.*, 2013).

2.4.3. Negative control of FA and glycerolipid metabolism during seed maturation

During seed maturation, the expression of FA-related genes is positively controlled by the master (LEC1, LEC2, ABI3 and FUS3) and secondary (WRI1 and L1L) regulators. FA synthesis is, however, metabolically expensive in term of energy and reducing equivalent, therefore requiring a tight control of this anabolic process during seed maturation.

It was recently shown that WRI1 can indirectly bind through other proteins with the upstream region of *WRI1* gene, therefore decreasing the expression of its own gene (Snell *et al.*, 2019). The TEOSINTE BRANCHED1/CYCLOIDEA/PROLIFERATING CELL FACTOR 4 (TCP4) is one of the proteins that interacts with the AP2 domain of WRI1. Once formed, the complex WRI1/TCP4 binds with the upstream region of *WRI1* and acts as a negative regulator of FA synthesis by decreasing the expression of *WRI1* gene (Kong *et al.*, 2020a; 2020b). In developing seeds, FA synthesis can be no longer regulated by WRI1 after the degradation of this transcription factor by the proteasome. The proteasomal degradation of WRI1 can be performed after the interaction of the AP2 transcription factor with the CULLIN3-based E3 ligase (CUL3) and the BTB/POZ-MATH (BPM) proteins (Chen *et al*., 2013). In developing seeds, the protein kinase KIN10 decreases WRI1 activity. KIN10 can phosphorylate WRI1 (Zhai *et al.*, 2017). The phosphorylated WRI1 is degraded by the proteasome, therefore decreasing the expression of FA-related genes under WRI1 control. KIN10 can be repressed by trehalose-6-phosphate (T6P), a disaccharide in which the synthesis is correlated with high sugar level in plants (Zhai *et al.*, 2018). The role of this disaccharide consists in inhibiting the degradation of WRI1 by KIN10 and thus promoting the stabilization of WRI1 necessary for the FA synthesis. WRI1 positively regulates the expression of the BIOTIN ATTACHMENT DOMAIN-CONTAINING (BADC) protein. The activation of BADC by WRI1 decreases the content of FA through the inhibition of the heteromeric ACC, one of the enzymatic complexes involved in the FA synthesis (Liu *et al.*, 2019). Some of the transcription factors containing tryptophan (W)-arginine (R)-lysine (K)-tyrosine (Y) sequence at N-terminus extremity negatively controlled seed maturation. Due to their amino acids sequence at N-terminus, these transcription factors are referred as WRKY. WRKY6 acts as a negative regulator of seed maturation by decreasing *ABI3* and *FUS3* expression (Song *et al*., 2020). WRI1 can also positively modulate the expression of *CTI*, an inhibitor of the heteromeric ACC (Ye *et al.*, 2020).

Myeloblastosis 96 (MYB96) positively controls the expression of genes involved in TAG synthesis, including *DGAT1* and *PDAT1* (Lee *et al.*, 2018). MYB115 and MYB118 are both transcription factors that are under the positive control of LEC2. Once expressed, MYB115 and MYB118 increase the expression of genes involved in the synthesis of the ω7 C16:1-ACP (*AAD2* and *AAD3*) mainly in the endosperm of Arabidopsis seeds (Troncoso-Ponce *et al.*, 2016). Unlike MYB96 and MYB115, MYB118 also acts as negative regulator of seed maturation. This transcription factor is, indeed, involved in the inhibition of LEC2, therefore repressing physiological processes involved in Arabidopsis seed maturation (Barthole *et al.*, 2014). MYB89, MYB79 and MYB123 negatively regulates FA synthesis **(Figure 14)**. MYB89 inhibits the expression of *WRI1* and *L1L*, as well as the expression of several FA- and glycerolipid-related genes, including *BCCP*, *KAS I*, *KCS*, *PLA2*, *FAE1*, *FAD2* and *FAD3* (Li *et al.*, 2017). MYB76 downregulates the expression of some FA- and lipid-related genes, including *FAD2*, *FAD3* and *FAE1* (Duan *et al.*, 2017). MYB123 reduces the expression of *FUS3*, therefore inhibiting seed oil synthesis in Arabidopsis. In addition, this transcription factor decreases VLCFA content by repressing the expression of *FAE1* (Wang *et al.*, 2014).

TRANSPARENT TESTA GLABRA 1 (TTG1) inhibits the expression of several FA-related genes, including *FAE1*, *FAD2*, *FAD3* and *BCCP2*, and genes involved in the synthesis of seed storage proteins. In developing seeds, FUS3 reduces the expression of *TTG1*, therefore decreasing the inhibitory action of TTG1 on the expression of genes involved in FA synthesis and storage protein accumulation. The reduction of *TTG1* expression thus results in promoting FA and storage protein synthesis. In order to maintain the rate of storage protein and FA accumulation in developing seeds, TTG1 can negatively regulate the expression of *LEC2* and *ABI3*, both transcription factors that positively modulates the expression of *FUS3*. The reduction of the expression of *FUS3* through the inhibition of LEC2 and ABI3 increases the expression of *TTG1*, therefore decreasing the expression of genes involved in FA and storage protein accumulation (Chen *et al.*, 2015). TRANSPARENT TESTA 8 (TT8) is a transcription factor that decreases the expression of several regulators involved in seed maturation, like *LEC1*, *LEC2* and *FUS3*. The expression of several FA- and glycerolipid-related genes (*CDP-DAG SYNTHASE*, *KAS II*, *FAB2*, *FAE1*, *FAD2* and *FAD3*) are down-regulated by TT8 (Chen *et al.*, 2014).

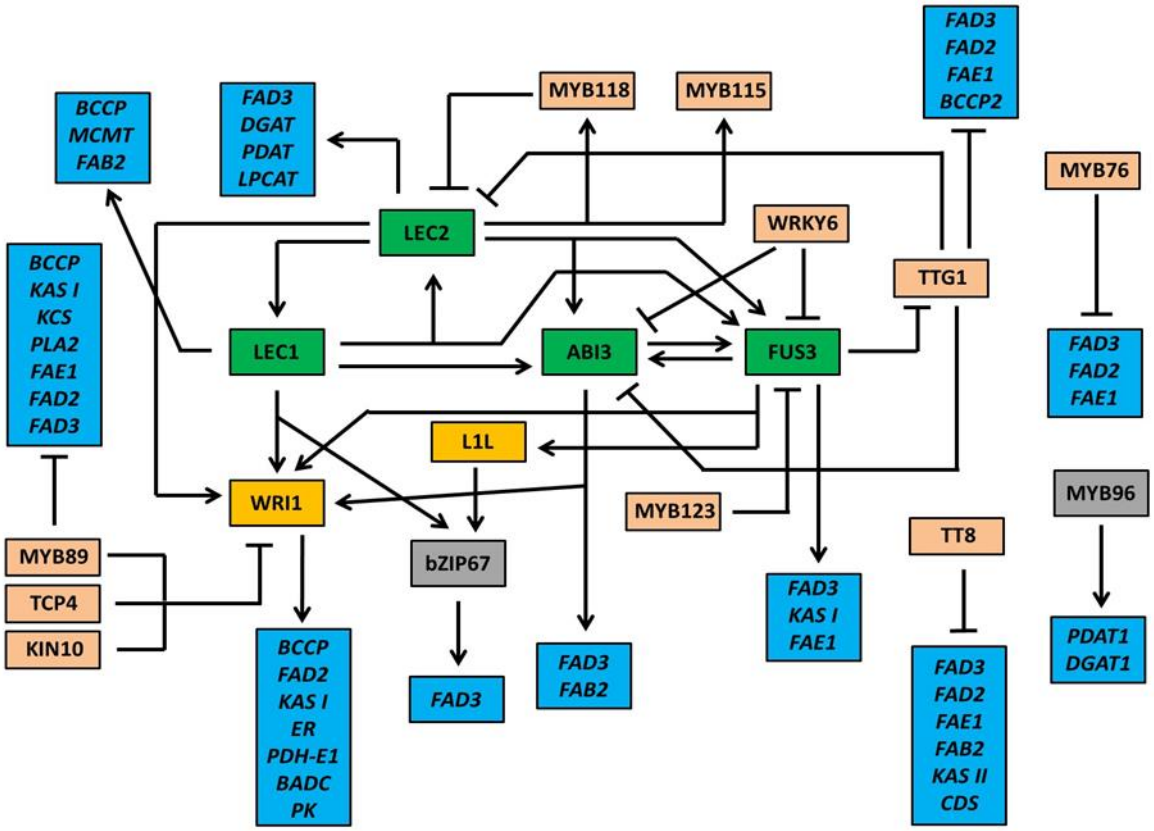

Figure 14. Transcription factors regulating FA and glycerolipid metabolism in Arabidopsis seeds. *In this figure, primary regulators, including LEAFY COTYLEDON 1 (LEC1), LEAFY COTYLEDON 2 (LEC2), ABSCISIC ACID INSENSITIVE 3 (ABI3) and FUSCA 3 (FUS3), are represented by green boxes. Secondary regulators, including WRINKLED 1 (WRI1) and LEC1-like (L1L), are illustrated by orange boxes. FA- and glycerolipid-related genes are represented by blue boxes. Pink boxes correspond to transcription factors that negatively regulates the expression of FA-related genes, as well as the expression of genes encoding for the primary and secondary regulators. Grey boxes correspond to transcription factors that positively regulates the expression of FA-related genes. Abbreviation: TCP4, TEOSINTE BRANCHED1/CYCLOIDEA/PROLIFERATING CELL FACTOR 4; BCCP, Biotin carboxyl Carrier Protein; FAD, FA desaturase; KAS, 3-ketoacyl-ACP synthase; ER, enoyl-ACP reductase; FAE1, FA elongase 1; DGAT1, diacylglycerol acyltransferase; PLA2, phospholipase A2; PDH-E1, component E1 of the pyruvate dehydrogenase complex; KCS, β-ketoacyl-CoA synthase; MCMT, malonyl-CoA: ACP transacylase; FAB2, FA biosynthesis 2; PDAT, phospholipid: DAG acyltransferase; LPCAT, lysophosphatidylcholine acyltransferase; CDS, CDP-DAG synthase; TTG1; TRANSPARENT TESTA GLABRA 1; TT8; TRANSPARENT TESTA 8 . Adapted from Kumar et al. (2020).*

3. Diurnal and circadian regulation of glycerolipid metabolism

Physiological processes associated to seed maturation, including seed oil accumulation, are tightly regulated through the action of a complex regulatory network composed of WRI1, LEC1, L1L, LEC2, ABI3, FUS3 and other transcription factors (Kumar *et al.*, 2020). It is well known that, in plants, physiological processes can also be rhythmically regulated by light within successive 24h light/dark cycles, this regulation is referred as diurnal. The synthesis of several glycerolipids is diurnally regulated, therefore describing an oscillatory profile within successive 24h light/dark cycles (Nakamura *et al.*, 2014a). The oscillation of these glycerolipids is considerably affected when plants are exposed from long-day to short-day conditions and is no longer observed under continuous light conditions (Nakamura *et al.*, 2014a; Nakamura, 2018). The composition of diurnally-regulated glycerolipids can be predicted since the oscillatory profile of these biomolecules remains similar between current and subsequent 24h light/dark cycles **(Figure 15)**.

Plants are constantly exposed to rhythmic environmental changes, including rhythmic variation of light (light/dark cycles) and temperature imposed by Earth's rotation. Plants, as sessile organisms, are not able to escape from these rhythmic external fluctuations. The anticipation to these rhythmic environmental changes is critical for maintaining plant physiology (Alfredo *et al.*, 2011). Another regulatory network, also composed of transcription factors, is involved in the regulation of physiological processes at a specific time of the day and night. This regulatory network, referred as the circadian clock, allows the anticipation of rhythmic environmental fluctuations. The circadian system is divided into three parts, including the input pathway, the central oscillator (circadian clock) and the output pathway **(Figure 16A)** (Mas, 2005; Oakenfull *et al.*, 2017). The input pathway consists in the perception of rhythmic external changes, including the increase of light and temperature, by photoreceptors (phytochrome and cryptochrome) and the transmission of these external information to the central oscillator. The synchronization of the central oscillator with the external environment allows the expression of clock transcription factors at a specific time of the daily light/dark cycle **(Figure 16A)**. Once expressed, transcription factors belonging to the central oscillator tightly control the expression of other clock components at a specific moment of the daily light/dark cycles, therefore providing timing information to the plant **(Figure 16B)**. The output pathway enables the synchronization of multiple physiological

processes with the daily light/dark cycles through the regulation of target genes by clock components at a specific moment of the day and the night **(Figure 16A)**. It is well known that clock components regulate the expression of several physiological processes, including lipid and carbohydrate synthesis, photosynthesis, flowering and stomatal aperture, at a specific time of the daily light/dark cycles (Mizoguchi *et al.*, 2005; Dodd *et al.*, 2005; Graf *et al.*, 2010; Pokhilko *et al.*, 2013; Hsiao *et al.*, 2014).

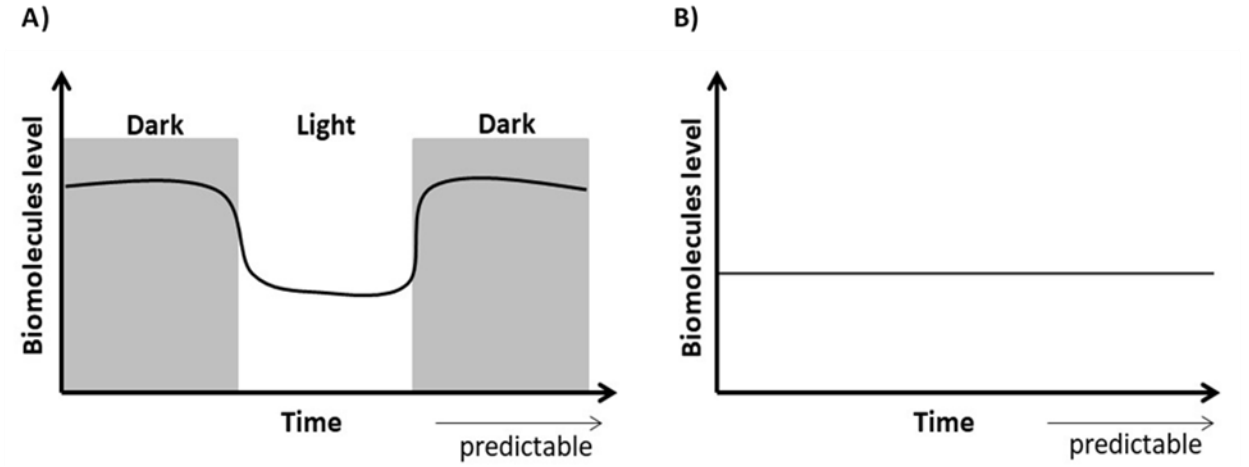

Figure 15. Diurnal regulation of biomolecule synthesis. *In plants, the synthesis of biomolecules can be rhythmically controlled by light within a 24h light/dark cycles. The composition of biomolecules can be rhythmically modified within a 24h light/dark cycle. A diurnal oscillatory profile can be observed within 24h light/dark cycle. A) This figure is an example of the diurnal oscillatory profile of biomolecules within 24h light/dark cycle. B) Diurnal oscillation, observed in A), is no longer observed when plants are exposed to continuous light conditions. Adapted from Nakamura et al. (2014) and Nakamura (2018).*

The circadian clock is composed of negative feedback loops. The negative central loop of the circadian clock is constituted of two morning expressed MYB-like transcription factors CIRCADIAN CLOCK ASSOCIATED 1 (CCA1) and LATE ELONGATED HYPOCOTYL (LHY) and a single evening expressed pseudo-response regulator (PRR) TIMING OF CAB EXPRESSION 1 (TOC1, also known as PRR1) **(Figure 16B)** (Alabadi *et al.*, 2001; Gendron *et al.*, 2012). The increase in the expression of *CCA1* and *LHY* at the beginning of the day period results in the inhibition of the expression of *TOC1* **(Figure 16B)** (Alabadi *et al.*, 2001). Conversely, TOC1 negatively regulates the expression of *CCA1* and *LHY* during the night **(Figure 16B)** (Gendron *et al.*, 2012). The other clock transcription factors, including the PSEUDO-RESPONSE REGULATOR (PRR) family (PRR5, PRR7 and PRR9), GIGANTEA (GI), ZEITLUPE (ZTL), EARLY FLOWERING 3 (ELF3), EARLY FLOWERING 4 (ELF4) and LUX ARRHYTHMO (LUX), are mainly involved in the reciprocal regulation of the expression of *CCA1*/*LHY* and *TOC1* during the day and the night, respectively **(Figure 16B)** (Adams *et al.*, 2015; Locke *et al.*, 2006).

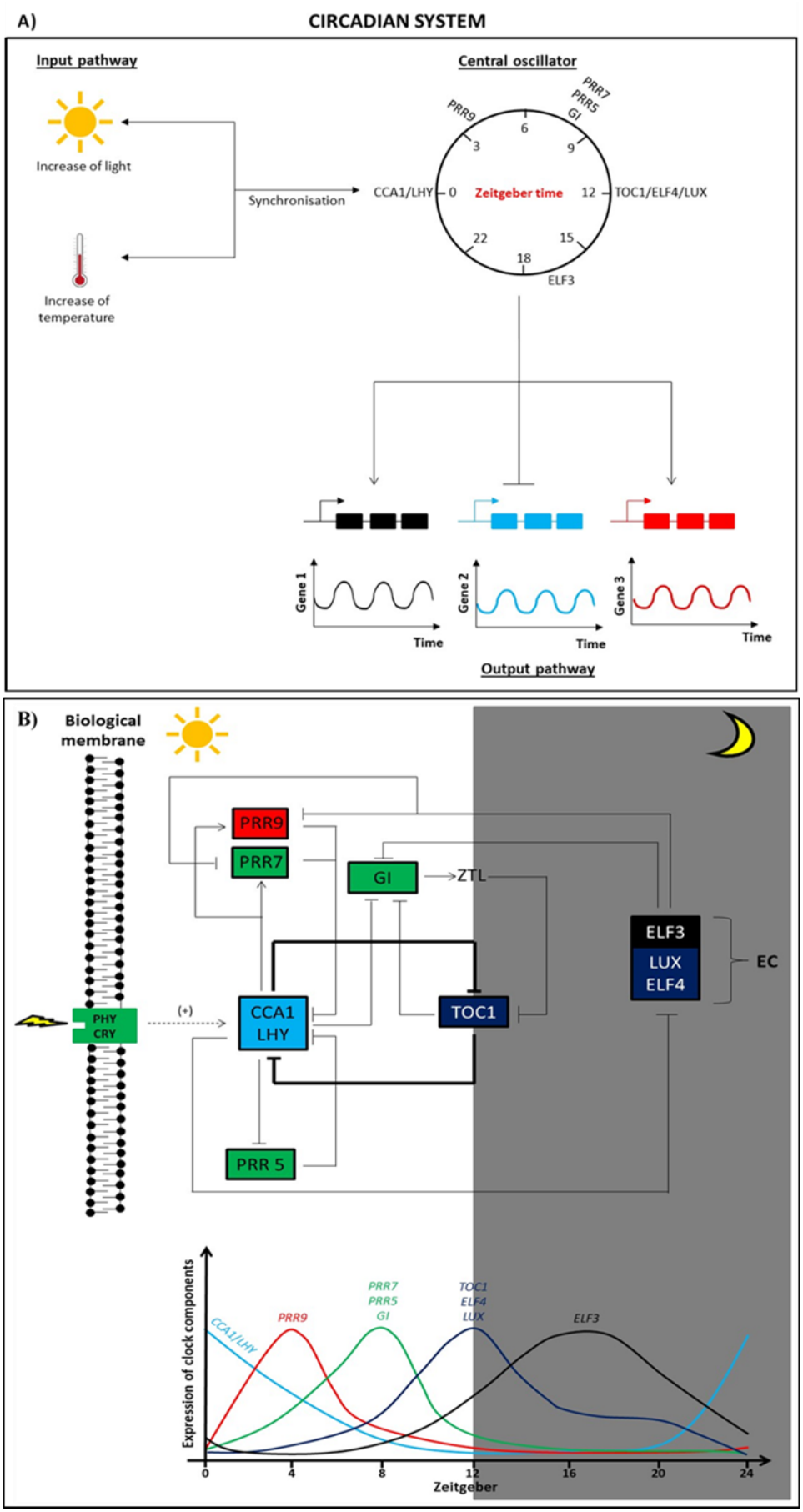
A)
CIRCADIAN SYSTEM
Input pathway
Increase of light
Increase of temperature
Synchronisation
Central oscillator
PRR9
PRR7
PRR5
GI
CCA1/LHY
Zeitgeber time
TOC1/ELF4/LUX
ELF3
Gene 1
Gene 2
Gene 3
Time
Output pathway
B)
Biological membrane
PRR9
PRR7
GI
ZTL
ELF3
LUX
ELF4
EC
PHY
CRY
(+)
CCA1
LHY
TOC1
PRR 5
Expression of clock components
PRR9
PRR7
PRR5
GI
TOC1
ELF4
LUX
ELF3
CCA1/LHY
Zeitgeber

Figure 16. The circadian system in plants. *A) This figure illustrates the circadian system composed of three parts: the input pathway, the central oscillator (circadian clock) and the output pathway. B) On the upper part of the figure is proposed a model for the plant circadian clock. The perception of light by phytochrome (PHY) and cryptochromes (CRY) enables the central oscillator to work. The central oscillator is composed of CCA1/LHY-TOC1 central loop, which is represented by two bold inhibitor arrows. Other transcription factors enable the regulation of clock component belonging to the central loop. Transcription factors that are represented with same color are expressed at the same time. On the lower part of the figure is provided the timing expression (expressed in Zeitgeber with Zeitgeber 0 corresponding to dawn) of each clock components. Abbreviations: CCA1, CIRCADIAN CLOCK-ASSOCIATED 1; LHY, LATE ELONGATED HYPOCOTYL; TOC1, TIMING OF CAB EXPRESSION 1; PRR, PSEUDO-RESPONSE REGULATOR; GI, GIGANTEA; ZTL, ZEITLUPE; ELF, EARLY FLOWERING; LUX, LUX ARRHYTHMO; EC, evening complex. Adapted from Huang and Nusinow (2016).*

The expression of each clock component is expressed in Zeitgeber time (ZT), a unit of time based on a precise moment within a 12h light/12h dark cycle. In a 12h light/12h dark cycle, ZT0 corresponds to the time of light on or dawn and ZT12 is the time of light off or dusk. The expression of *CCA1*/*LHY* and *TOC1* oscillates in a 24h period reaching a maximum at dawn (ZT0) in the case of *CCA1* and *LHY* and at dusk (ZT12) for *TOC1* **(Figure 16B)** (Huang and Nusinow, 2016). The expression of the other transcription factors also oscillates in a 24h period reaching maximum of expression at ZT4 for *PRR9*, ZT8 for *PRR5*, *PRR7* and *GI*, ZT12 for *ELF4* and *LUX* and between ZT16 and 18 for *ELF3* **(Figure 16B)** (Huang and Nusinow, 2016).

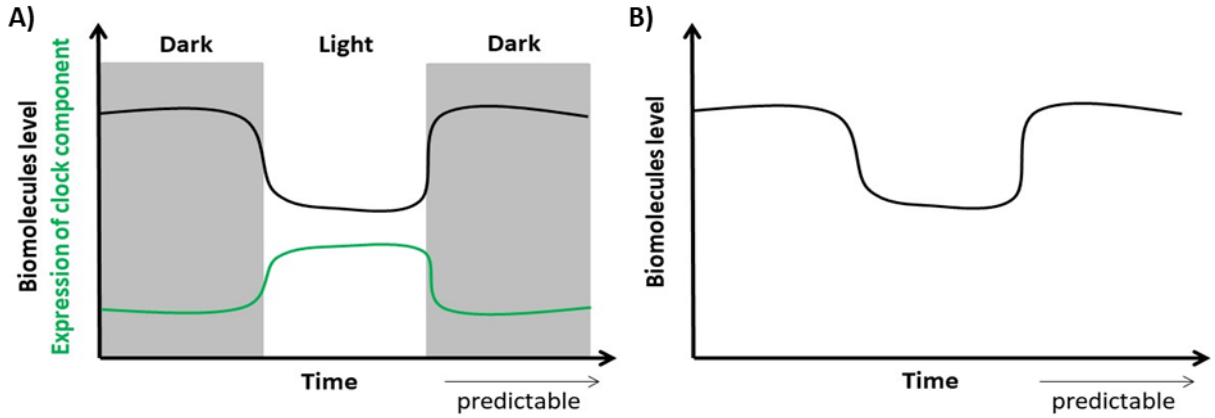

Figure 17. Circadian regulation of biomolecule synthesis. *In plants, the synthesis of biomolecules can be rhythmically controlled by transcription factors belonging to the circadian clock. A) The composition of biomolecules under the control of clock components oscillates simultaneously with the oscillatory expression profile of the corresponding clock components within a 24h light/dark cycle. B) The composition of biomolecules regulated by the circadian clock still oscillates in continuous light conditions. Adapted from Nakamura (2018).*

Each of these clock components provides timing information to the plant, which is crucial for ensuring their biological functions at a specific time of the day or night (Roden *et al.*, 2002). Once expressed, clock components can regulate the expression of genes involved in many physiological processes (photosynthesis, carbohydrate synthesis, flowering, stomatal aperture, etc) at a specific moment of the day or night. The expression of genes controlled by the circadian clock oscillates in a 24 h period. A correlation should be observed between the

oscillatory expression of a given clock component and the oscillatory expression of genes controlled by this clock component (Nakamura *et al.*, 2014b). The oscillatory expression of genes controlled by the circadian clock remains unchanged during diurnal changes (short-day to long-day) or exposition of plants to continuous conditions **(Figure 17)** (Nakamura, 2018).

3.1. Diurnal regulation of lipid metabolism

Genes and enzymes involved in FA and glycerolipid synthesis can be diurnally regulated by light. It was revealed that the *de novo* intraplastidial FA synthesis is preferentially performed during the light period since the activity of the plastidial acetyl-CoA carboxylase (ACC) in plants is higher in light than in dark condition (Ohlrogge *et al.*, 1997; Hunter *et al.*, 1998). A diurnal oscillatory profile has been observed for C18:1, C18:2 and C18:3 in Arabidopsis leaves exposed under long-day condition (16h light/8h dark). The synthesis of C18:1 is increased in light and decreased in dark, while the production of C18:2 and C18:3 is conversely increased in dark and reduced in light (Ekman *et al.*, 2007). The diurnal profile observed for C18:2 and C18:3 is not directly explained by a diurnal regulation of C18:1 and C18:2 desaturase enzymes. It was rather proposed that the diurnal profile observed for C18:2 and C18:3 is due to the positive action of light on the *de novo* intraplastidial FA synthesis combined with the desaturation of C18:1 and C18:2 that are neither stimulated nor inhibited by light (Browse *et al.*, 1981). Nakamura *et al.* (2014a) have then studied the potential diurnal oscillatory profile of PC and PE species in Arabidopsis seedlings exposed in short- (8h light/16h dark) and long-day (16h light/8h dark) conditions. A diurnal oscillatory profile was observed for PC species under short- and long-day, while a more stable profile was noticed for PE species under short- and long-day. It was shown that the synthesis of PC species containing polyunsaturated FA, including PC 36:5 and 36:6, is increased in dark condition and decreased in light condition. Conversely, the synthesis of PC containing less polyunsaturated FA (PC 36:1, PC 36:2, PC 36:3 and PC 34:1) is increased in light period and decreased in dark period. The diurnal oscillatory profile of PC species observed in Arabidopsis seedlings reflects the diurnal oscillatory profile of FA obtained in previous studies **(Figure 18)** (Browse *et al.*, 1981; Ekman *et al.*, 2007). Maata *et al.* (2012) have been focused on the diurnal oscillatory profile of other glycerolipids in Arabidopsis leaves exposed in 12h light/12h dark cycles. The synthesis of all PA and PS species is increased in dark condition, while PG and MGDG species are synthesized either in light or dark periods according to their constitution in FA as previously shown for PC

(Nakamura *et al.*, 2014a). PG and MGDG containing less polyunsaturated FA (PG 34:1; MGDG 34:2, MGDG 34:3 and MGDG 36:2) are rather produced in light than in dark condition, while PG and MGDG containing at least a single C18:3 (PG 34:3 and PG 36:3; MGDG 34:6 and MGDG 36:6) are rather synthesized in dark than in light periods which is consistent with the diurnal oscillatory profile of polyunsaturated FA described in previous studies **(Figure 18)** (Browse *et al.*, 1981; Ekman *et al.*, 2007).

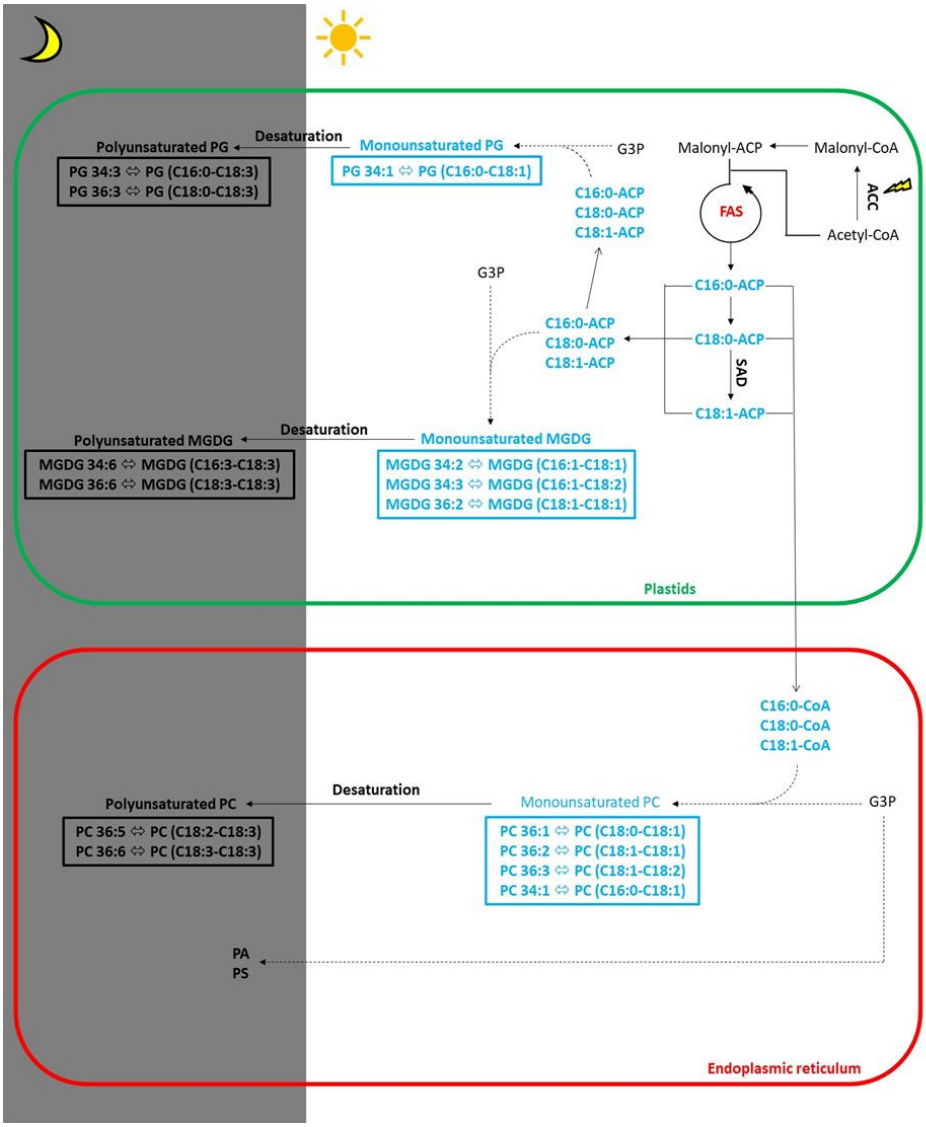

Figure 18. Diurnal regulation of FA and glycerolipid synthesis. *In this figure, the yellow lightning corresponds to the diurnal and positive regulation of ACC by light. FA and glycerolipids synthesized during light and night periods are represented in blue and black bold, respectively. The activity of ACC increases in presence of light and decreases in the lack of light, while the activity of C18:1 and C18:2 desaturases remain unchanged in presence and lack of light. C18:1 is no longer accumulated during the night period but still converted into C18:2 and C18:3. This results in the decrease of C18:1 content and the increase of C18:2 and C18:3 content during the night period. Adapted from Nakamura et al. (2014) and Maata et al. (2012).*

3.2. Regulation of lipid metabolism by the circadian clock

3.2.1. Potential regulation of lipid-related genes by circadian clock

Previous studies have been performed with the aim of the identification of lipid-related genes potentially under the control of the circadian clock in plants (Hudson, 2010; Nakamura *et al.*, 2014b). Soybean plants have first been exposed to 12h light/12h dark conditions for 10 weeks and then in 24h continuous light conditions for three days. In continuous light conditions, each 24h period can be divided into two intervals of 12h in which plants are first exposed to light and then under subjective dark (12h light/12h subjective dark). Subjective dark refers to a light exposure interval of 12h that corresponds to the portion of the diurnal cycle in which plants were exposed to dark. Soybean seeds were harvested each 4h between 24 and 72h after the exposition of plants to continuous light (Hudson, 2010). In order to identify genes under the clock control in soybean seeds, transcriptomic analysis was performed on microarray containing probes that represents 26,006 genes potentially expressed in developing soybean seeds. Genes presenting cycling profiles in continuous light were identified. Hudson (2010) has revealed cycling expression profile in continuous light for 479 genes in soybean developing seeds. Further analysis has shown that 14 genes with predicted functions in lipid synthesis are controlled by the circadian clock (Hudson, 2010). This includes *FAD2*, a gene involved in the introduction of double bonds to monounsaturated FA moieties PC (Okuley *et al.*, 1994; Hudson, 2010). An online Arabidopsis circadian microarray data referred as the “Diurnal” tool (http:// diurnal.mocklerlab.org/) was then used in order to identify ortholog genes potentially under the clock control in Arabidopsis seedlings and leaves. This *in silico* study was performed by focusing on the 479 genes that revealed cycling expression profiles in continuous light conditions in soybean seeds (Hudson, 2010). Circadian expression pattern has been observed for a total of 221 ortholog genes, while the potential role of the circadian clock in the regulation of 236 ortholog genes has not been shown in Arabidopsis leaves and seedlings (Hudson, 2010).

Nakamura *et al.* (2014b) have studied the potential role of the circadian clock in the regulation of the expression of glycerolipid-related genes in Arabidopsis leaves using public microarray data found in the “Diurnal” tool (http:// diurnal.mocklerlab.org/). Using this online software, the oscillatory expression of glycerolipid-related genes was reconstituted in short-day (SD: 8 h light/16 h dark), long-day (LD: 16 h light/8 h dark) and continuous light (LL:

24 h exposed in light) conditions. The expression of glycerolipid-related genes was supposed to be diurnally controlled if the oscillatory expression of these genes is affected between SD and LD, while the expression of glycerolipid-related genes is supposed to be regulated by the circadian clock if the oscillatory expression profile of these genes is unchanged between SD and LD and still observed in LL. This *in silico* study has revealed an oscillatory expression profile for 12 glycerolipid-related genes in Arabidopsis leaves. 9 over these 12 glycerolipid-related genes have shown to be potentially regulated by the circadian clock since the oscillatory expression of these 9 genes seems to be not affected between SD and LD and still observed in LL **(Figure 19)**. These 9 genes correspond to the CDP-DAG synthase (*CDS1,4*), LPA acyltransferase (*LPAT5*), aminoalcohol aminophosphotransferase (*AAPT2*), choline kinase (*CK5*), CTP: phosphorylethanolamine cytidyltransferase (*PECT1*), PS decarboxylase (*PSD3*), DAG acyltransferase (*DGAT1*), phospholipid: DAG acyltransferase (*PDAT1*) and DGDG synthase (*DGD1*) (Nakamura *et al.*, 2014b).

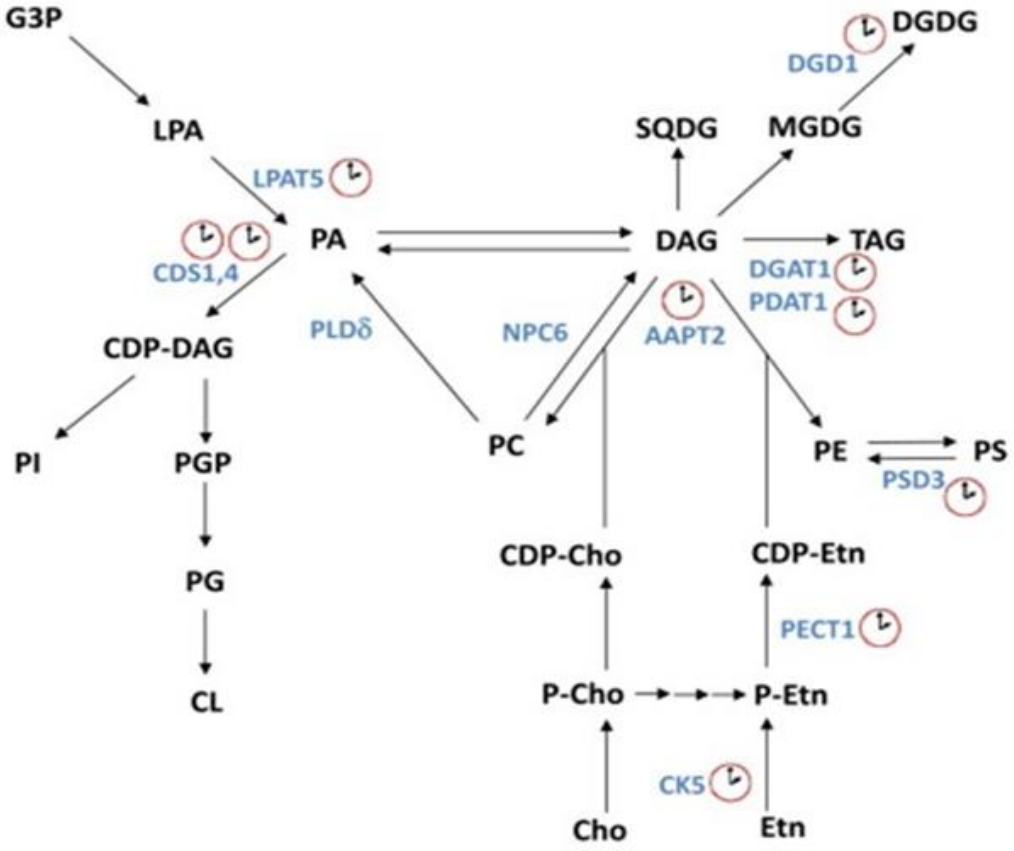

Figure 19. Circadian and diurnal regulation of glycerolipid-related genes. *In silico studies has been performed using microarray data contained within an online database (http:// diurnal.mocklerlab.org/). These microarray data were generated from plants exposed to SD, LD and LL. Genes written in blue are potentially regulated by light, while enzymatic reactions represented by clock are potentially regulated by circadian clock (Nakamura et al., 2014).*

The potential role of the circadian clock in the regulation of the expression of *PECT* was then experimentally checked by comparing the oscillatory expression profile of *PECT* between SD and LD. It was shown that the oscillatory expression of *PECT* is not affected by the diurnal changes (from SD to LD) and well correlated with the oscillatory expression of *GI*, confirming what it was suggested by *in silico* study regarding the role of the circadian clock in the regulation of *PECT*.

3.2.2. Role of CCA1/LHY in the control of glycerolipid-related genes

The potential role of CCA1/LHY in the regulation of glycerolipid metabolism has first been studied in germinating Arabidopsis seeds (Hsiao *et al.*, 2014). It was first revealed that the amount of FA and TAG is similar between mature *cca1lhy* and wild-type seeds. Differences in the amount of these biomolecules increases between *cca1lhy* and wild-type seedlings from four to five days after germination. At this developmental stage, the amount of FA and TAG is higher in *cca1lhy* than wild-type seedlings. Oil bodies are still retained five days after germination in *cca1lhy* seedlings, while no longer observed in the wild-type. Results generated by Hsiao *et al.* (2014) have been explained by lower expression of genes involved in the β-oxidation (*MFP2*, *KAT2* and ACX2) in *cca1lhy* than in wild-type during the germination. Hsiao et al., (2014) have shown that CCA1/LHY is involved in the mobilization of storage lipids during germination through its role in the regulation of β-oxidation genes.

PA, besides a precursor of other glycerolipids, including membrane and storage lipids, is a molecule involved in signal transduction, vesicle trafficking and other cellular functions (Wang *et al.*, 2006; Testerink and Munnik, 2011; Bullen and Soldati-Favre, 2016). PA species can specifically interact with proteins modulating their activities (Zhang *et al.*, 2004). Recently, the potential regulation of clock components by PA has been studied by Kim *et al.* (2019). It was first shown that CCA1/LHY interacts with PA species, decreasing the interaction of both morning MYB-like transcription factors with *TOC1* promoter. The oscillatory expression profile of *TOC1* has a period close to 24 h in the wild-type. This period increases to 25.7 h in *pah*, a mutant characterized by the increase in PA biosynthesis. It was revealed that PA negatively regulates the circadian rhythm. The potential role of CCA1/LHY in the regulation of glycerolipids synthesis has also been studied in Arabidopsis *cca1lhy* and wild-type seedlings grown in 16 h light/8 h dark (Kim *et al.*, 2019). Lipid oscillation has been reconstituted for 36:4 PG, 38:5 PS, 36:6 PA and 34:4 PA in the wild-type but no longer observe in *cca1lhy*. The

synthesis of PA in Arabidopsis seedlings is under the control of the morning MYB-like CCA1/LHY. Taken altogether, Kim *et al.* (2019) have revealed that CCA1/LHY is involved in the synthesis of PA, while the accumulation of this glycerolipid intermediate affects the circadian rhythm in order to control glycerolipid level within plant cells.

SECTION 2: PhD PROJECT

PhD PROJECT

1. Biological context

Arable land is constantly decreasing simultaneously with the increase of the World's population and the negative effect of the climate changes[3]. Redistributing of arable land, particularly to northern and cooler latitudes (Zabel *et al.*, 2014) will require adaptation of crops to new daylengths. The development and survival of plants can be considerably affected when exposed to new environmental fluctuations. The presence of the circadian clock in plants allows anticipating these new rhythmic environmental fluctuations and maintaining plant physiology (Mas, 2005; Oakenfull *et al*., 2017). It is well known that the circadian clock is involved in the regulation of several physiological processes, including the carbohydrate synthesis, the photosynthesis, the flowering and the stomatal aperture (Mizuguchi *et al.*, 2005; Dodd *et al.*, 2005; Graf *et al.*, 2010; Pokhilko *et al.*, 2013). However, the potential involvement of the circadian clock in the synthesis of seed storage oils, the main component of commercial vegetable oils, has been sparsely studied. Previous *in silico* studies have revealed a potential role of the circadian clock in the regulation of several lipid-related genes in leaves (Nakamura *et al.*, 2014b); Hsiao *et al.,* (2014) and Kim *et al.,* (2019) have shown respectively that the mobilization of storage lipids in germinating Arabidopsis seeds and the synthesis of PA in Arabidopsis seedlings are under the control of the morning MYB-like CCA1/LHY clock components. Microarray analysis has also shown that a total of 14 lipid-related genes are under the control of the circadian clock in soybean developing seeds (Hudson, 2010). The study of the connection between the internal timekeeper and seed lipid metabolism could help understanding the role played by the former in the synthesis and accumulation of seed reserves.

2. Objective and strategies of the current PhD project

To the best of our knowledge, the interaction between components of the central oscillator of the circadian system (CCA1/LHY, PRR5, PRR7, PRR9 and TOC1) and lipid metabolism in Arabidopsis seeds has been only partially addressed. The objective of this PhD project is investigating the connection between these two important physiological processes.

[3] FAO, World agriculture towards 2030/2050. FAO Headquarters, Rome, 1-147 June. 2012.

2.1. Identification of clock components involved in FA and glycerolipid synthesis in seeds

The first and second part of the PhD project consisted in the identification of clock components potentially participating in the regulation of FA and glycerolipid metabolism in Arabidopsis seeds. FA and glycerolipids profiles were characterized in Arabidopsis mature seeds **(Step 1 and 2, Figure 20)** from different circadian clock mutants (*toc1-1*, *toc1-2*, TOC1-ox, *prr5-1*, *prr7-3*, *prr9-1* and *cca1-11 lhy-21*) and respective wild-types (WT: C24, Col-0 and Ws). Clock components were identified as potentially involved in the regulation of FA and glycerolipid synthesis if significant differences were observed between clock mutants and their respective WT. Clock mutants associated to high FA and glycerolipid composition changes in Arabidopsis seeds were then selected for further characterization of their FA and glycerolipid profile in seedlings and leaves. The objective was revealing if the regulation of FA metabolism potentially observed in seeds was specifically associated to seed maturation **(Figure 20)**.

2.2. Identification of glycerolipid-related genes under the control of clock components

Once clock components associated to FA synthesis were identified, the third part focused on identifying lipid-related genes under the control of these transcription factors. In order to identify these target genes, the expression level of several potentially controlled genes was compared between developing mutant seeds and their WT **(Step 3, Figure 20)**.

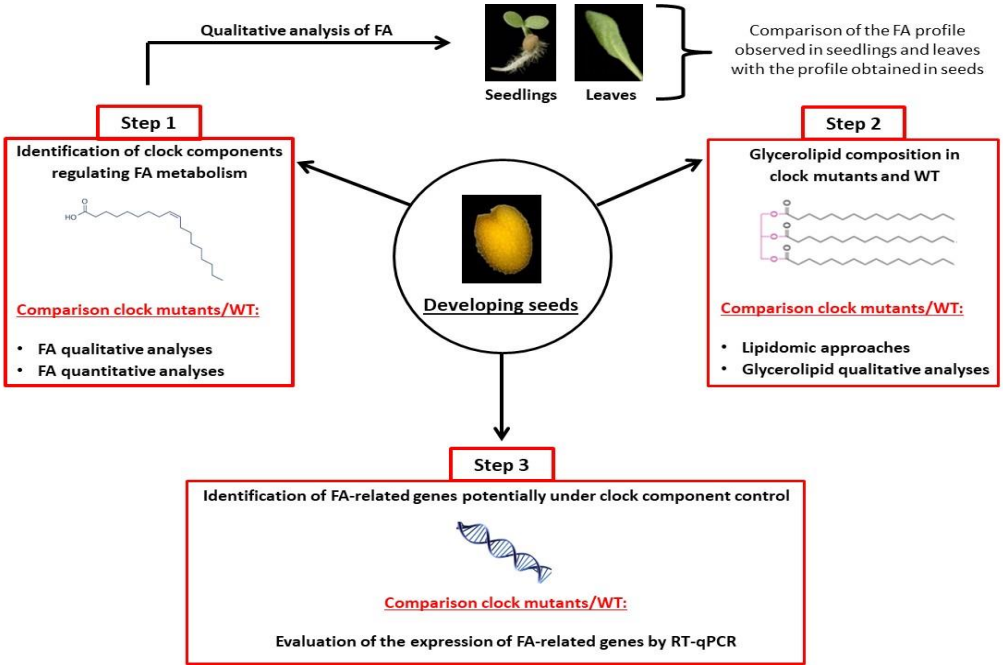

Figure 20. Strategies of the PhD project. *The PhD project is divided into three main steps. The first and second step consists in identifying clock components involved in the regulation of FA and glycerolipid metabolism. The third step enables the identification of glycerolipid-related genes under the control of clock components.*

SECTION 3: MATERIALS AND METHODS

MATERIALS AND METHODS

1. Biological materials and growth conditions

1.1. Arabidopsis mature seeds

The *Arabidopsis thaliana* (L.) accession Columbia (Col-0), C24, Ws and mutants used in this project are summarized in **Table 1**. These mutants, *toc1-1*, *toc1-2*, TOC1-ox, *prr5-1*, *prr7-3*, *prr9-1* and *cca1-1 lhy-21* were kindly provided by Dr. Manuel Rodriguez-Concepcion (Institute of Molecular & Cellular Biology of Plants, Spain), Dr. Takafumi Yamashino (Nagoya University, Japan), Dr. Elena Monte (Center for Research in Agricultural Genomics, Spain) and Professor Mee Len Chye (The University of Hong Kong).

Both *toc1-1* and *toc1-2* mutants were characterized and described in the literature (Strayer *et al.*, 2000; Millar *et al.*, 1995). The loss-of-function *toc1-1* mutant was generated from C24 ecotype, while *toc1-2* mutant comes from Col-0 background. In the *toc1-1* mutant, a missense mutation is present in the exon 6 of *TOC1* gene. The modification of a cytidine into thymidine was responsible of the production of a mutated TOC1 protein in which the alanine 562 of the DNA-binding domain was changed into a valine residue. The consequence of this mutation was a reduction of the DNA-binding properties of TOC1 (Gendron *et al.*, 2012). In the loss-of-function *toc1-2* mutant, the mutation was performed in the exon 1 of *TOC1* gene. The *toc1*-2 mutation is characterized by a modification of the last guanidine of the exon 1 into adenosine. The consequence of this mutation is a production of 94 % of *TOC1* transcript in which the 13 nucleotides following the sequence of the exon 1 were not correctly spliced in *toc1-2*, whereas the splicing has been performed between the exon 1 and 2 for only 6 % of *TOC1* transcript in the same mutant. Thereby, *toc1-2* Arabidopsis mutant was mainly involved in the production of truncated and non-functional TOC1 protein composed of only 59 amino acids, while the non-truncated protein was sparsely produced and characterized by a valine modified into methionine within the receiver domain. The development of *toc1-2* plant was also greatly altered by the mutation as evidenced by its dwarf size in comparison with its respective WT (Col-0) **(Figure 21)**.

The overexpressing TOC1 mutant (TOC1-ox) was provided by Dr. Yamashino. TOC1-ox mutant was generated from Columbia-0 (Col-0). The overexpression of *TOC1* gene was performed by the insertion of the amplified *TOC1* cDNA fragment within a plasmid

containing the *Cauliflower mosaic virus* 35S promoter (Makino *et al.*, 2002).

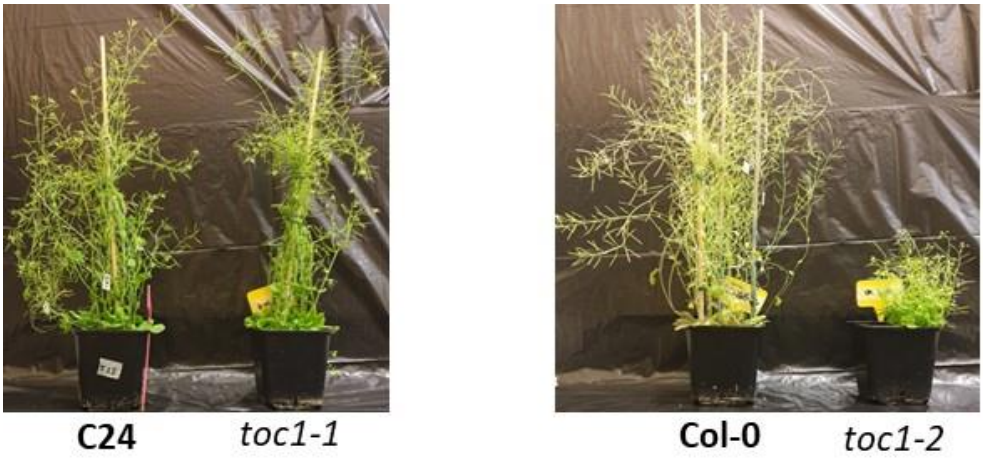

Figure 21. Phenotype of *toc1* and respective WT plants. *The morphology of each toc1 mutant was compared with its respective WT. The development of toc1-2 plants is considerably altered in comparison with its respective WT Col-0.*

The loss-of-function *cca1-11 lhy-21* was generated from Ws. This double mutant was generated by crossing *cca1-11* with *lhy-21*. The *lhy-21* and *cca1-11* simple mutants were created by the insertion of the T-DNA in the exon 7 of the *LHY* sequence and the region 80 bp upstream from the ATG codon of the *CCA1* sequence, respectively (Hall *et al.*, 2003).

The *prr5-1*, *prr7-3* and *prr9-1* mutants were generated from Col-0. The *prr5-1* mutant was created by the insertion of T-DNA in the first exon upstream to the initiation codon in the 5'UTR region of *PRR5*. In *prr7-3* mutant, T-DNA was inserted in the exon 2 of *PRR7* downstream to the initiation codon. The *prr9-1* mutant was characterized by the insertion of T-DNA in the exon 2 of *PRR9* downstream to the initiation codon (Michael *et al.*, 2003).

Table 1. List of circadian clock mutants and respective WT

Mutant	Type of mutation	WT
toc1-1	Substitution in exon 6 of *TOC1*	C24
toc1-2	Substitution in exon 1 of *TOC1*	Col-0
TOC1-ox	Overexpression of *TOC1* using *35S::TOC1* plasmid	Col-0
prr5-1	T-DNA insertion	Col-0
prr7-3	T-DNA insertion	Col-0
prr9-1	T-DNA insertion	Col-0
cca1-11 lhy-21	T-DNA insertion in *CCA1* (*cca1-11*) and *LHY* (*lhy-21*) Crossing between *cca1-11* and *lhy-21*	Ws

1.2. Harvesting of 16 days after flowering (DAF) Arabidopsis developing seeds

1.2.1. Step 1: Pre-culture of Arabidopsis seeds in Murashige and Skoog medium

Seeds were pre-cultivated in Murashige and Skoog medium (MS medium). MS medium was first prepared using the protocol described by Lindsey *et al.* (2017). The medium was prepared for a total volume of 500 mL. Thereby, 2.15 g of "Murashige and Skoog (MS) Basal Medium" powder was first added to 200 mL of milli-q water. MS medium contains phosphate as a source of energy (170 mg/L of potassium phosphate monobasic), 2 mg/L of glycine as a source of amino acids, enzymatic cofactors (0.1 mg/L of thiamine, 0.5 mg/L of pyridoxine, 0.5 mg/L of nicotinic acid and 100 mg/L of myo-inositol) and microelements containing magnesium, calcium, iron and manganese. 5 g of sucrose (1 % w/v: 10 g/L) were also introduced to the 200 mL of dissolved MS medium for promoting Arabidopsis growth (Eckstein *et al.*, 2012). 1M KOH was then carefully added to stabilize the pH value at 5.7. Finally, 4 g of agar and 300 mL of milli-q water was added to the 200 mL of sucrose-containing MS medium. In order to avoid micro-organisms contamination, the medium was immediately autoclaved at 121 °C for 20 min. The autoclaved medium was poured in Petri dishes under sterile conditions. Petri dishes were then sealed with paraffin plastic film and stored at 4 °C.

The sterilization of WT and mutant seeds was performed prior to seed preculture in order to prevent contamination **(Step 1, Figure 22)**. This step was carried out in a laminar flow hood. Seeds were first sterilized by adding 1 mL of 70 % ethanol + 0.01 % of SDS in 1.5 mL tube for 3 min and shaken in the meantime. The supernatant was then removed and seeds were washed twice with 1 mL of autoclaved milli-q water. Thereafter, seeds were sterilized for a second time by adding 1 mL of 20 % of the commercial bleach solution for 20 min and shaken every 2 min. The supernatant was immediately removed after 20 min of treatment by 20 % of the commercial bleach solution to prevent a decrease of the percentage of germinated seeds (Lindsey *et al*., 2017). Seeds were washed three times by adding 1 mL of autoclaved milli-q water. In the next step, 15 to 20 seeds were sown on MS medium and Petri dishes were stored in dark at 4 °C for 3-4 days to remove seed dormancy (Cutler *et al*., 1996). Seeds were then germinated within a plant tissue culture growth chamber (Sanyo Versatile Environmental Test Chamber), which is equipped with 15 white light tubes and connected with a water-containing tank whose the role is maintaining the humidity within the growth chamber. The resulting seedlings were exposed (for 2-3 weeks) in 12h light (intensity of the light: 250 µmol

photon.m^{-2}.sec^{-1}) and 12h dark condition, at 22 °C for 24h and 70 % of humidity. The next step was performed after obtaining well-developed seedlings.

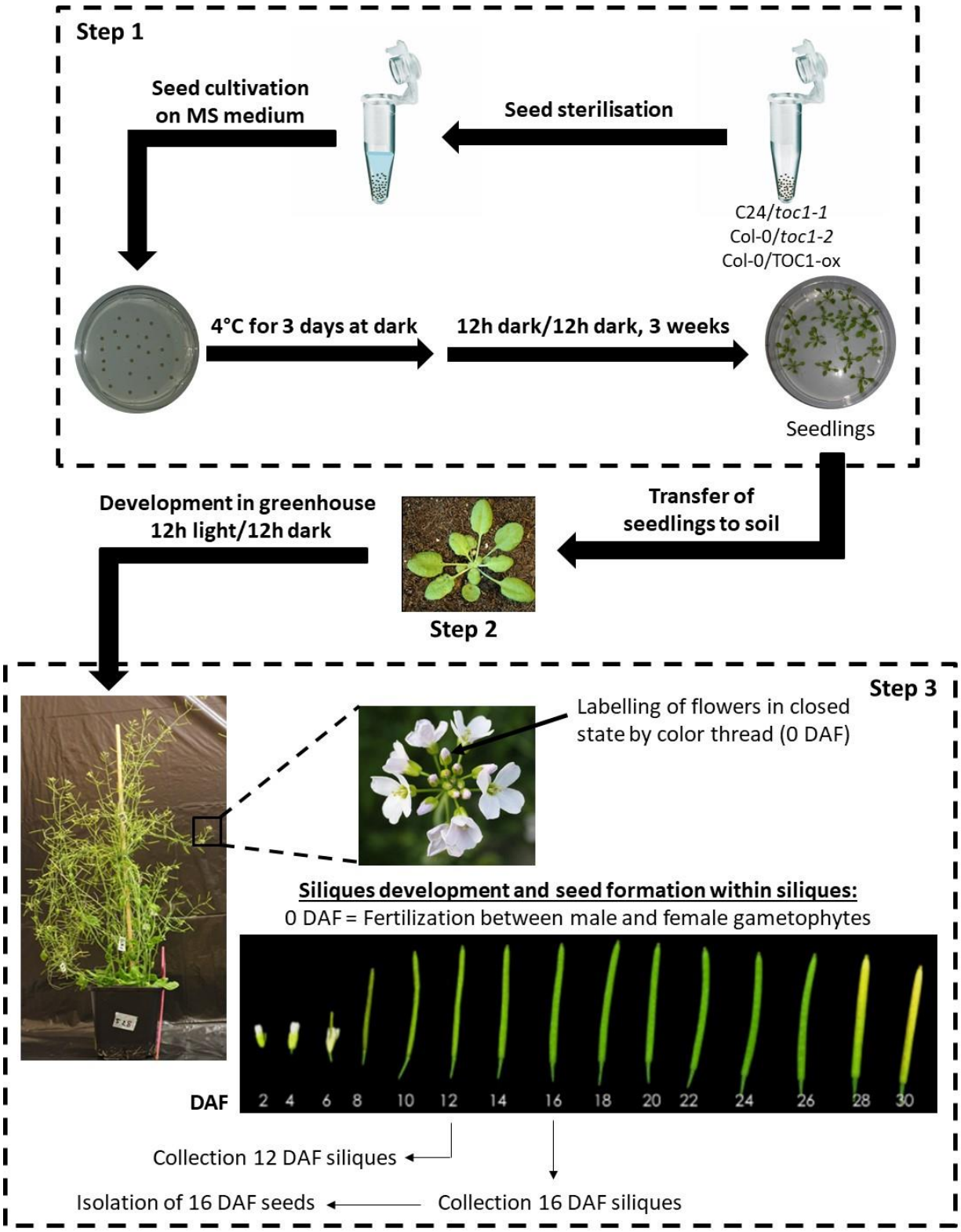

Figure 22. Workflow allowing the accumulation of 12 and 16 DAF Arabidopsis siliques. *The first step corresponds to the preculture of Arabidopsis seeds in MS medium. The second step consists in the transfer of seedlings to soil, allowing the growth of seedlings into adult plants with flowers. The third step enables the labelling of flowers and the collection of 12 and 16 DAF siliques.*

1.2.2. Step 2: Transfer of seedlings from MS medium to soil

The objective of this step consists in soiling seedlings for promoting their development into plants with flowers **(Step 2, Figure 22)**. The soil was first autoclaved (120 °C for 30 min) prior to the transfer of seedlings. 9 x 9 x 9.5 cm square pots, used for Arabidopsis plants, were filled with autoclaved soil and left on plates. Arabidopsis seedlings were carefully transferred from MS medium to soil, slightly watered and sheltered by a plastic cover in order to preserve the environment humidity. All these steps were performed within the level 2 containment greenhouse facility at "UMR CNRS 7025, Génie Enzymatique et Cellulaire" unit research. The greenhouse contains plant tissue culture growth chambers. Each growth chamber is equipped by cooling systems whose role is maintaining the temperature of the chamber at 24 °C whatever the external temperature. A total of eight mercury light lamps enable to provide a light intensity of 400 µmol photon.m^{-2}.sec^{-1} in each growth chamber. Seedlings were thus left in a greenhouse at 24 °C, 12h light/12h dark (Light period: from 7 a.m. to 7 p.m.; Dark period: from 7 p.m. to 7 a.m.) and 50 % of humidity for 2-3 months allowing its development into plants with flowers.

1.2.3. Step 3: Flower labelling and 12 and 16 DAF siliques collection

During the flowering processes (0 DAF), flowers were labelled using color threads **(Step 3, Figure 22)**. Each color thread was associated to a date of labelling. The labelling date corresponded to the day in which the fertilization (0 DAF) was occurring between the male and female gametophytes. Only labelled siliques were collected in liquid nitrogen 1h before dark period (Collection time: 6 p.m.) during the twelfth and sixteenth day after flowering. 12 and 16 DAF siliques were then stored at -80 °C.

1.3. Arabidopsis seedlings and leaves

1.3.1. Collection of Arabidopsis seedlings

Arabidopsis mutants (*toc1-1* and *toc1-2*) and WT (C24 and Col-0) seeds were cultivated in a sterile filter in MS medium. In order to remove seed dormancy, petri dishes were then stored at 4 °C in dark for 4 days. Seeds were germinated and the resulting seedlings were grown within a plant tissue culture growth chamber (Sanyo Versatile Environmental Test Chamber) in 12h light (intensity of white light: 250 µmol photon.m^{-2}.sec^{-1}) and 12h dark cycle, at 22 °C and 70 % of humidity for 1 month.

After 1 month growth, Arabidopsis seedlings (WT and *toc1*) remain exposed in 12h light (Light period: from 1 a.m. to 1 p.m.)/12h dark (Dark period: from 1 p.m. to 1 a.m.) cycle for one more day (Sanyo Versatile Environmental Test chamber). Seedlings were collected 7h after the beginning of the light period at 8 a.m. (collection in light condition). Once collected, seedlings were grinded in liquid nitrogen and immediately stored at -80 °C.

1.3.2. Collection of Arabidopsis leaves

Arabidopsis mutants (*toc1-1* and *toc1-2*) and respective WT (C24 and Col-0) mature seeds were cultivated in a sterile MS medium. Petri dishes were then stored at 4 °C in dark for 4 days. The germination and development of seedlings was performed in 12h light (Light period: from 1 a.m. to 1 p.m.)/12h dark (Dark period: from 1 p.m. to 1 a.m.) cycle, at 22 °C and 70 % of humidity for 3 weeks (Sanyo Versatile Environmental Test Chamber). Seedlings were then transferred to autoclaved soil and left in the greenhouse at 24 °C, 12h light/12h dark (Light period: from 7 a.m. to 7 p.m.; Dark period: from 7 p.m. to 7 a.m.) and 50 % of humidity for 2 weeks. Once scape reaches a height of 5 cm, leaves were collected 8h after the beginning of the light period using liquid nitrogen. Leaves were immediately stored at -80 °C.

2. Methods

2.1. FA methyl ester (FAME) analysis

2.1.1. FAMES extraction

The "whole seed transmethylation" protocol, described in the acyl-lipid metabolism chapter from the *Arabidopsis book* (Li-Beisson *et al*., 2013), was carried out for the extraction of FAMES. This protocol was used for the extraction of FAMES from Arabidopsis seeds but also adapted to seedlings and leaves samples. A mix containing 5 % of H_2SO_4 in methanol, 50 µg/mL of internal standard (heptadecanoic acid, C17:0, for seed samples or pentadecanoic acid, C15:0, for seedlings or leaves samples) and 50 µg/µL of butylated hydroxytoluene (BHT) was prepared prior to the extraction of FAMES. Thereafter, 1 mL of the mix and 300 µL of toluene, as co-solvent, were added to 50 non-desiccated seeds (1 mg of non-desiccated seeds), 5 mg of seedlings or 5 mg of leaves in a glass tube closed by a screw polypropylene cap. Each sample was vortexed for 30 sec. Samples were then heated at 85 °C for 90 min which promote the hydrolysis of lipids by H_2SO_4 and the esterification of the released FA by methanol. FA were thus derivatized into FAMES. Samples were then cooled for 5 min at room temperature. In the next step, a two-phase system was formed by adding 1.5 mL of 0.9 % NaCl and 1 mL of heptane, instead of hexane as described in the protocol described in the publication by Li-Beisson *et al*. (2013). Samples were vortexed and centrifuged for 2 min at 4000 rpm. The heptane fraction, containing FAMES, were then transferred in a 2 mL screw vials 9 mm clear glass vials and evaporated under nitrogen stream. FAMES were resuspended in 50 µL of heptane. Samples were vortexed and transferred in a new 2 mL vial equipped by a 15 mm insert and closed by a blue polypropylene cap. FAMES extract (extracted from seeds, seedlings or leaves), as well as blanks and a mix of 37 FAMES authentic standards (Sigma-Aldrich), were then analyzed by Gas Chromatography with Flame-Ionization Detector (GC-FID).

2.1.2. GC-FID methods

The GC-FID used to analyze FAMES is a GC-FID 2010 Plus From Shimadzu®. GC-FID methods (autosampler, injector, column and FID methods) were settled by using the GC Real Time Analysis module of the GC solution software.

2.1.2.1. Autosampler method

GC-FID system was equipped by an AOC-20i+s autosampler. For each run, 2 µL of sample were injected towards the GC-FID injector by piercing the septum with a 10 µL syringe. The sample was promptly taken (Plunger speed suction) and injected (Plunger speed injection) by the syringe. In order to avoid loss of sample, the syringe was also inserted with a high speed to the GC-FID injector. The acquisition of the chromatogram was followed by a single syringe washing step with heptane (Post-run rinse). The syringe was also cleaned up twice with the sample prior the injection of the latter towards the injector.

2.1.2.2. Injector method

In order to inject the different types of FAMES in the GC column, these biomolecules were evaporated by setting the temperature of the SP1 injector at 250 °C. FA were also led to the GC column by dihydrogen (H_2) as a carrier gas exerting a pressure of 64.7 kPa. The split injection mode was preferred to the splitless since FAMES were highly concentrated by adding a small volume of heptane (50 µL) to the lipid extract which contributes in the increase of the risk of GC column saturation. The total gas flow, fixed at 38.6 mL/min, was divided into the purge flow, which had been set at 3 mL/min to prevent contamination from the septum, the column flow, which had been fixed at 1.15 mL/min, and the split flow, which had been settled at 34.45 mL/min. The split ratio was thus fixed at 30.

2.1.2.3. Column method

The BPX70 column (length = 30 m, inner diameter = 0.25 mm, film thickness = 0.25 µm and column maximum temperature = 260 °C) was used for the separation of FAMES according to their evaporation temperature. The temperature of the oven that contains the BPX70 column was first hold for 2 min at 120 °C and then increased by 8 °C/min up to 250 °C. The linear velocity, defined by the travel length of the carrier gas in the GC column per unit of time and calculated by dividing the length of the GC column with the retention time of the heptane solvent (1.3 min), was also settled at 38.4 cm/sec.

2.1.2.4. Flame ionization detector (FID) method

Flame ionization detector (FID1) was used for detecting FAMES separated by the GC column. The temperature of the FID detector was set at 280 °C. The flame, allowing the

ionization of FAMES prior to their detection, was created by the combustion between H_2 and air (oxygen) gases who's the flow was settled at 40 and 400 mL/min, respectively. The makeup gases (H_2: flow fixed at 15 mL/min) was also used in order to prevent the increase of the peak width in the GC chromatogram and thus improve the resolution of the analysis.

2.1.3. Data processing

2.1.3.1. Peak identification and integration

The identification and integration of peaks were performed by using the "GC PostRun" module of the GC solution software. The identification of peaks was first performed by comparing the retention time of the chromatogram peaks acquired from samples (seeds, leaves or seedlings) with those acquired from authentic standards of FAMES. Equivalent chain length (ECL) of a given FAME were calculated and compared with the experimental one (Ackman, 1967). FAMES were also injected by GC-MS (Q Exactive™, Thermo®) in order to confirm the annotation of FAMES (Merlier *et al*., 2019). Once FAMES were identified, peaks were manually integrated for the determination of peak area. Data were then exported into an excel file.

2.1.3.2. Qualitative analysis of FAMES

The qualitative analysis of FAMES was performed by processing data from mature and developing seeds, seedlings and leaves samples. The total area of peaks was first calculated by the sum of the area of each identified peak in the chromatogram (except the area of peaks corresponding to the internal standard, heptane and BHT). The contribution of each FAMES (expressed in mol%) was then determined by dividing the area of the peak corresponding to a given FAMES with the total area of peaks, the ratio being reduced to a total of 100 %. The contribution of FAMES was compared between Arabidopsis circadian clock mutants (*toc1-1*, *toc1-2*, TOC1-ox, *prr5-1*, *prr7-3*, *prr9-1* and *cca1-11 lhy*-21) and their respective WT (C24, Col-0 or WS) by using the univariate Student test (t-test, unpaired samples). This statistical analysis was thus performed by using the online software BiostaTGV (http://biostatgv.sentiweb.fr/). The contribution of FAME was significantly different between mutants and WT when associated with a p-value < 0.05.

2.1.3.3. Quantitative analysis of FAMES

The quantitative analysis of FAMES was also performed on developing and mature seeds from Arabidopsis WT (C24, Col0 and WS) and mutants (*toc1-1*, *toc1-2*, TOC1-ox and *cca1lhy*) plants. The amount of each FA (expressed in µg) was first determined by using the information from the internal standard (the area of the peak corresponding to the internal standard C17:0 and the amount of C17:0 introduced in the sample = 50 µg) and FAME (the area of the peak corresponding to a given FA). The following formula was thus applied for the determination of FAME amount:

$$Amount\ of\ fatty\ acid\ (\mu g) = \frac{Peak\ area\ of\ FAME\ \times Amount\ of\ C17{:}0}{Peak\ area\ of\ C17{:}0}$$

The total amount of FA (expressed in µg) was then calculated by the sum of the amount of each FA. The total amount of FA per seed, as well as the total amount of FA per weight of seed, was then determined by dividing the total amount of FA by the number (50 seeds) or weight of seeds (1 mg), respectively. The total amount of FA per seed or weight of seeds was compared between Arabidopsis mutants and their respective WT by using the univariate Student test (t-test, unpaired samples and bilateral test). These statistical analyses were performed by using the online software BiostaTGV (http://biostatgv.sentiweb.fr/). The difference in the total amount of FA was considered as significant between the mutants and WT when associated with a p-value < 0.05.

2.2. MS-based lipidomic

2.2.1. Workflow

Lipidomic studies begins with the extraction of lipids found within biological samples (seeds) that are collected from circadian clock mutants (*toc1-1*, *toc1-2* and TOC1-ox) and respective WT (C24 and Col-0) plants **(Figure 23, Step 1)**.

Once extracted, these lipids were analyzed by liquid chromatography coupled with a hybrid quadrupole time-of-flight (HPLC-QTOF) **(Figure 23, Step 2)**. During this second step, lipids were first separated by liquid chromatography (HPLC) according to their physicochemical properties allowing the acquisition of chromatogram (each chromatographic peak corresponding to a lipid species). Once eluted, each lipid species was ionized by electrospray ionization source (ESI) and analyzed by Ultra High Definition (UHD) Accurate Mass

Q-TOF. MS1 spectra were acquired in order to characterize molecules. Daughter ions were also detected by the QTOF detector allowing the generation of mass spectrum (MS/MS spectrum) per chromatographic peak.

The acquisition of chromatographic and mass spectrum (MS/MS) data is followed by its importation within MS-DIAL 4 software enabling the processing of the data **(Figure 23, Step 3)** (Tsugawa *et al.*, 2020). Once imported, chromatographic and mass spectrum data were displayed in the software **(Figure 23, Step 4 and 7)**. From this stage, the objective is annotating each chromatographic peak by comparing MS1, MS/MS spectra and retention time to LipidBlast database **(Figure 23, Step 5, 6 and 7)**. The annotation is putative at level 2. Each annotated chromatographic peak was then integrated and exported into a peak table containing the contribution of lipid species in each sample (mutant and WT) **(Figure 23, Step 8 and 9)**. The contribution of each lipid species was then compared between mutants and WT using online statistical analysis software **(Figure 23, Step 10).**

2.2.2. Glycerolipid extraction from Arabidopsis mature seeds and seedlings

2.2.2.1. Extraction from Arabidopsis mature seeds

A Folch lipid extraction method was performed on different mutant (*toc1-1* and *toc1-2*) and respective WT (C24 and Col-0) of Arabidopsis mature seeds (Folch *et al*., 1951). 1 mL of chloroform/methanol (2/1, v/v) containing 0.01 % (w/v) of BHT, 100 µg/mL of internal standards (TAG 51:0 and PC 34:0) was added to 20 mg of non-desiccate mature seeds. 400 µL of water were then added to sample. Seeds were immediately grinded by beads using a Precellys (5500 rpm, 3 x 90 sec). Samples were then cooled on ice for 2h and centrifuged for 5 min at 4 °C and 13000 rpm allowing the formation of a two-phase system. Lipids-containing chloroform were transferred in a 2 mL vial and evaporated under nitrogen stream. Lipids were resuspended in 400 µL of chloroform. 50 µL of lipid extract were transferred in a 2 mL vial equipped by a 15 mm insert and diluted with 150 µL of chloroform. Samples, including lipid extract from WT and mutants, the blank, internal standard and the quality control (QC) were then analyzed by HPLC-QTOF.

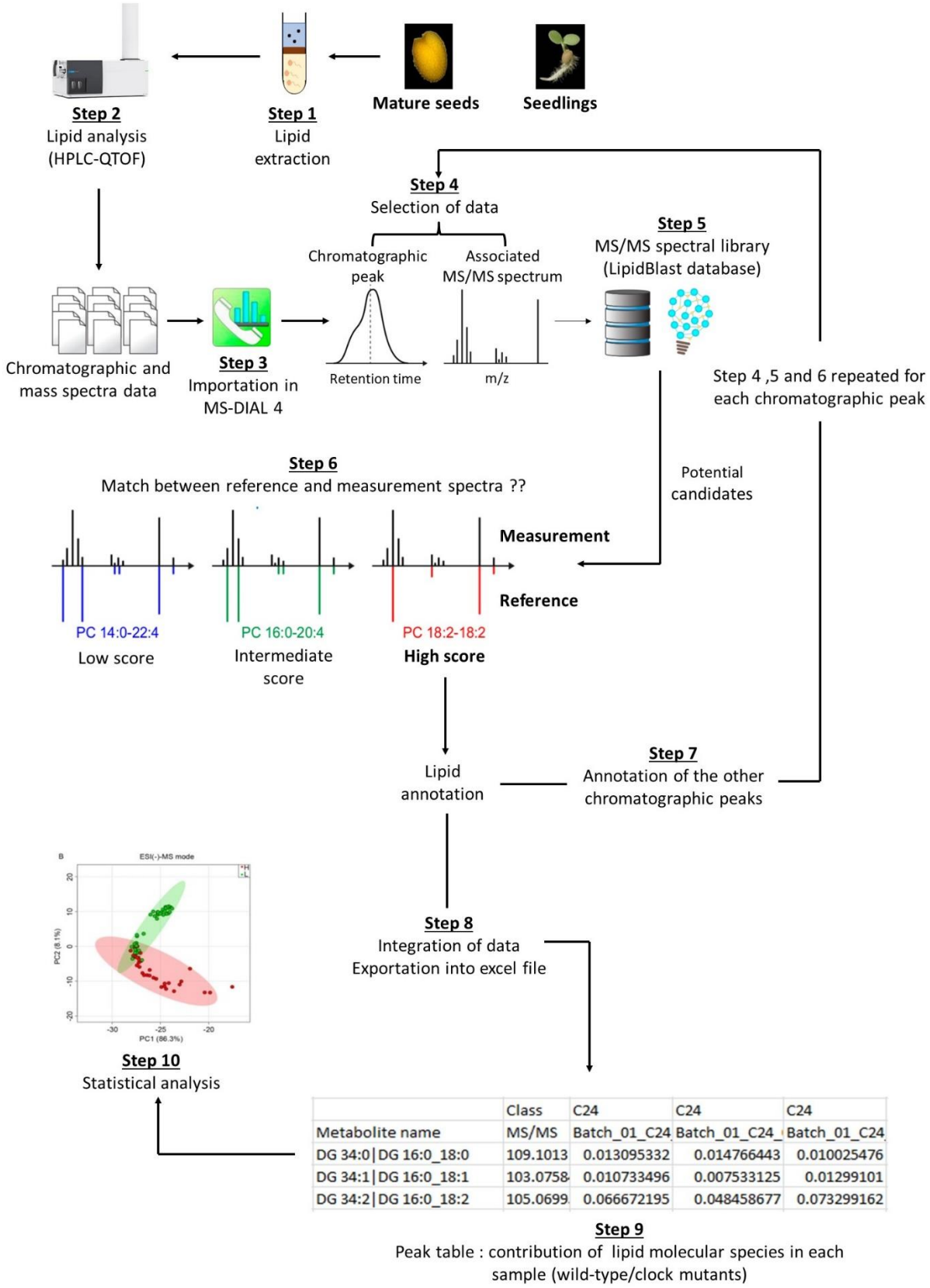

	Class	C24	C24	C24
Metabolite name	MS/MS	Batch_01_C24	Batch_01_C24_	Batch_01_C24
DG 34:0|DG 16:0_18:0	109.1013	0.013095332	0.014766443	0.010025476
DG 34:1|DG 16:0_18:1	103.0758	0.010733496	0.007533125	0.01299101
DG 34:2|DG 16:0_18:2	105.0699	0.066672195	0.048458677	0.073299162

Figure 23. Lipidomic workflow enables studying the role of circadian clock in the regulation of lipid metabolism. *Lipidomic approaches are divided into ten successive steps from glycerolipid extraction to the statistical analyses of our data. This figure is adapted from Tsugawa et al. (2020).*

2.2.2.2. Extraction from Arabidopsis seedlings

Glycerolipid extraction was performed on *toc1-1* and C24 seedlings. The following protocol was inspired from the one described in the MS-DIAL 4 publication (Tsugawa et al., 2020). In the first step, 1 mL of a methyl tert-butyl ether (MTBE)/methanol mix (3/1, v/v) containing 1 µM of internal standard (SPLASH Lipidomix, Avanti Polar Lipids, inc.) and 0.01 % of BHT was added to 100 mg of seedlings (Tube A). Samples were then vortexed vigorously. The addition of 400 µL of water was followed by the homogenization of samples by a Precellys (5500 rpm, 3 x 90 sec). Samples were cooled on ice for 15 min and centrifuged at 3,000 x g for 10 min at 4 °C. The glycerolipid-containing organic upper phase was then transferred in a new 1.5 mL tubes (Tube B) and glycerolipids were extracted for a second time by adding 750 µL of MTBE to seedling samples (Tube A). All steps described above, except the step consisting in the addition of water, were performed until obtaining a two-phase system. The upper phase (Tube A) was combined with the previous glycerolipid extract (Tube B). The combined glycerolipid extract (Tube B) was evaporated under a nitrogen stream and resuspended in 60 µL of isopropanol. The glycerolipid extract was then centrifuged at 14,000 x g for 10 min at 4 °C and supernatant was transferred in 2 mL vial equipped by a 15 mm insert. Samples, blank, internal standard and QC were then analyzed by HPLC-QTOF.

2.2.3. Glycerolipid species analysis by HPLC-QTOF

HPLC was performed based on a modified protocol from the publication by Tsugawa *et al.* (2020). Lipids were first separated by using the ACQUITY UPLC CSH C18 column (100 × 2.1 mm; 1.7 µm) and ACQUITY UPLC CSH C18 VanGuard pre-column (5 × 2.1 mm; 1.7 µm) maintained at 60 °C on a high-performance liquid chromatograph (HPLC) 1290 (Agilent Technologies). 3 and 5 µL of samples were then injected in positive (ESI+) and negative (ESI-) mode, respectively. Separation was done at 65 °C at 0.6 mL/min by using two mobile phases (A and B). The mobile phase A were composed by a mix of acetonitrile and water (60/40, v/v) and a mix of isopropanol and acetonitrile (90/10, v/v), respectively. In the positive mode, 10 mM of ammonium formate and 0.1 % of formic acid were added to the mobile phase A and B mainly for the generation of $[M+H]^+$ and $[M+NH_4]^+$ adducts by the electrospray ionization (ESI+). In the negative mode, only 10 mM of ammonium acetate was added to the mobile phase A and B mainly for the production of $[M-H]^-$ and other types of adducts by the electrospray ionization (ESI-).

In POS mode, the separation was done in 18 min. The gradient was as follows: B, 0 to 2.40 min, 30 %; 2.40 to 3 min, 48 %; 3 to 13.25 min, 82 %; 13.25 to 13.90 min, 99 %; 13.90 to 14.40 min, 99 %; 14.40 to 14.50 min, 15 %; 14.50 to 18 min, 15 %. In NEG mode, the separation was done in 13.50 min. The gradient was as follows: B, 0 to 2 min, 30 %; 2 to 2.50 min, 43 %; 2.50 to 9.50 min, 76 %; 9.50 to 9.60 min, 99 %; 9.60 to 10.50 min, 99 %; 10.50 to 10.60 min, 15 %; 10.60 to 13.50 min, 15 %. LC-electrospray ionization (ESI)-HRMS2 analyses were achieved by coupling the LC system to a hybrid quadrupole time of flight (QTOF) mass spectrometer Agilent 6538 (Agilent Technologies) equipped with dual electrospray ionization (ESI). The source temperature, fragmentor, and the skimmer were set up at 350 °C, 150 V, and 65 V, respectively. The nebulization, consisting in the formation of a lipid-containing droplet spray, and the transfer of ions into the MS system was carried out by settling the nozzle and capillary voltage to +/- 1 kV and +/- 3.5 kV, respectively. In order to improve the nebulization process, the pressure of the nebulizer nitrogen gas was settled at 35 psi. The collimation of the nebulizer spray was performed by setting the temperature and flow of the sheath nitrogen gas at 350 °C and 11 L/min, respectively. The temperature and the flow of the drying nitrogen gas, crucial for the evaporation of the droplet solvent and the coulomb-explosion-induced lipid ionization, were fixed at 200 °C and 14 L/min, respectively. The collision energy, allowing the fragmentation of parent ions within the collision cell, was settled at +40 eV in Pos Mode and -40 eV in Neg Mode. The MS1 and MS/MS acquisition speed were both settled to 2 spectra/sec with a mass range between m/z = 100 and 1200. MS2 scans were performed on the sixth most intense ions. Two internal reference masses were used for in-run calibration of the mass spectrometer (121.0509 and 922.0098 in positive-ion mode and 112.9856 and 1033.9881 in negative-ion mode). MassHunter B.07 software enabled the control of the parameters of the machine and acquired and processed the data.

2.2.4. Data processing by MS-DIAL

2.2.4.1. Data import in MS-DIAL 4

MS-DIAL 4 was used in order to obtain lipidomic data as described by Tsugawa *et al*. (2020). Chromatograms and mass spectra were first converted in a mzML format. Lipidomic centroid data, acquired by using a conventional LC-MS method and the soft ionization ESI in positive and negative mode, were named as sample, quality control (QC), standard or blank in MS-DIAL 4. The analytical injection order was also indicated in the case of the data

normalization by the QC (LOWESS).

Several parameters were then fixed prior to the import of the data. The mass accuracy tolerance in MS1 and MS2, allowing the recognition of a peak in the m/z ratio interval in each MS1 and MS/MS spectrum, were settled at 0.01 and 0.025 Da, respectively. Chromatographic, MS1 and MS2 peaks were detected by settling the chromatogram intensity threshold (minimum height peak) at 8×10^3 and cutting MS and MS/MS spectra in 0.1 Da slices, respectively. Reference ions (Positive mode: m/z = 121.0509 and 922.0098; Negative mode: m/z = 112.9856 and m/z = 1033.9881), previously used for the rectification of m/z values during the analysis by HPLC-QTOF, were excluded during the import of the data (tolerance in MS1: 0.01 Da). The exclusion of the MS2 region downstream of the precursor ion was also carried out during the import of the data. Peak deconvolution, allowing the separation of chromatographic peaks with similar retention time, was performed by settling the sigma window value at 0.5. Chromatogram and mass spectra were also aligned with a 1 min and 0.025 Da tolerances, respectively. The MS1 and MS2 tolerance, allowing the comparison of the experimental MS1 and MS/MS spectra with the reference spectra of different lipid adducts from LipidBlast database (Positive mode: $[M+H]^+$, $[M+NH_4]^+$ and $[M+Na]^+$ adducts; Negative mode: [M-H]-, $[M-H_2O-H]^-$, $[M+FA-H]^-$ and $[M+Hac-H]^-$ adducts), was fixed at 0.01 and 0.05 Da, respectively. The identification score cut off was set up at 80 %.

2.2.4.2. Data curation, normalization and exportation

Once imported, data curation was performed in order to remove all false positive found in the data. Data were first filtered by selecting ions whose MS/MS spectra were acquired and matched with the reference spectra containing in the LipidBlast database. The retention time, alignment and integration of each selected chromatographic peak was then manually corrected by using the “EIC aligned spot” module of MS-DIAL 4 as described in the publication by Tsugawa *et al.* (2020).

Curation was performed and the data were then normalized by the appropriate internal standard by using the normalization module of MS-DIAL 4. The normalized data (represented in peak height) were exported into an excel file. In the excel file, we kept the lipids annotated in level 2 (MS1, MS/MS spectrum and retention time predicted) and normalized data was used for lipidomic quantification. The contribution of each lipid

molecular species was then determined by dividing the height of a chromatographic peak (corresponding to a lipid molecular species) with the sum of the height of each annotated chromatographic peak. The peak table (variables x observations) was thus providing the contribution of lipid molecular species in mol% (variables) in each sample (observations).

2.2.5. Statistical analyses of data from Arabidopsis mature seeds and seedlings

2.2.5.1. Data import

The peak table (variables x observations = "contribution of lipid molecular species" x unpaired samples) was converted into ".csv" format. The peak table, in which unpaired samples have been organized in columns, was imported in *metaboanalyst* software (https://www.metaboanalyst.ca/MetaboAnalyst/upload/StatUploadView.xhtml).

2.2.5.2. Univariate test and multivariate statistical analyses

Principal component analysis (PCA) was first performed for the visualization of a potential discrimination in lipidomic between mutants (*toc1-1* and *toc1-2*) and respective WT (C24 and Col-0) in a 2D projection. In order to explain the potential discrimination observed between mutants and WT in PCA, t-test was performed for each variable**.** Variables were significantly different between mutants and its respective WT when associated with a p-value < 0.05. Results were represented in form of heatmaps and histogram for each variable with a p-value < 0.05 in order to easily visualize the group (mutant or WT) for which lipid molecular species were highly or weakly represented.

2.3. Expression of lipid-related genes

2.3.1. RNA extraction from 16 DAF developing seeds and 12 DAF developing siliques

A total elimination of the enzyme involved in the degradation of RNA, also known as RNase, was first required prior the extraction of total RNA. 1.5- and 2-mL Eppendorf tubes were thus autoclaved at 121 °C for 20 min. Mortar and pestle, which are used for grinding immature seeds, were also heated for 2h at 200 °C. In the meantime, the fume hood and all materials (pliers, pipet, centrifuge, tip boxes, etc) were washed with 70 % ethanol. Once the RNase has been eliminated from the material and bench, 16 DAF siliques previously collected from WT and mutant plants and stored at -80 °C were dissected on clean aluminum foil by using RNase free pliers. 16 DAF developing seeds collected from 40 siliques were then

transferred to 1.5 mL autoclaved Eppendorf tubes in liquid nitrogen and stored at -80 °C. In order to avoid any risk of RNA degradation or contamination, the RNA extraction was performed using filter tips.

The following RNA extraction was optimized from the protocol by Piskurewicz and Lopez-Molina (2011). RNA extraction was performed on 12 DAF developing siliques and 16 DAF developing seeds. Biological samples were first ground in liquid nitrogen by using RNAse free mortar and pestle. Once ground, samples were then transferred in 2 mL of ice-cold extraction buffer composed by 2 % of β-mercaptoethanol freshly added to 8 M of LiCl. Samples were homogenized and stored overnight at 4 °C. Samples were homogenized for a second time and centrifuged at 17,000 x g for 10 sec at 4 °C. The supernatant was transferred in a new 2 mL Eppendorf tube while avoiding the inclusion of insoluble debris. The RNA-containing supernatant was centrifuged at 17,000 x g for 30 min at 4 °C. The supernatant was removed and the RNA-containing pellet was resuspended by vortexing in 750 µL of ice-cold 75 % ethanol. Sample was centrifuged at 17,000 x g for 5 min at 4 °C and the supernatant was discarded while avoiding the resuspension of the RNA-containing pellet. The residual ethanol was evaporated by leaving the tube open at room temperature for 5-10 min. The RNA-containing pellet was resuspended in 600 µL of solubilization buffer containing 2 % of β-mercaptoethanol freshly added to 0.5 % SDS, 100 mM NaCl, 25 mM EDTA and 10 mM Tris-HCl (pH = 7.6). The supernatant was washed by adding 600 µL of phenol/chloroform/isoamyl alcohol mix (25/24/1, v/v/v) which were immediately vortexed for 30 sec and centrifuged at 17,000 x g for 5 min at room temperature. The RNA-containing upper phase was transferred in a 1.5 mL Eppendorf tube and the washing step was repeated twice. 400 µL of RNA-containing supernatant was recovered after the last washing step. The addition of 27 µL 4M NaCl and 800 µL of ice-cold 100 % ethanol, as well as the storage of sample at -80 °C for 30 min, was performed for the precipitation of RNA. Sample was then centrifuged at 17,000 x g for 15 min at 4 °C. The supernatant was discarded while avoiding the resuspension of the RNA-containing pellet. The pellet was washed three times by adding 500 µL of ice-cold 75 % ethanol. Each washing step was followed by a centrifugation of sample at 17,000 x g for 5 min at 4 °C. Once washing was performed, the pellet was resuspended in 30 µL of sterile water.

2.3.2. Verification of nucleic acid quality

The quality of the RNA isolated from 16 DAF Arabidopsis seeds was checked by

using the NanoDrop 2000 spectrophotometer. Samples whose nucleic acid (RNA and genomic DNA with a maximum of absorbance at 260 nm) were not contaminated with protein (maximum of absorbance at 280 nm, 1.8 < A260/A280 ratio < 2.1) was selected for further analyses by RT-qPCR (Desjardin *et al.*, 2010).

2.3.3. Elimination of genomic DNA

The RNA extraction protocol described in the publication by Piskurewicz and Lopez-Molina (2011) was followed by the degradation of the genomic DNA. Samples were treated by a recombinant and modified form of the DNase I provided in the TURBO DNA-*free*™ kit (Fisher Scientific, Invitrogen, reference: AM1907). The modified DNase I was used for the degradation of residual DNA with higher efficiency in comparison to the WT DNase I. Once the residual DNA was degraded, the elimination of the modified DNase I was performed by using the DNase Inactivation Reagent.

The routine DNase treatment method was chosen for samples with a concentration of RNA lower than 200 ng/µL. The routine DNase treatment protocol was described in the TURBO DNA-*free*™ kit instruction: https://assets.fishersci.com/TFS-Assets/LSG/manuals/1907M_turbodnafree_UG.pdf. Once the residual DNA was eliminated, the RNA concentration was estimated by using the NanoDrop 2000 spectrophotometer.

2.3.4. Verification of the RNA integrity by agarose gel

RNA integrity was checked by detecting only 18S (1.8 kb) and 28S (4.8 kb) rRNA bands in a 1.2 % agarose gel (Oliveira *et al.*, 2016). This step was only performed during the optimization of the RNA extraction protocol because of the weak concentration of RNA (between 20 to 50 ng/µL of RNA in each sample) extracted from 16 DAF Arabidopsis seeds of interest. The 1.2 % agarose gel was performed in a total volume of 30 mL TAE 1X. 360 mg of agarose powder were thus added to 30 mL of TAE 1X. The solution was heated in the microwave until a complete resuspension of the agarose powder in the TAE 1X. 3 µL of 10,000X SYBR™ Safe DNA Gel Stain (final concentration: 1X) were added to the 1.2 % agarose when the temperature of the agarose solution was lower than 40 °C. The solution was carefully mixed and poured in the 30 mL electrophoresis plate. Once poured into the electrophoresis plate, an eight-tooth comb was added to the agarose solution in order to create well in the upper part of the agarose gel. An approximately 20 min waiting time was required for the

solidification of the agarose solution within the electrophoresis plate. The comb was then carefully removed from the agarose gel. The electrophoresis plate was placed within an electrophoresis tank filled with TAE 1X buffer. For the migration of the negatively charged RNA, the electrophoresis wells were actually oriented toward the negative pole of the electrophoresis tank.

In the meantime, 3 µL of 6X DNA loading dye buffer blue were added to 15 µL of RNA samples (final concentration of the loading dye: 1X). 10 µL of the SmartLadder (0.2-10 kb) and 900 ng of RNA samples were then loaded within the wells of the electrophoresis gel. RNA migration was then performed at 85 Volts for 40 min from the negative to the positive pole of the electrophoresis 1.2 % agarose gel within the electrophoresis tank. RNA bands were finally revealed by exposing the 1.2 % agarose gel to ultraviolet (UV).

2.3.5. Reverse transcription

The reverse transcription was carried out for the synthesis of the first strand of cDNA from the previously extracted RNA. 100 pmol of Oligo(dT)$_{18}$ (Reference: SO132, Scientific™, initial concentration: 100 µM) were first added to 0.1-5 µg of RNA in a total volume of 12.5 µL. 4µL of the 5X Reaction Buffer (Reference: EP0441, Thermo Scientific™, final concentration = 1X), 20 U of the Ribolock RNase inhibitor (Reference: EO0381, Thermo Scientific™, initial concentration: 40 U/µL), 20 nmol of each dNTP (Reference: R0191, Thermo Scientific™, initial concentration of each dNTP: 10 mM) and 200 U of the RevertAid Reverse Transcriptase (Reference: EP0441, Thermo Scientific™, initial concentration: 200 U/µL) were then added to the 12.5 µL of the RNA/Oligo(dT)$_{18}$ mix in order to obtain 20 µL of the reverse transcription reaction mix. The cDNA synthesis was performed by incubating the reaction mix at 42 °C for 1h before heating at 70 °C for 10 min. For each replicate (WT and *toc1* mutants), the cDNA has been diluted to 1/20th prior the evaluation of the expression of lipid-metabolism-associated genes by quantitative PCR (qPCR).

2.3.6. Expression of target genes by qPCR

2.3.6.1. Preparation of the qPCR reaction mixes

qPCR was performed in the molecular biology platform “Centre de Ressources Régionales en Biologie Moléculaire” (CRRBM) located in the University of Picardie Jules Verne (UPJV) in Amiens. The expression of five lipid-related genes (*FAD3*, *FAD2*, *FAE1*, *bZIP67* and

WRI1) and circadian clock genes (*TOC1*) was evaluated by qPCR using sequence-specific forward and reverse primers whose sequences were indicated in the **Table 2**. Real-Time RT-PCR data normalization was performed using *EF1α* as reference genes, which expression stability was firstly validated for the considered developmental stages (12 DAF siliques and 16 DAF seeds). Lyophilized forward and reverse primers were first resuspended in a volume of sterile milli-q water for reaching 100 µM of primer stock solutions as indicated in the oligonucleotide synthesis report provided by Eurofins Genomics France SAS. A mix containing 10 µM of the cDNA-sequence-specific forward and reverse primers (10 µM R+F primers) was then prepared for each target and housekeeping cDNA sequence to be amplified by qPCR. The primer mix was finally prepared in a 2-mL autoclaved Eppendorf tube by diluting 0.5(2n+2) µL of the corresponding 10 µM R+F primer with 2.1(2n+2) µL of sterile milli-Q water and 4.6(2n+2) µL of LightCycler® 480 SYBR® Green I Master (Roche, reference: 04 887 352 001) which is constituted by the FastStart Taq DNA Polymerase, dNTP mix, reaction buffer, SYBR Green I dye and $MgCl_2$. Each reagent volume (0.5 µL of 10 µM primer mix, 2.1 µL of sterile milli-q water and 4.6 µL of LightCycler® 480 SYBR® Green I Master) was multiplied by 2n since the amplification of a given cDNA from each sample (n cDNA sample) was performed twice using the corresponding R+F primer (two technical replicates per cDNA sample). The addition of two volumes of each reagent was also required for the realization of the "no template control" (NTC or blank) that consisted in checking the potential dimerization between the reverse and forward primers in the lack of the cDNA template.

Once all primer mixes were prepared, 96-well qPCR plate was filled by adding 15 µL of the $1/20^{th}$ diluted cDNA or water (for the NTC) in each well. The 96-well qPCR plate was then sealed by an adhesive PCR plate film and a small centrifugation of the PCR plate was performed in order to spin down all the cDNA volume at the bottom of the wells. The 2-mL-Eppendorf-contained primer mixes and the 96-well-plate-contained cDNA were then placed in the Automate Freedom platform EVO 150®-TECAN®. The final qPCR reaction mixes were thus automatically prepared by transferring 7.2 µL of the primer mix and 2 µL of cDNA (or water) in each well of the 384-well plate (final concentration of the primer: 0.5 µM). The 384-well plate was finally sealed by an adhesive PCR plate film and qPCR reaction mixes were homogenized using a PCR plate vortex.

Table 2. List of primers targeting reference and lipid-related genes

Genes	Forward (5' -> 3')	Reverse (5' -> 3')
Elongation factor (*EF1α*, reference gene)	TCGATTGCCACACCTCTCAC (Tm= 59.4 °C)	GGCTTGGTTGGGGTCATCTT (Tm= 59.4 °C)
Timing of CAB expression 1 (*TOC1*)	TCTTCGCAGAATCCCTGTGAT (Tm= 57.9 °C)	GCTGCACCTAGCTTCAAGCA (Tm= 59.4 °C)
FA desaturase 3 (*FAD3*)	ATCTTTCGTCTTCGGTCCACT (Tm= 57.9 °C)	GGCAACTTCTCATCGTGACC (Tm= 59.4 °C)
FA desaturase 2 (*FAD2*)	CGGAAACCGACACCACAAA (Tm=56.7 °C)	TTCAGATCTCCCACCGAGAAA (Tm=57.9 °C)
FA elongase 1 (*FAE1*)	GGTGGCTCTACGCAATGTCA (Tm= 59.4 °C)	ACCGACCGTTTTGGACATGA (Tm= 57.3 °C)
bZIP67	AAGAGCTTTGGAGCGATGAA (Tm= 55.3 °C)	CACCTCCTTCGTTGTCGTTT (Tm= 57.3 °C)
WRINKLED 1 (WRI1)	CGCCGCCAGAGCAGTGGTTT (Tm= 63.5 °C)	GCAGCAGCTTCCTCCTGCGT (Tm= 63.5 °C)

2.3.6.2. cDNA amplification by qPCR

The amplification of the cDNA by qPCR was performed using the LightCycler® 480 PCR instrument. The activation of the FastStart Taq DNA Polymerase was first carried out by pre-incubating qPCR reaction mixes at 95 °C for 5 min (ramp rate: 4.8 °C/sec). A total of 45 cycles of cDNA denaturation, primer annealing and extension was then performed by incubating qPCR reaction mixes at 95 °C for 10 sec (ramp rate: 4.8 °C/sec), 60 °C for 15 sec (ramp rate: 2.5 °C/sec) and 72 °C for 10 sec (ramp rate: 4.8 °C/sec), respectively. The extension time was prior calculated by dividing the amplicon size (100-150 bp) over 25 (extension time about 6 sec), as advised in the LightCycler® 480 SYBR® Green I Master kit instruction, with an additional extension time of 4 sec in order to ensure maximum efficiency of the cDNA amplification.

Each cycle of the cDNA amplification was characterized by the incorporation of the SYBR green (excitation: 465 nm) as a DNA intercalating dye (SYBR green) whose the fluorescence was emitted at 510 nm when associated to the cDNA double strand. The amplification was thus followed by the increase in the intensity of the fluorescence along with

the number of cycles, especially between 15 and 30 amplification cycles. The detection of the fluorescence at 510 nm allowed the establishment of the amplification curve of each cDNA in the LightCycler® 480 v1.5.0.39 software: fluorescence intensity = f (number of cycle). In theory, the amplification curve is only described as an exponential function: $N = No \times 2^n$ (with No: the initial number of cDNA and N: the number of cDNA after n cycle of amplification). However, the experimental amplification curve was divided into three phases: the exponential, linear and plateau phases. The exponential phase from the experimental curve has been described as following a similar mathematical function than the theoretical curve since only the amplification of the cDNA occurs during this phase. This mathematical function was no longer observed in the linear and plateau phases. A competition between the cDNA renaturation and hybridization of primers with cDNA strands was, indeed, observed during the linear phase, therefore reducing the rate of the cDNA amplification. During the plateau phase, the rate of the amplification reaction is considerably decreased simultaneously with the amount of primer in the sample. Only the exponential phase was therefore used for the quantification of cDNA in each sample. The exponential phase of the experimental amplification curve was used for the determination of the Ct (cycle threshold) value for each cDNA (reference or target genes). Ct corresponded to the number of cycles for reaching a fluorescence threshold. The Ct value was inversely proportional to the amount of cDNA in the sample. Low Ct values reflects high gene expression in a given condition (WT and mutant). Conversely, high Ct value revealed low gene expression in a given condition (WT and mutant).

2.3.6.3. Establishment of melting curves and peaks

The amplification of cDNA was prior performed using primers which have been designed in order to promote their hybridization to specific cDNA sequences. However, the possibility was not excluded that non-specific hybridizations may experimentally occur within the same qPCR reaction mix getting at least two PCR products. Once the cDNA amplification step was performed, the specificity of each primer was checked by the determination of the number of PCR products obtained in each qPCR reaction mix. Each PCR product was actually associated to a single and sequence-specific melting temperature (Tm) from which 50 % of the double-stranded PCR products dissociate into single-stranded cDNA. The specificity of each primer was thus verified by the determination of a single Tm in each qPCR reaction mix.

The denaturation and immediate renaturation of the PCR products was first

performed by incubating qPCR reaction mixes at 95 °C for 5 sec (ramp rate: 4.8 °C/sec) and 65 °C for 1 min (ramp rate: 2.5 °C/sec), respectively. The dissociation of each SYBR-green-associated PCR product was then performed by gradually increasing the temperature of the qPCR reaction mixes from 65 to 97 °C by 0.1 °C/sec. During the dissociation step, the intensity of the SYBR-green-emitted fluorescence was continuously monitored from 65 to 97 °C (5 acquisitions/°C) allowing the establishment of the melting curve "fluorescence = f (temperature)" and melting peak "d(fluorescence)/dT = f (temperature)" for each cDNA. The dissociation of the double-stranded PCR product into single-stranded cDNA was thus represented by a decrease of the fluorescence intensity in the melting curve given that SYBR green is an intercalating dye that only fluoresces when associated to the cDNA double strand. The number of peaks, whose the top corresponds to the Tm of the PCR product in the melting peak representation, allowed the determination of the number of PCR products obtained in each qPCR reaction mix after the cDNA amplification step. The presence of a single Tm peak in a melting peak representation thus reflects that the corresponding primers hybridize to a specific cDNA sequence.

2.3.6.4. Determination of the cDNA amplification efficiency

Each cycle of the cDNA amplification that occurs within the exponential phase of the amplification curve was theoretically characterized by a 2-fold increase of the cDNA amount. Although the amplification efficiency was theoretically at 100 %, the percentage may be experimentally altered according to the sequence of primers which slightly modifies the number of cDNA produced per single cDNA per cycle. The determination of the efficiency was thus critical for the quantification of each target cDNA in the sample.

The first step consists in diluting cDNA to $1/20^{th}$, $1/40^{th}$, $1/80^{th}$, $1/160^{th}$ and $1/320^{th}$ by adding the corresponding water volume. The dilution of each cDNA was performed in triplicates. 2 µL of diluted cDNA (or water) was then added to 7.2 µL of primer mix in each well of the 384-well plate. For each qPCR reaction mix, the value of Ct was then determined as previously described in the above section "cDNA amplification by qPCR" of the materials and methods. The efficiency curve Ct = f ($\log_{10}$ dilution factor) was associated to the equation Ct = a x $\log_{10}$ dilution factor + b (a: the slope of the curve; b: the value of the Ct obtained from the non-diluted cDNA sample). The efficiency percentage was then calculated as followed:

$$Efficiency\ (\%) = \left(10^{\left(\frac{-1}{slope}\right)} - 1\right) \text{ x } 100$$

with the efficiency of the amplification at 100 % that corresponds to the synthesis of 2 molecules of cDNA/single molecule of cDNA/amplification cycle.

2.3.6.5. Data processing

The determination of Ct values and cDNA amplification efficiency was followed by the evaluation of the expression of target and reference genes in 16 DAF immature seeds previously collected from mutant and respective WT plants. The expression of target and reference genes was calculated as followed:

$$Expression\ of\ target/ref\ genes = \left[\frac{1}{(1 + Efficiency)^{Ct}}\right]_{\text{Target/Ref}}$$

with "1+ *Efficiency*" corresponding to the number of cDNA produced per molecule of cDNA per cycle (the efficiency was not expressed in percentage in this formula).

The expression of target genes was then normalized by *EF1α* as a reference gene whose the expression should not be affected whatever the developmental stage, the mutation or the time of collection. The normalized ratio was calculated for each target gene in the mutant and WT as followed:

$$Normalized\ ratio = \frac{\left[\frac{1}{(1 + Efficiency)^{Ct}}\right] \text{Target}}{\left[\frac{1}{(1 + Efficiency)^{Ct}}\right] \text{Ref}}$$

The normalized expression of each target gene (lipid-metabolism-associated gene) was finally compared between circadian clock mutants and respective WT by using the univariate Student test (t-test, unpaired samples and bilateral test). These statistical analyses were performed by using the online software BiostaTGV (http://biostatgv.sentiweb.fr/). The difference in the expression of lipid-metabolism-associated genes was considered as significant between the mutants and WT when associated with a p-value < 0.05.

SECTION 4: RESULTS AND DISCUSSIONS

RESULTS AND DISCUSSIONS

1. Role of clock components in the synthesis of FA in Arabidopsis seeds

The objective of this initial part of the present project was characterizing the mature seed FA composition of eight clock mutants (*toc1-1*, *toc1-2*, TOC1-ox, *prr5-1*, *prr7-3*, *prr9-1* and *cca1-11 lhy*-21) and their three respective WT (C24, Col-0 and Ws). The aim of this analysis was identifying clock components related to the synthesis of FA in Arabidopsis developing seeds. Following this initial characterization, clock mutants associated to FA modifications in Arabidopsis seeds were selected for further characterizations of their FA composition in seedlings and leaves.

1.1. Identification of clock components related to FA metabolism in seeds

1.1.1. FA qualitative and quantitative analyses in clock mutant mature seeds

In order to identify clock components involved in the synthesis and regulation of FA in Arabidopsis seeds, FA were extracted from WT and clock mutant mature seeds and analysed by GC-FID at the "UMR CNRS 7025, Génie Enzymatique et Cellulaire (GEC)" unit research. The acquisition of chromatograms from mature WT and clock mutant seeds allowed the identification of nine FA, including palmitic (C16:0), stearic (C18:0), oleic (C18:1), linoleic (C18:2), linolenic (C18:3), arachidic (C20:0), eicosenoic (C20:1), eicosadienoic (C20:2) and docosenoic (C22:1) acids. The mole percent corresponding to each FA and the FA total amount were calculated in each clock mutant and respective WT. The mole percent of each FA in Col-0 were then compared with data already published by Robert *et al.* (2005), Li *et al.* (2006) and Shrestha *et al.* (2016). During the execution of this project, the whole seed acid-catalyzed transmethylation protocol was used to generate fatty acid methyl esters (FAMEs) from mature seeds (Li-Beisson *et al.*, 2013), these FAMEs were later analysed by GC-FID (Materials & Methods, 2.1.2.). This protocol consists in the transesterification of FA directly from Arabidopsis seeds without performing a prior glycerolipid extraction step. In a similar way, FAMES were also directly generated and extracted by Robert *et al.* (2005) and Li *et al.* (2006). However, in the case of the work published by Shrestha *et al.* (2016), TAG, the main source of FA in oilseeds, were separated by thin layer chromatography before transmethylation. Moreover, in spite of experimental differences between protocols described in the above-cited publications and the one used in this thesis, similar FA profiles were obtained from Col-

0 mature seeds **(Table 3)**. Major FA were C18:2 (29.5 %), C20:1 (20.8 %), C18:3 (16.5 %), C18:1 (17.6 %), C16:0 (7.2 %), C18:0 (3 %), C20:0 (1.9 %), C20:2 (1.8 %) and C22:1 (1.7 %).

Table 3. Comparison of FA profiles obtained from Col-0 Arabidopsis mature seeds. *Values are expressed in mol% ± standard deviation, N.S.: not specified; (n = 9).*

FA	Present study	Li *et al.* (2006)	Shrestha *et al.* (2016)	Robert *et al.* (2005)
C16:0	7.2 ± 0.2	8.7 ± 0.1	7.6 ± 0.0	7.2 ± N.S.
C18:0	3.0 ± 0.1	3.6 ± 0.1	3.0 ± 0.0	2.9 ± N.S.
C18:1	17.6 ± 0.7	15.0 ± 0.2	15.7 ± 0.1	20.0 ± N.S.
C18:2	29.5 ± 0.3	29.0 ± 0.3	28.6 ± 0.1	27.5 ± N.S.
C18:3	16.5 ± 0.7	19.2 ± 0.1	17.6 ± 0.0	15.1 ± N.S.
C20:0	1.9 ± 0.1	2.2 ± 0.1	2.1 ± 0.0	2.2 ± N.S.
C20:1	20.8 ± 0.4	20.2 ± 0.1	20.0 ± 0.1	22.0 ± N.S.
C20:2	1.8 ± 0.1	2.0 ± 0.1	< 1.3	0.1 ± N.S.
C22:1	1.7 ± 0.1	1.7 ± 0.1	1.7 ± 0.0	1.5 ± N.S.

Once the method implemented in this PhD project was successfully compared to the state-of-art methods, qualitative and quantitative FA seed content in several clock mutants were analyzed.

The potential role of PRR5, PRR7 and PRR9 in the regulation of FA metabolism was studied using *prr5-1*, *prr7-3* and *prr9-1* mutants (Michael *et al.*, 2003). FA qualitative analysis showed significant differences in the case of six FA between *prr9-1* and Col-0 mature seeds (p-value < 0.05). Results revealed that the mole percent of C18:3, C20:1 and C22:1 were significantly higher in *prr9-1* seeds, while C18:0, C18:1 and C18:2 were significantly lower than in Col-0 seeds **(Figure 24A)**. Differences observed between Col-0 and *prr9-1* were estimated to 0.1 % for C18:0 and C22:1, 1.6 % for C18:1 and C18:3 and 0.9 % for C18:2 and C20:1. The quantitative analyses also showed significant differences in the total amount of FA per seed (p-value < 0.01) and total amount per mg of seeds (p-value < 0.05) between Col-0 and *prr9-1*, 1.06 and 1.08 folds decrease respectively **(Figure 24B)**.

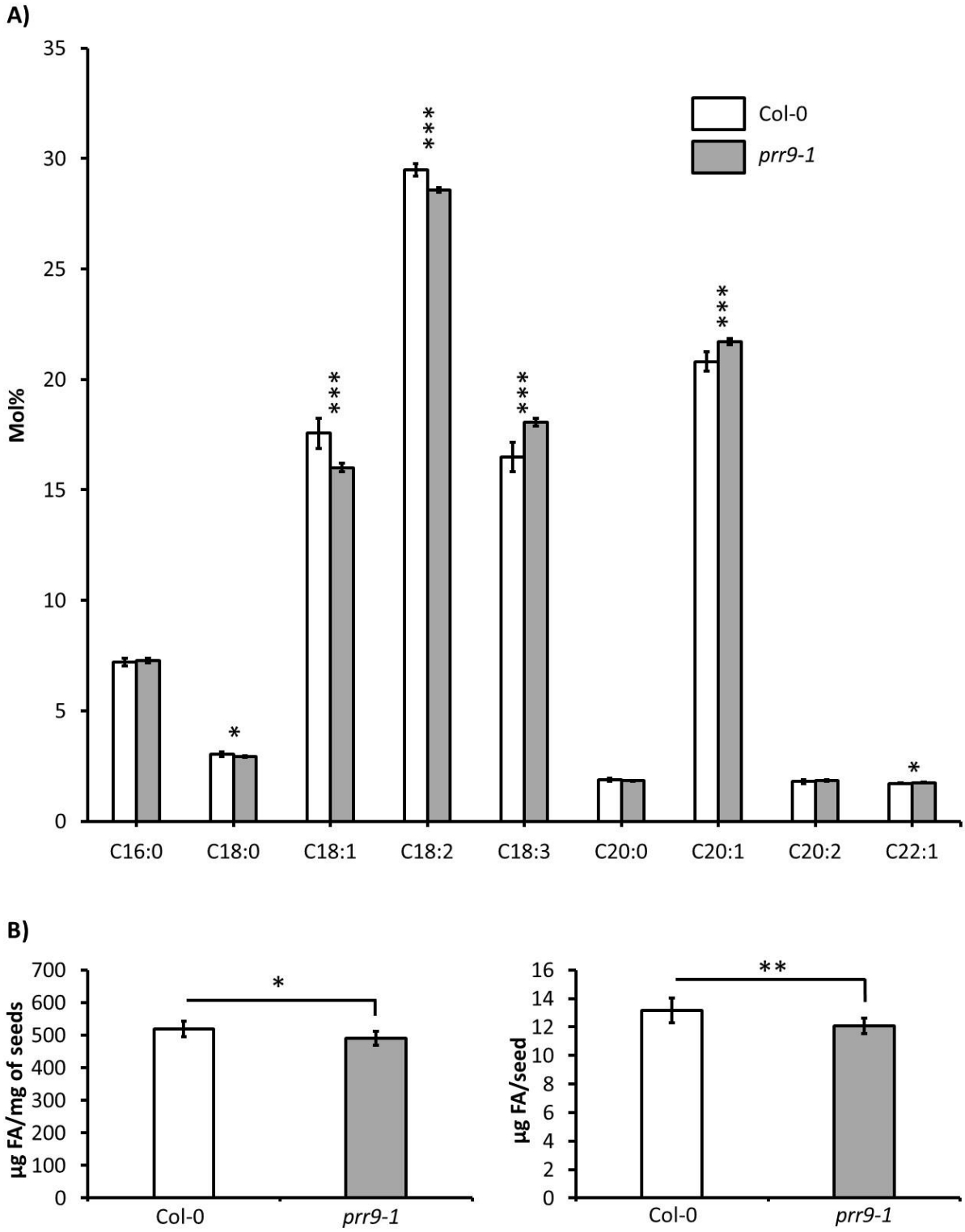

Figure 24. Differences in FA composition between Col-0 and *prr9-1* mature seeds. *A) The qualitative analysis of FA (mol %) and B) the quantitative analyses of FA (µg/seed and µg/mg) were performed using GC-FID data acquired from Col-0 and prr9-1. The statistical significance was evaluated with a bilateral student test using unpaired samples (n = 9; p < 0.05: *, p < 0.01: ** and p < 0.001: ***). Numerical data were indicated in Supplementary Table 1.*

Qualitative analysis showed significant differences in the case of five FA between Col-0 and *prr7-3*. These changes concerned C18:0, C18:2, C20:0, C16:0 and C18:3 **(Figure 25A)**.

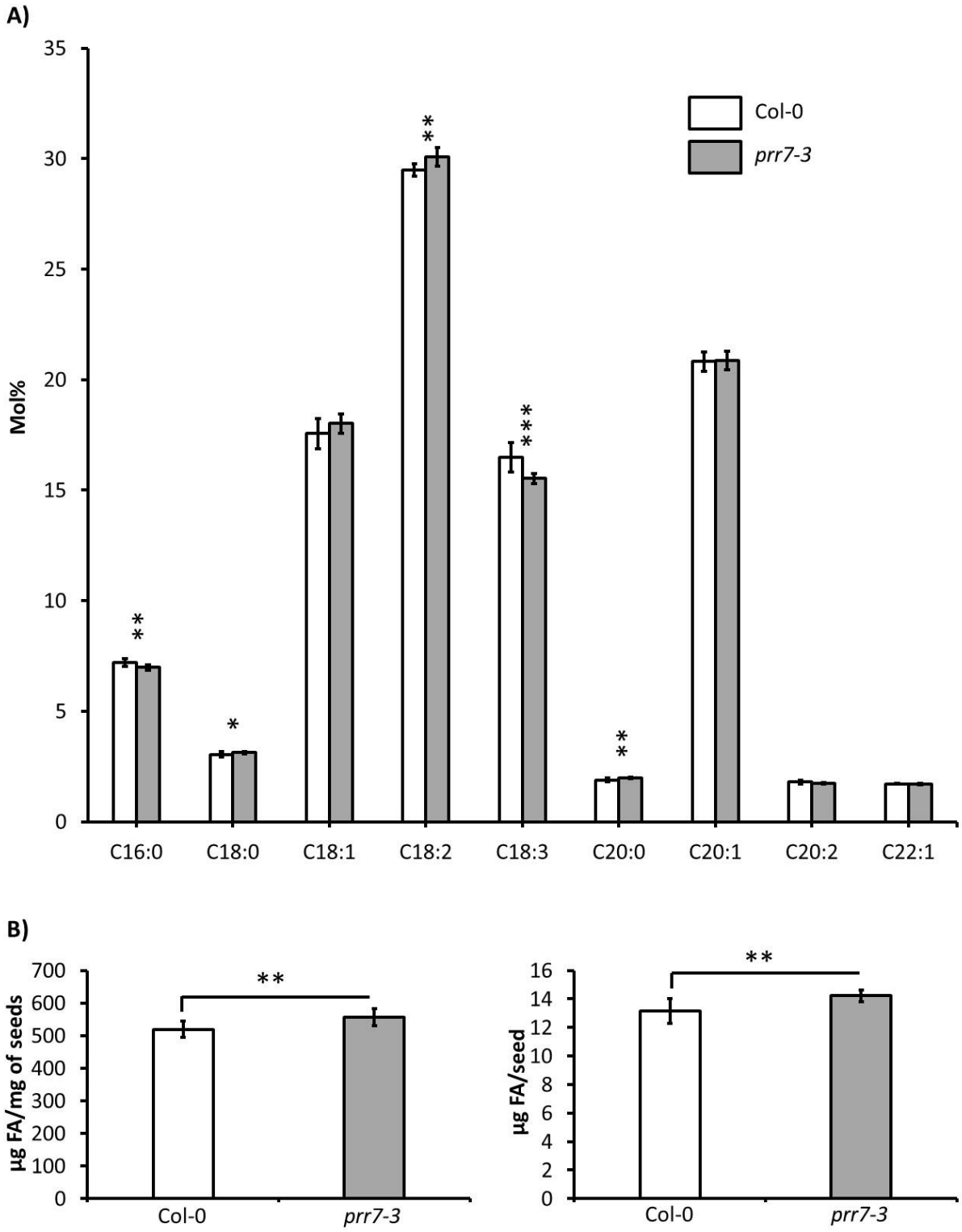

Figure 25. Differences in FA composition between Col-0 and *prr7-3* mature seeds. *A) FA qualitative analysis (mol %) and B) FA quantitative analyses (µg/seed and µg/mg) were performed using GC-FID data acquired from Col-0 and prr7-3. The statistical significance was evaluated with a bilateral student test using unpaired samples (n = 9; p < 0.05: *, p < 0.01: ** and p < 0.001: ***). Numerical data were indicated in Supplementary Table 2.*

The mole percents of C18:0 (p-value < 0.05), C18:2 (p-value < 0.01) and C20:0 (p-value < 0.01) were significantly increased in *prr7-3* mature seeds, while the percentages were significantly higher for C16:0 (p-value < 0.01) and C18:3 (p-value < 0.001) in WT **(Figure 25A)**. Differences observed between Col-0 and *prr7-3* were estimated to 0.1 % for C18:0 and C20:0, 0.2 % for C16:0, 0.6 % for C18:2 and 1 % for C18:3. The quantitative analyses showed significant differences in the total amount of FA per seed and the total amount of FA per mg of seeds between Col-0 and *prr7-3* (p-value < 0.01), 1.07 and 1.08 folds increase respectively **(Figure 25B)**.

The qualitative analysis of FA revealed significant differences in the case of three FA between Col-0 and *prr5-1*. The mole percents of C18:0 and C20:0 were significantly higher in *prr5-1* seeds, while the percentage of C16:0 was significantly increased in Col-0 seeds **(Figure 26A)**. Differences between Col-0 and *prr5-1* were estimated to 0.2 % for C20:0, 0.3 % for C16:0 and 0.5 % for C18:0. The quantitative analyses of FA showed significant differences in the total amount of FA per mg of seeds between Col-0 and *prr5-1*. The amount was increased 1.05 folds in *prr5-1*. No significant difference was observed for the total amount of FA per seed **(Figure 26B)**.

The potential role of CCA1-LHY in the regulation of FA metabolism in developing seeds was studied using *cca1-11 lhy-21* mutant (Hall et al., 2003). The qualitative analysis of FA showed significant differences (p-value < 0.001) in the case of three FA. C18:0 and C20:0 were significantly higher in *cca1-11 lhy-21* mature seeds, while C18:1 was significantly increased in WT mature seeds **(Figure 27A)**. Differences between WT and *cca1-11 lhy-21* were estimated to 0.6 %, 0.4 % and 0.8 % for C18:0, C20:0 and C18:1, respectively.

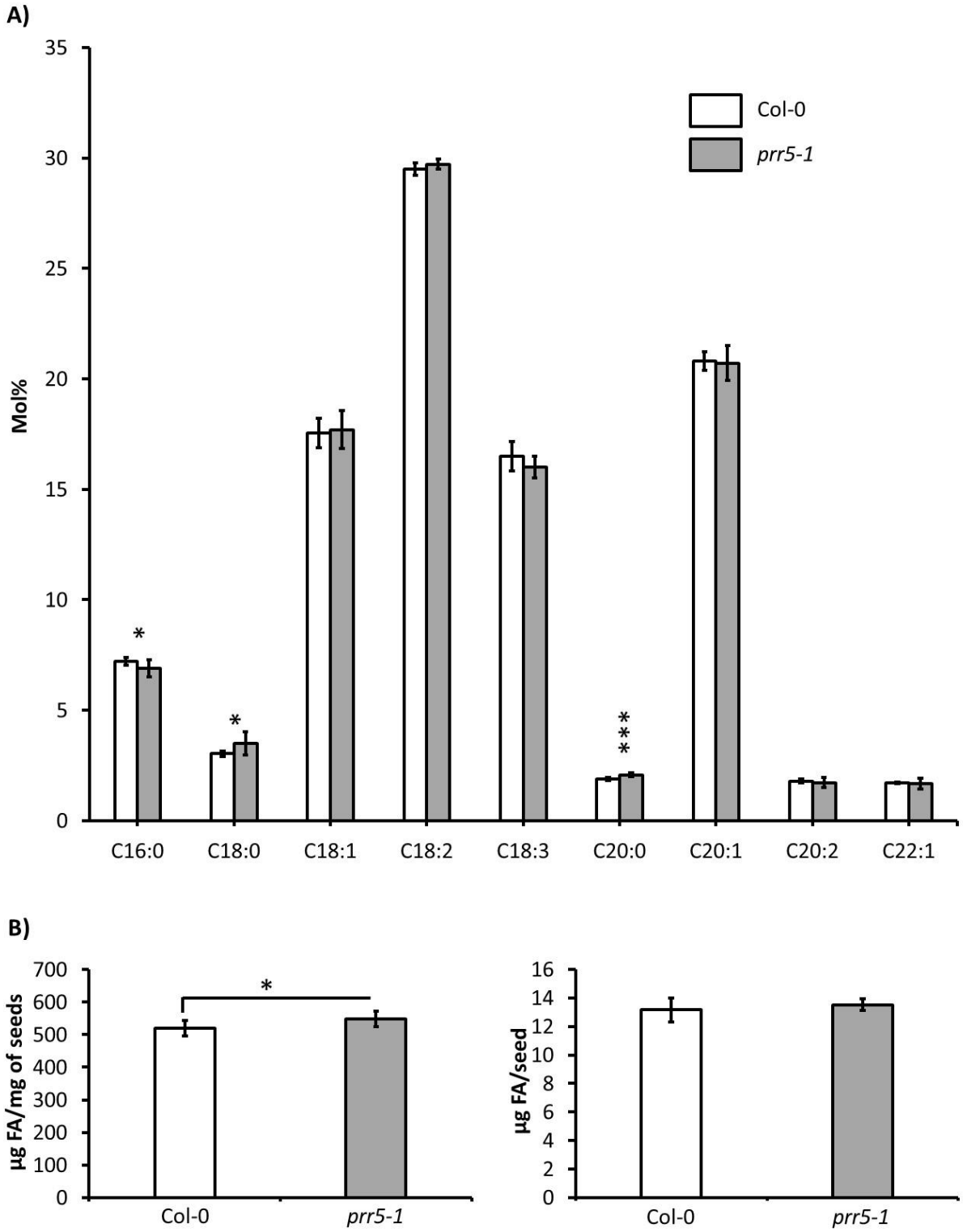

Figure 26. Differences in FA composition between Col-0 and *prr5-1* mature seeds. *A) The qualitative analysis of FA (mol %) and B) the quantitative analyses of FA (µg/seed and µg/mg) were performed using GC-FID data acquired from Col-0 and prr5-1. The statistical significance was evaluated with a bilateral student test using unpaired samples (n = 9; p < 0.05: *, p < 0.01: ** and p < 0.001: ***). Numerical data were indicated in Supplementary Table 3.*

The quantitative analyses of FA did not show significant difference in the total amount of FA between *cca1-11 lhy-21* and its WT **(Figure 27B)**.

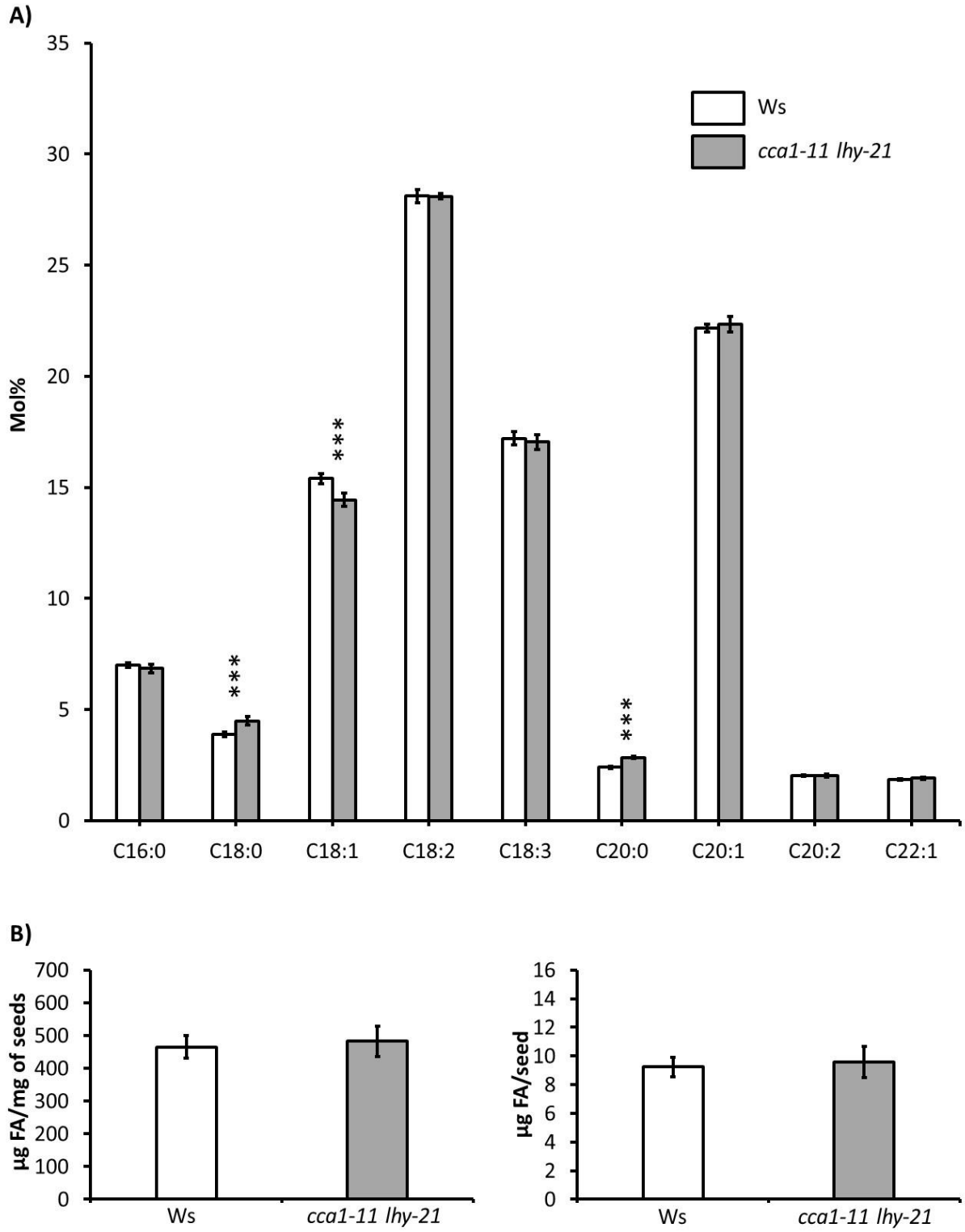

Figure 27. Differences in FA composition between Ws and *cca1-11 lhy-21* mature seeds. *A) The qualitative analysis of FA (mol %) and B) the quantitative analyses of FA (µg/seed and µg/mg) were performed using GC-FID data acquired from Ws and cca1-11 lhy-21. The statistical significance was evaluated with a bilateral student test using unpaired samples (n = 18; p < 0.05: *, p < 0.01: ** and p < 0.001: ***). Numerical data were indicated in Supplementary Table 4.*

This result is consistent with the one generated by Hsiao *et al.* (2014), where differences in FA and TAG composition between *cca1-lhy* and its WT were found during germination and not in mature seeds. These metabolic differences during germination point out to the role of CCA1-LHY in the control of storage lipid mobilization. CCA1-LHY have also been identified participating in the regulation of PA synthesis in Arabidopsis seedlings (Kim *et al.*, 2019). Similarities between FA composition observed in *cca1-lhy* and its WT mature seeds **(Figure 27)** suggested that both clock components are rather involved in the regulation of FA and glycerolipid metabolism in germinating seedlings than in developing seeds.

The potential role of TOC1 in the regulation of FA seed metabolism was studied in two different *toc1* loss-of-function mutants (*toc1-1* and *toc1-2*) and TOC1 overexpression (TOC1-ox) plants.

The *toc1-1* mutation decreased the DNA binding properties of TOC1, while *toc1-2* produced non-functional TOC1 proteins (Strayer *et al.*, 2000; Gendron *et al.*, 2012). Both *toc1* mutants were generated from two different genetic background, C24 and Col-0 respectively. Differences in genetic backgrounds may potentially lead to phenotypic differences between C24 and Col-0, resulting in the alteration of the FA profiles between both *toc1* mutants generated from C24 (*toc1-1*) and Col-0 (*toc1-2*).

FA composition were analyzed in both *toc1* mutants if similar FA profiles were observed between their respective WT in mature seeds. FA were qualitatively and quantitatively analyzed in C24 and Col-0 mature seeds **(Figure 28)**.

The FA qualitative analysis showed no significant difference (p-value > 0.05) in the mole percents of seven FA between Col-0 and C24. Statistical differences were observed for C18:1 and C18:3 **(Figure 28A)**. Differences between C24 and Col-0 were estimated around 0.7 % for C18:1 and 0.6 % for C18:3. The quantitative analyses did not reveal significant differences (p-value > 0.05) in the total amount of FA per mg of seeds and the total amount of FA per seed between C24 and Col-0 **(Figure 28B)**. FA qualitative and quantitative analyses showed similarities in FA profiles between C24 and Col-0 in mature seeds **(Figure 28A and 28B)**.

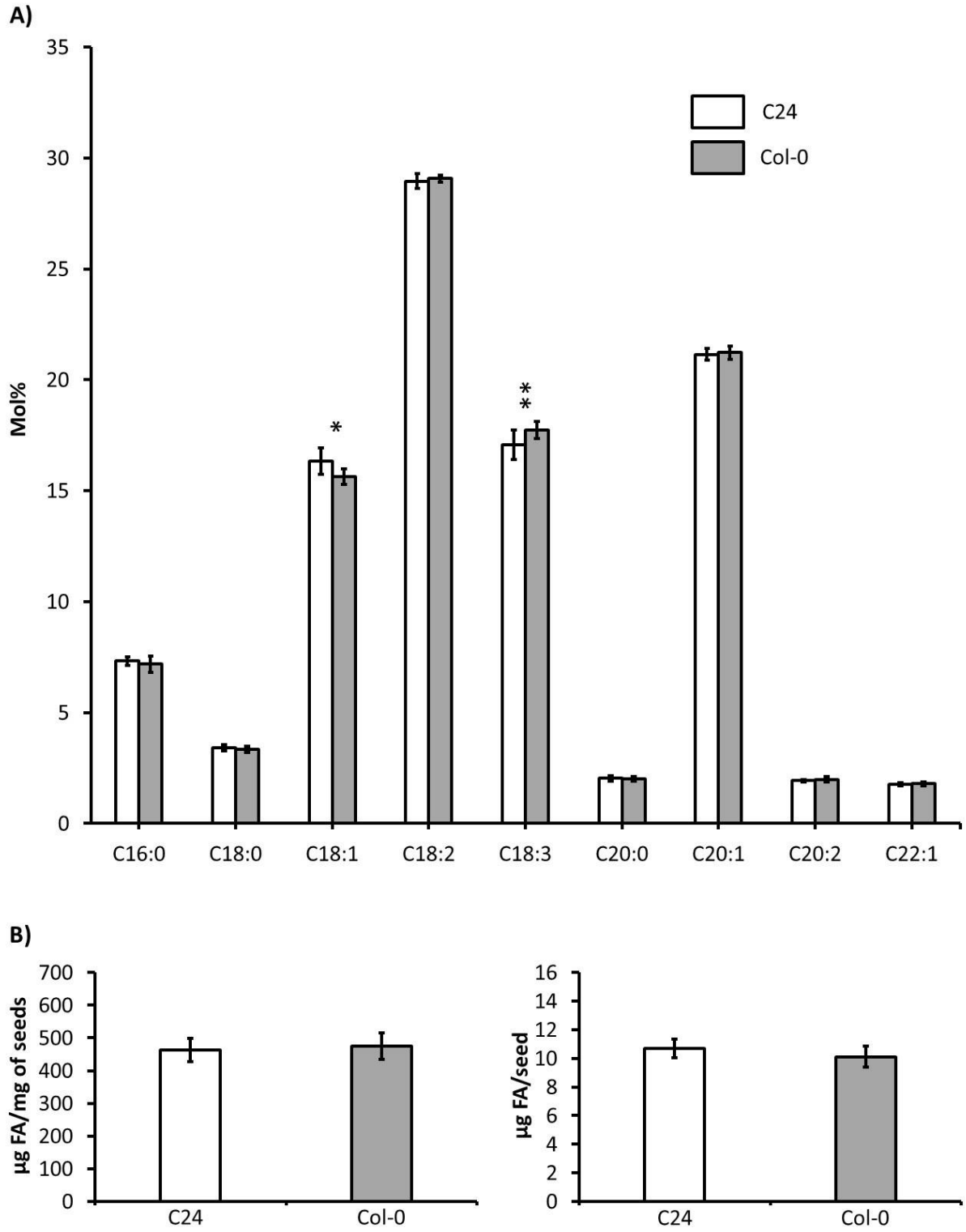

Figure 28. Differences in FA composition between Col-0 and C24 mature seeds. *A) The qualitative analysis of FA (mol %) and B) the quantitative analyses of FA (µg/seed and µg/mg) were performed using GC-FID data acquired from Col-0 and C24. The statistical significance was evaluated with a bilateral student test using unpaired samples (n = 17; p < 0.05: *, p < 0.01: ** and p < 0.001: ***). Numerical data were indicated in Supplementary Table 5.*

FA were qualitatively and quantitatively analyzed in both *toc1* mutant mature seeds **(Figure 29 and 30)**.

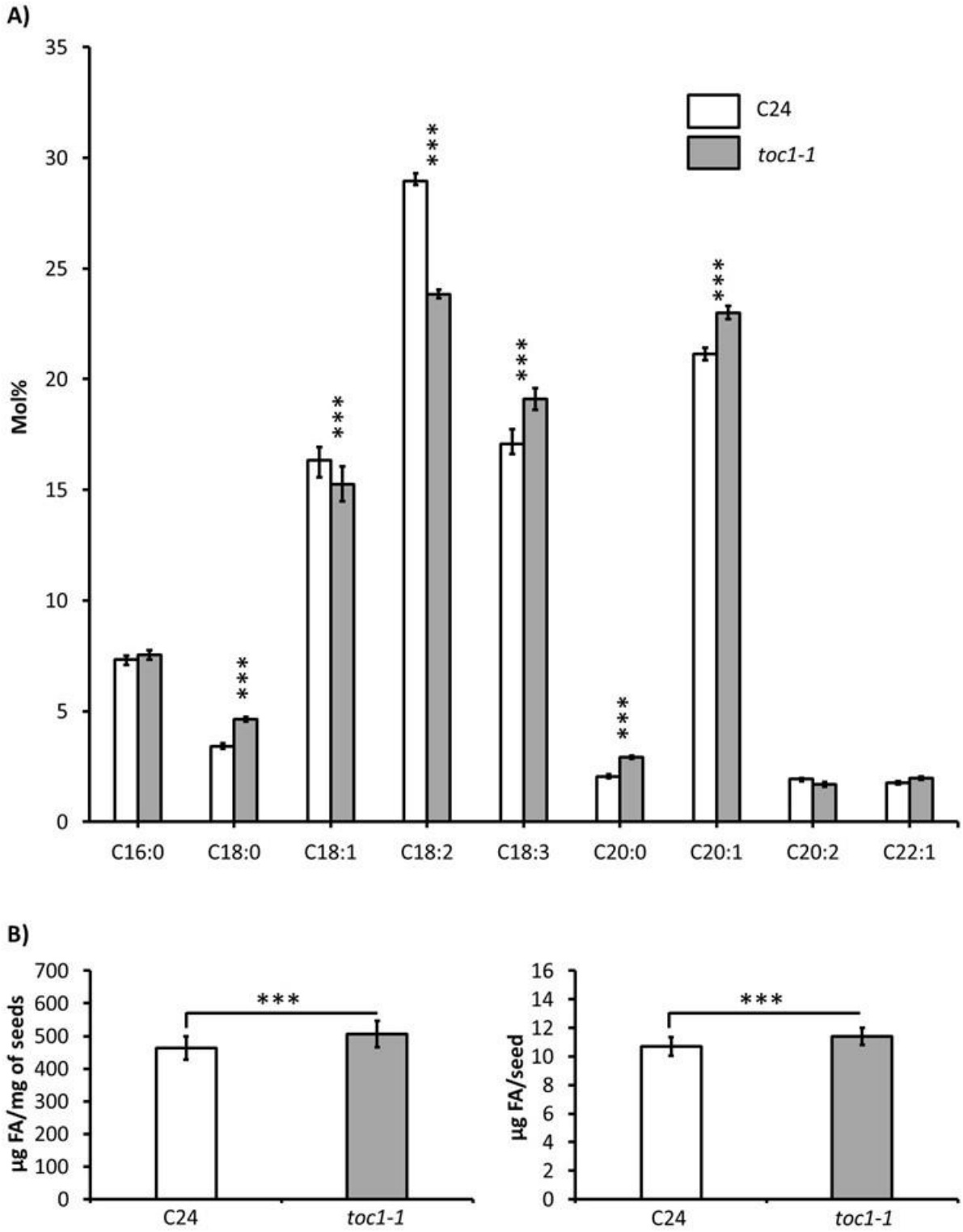

Figure 29. **Differences in FA composition between C24 and *toc1-1* mature seeds.** *A) FA qualitative analysis (mol %) and B) FA quantitative analyses (µg/seed and µg/mg) were performed using GC-FID data acquired from C24 and toc1-1. The statistical significance was evaluated by a bilateral student test using unpaired samples (n = 17; p < 0.05: *, p < 0.01: ** and p < 0.001: ***). Numerical data were indicated in Supplementary Table 6.*

The FA qualitative analyses showed significant differences (p-value < 0.001) in the case of six FA between both *toc1* mutants and their respective WT. C18:0, C18:3, C20:0 and C20:1 were significantly higher in both *toc1* mutants, while C18:1 and C18:2 were significantly increased in their respective WT **(Figure 29A and 30A)**. These differences represent 5.1 % for C18:2, 2 % for C18:3 and 1.9 % for C20:1 in the case of *toc1-1* and 4.7 %, 2.2 % and 1.2 % in the case of *toc1-2***,** while modifications in the percentages of the nine FA between the other clock mutants and their respective WT were lower than 2 %. The qualitative analyses revealed similar FA profiles in both *toc1* mutants **(Figure 29A and 30A)**. The quantitative analyses revealed similarities between both loss-of-function *toc1* mutants, 1.10 folds and 1.20 folds increase in the total amount of FA per mg of seeds and total amount of FA per seed in both *toc1* mutants respectively (p-value < 0.001) **(Figure 29B and 30B)**.

FA were qualitatively and quantitatively analyzed in the overexpressing mutant TOC1-ox and its respective WT (Col-0). The FA qualitative analysis showed significant differences (p-value < 0.001) for seven FA. The molar percents of C16:0, C18:0, C18:2 and C18:3 were significantly higher in TOC1-ox, while C20:1, C20:2 and C22:1 were significantly increased in Col-0 **(Figure 31A)**. Unlike *toc1-1* and *toc1-2*, differences observed between Col-0 and TOC1-ox were lower than 2 %. These differences were estimated to 0.4 % for C18:0 and C18:3, 0.6 % for C16:0 and C22:1, 0.1 % for C20:2, 1 % for C18:2 and 1.7 % for C20:1. Qualitative analysis of FA performed in Col-0 and TOC1-ox **(Figure 31A)** did not reveal an inverted FA profile in comparison with results obtained in both loss-of-function *toc1* mutants **(Figure 29A and 30A)**. The FA quantitative analyses showed that the total amount of FA per mg of seeds was 1.12 folds decreased in TOC1-ox and the total amount of FA per seed was 1.19 folds decreased in the overexpressing mutant (p < 0.001) **(Figure 31B)**, while the FA total amount was increased in both *toc1* mutants **(Figure 29B and 30B)**.

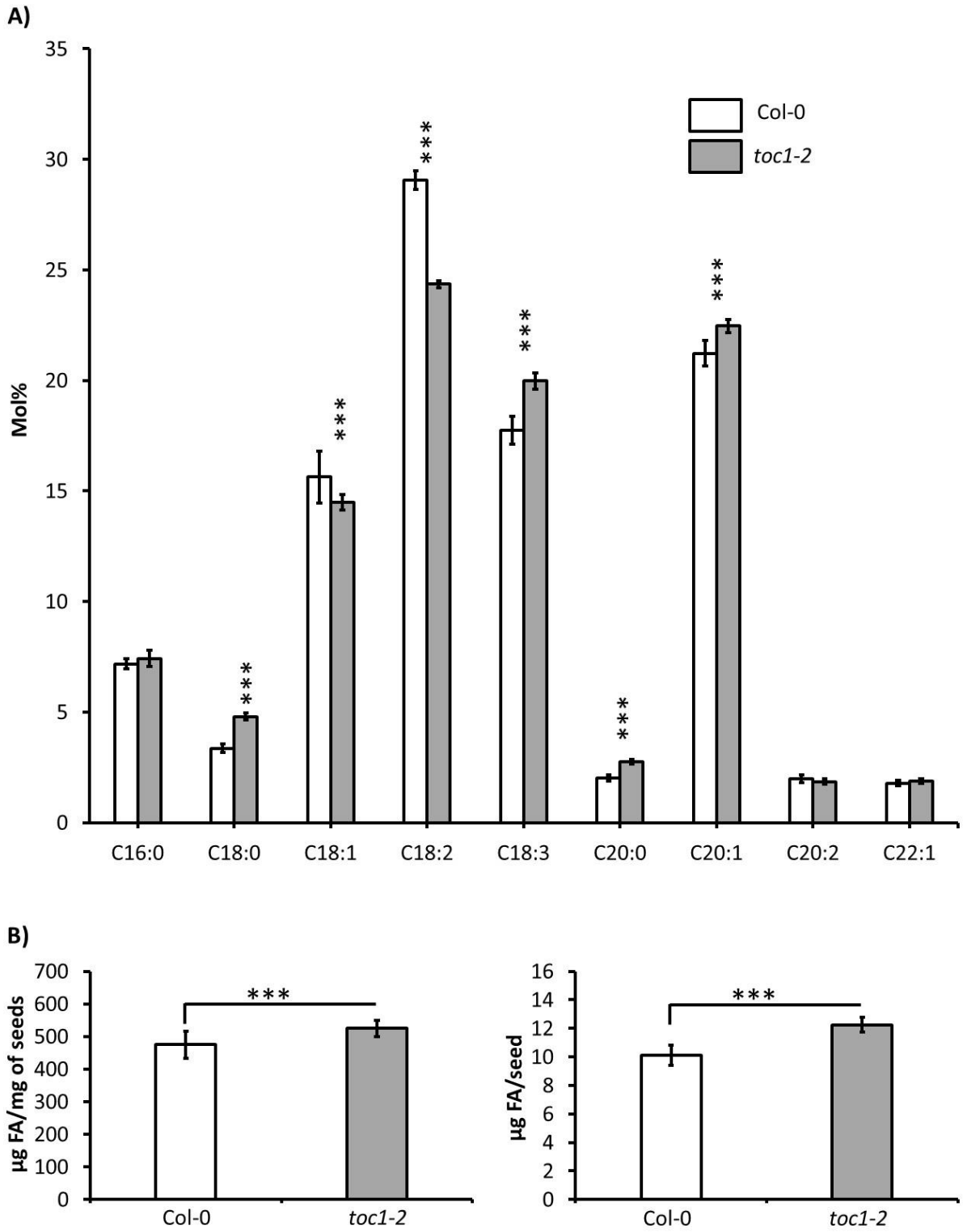

Figure 30. Differences in FA composition between Col-0 and *toc1-2* mature seeds. *A) The qualitative analysis of FA (mol %) and B) the quantitative analyses of FA (µg/seed and µg/mg) were performed using GC-FID data acquired from Col-0 and toc1-2. The statistical significance was evaluated with a bilateral student test using unpaired samples (n = 17; p < 0.05: *, p < 0.01: ** and p < 0.001: ***). Numerical data were indicated in Supplementary Table 6.*

1.1.2. Identification of candidate genes potentially regulated by TOC1

The circadian rhythm is disturbed in *prr5-1*, *prr7-3*, *cca1-11 lhy-21*, TOC1-ox, *toc1-1* and *toc1-2* and not in *prr9-1* (Michael *et al.*, 2003; Alabadi *et al.*, 2001; Makino et al., 2002; Lu *et al.*, 2009; Graf *et al.*, 2010). The circadian period was estimated to 23h in *prr5-1*, 26h in *prr7-3*, 20h in *toc1-1* and *toc1-2*, 30h in TOC1-ox, 17h in *cca1-11 lhy-21* and similar to the WT in *prr9-1* (24h). The circadian system was affected in *prr5-1*, *prr7-3*, *cca1-11 lhy-21*, TOC1-ox and both *toc1*, leading to the desynchronization of the central oscillator with the daily light/dark cycle. Several physiological processes under the control of the circadian clock, including the chlorophyll synthesis and the starch degradation, were altered because of the desynchronization of the internal timekeeper with the external environment (Dodd *et al.*, 2005; Graf *et al.*, 2010).

For instance, Dodd *et al.* (2005) studied the role of the circadian clock in the synthesis of chlorophyll. Higher amount of chlorophyll was obtained in WT leaves (circadian rhythm: 24h) grown in 12h light/12h dark than in 10h light/10h dark and 14h light/14h dark. In contrast, higher chlorophyll content was observed in *toc1-1* (circadian rhythm: 20h) leaves exposed to 10h light/10h dark than in 14h light/14h dark. Dodd *et al.* (2005) showed that chlorophyll synthesis was enhanced when the central oscillator was synchronized with the daily light/dark cycles.

Graf *et al.* (2010) worked on the involvement of the circadian clock in the degradation of starch during the night period. Starch reserves accumulate during the day period and are mobilized when plants are not exposed to light, therefore ensuring the production of energy during the whole night period (Gibon *et al.*, 2009). Starch was almost consumed by the end of the night period in WT (circadian rhythm: 24h) plants grown under 12h light/12h dark cycles, while starch reserves were exhausted 3 to 4h before the end of the night period in *cca1-lhy* (circadian rhythm: 17h) exposed under 12h light/12h dark. Starch exhaustion was no longer observed during the night period in *cca1-lhy* (circadian rhythm: 17h) plants grown under 8.5h light/8.5h dark. The regulation of the starch degradation was ensured when the central oscillator was synchronized with the daily light/dark cycle (Graf *et al.*, 2010).

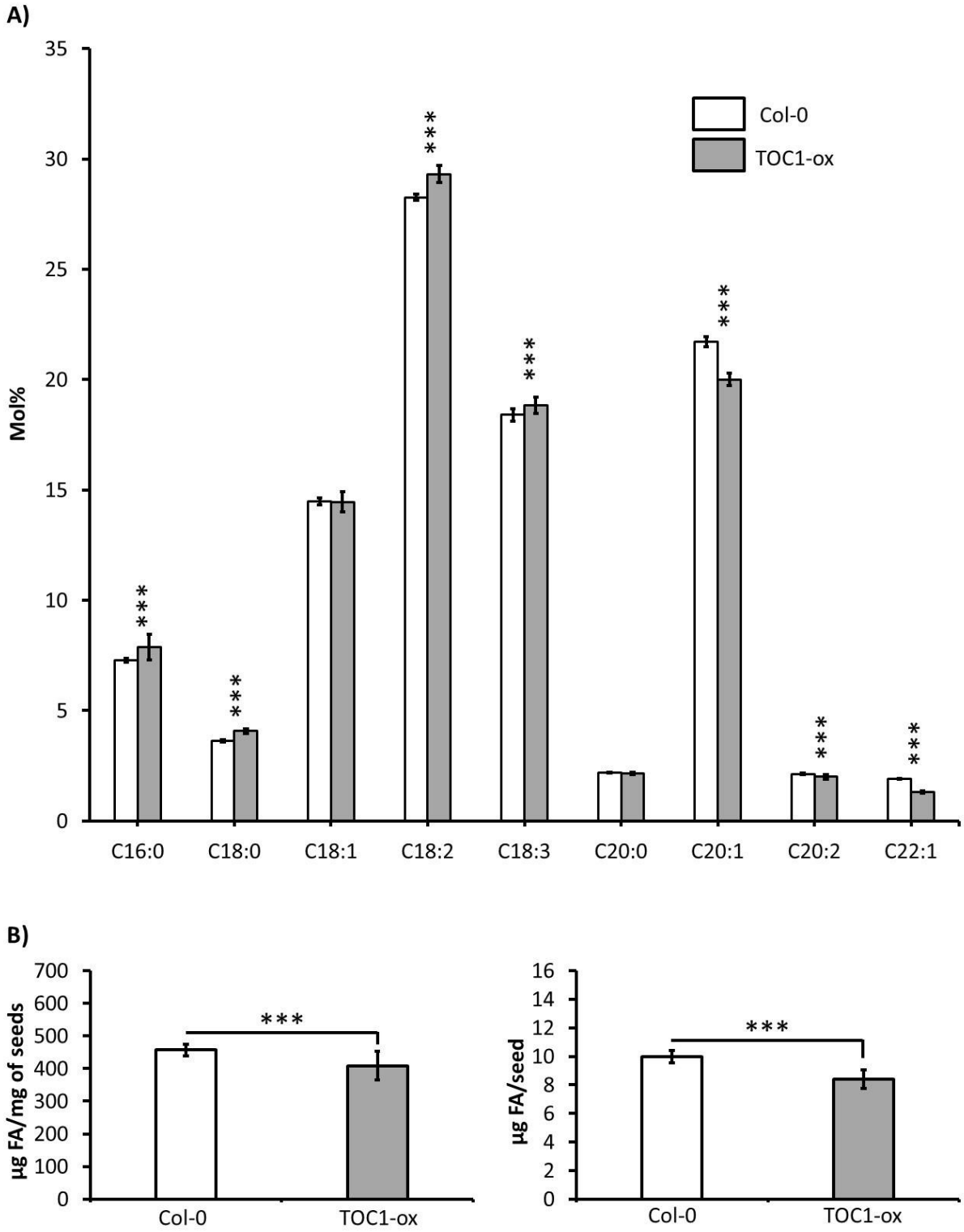

Figure 31. Differences in FA composition between Col-0 and TOC1-ox mature seeds. *A) The qualitative analysis of FA (mol %) and B) the quantitative analyses of FA (µg/seed and µg/mg) were performed using GC-FID data acquired from Col-0 and toc1-2. The statistical significance was evaluated with a bilateral student test using unpaired samples (n = 18; p < 0.05: *, p < 0.01: ** and p < 0.001: ***). Numerical data were indicated in Supplementary Table 7.*

In the case of FA metabolism in Arabidopsis seeds, changes in FA composition were higher in both *toc1* mutants (circadian rhythm: 20h) than in *cca1-11 lhy-21* (circadian rhythm: 17h) and TOC1-ox (circadian rhythm: 30h) seeds under 12h light/12h dark cycles **(Figure 27, 29, 30 and 31)**. In addition, FA modifications were rather observed in *prr9-1* (circadian rhythm: 24h) than in *prr7-3* (circadian rhythm: 26h) and *prr5-1* (circadian rhythm: 23h) seeds collected from plants exposed under 12h light/12h dark cycles **(Figure 24, 25 and 26)**. Differences between clock mutants and their respective WT were not related to the desynchronization of the central oscillator with the daily light/dark cycles. The alteration of the FA content in clock mutants may be explained by the potential involvement of clock components in the regulation of FA-related genes during seed maturation. Differences observed between both *toc1* mutants and their respective WT reached up to 5 %, while modifications in FA composition between the other clock mutants (*prr5-1*, *prr7-3*, *prr9-1* and *cca1-11 lhy-21*) and their respective WT were lower than 2 %. Both *toc1* mutants were generated from different genetic backgrounds (C24 and Col-0). Similar FA profiles were obtained in both *toc1* mutants despite that TOC1 function was deeper altered in *toc1-2* than in *toc1-1*.

Lemieux *et al.* (1990) have previously characterized Arabidopsis mutant lines generated by random mutagenesis, including BL1 and JB11 lines. BL1 was deficient in C18:2 desaturation and this line was characterized by a reduction of C18:3 content in their seeds. On the contrary, JB11 was referred as *enhanced linolenate accumulation 1* (*ela1*) line since the mutation increased C18:3 seed content. The percentages of C18:0, C18:3, C20:0 and C20:1 were higher in JB11 line than in its respective WT, while C18:1 and C18:2 were increased in the respective WT (Lemieux *et al.*, 1990). This FA profile is similar to the one obtained in both *toc1* mutants **(Figure 29A and 30A)**. This similarity suggests a potential role of TOC1 in the regulation of at least one C18:3-producing desaturase. The plastid-localized FAD7 and FAD8 and the microsomal FAD3, involved in the conversion of C18:2 into C18:3 moieties glycerolipids, may be partially regulated by TOC1. The use of the "Electronic Fluorescent Pictograph (Arabidopsis eFP Browser)" (http://www.bar.utoronto.ca/) and previous studies (Browse *et al.*, 1993; McConn *et al.*, 1994) have, however, revealed higher expression of *FAD3* than *FAD7* and *FAD8* in Arabidopsis developing seeds. Moreover, it has been described that the expression of *FAD3* is controlled by bZIP67 (Mendes *et al.*, 2013). Therefore, TOC1 may,

directly or indirectly through bZIP67, partially controls the expression of *FAD3* in Arabidopsis seeds.

FAE1 is one of the 21 genes encoding for the β-ketoacyl-CoA synthase. This gene is highly expressed in Arabidopsis developing seeds (James *et al.*, 1995). The alteration of *FAE1* in Arabidopsis seeds leads to a sharp decrease in C20:1 content and the increase in the proportion of C18:1. One of the roles associated to *FAE1* was converting C18:1 into C20:1 in Arabidopsis developing seeds (James *et al.*, 1995; Millar and Kunst, 1997). Our data revealed that C18:1 was decreased in both *toc1* mutants, while C20:1 was increased in both *toc1* mutants **(Figure 29A and 30A)**. TOC1 may potentially also participates in the regulation of the expression of *FAE1*.

FA synthesis is positively regulated by WRI1 during seed maturation (Focks and Benning, 1998; Baud *et al.*, 2007b). Our data showed significant increase and decrease in the total amount of FA in both *toc1* mutants and TOC1-ox, respectively **(Figure 29B, 30B and 31B)**. It was thus suggested that TOC1 could participate in the regulation of *WRI1* expression.

1.2. Investigation of the potential role of TOC1 in FA synthesis in seedlings and leaves

Results generated in both *toc1* mature seed mutants showed a potential regulation of FA metabolism by TOC1 in developing seeds. The next objective was investigating the potential role of TOC1 in the regulation of FA metabolism in leaves and seedlings. FA qualitative analyses were carried out in both *toc1* mutants and WT seedlings and leaves.

FA were extracted from both *toc1* mutants (*toc1-1* and *toc1-2*) and respective WT (C24 and Col-0) leaves and seedlings. The acquisition of chromatogram from seedlings and leaves allowed the identification of eight FA, including palmitic (C16:0), palmitoleic (C16:1), hexadecadienoic (C16:2), hexadecatrienoic (C16:3), stearic (C18:0), oleic (C18:1), linoleic (C18:2) and linolenic (C18:3) acids. The mole percent of each individual FA was calculated using GC-FID data acquired from leaves and seedlings. Our data were compared with the one already published by Miquel *et al.* (1992) and Browse *et al.* (1986).

The transmethylation protocol was used for the extraction of FAMEs from leaves and seedlings. FA were directly transmethylated from these tissues without performing a prior glycerolipid extraction step. This protocol was similar to the one used by Miquel *et al.* (1992) and Browse *et al.* (1986). The comparison of data generated from Col-0 leaves in this present

study with those published by Miquel *et al.* (1992) and Browse *et al.* (1986) showed similar FA profiles **(Table 4)**. In leaves, major FA corresponded to C18:3 (43.8 %), C18:2 (19.1 %), C16:0 (15.2 %), C16:3 (13 %), C18:1 (4.7 %), C16:1 (2 %), C18:0 (1.6 %) and C16:2 (0.5 %).

Table 4. Comparison of FA profiles obtained from Col-0 Arabidopsis leaves. *Values are expressed in mol% ± standard deviation, N.S.: not specified, (n = 27).*

FA	Present study	Miquel *et al.* (1992)	Browse *et al.* (1986)
C16:0	15.2 ± 0.2	15.0 ± 0.1	15.8 ± N.S.
C16:1	2.0 ± 0.1	3.8 ± 0.0	2.4 ± N.S.
C16:2	0.5 ± 0.0	1.1 ± 0.0	0.3 ± N.S.
C16:3	13.0 ± 1.0	13.8 ± 0.2	10.7 ± N.S.
C18:0	1.6 ± 0.2	1.0 ± 0.0	1.3 ± N.S.
C18:1	4.7 ± 0.8	3.5 ± 0.1	3.7 ± N.S.
C18:2	19.1 ± 0.7	15.7 ± 0.2	17.0 ± N.S.
C18:3	43.8 ± 0.7	46.0 ± 0.2	48.7 ± N.S.

1.2.1. Characterization of the FA profiles in *toc1* mutant seedlings

FA were qualitatively analyzed in both *toc1* (*toc1-1* and *toc1-2*) mutants and their respective WT seedlings **(Figure 32)**. FA qualitative analysis showed significant modifications (p-value < 0.05) in the case of four FA between *toc1-1* and C24 seedlings. These four FA correspond to C16:0, C16:3, C18:1 and C18:2. The mole percents of C16:0 and C16:3 were increased in *toc1-1* seedlings, while C18:1 and C18:2 were higher in C24 seedlings **(Figure 32A)**. Differences between C24 and *toc1-1* seedlings were estimated to 0.2 % for C18:1 and 1.9 % for C18:2, while changes were evaluated to 1.1 % for C18:1 and 5.1 % for C18:2 in mature seeds. Unlike mature seeds, the mole percents of C18:0 and C18:3 were not significantly modified (p-value > 0.05) between C24 and *toc1-1* seedlings. Results revealed that FA profiles were less altered in *toc1-1* seedlings than in *toc1-1* mature seeds **(Figure 29A and 32A).**

FA qualitative analysis showed significant modifications (p-value < 0.05) in the case of five FA between Col-0 and *toc1-2* seedlings, corresponding to C16:0, C16:3, C18:0, C18:1 and C18:2. C16:0 and C18:0 were increased in *toc1-2* seedlings, while C16:3, C18:1 and C18:2 were higher in WT seedlings **(Figure 32B)**. Differences between Col-0 and *toc1-2* seedlings were estimated to 0.6 % for C18:0, 0.1 % for C18:1 and 2 % for C18:2, while changes were evaluated to 1.4 % for C18:0, 1.2 % for C18:1 and 4.7 % for C18:2 in mature seeds. Unlike mature seeds, the mole percent of C18:3 was not significantly changed (p-value > 0.05) between Col-0 and *toc1-2* seedlings **(Figure 30A and 32A)**. Results showed that FA profile were

less affected in *toc1-2* seedlings than in *toc1-2* mature seeds.

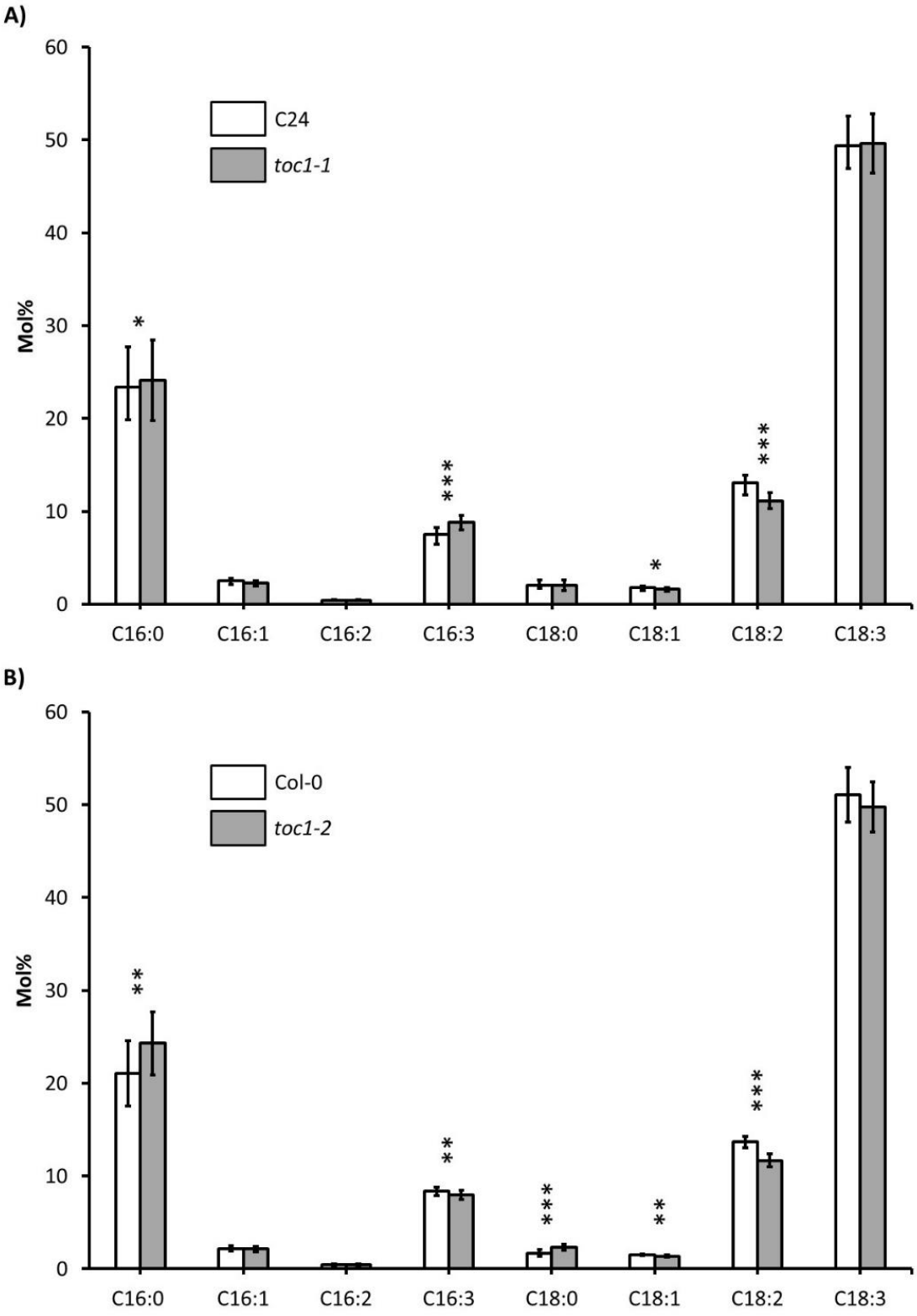

Figure 32. Differences in FA composition between *toc1* and respective WT seedlings. *The qualitative analyses of FA (mol %) was performed using GC-FID data acquired from A) C24 and toc1-1 seedlings and B) Col-0 and toc1-2 seedlings. The statistical significance was evaluated with a bilateral student test using unpaired samples (n = 27; p < 0.05: *, p < 0.01: ** and p < 0.001: ***). Numerical data were indicated in Supplementary Table 9.*

1.2.2. Characterization of the FA profiles in *toc1* mutant leaves

FA were qualitatively analyzed in both *toc1* (*toc1-1* and *toc1-2*) mutants and their respective WT leaves **(Figure 33)**. FA qualitative analysis showed significant modifications in the case of two FA between C24 and *toc1-1* leaves. These two FA corresponding to C16:1 and C18:2 was significantly higher (p-value < 0.05) in C24 leaves **(Figure 33A)**. Difference between Arabidopsis C24 and *toc1-1* leaves was estimated to 3.5 % for C18:2 in comparison to 5.1 % for this FA in mature seeds. Unlike mature seeds, C18:0, C18:1 and C18:3 were not significantly altered (p-value > 0.05) between C24 and *toc1-1* leaves **(Figure 29A and 33A)**. Results revealed that FA profile were less affected in *toc1-1* seedlings than in *toc1-1* seeds.

FA qualitative analysis showed significant modifications (p-value < 0.05) in the case of eight FA between Col-0 and *toc1-2* leaves. The percentages of C16:0, C18:0, C18:1 and C18:2 were significantly higher in *toc1-2* leaves **(Figure 33B)**, while C16:1, C16:2, C16:3 and C18:3 were significantly decreased in *toc1-2* leaves. Differences between Col-0 and *toc1-2* leaves were estimated to 0.3 % for C18:0, 1.2 % for C18:1, 1 % for C18:2 and 2.6 % for C18:3, while these changes were evaluated to 1.4 % for C18:0, 1.2 % for C18:1, 4.7 % for C18:2 and 2.2 % for C18:3 in mature seeds. C18:1 and C18:2 were increased in *toc1-2* leaves, while these two FA were significantly higher in Col-0 mature seeds. Unlike mature seeds, C18:3 content in leaves was significantly lower in *toc1-2* than in its respective WT **(Figure 30A and 33B)**.

1.2.3. FA profiles in *toc1* specifically associated to seed maturation

FA analyses performed in mature seeds showed similarities in the FA profiles between both *toc1* mutants generated from two different genetic background, C24 and Col-0 respectively **(Figure 29 and 30)**. The decrease of C18:2 combined with the increase of C18:3 seed contents in both *toc1* mutants allowed hypothesizing about the potential role of TOC1 in the regulation of *FAD3* and *bZIP67* during seed maturation **(Figure 29 and 30)**.

Unlike mature seeds, FA profiles in both *toc1* mutant seedlings were not highly modified in comparison to the obtained from their respective WT. C18:2 content was significantly decreased in both *toc1* seedlings mutants. In the case of a potential regulation of *FAD3* by TOC1 in developing seedlings, the decrease of C18:2 observed in *toc1-1* and *toc1-2* seedlings should also be associated to the increase of C18:3 content in both *toc1* mutants. No significant difference in C18:3 content was, however, observed between both *toc1* seedlings

mutants and their respective WT **(Figure 32A and 32B)**.

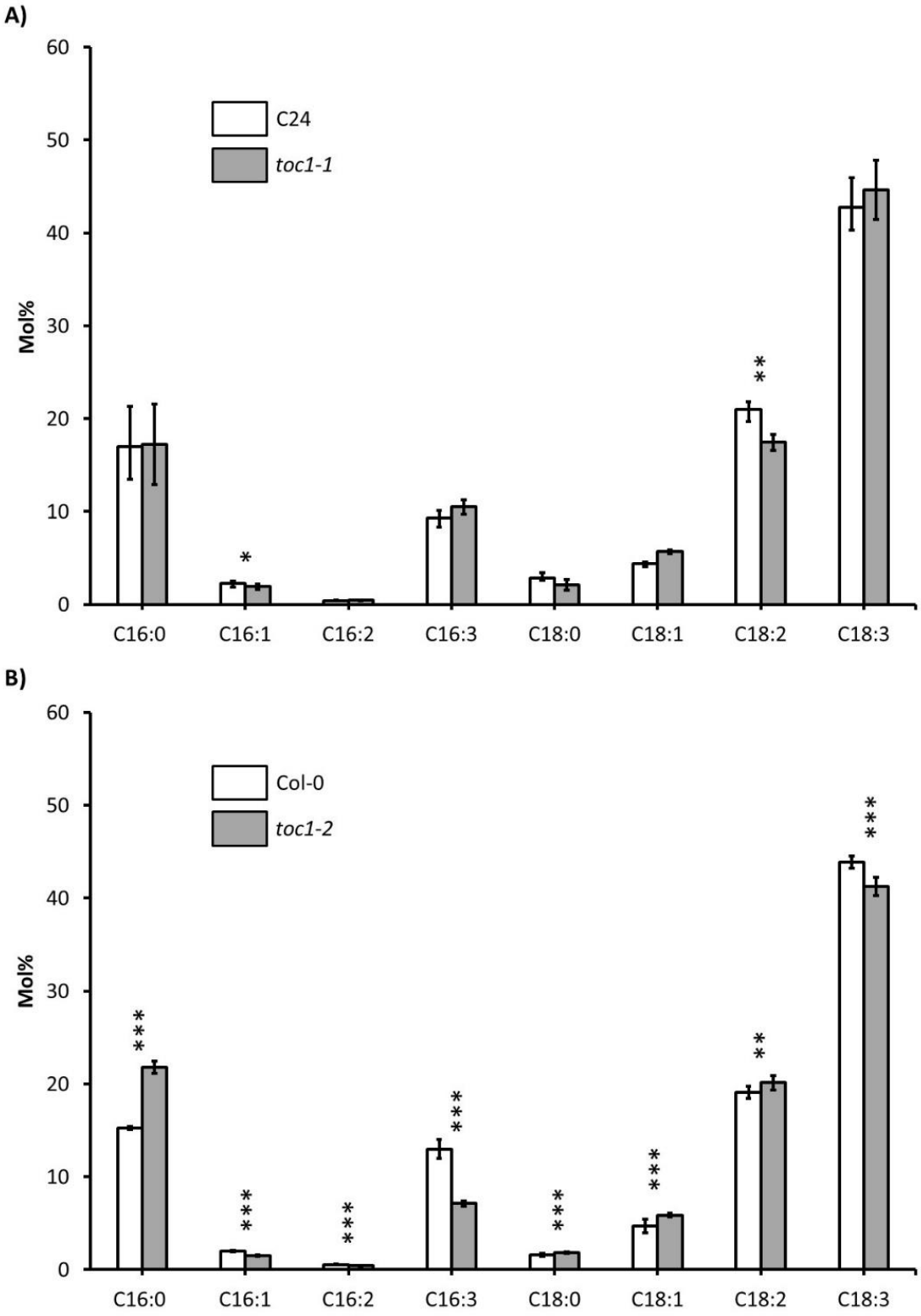

Figure 33. Differences in FA composition between *toc1* and respective WT leaves. *The qualitative analyses of FA (mol %) was performed using GC-FID data acquired from A) C24 and toc1-1 leaves and B) Col-0 and toc1-2 leaves. The statistical significance was evaluated with a bilateral student test using unpaired samples (n = 27; p < 0.05: *, p < 0.01: ** and p < 0.001: ***). Numerical data were indicated in Supplementary Table 10.*

Results generated from leaves showed no similarities in FA profiles between both *toc1* mutants **(Figure 33A and 33B)**. FA composition in *toc1-1* mutant leaves was similar to its respective WT leaves **(Figure 33A)**. FA profile in *toc1-2* leaves was, however, altered in comparison to its WT **(Figure 33B),** this modification was probably due to a more important global phenotype in *toc1-2* than in WT plants **(Figure 21)**.

FA analyses did not reveal a regular FA phenotype in leaves and seedlings for both *toc1* mutants in comparison to the FA profile obtained in mature seeds. FA profiles observed in both *toc1* mutant seeds were specifically associated to seed maturation.

2. Glycerolipid composition in *toc1* and TOC1-ox mutants

The next objective consisted in studying the glycerolipid composition of TOC1-ox and both *toc1* mutant mature seeds and characterizing the glycerolipid profiles of *toc1-1* seedlings.

2.1. Lipidomic analyses in mature seeds

2.1.1. Characterization of glycerolipid profiles in *toc1* and TOC1-ox mature seeds

Glycerolipids were qualitatively analyzed in *toc1-1*, *toc1-2* and TOC1-ox mutant mature seeds. The percentages of each glycerolipid species in *toc1-1*, *toc1-2* and TOC1-ox mutants were calculated and compared with data generated from their respective WT (C24 and Col-0) mature seeds.

Once extracted from mature seeds, glycerolipids were analyzed by HPLC-QTOF in positive and negative modes. No chromatographic peak was detected when glycerolipids were analyzed in negative mode. Indeed, 93 % of glycerolipids accumulated during seed maturation correspond to TAG (Baud *et al.*, 2002). This neutral glycerolipid was, however, detected in positive mode but not in negative mode (Harshfield *et al.*, 2019). Chromatographic and mass spectral data were, therefore, acquired in positive mode. The acquired chromatographic and mass spectral data were imported in MS-DIAL 4 software (Tsugawa *et al.*, 2020). Chromatographic peaks were annotated using mass information. Retention time, MS and MS2 spectra were compared with reference data contained within the LipidBlast database (Materials and Methods, 2.2.). A total of 118 glycerolipids species were annotated putatively in positive mode, including 18 DAG, 4 DGDG, 4 LPC, 1 MGDG, 19 PC, 11 PE and 61 TAG. These 118 species were indicated in **Supplementary Table 11**.

Phenotypic differences may be potentially observed between C24 and Col-0 because of differences in genetic backgrounds between both WT. Lipidomic data were first compared between C24 and Col-0. The peak table file containing the qualitative data (mol%) of the 118 annotated glycerolipid species was imported in Metaboanalyst (Pang *et al.*, 2022). This online statistical software was used for the detection of potential lipidomic differences between both WT. A t-test was performed for each of these 118 lipid molecular species. The t-test showed that 106 glycerolipids species were not significantly modified between C24 and

Col-0 (p-value > 0.05), whereas 12 glycerolipid species were significantly different between both WT (p-value < 0.05). These 12 glycerolipid species correspond to TAG 60:8 (TAG C20:2-C18:3-C22:3), TAG 58:8 (TAG C18:3-C18:3-C22:2), TAG 60:6 (TAG C20:2-C22:1-C18:3), TAG 50:3 (TAG C16:0-C16:0-C18:3), TAG 60:5 (TAG C20:1-C22:1-C18:3), TAG 58:7 (TAG C18:3-C18:3-C22:1), TAG 60:4 (TAG C20:1-C22:1-C18:2), TAG 58:3 (TAG C18:1-C20:1-C20:1), TAG 58:6 (TAG C18:3-C20:2-C20:1), TAG 58:4 (TAG C18:2-C20:1-C20:1), TAG 58:5 (TAG C18:2-C20:2-C20:1) and TAG 54:6 (TAG C18:1-C18:2-C18:3) **(Supplementary Table 11)**. Differences between C24 and Col-0 were estimated to 0.001 % for TAG 60:8 (TAG C20:2-C18:3-C22:3), 0.006 % for TAG 58:8 (TAG C18:3-C18:3-C22:2), 0.02 % for TAG 60:6 (TAG C20:2-C22:1-C18:3), 0.03 % for TAG 50:3 (TAG C16:0-C16:0-C18:3), 0.05 % for TAG 60:5 (TAG C20:1-C22:1-C18:3), 0.06 % for TAG 58:7 (TAG C18:3-C18:3-C22:1) and TAG 60:4 (TAG C20:1-C22:1-C18:2), 0.1 % for TAG 58:3 (TAG C18:1-C20:1-C20:1), 0.13 % for TAG 58:6 (TAG C18:3-C20:2-C20:1), 0.16 % for TAG 58:4 (TAG C18:2-C20:1-C20:1) and TAG 58:5 (TAG C18:2-C20:2-C20:1) and 0.23 % for TAG 54:6 (TAG C18:1-C18:2-C18:3). Differences in the mole percents of these 12 glycerolipid species were comprised between 0.001 % and 0.23 %. Glycerolipid profile in Col-0 mature seeds was, therefore, close to the profile observed in C24 mature seeds **(Figure 34A)**.

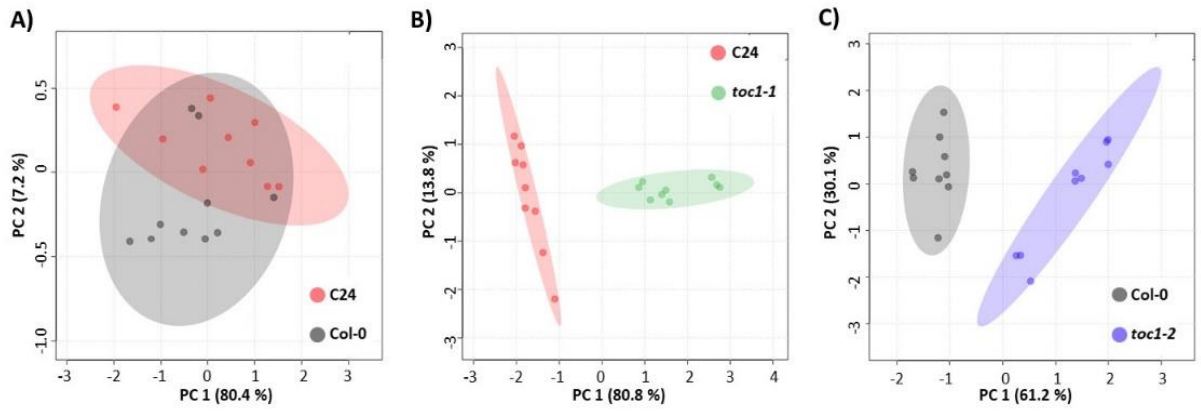

Figure 34. Lipidomic differences between WT and *toc1* seeds observed by principal component analysis (PCA). *A) Comparison between C24 (red) and Col-0 (black) by PCA. The PCA explains 87.6 % of the total variabilities: 80.4 % for the first principal components (PC1) and 7.2 % for the second principal components (PC2). B) Comparison between C24 (red) and toc1-1 (green) by PCA. PC1 and PC2 explain 80.8 and 13.8 % of variabilities. C) Comparison between Col-0 (black) and toc1-2 (purple) by PCA. PC1 and PC2 explain 61.2 and 30.1 % of variabilities.*

Peak table files containing the molar percents of the 118 glycerolipid species in both *toc1* mutants and their respective WT mature seeds were then imported in Metaboanalyst website (Pang *et al.*, 2022). PCA showed discrimination between both *toc1* mutants and their respective WT groups **(Figure 34B and 34C)**. Lipidomic differences were observed between both *toc1* mutants and their respective WT. Student tests were performed

for each annotated glycerolipid species in order to explain discriminations observed between both *toc1* mutants and their respective WT. Results were represented in form of heatmaps **(Supplementary Figure 1)** and histograms **(Figure 35 and 36)**. Student test was carried out using lipidomic data acquired in positive mode from both loss-of-function *toc1* mutants and their respective WT mature seeds. This univariate statistical analysis showed significant differences in the mole percents of 43 glycerolipid species between C24 and *toc1-1*, while significant modifications was revealed for 50 glycerolipid species between Col-0 and *toc1-2*. 35 over the 43 species discriminated in *toc1-1* were also significantly modified in *toc1-2*. These 35 glycerolipid species were highlighted in yellow in **Supplementary Figure 1**. Histogram for each of these 35 species showed similar modifications between both *toc1* mutants and their respective WT **(Figure 35 and 36)**. In addition, our results revealed no significant difference between C24 and Col-0 except for 12 glycerolipid species in which differences were significantly lower than 0.23 %. Glycerolipid profile observed in Col-0 was close to the profile obtained in C24. It was concluded that the mole percents of the 35 discriminated species were similar in both *toc1* mutants generated from C24 and Col-0. Differences in the mole percents of these 35 species between both *toc1* mutants and their respective WT reached up to 1.62 % in the case of *toc1-1* and 1.05 % in the case of *toc1-2*.

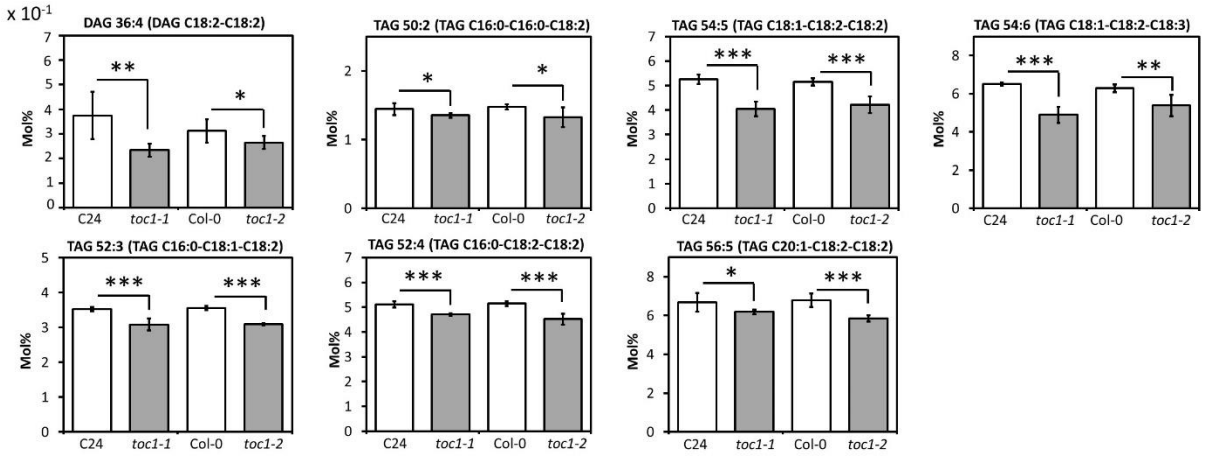

Figure 35. Differences in glycerolipid composition between *toc1* and WT mature seeds. *These histograms showed differences in the percentage of seven glycerolipid species in WT and clock mutants. These species mostly correspond to TAG containing C18:1 and C18:2. The statistical significance was evaluated with a bilateral student test using unpaired samples (n = 9; p < 0.05: *, p < 0.01: ** and p < 0.001: ***). Numerical data were indicated in Supplementary Table 12a.*

The qualitative analyses of glycerolipids showed that a total of 24 TAG containing C18:0, C18:3, C20:0 and C20:1 were significantly increased in both *toc1* mutant mature seeds **(Figure 36)**. On the contrary, the mole percents of seven C18:1 and C18:2 moieties TAG were

significantly higher in both WT than in both *toc1* seeds **(Figure 35)**.

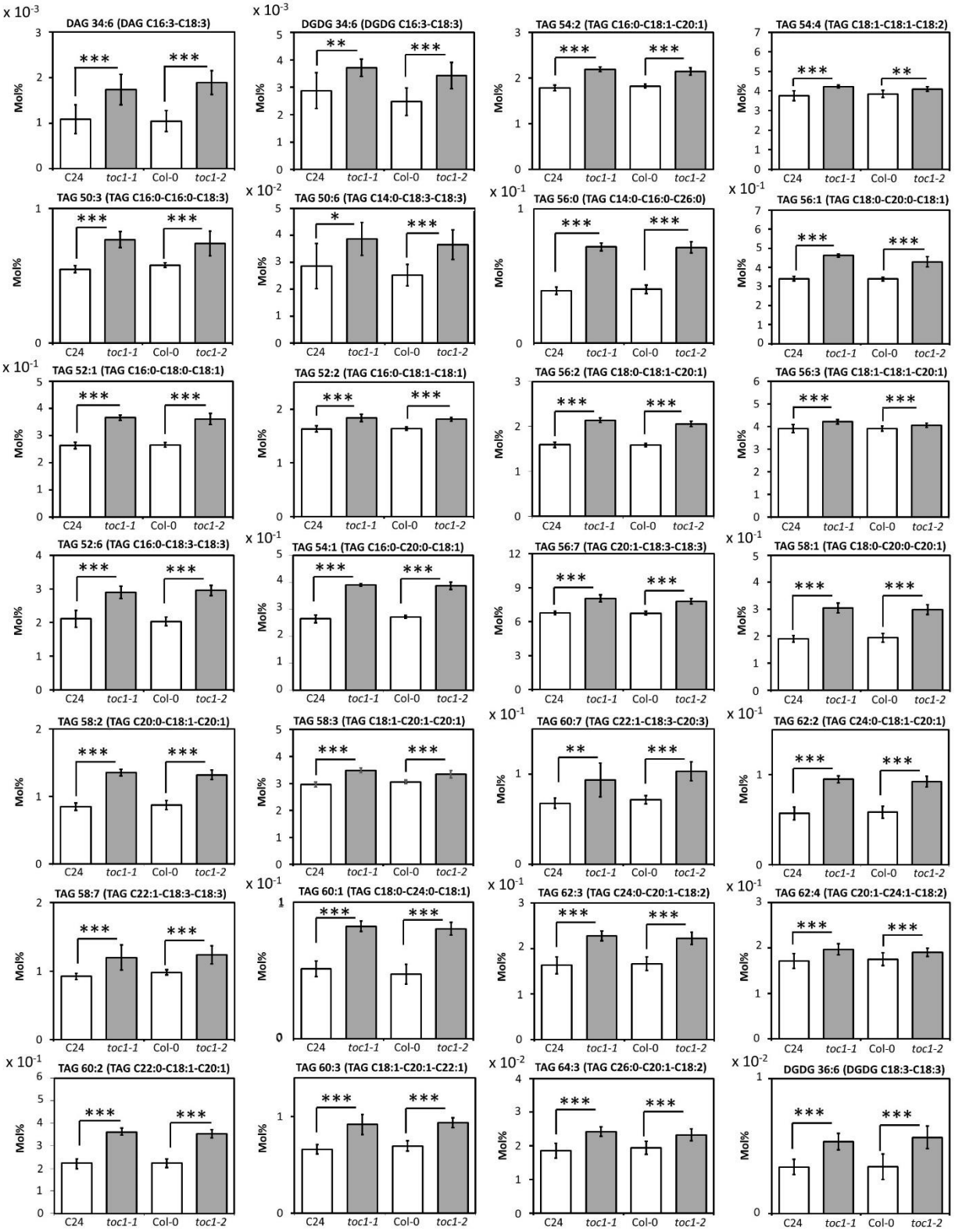

Figure 36. Differences in glycerolipid profile between *toc1* and WT mature seeds. *These histograms showed differences in the percentage of 28 glycerolipid species in WT and clock mutants. These species mostly correspond to TAG containing C18:0 and C18:3, C20:0 and C20:1. The statistical significance was evaluated with a bilateral student test using unpaired samples (n = 9; p < 0.05: *, p < 0.01: ** and p < 0.001: ***). Numerical data were indicated in Supplementary Table 12a.*

Further statistical analyses were carried out using lipidomic data generated from TOC1-ox and Col-0 mature seeds. Student test showed that the molar percents of 83 glycerolipid species were not significantly different between Col-0 and TOC1-ox (p-value > 0.05), while the percentages of the other glycerolipid species were significantly modified between the overexpressing mutant and its respective WT (p-value < 0.05). The name of glycerolipid species discriminated between Col-0 and TOC1-ox were indicated in the heatmap of the **Supplementary Figure 2**.

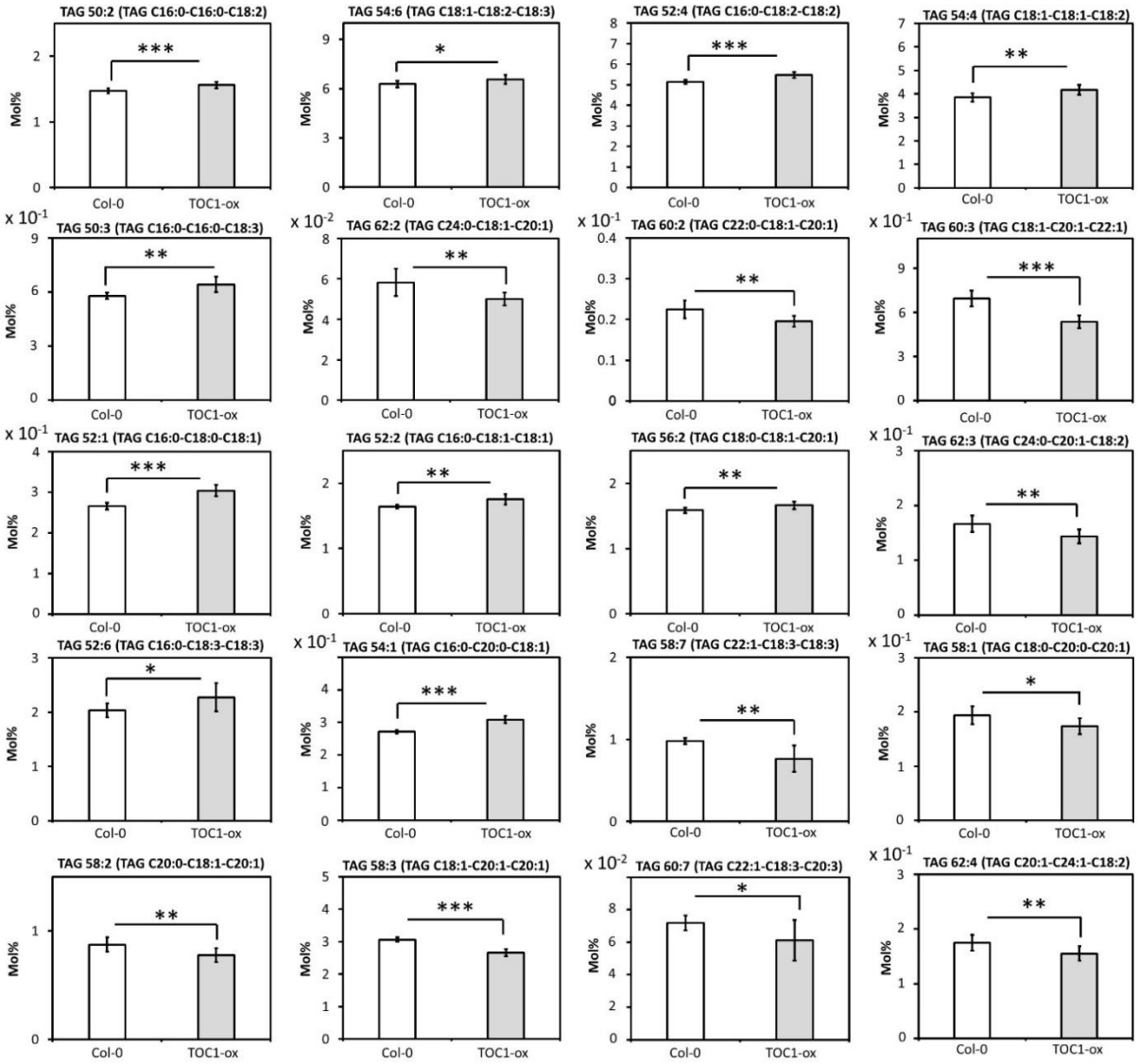

Figure 37. Differences in glycerolipid profiles between Col-0 and TOC1-ox mature seeds. *Histograms showed differences in the percentage of 20 glycerolipid species between Col-0 and TOC1-ox. These 20 species were also significantly modified between both toc mutants and their respective WT. The statistical significance was evaluated with a bilateral student test using unpaired samples (n = 9; p < 0.05: *, p < 0.01: ** and p < 0.001: ***). Numerical data were indicated in Supplementary Table 12b.*

Statistical analyses were also performed between Col-0 and TOC1-ox by focusing on the 35 species in which the mole percents were modified between both *toc1* mutants and their respective WT. Our results showed that 15 over the 35 species modified between both *toc1* mutants and their respective WT were not significantly changed between TOC1-ox and Col-0 (p-value > 0.05). The 20 other species modified between both *toc1* mutants and their respective WT were also significantly changed between TOC1-ox and Col-0 (p-value < 0.05). These 20 glycerolipid species were highlighted in green in the heatmap of the **Supplementary Figure 2**. Modifications observed between Col-0 and TOC1-ox for these 20 species were showed in **Figure 37.** Differences in the mole percents of these 20 species between Col-0 and TOC1-ox were lower than 0.4 %, while differences in the mole percents of these 20 species between *toc1-2* mutants and their respective WT reached up to 0.92 %. In addition, the non-statistical significance observed between Col-0 and TOC1-ox for 83 species allowed concluding that the glycerolipid profiles obtained in TOC1-ox were close to the profile observed in Col-0.

Given that the glycerolipid profile in TOC1-ox were close to the profile in Col-0, the mole percents of the 35 species modified between Col-0 and *toc1-2* may be also changed between TOC1-ox and *toc1-2*. In order to confirm this hypothesis, statistical analyses were performed between *toc1-2* and TOC1-ox, both mutants generated from the same genetic background (Col-0), by focusing on these 35 species.

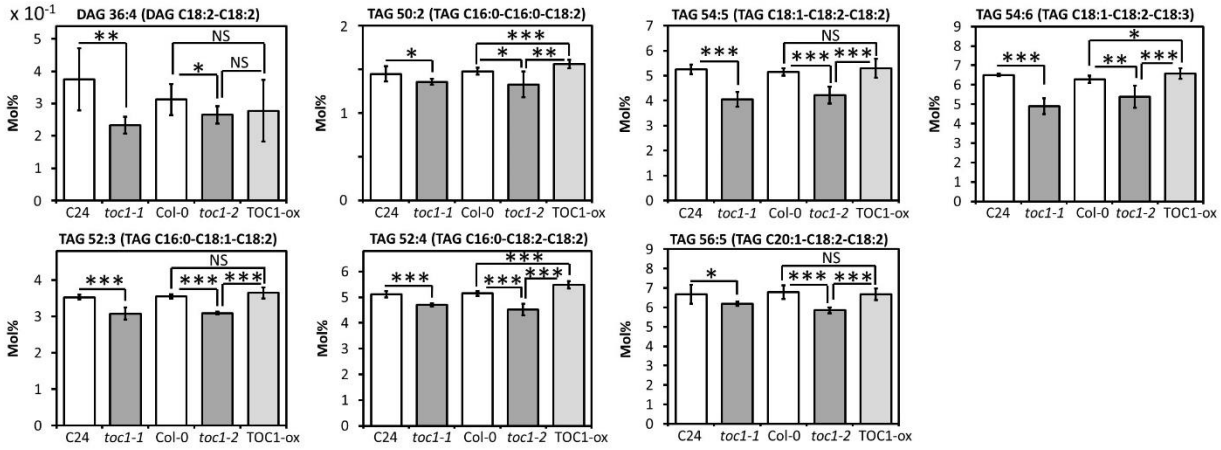

Figure 38. Lipidomic differences between clock mutants and WT mature seeds. *Histograms showed differences in the percentage of seven species between WT and clock mutants. These species mostly correspond to C18:1 and C18:2 moieties TAG. The statistical significance was evaluated with a bilateral student test using unpaired samples (n = 9; p < 0.05: *, p < 0.01: ** and p < 0.001: ***). Numerical data were indicated in Supplementary Table 12c.*

Student tests revealed significant differences between TOC1-ox and *toc1-2* for 32 over the 35 species modified between Col-0 and *toc1-2* **(Figure 38 and 39)**.

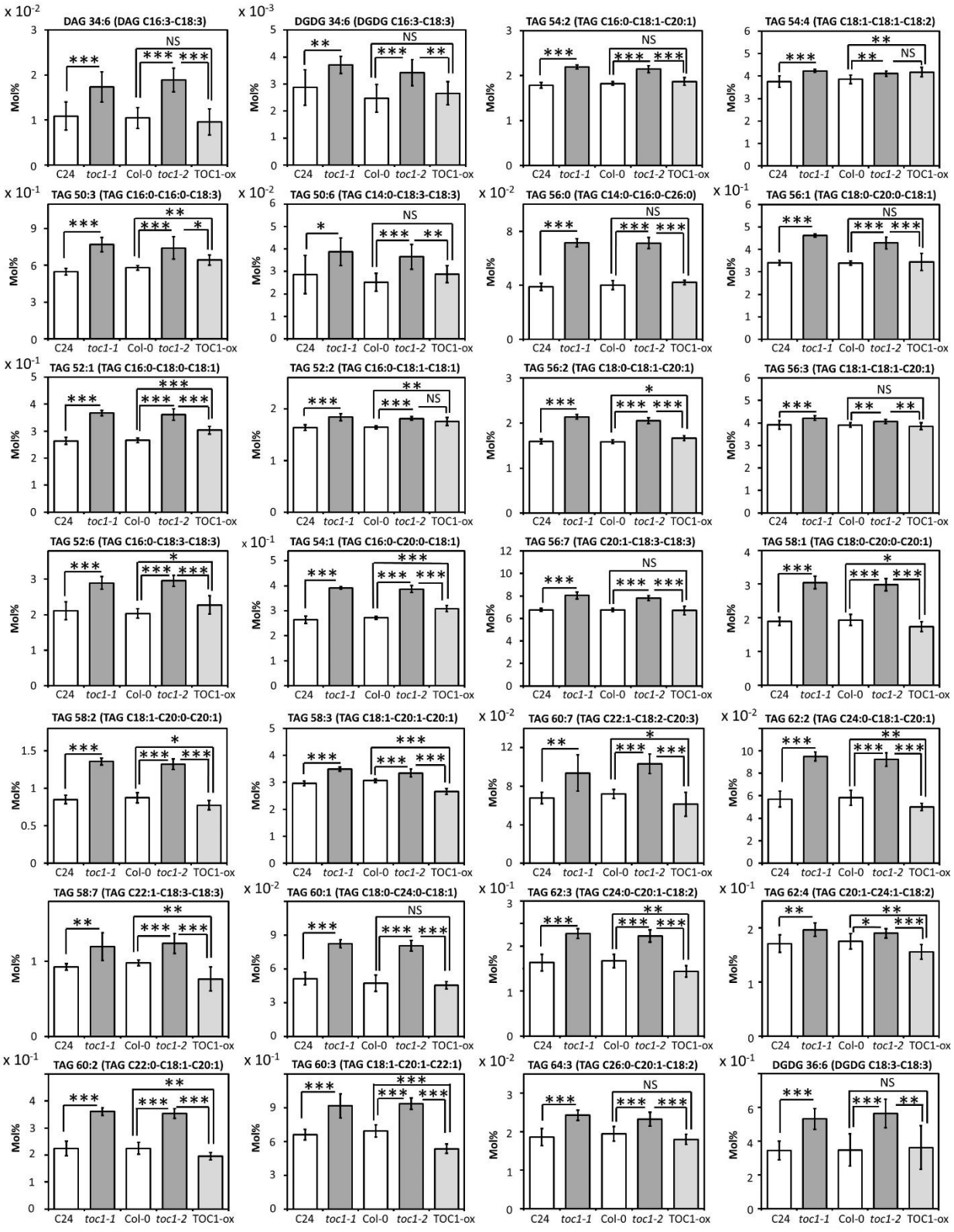

Figure 39. Lipidomic differences between clock mutants and WT mature seeds. *Histograms showed differences in the percentage of 28 species between WT and clock mutants. These species mostly correspond to TAG containing C18:0, C18:3, C20:0 and C20:1. The statistical significance was evaluated with a bilateral student test using unpaired samples (n = 9; p < 0.05: *, p < 0.01: ** and p < 0.001: ***). Numerical data were indicated in Supplementary Table 12c.*

The mole percents of 24 TAGs containing C18:0, C18:3, C20:0 and C20:1 were significantly higher in *toc1-2* than in TOC1-ox. On the contrary, the mole percent of six C18:1 and C18:2 moieties TAGs were significantly increased in TOC1-ox (**Figure 38 and 39**). Differences significantly observed between TOC1-ox and *toc1-2* were comprised 0.001 and 1.18 %, while modifications significantly observed between Col-0 and *toc1-2* were estimated between 0.001 and 1.05 %. Similar results were obtained when the glycerolipid profiles in *toc1-2* were compared with the profiles observed in the overexpressing mutant (TOC1-ox) and with the profiles observed in Col-0 mature seeds **(Figure 38 and 39)**.

2.1.2. Lipidomic differences between both *toc1* mutants and their WT seeds

Lipidomic studies showed that a total of 31 TAG species were discriminated between both *toc1* mutants and their respective WT mature seeds **(Supplementary Figure 1)**. This neutral glycerolipid can be synthesized from the acylation of DAG by DGAT or through the action of the PDAT on PC **(Figure 11)** (Li-Beisson *et al.*, 2013).

Katavic *et al.* (1995) have previously characterized an Arabidopsis mutant line generated by random mutagenesis known as AS11 line. This line was characterized by the reduction in DGAT activity, leading to the increase of DAG and decrease of TAG contents in seeds (Katavic *et al.*, 1995). Katavic *et al.* (1995) showed that DAG content reached up to 12 % of total glycerolipid in the loss-of-function *dgat1-1* mutant, while the percentage of DAG were close to 1 % of the total glycerolipid in WT seeds. In another study, Fan *et al.* (2013) revealed that TAGs were accumulated when *PDAT1* was ectopically overexpressed in leaves. On the contrary, PC content was decreased by 19 % in the overexpressing *PDAT1* mutant (Fan *et al.*, 2013). Both studies showed that the alteration of the expression of genes involved in TAG biosynthesis (*PDAT1* and *DGAT1*) led to the modification of TAG, DAG and PC contents (Katavic *et al.*, 1995; Fan *et al.*, 2013). In the case of a potential regulation of genes involved in TAG biosynthesis by TOC1, modifications between both *toc1* mutants and their respective WT should be observed for three glycerolipids: TAG, DAG and PC (Katavic *et al.*, 1995; Fan *et al.*, 2013). Lipidomic studies revealed that 88.6 % of the glycerolipids significantly modified between both *toc1* mutants and their respective WT corresponded to TAG. Only 11.4 % of the glycerolipids significantly modified between both *toc1* mutants and their respective WT corresponded to DGDG (5.7 %) and DAG (5.7 %). PC species were not significantly modified between both *toc1* mutants and their respective WT mature seeds **(Figure 38 and 39)**. Our

results also revealed that the molar percents of total DAG were not significantly changed between both *toc1* mutants and their respective WT mature seeds **(Figure 40)**.

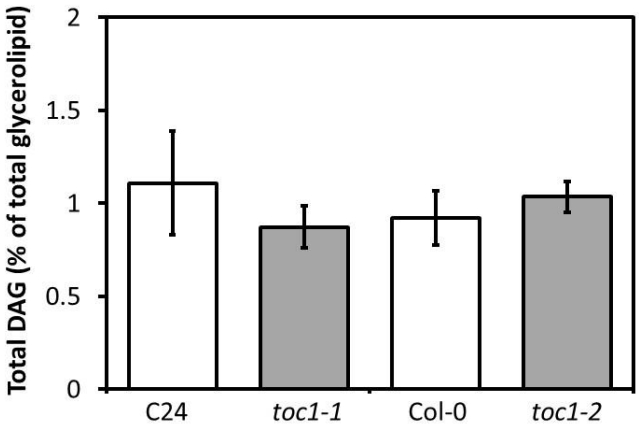

Figure 40. Differences in total DAG between *toc1* and WT mature seeds. *Histograms showed differences in the percentage of total DAG between WT and toc1. The statistical significance was evaluated with a bilateral student test using unpaired samples (n = 9; p < 0.05: *, p < 0.01: ** and p < 0.001: ***).*

Instead, our results showed that the percentages of most TAG species containing C18:0, C18:3, C20:0 and C20:1 were significantly increased in both *toc1* mutant mature seeds, whereas TAG species composed of C18:1 and C18:2 were significantly higher in WT mature seeds **(Figure 38 and 39)**. Lipidomics differences **(Figure 38 and 39)** reflect the FA profiles observed in both *toc1* mutants **(Figure 29A and 30A)**. Thereby, glycerolipid compositions obtained in both *toc1* mutant mature seeds were the consequence of the FA modifications.

2.2. Lipidomic analyses in seedlings

2.2.1. Characterization of glycerolipid profiles in *toc1-1* seedlings

In this part, lipidomic approaches were only performed in *toc1-1* and C24 seedlings but not in *toc1-2* and its respective WT. Indeed, like in the previous section (Results and discussion, 1.2.1.), glycerolipid profile in *toc1-2* seedlings must have been altered in comparison to its respective WT because of a more important global phenotype in *toc1-2* than in its respective WT plants **(Figure 21)**.

During seed maturation, TAG was accumulated within cotyledons (Baud *et al.*, 2002). This neutral glycerolipid was mobilized during the early germination (Graham, 2008), while membrane glycerolipids were rather synthesized in developing seedlings (Ohlrogge and Browse, 1995; Shrestha *et al.*, 2016). Membrane glycerolipids include phospholipids (PA, PC, PE, PI, PG and PS), sulfolipids (SQDG) and galactolipids (MGDG and DGDG). It was shown that

MGDG, PA, PC, PE, PG, PI and SQDG were detected in negative mode, while DAG, DGDG, MGDG, PC, PE, PG, SQDG and TAG were detected in positive mode (Harshfield *et al.*, 2019). Once extracted from seedlings, glycerolipids were analyzed by HPLC-QTOF in both positive and negative modes. The acquired chromatographic and mass spectra data were imported in MS-DIAL 4 software (Tsugawa *et al.*, 2020). Peaks found in each chromatogram were annotated using LipidBlast database (Materials and Methods, 2.2.). In the positive mode, a total of 49 glycerolipid species were annotated, including 6 DAG, 4 DGDG, 7 MGDG, 17 PC, 10 PE, 1 PG and 4 TAG. 20 over the 49 annotated glycerolipids were composed of C18:2, while 23 over the 49 annotated glycerolipid species were composed of C18:3. The six other glycerolipid species were constituted of C18:0, C18:1 and sixteen-carbon FA. The names of the 49 species were indicated in **Supplementary Table 13**. In the negative mode, a total of 51 glycerolipid species were annotated, including 11 MGDG, 3 PA, 8 PC, 9 PE, 9 PG, 3 PI and 8 SQDG. 11 over the 51 annotated glycerolipids were composed of C18:2, while 29 over the 51 annotated glycerolipid species were composed of C18:3. The 11 other glycerolipid species were constituted of C18:0, C18:1 and sixteen-carbon FA. The names of these 51 species were indicated in the **Supplementary Table 14.**

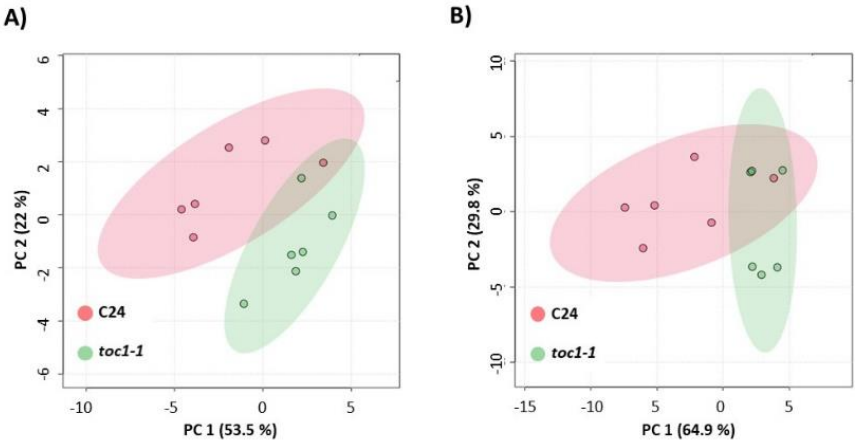

Figure 41. Lipidomic differences between C24 and *toc1-1* seedlings observed by principal component analysis (PCA). *Comparison between C24 (red) and toc1-1 (green) by PCA. A) The PCA was performed using lipidomic data acquired in positive mode. This PCA explains 75.5 % of the total variabilities: 53.5 % for the first principal components (PC 1) and 22 % for the second principal components (PC2). B) The PCA was performed using lipidomic data acquired in negative mode. This PCA explains 94.7 % of the total variabilities: 64.9 % for the first principal components (PC 1) and 29.8 % for the second principal components (PC2).*

Lipidomic data were compared between C24 and *toc1-1* seedlings. Peak table files containing the qualitative data (mol%) of the 49 glycerolipid species acquired in positive mode and 51 glycerolipid species acquired in negative mode were imported in Metaboanalyst (Pang *et al.*, 2022). PCA were performed in order to detect potential discrimination between C24 and *toc1-1* in seedlings. PCA showed discriminations between C24 and *toc1-1* seedlings using lipidomic data acquired in positive and negative modes **(Figure 41)**.

In order to explain discriminations observed in the PCA, a student test (t-test) was performed for each of the 49 glycerolipid species acquired in positive mode. The t-test showed significant differences (p-value < 0.05) in the molar percents of 16 glycerolipid species between C24 and *toc1-1* seedlings. The molar percents of the 33 other glycerolipid species were not significantly modified between C24 and *toc1-1* seedlings **(Supplementary Table 13)**. A student test was also performed for each of the 51 glycerolipid species acquired in negative mode. The t-test showed significant differences in the case of 19 glycerolipid species between C24 and *toc1-1* seedlings. The 32 other glycerolipid species were not significantly modified between C24 and *toc1-1* seedlings **(Supplementary Table 14).**

Lipidomic data acquired in positive and negative modes showed that the mole percents of four C18:2 species (SQDG 34:2, DAG 36:4, DAG 36:3 and TAG 54:6) were significantly decreased in WT seedlings **(Figure 42)**. Differences in the mole percents of these four C18:2 species between C24 and *toc1-1* seedlings were ranged between 0.07 and 0.73 %. The mole percents of five C18:2 species (PE 34:2, PC 34:2, PE 42:2, PC 34:5 and PC 38:2) were significantly increased in WT seedlings **(Figure 42)**. Differences in the mole percents of these five species between C24 and *toc1-1* seedlings were comprised between 0.04 and 2 %. The increase of these five C18:2 species in C24 seedlings may potentially explain the increase of the diunsaturated C18:2 FA content in WT seedlings **(Figure 32A)**.

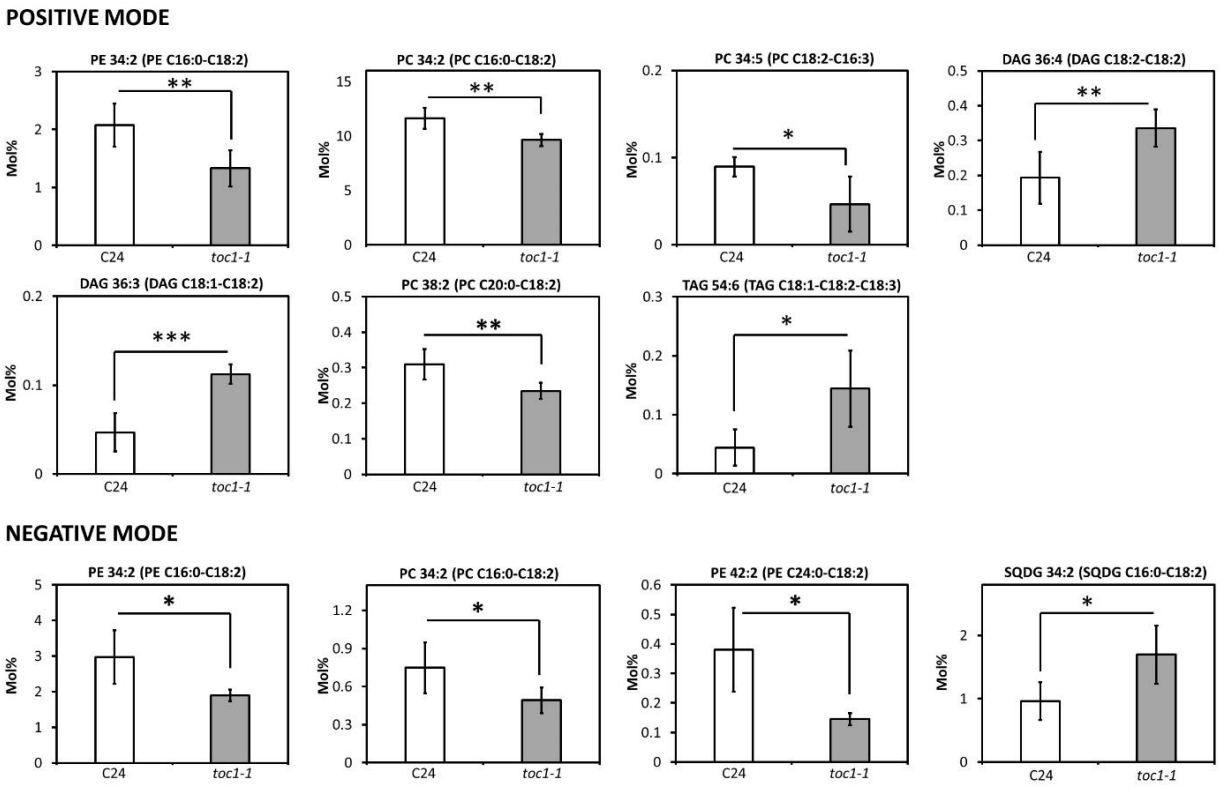

Figure 42. Lipidomic differences between C24 and *toc1-1* seedlings. *These histograms showed differences in the percentage of glycerolipid species containing C18:2 between C24 and toc1-1 seedlings using lipidomic data acquired by HPLC-QTOF in positive and negative modes. The statistical significance was evaluated by a bilateral student test using unpaired samples (n = 9; p < 0.05: *, p < 0.01: ** and p < 0.001: ***). Numerical data were indicated in Supplementary Table 15.*

Lipidomic data acquired in positive and negative modes showed that the mole percents of six C18:3 species (DAG 34:3, PC 32:3, PA 34:3, MGDG 34:6, SQDG 36:3 and SQDG 36:5) were significantly increased in *toc1-1* seedlings **(Figure 43)**. Differences in the mole percents of these six C18:3 species were ranged between 0.046 and 5.42 %. The mole percents of eleven C18:3 species (PC 34:3, PC 36:6, PC 38:3, PE 34:3, PG 34:4, PA 36:6, MGDG 34:5, MGDG 36:5, PI 34:3, PI 36:5 and PI 36:6) were significantly decreased in *toc1-1* seedlings **(Figure 43)**. Differences in the mole percents of these eleven C18:3 species were comprised between 0.056 and 1.19 %. The increase of six C18:3 species combined with the decrease of eleven C18:3 species may potentially explain the non-statistical significance obtained between C24 and *toc1-1* seedlings for C18:3 **(Figure 32A)**.

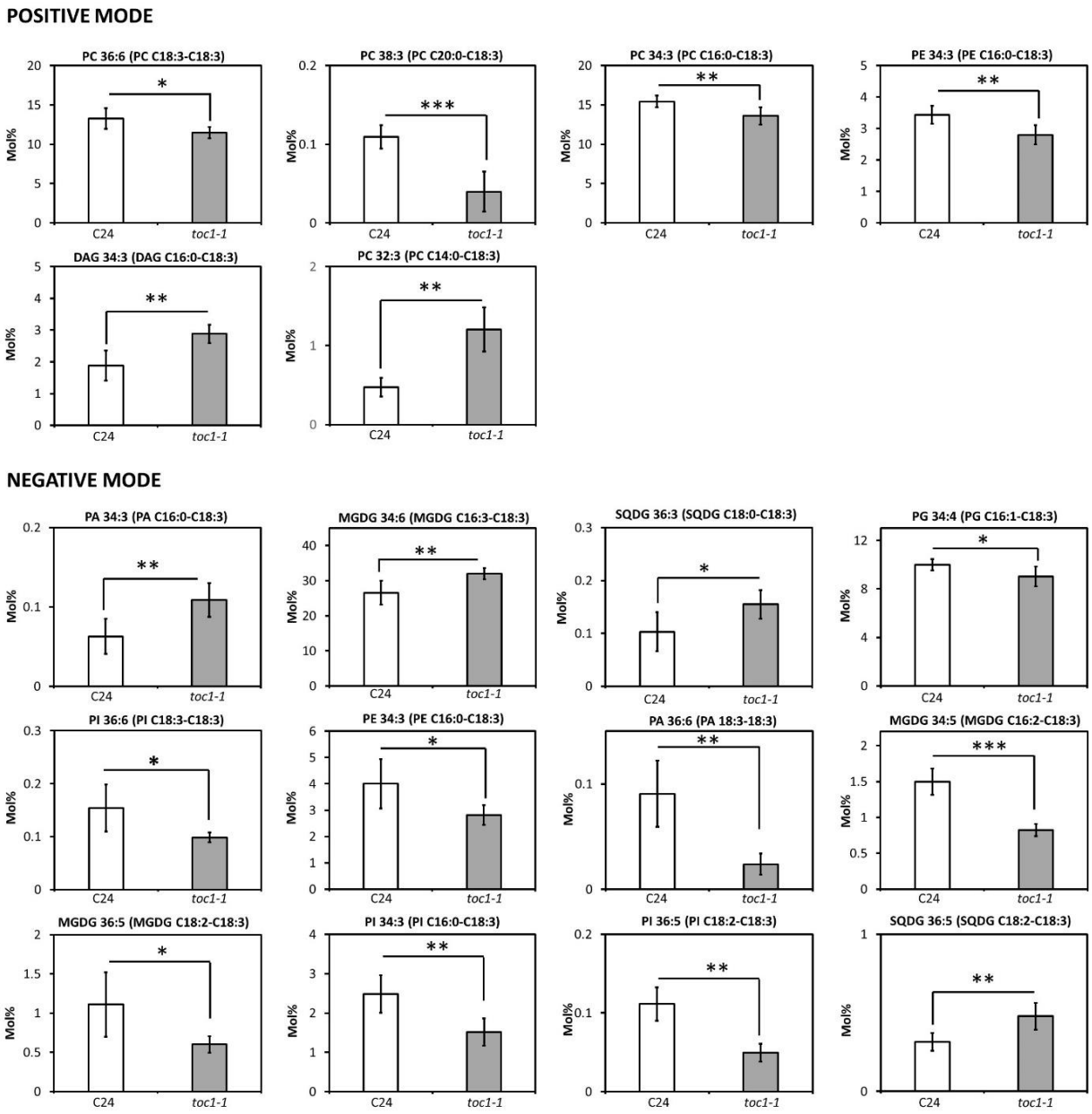

Figure 43. Lipidomic differences between C24 and *toc1-1* seedlings. *These histograms showed differences in the percentage of glycerolipid species containing C18:3 between C24 and toc1-1 seedlings using lipidomic data acquired by HPLC-QTOF in positive and negative modes. The statistical significance was evaluated with a bilateral student test using unpaired samples (n = 9; p < 0.05: *, p < 0.01: ** and p < 0.001: ***). Numerical data were indicated in Supplementary Table 15.*

2.2.2. Mole percents of the total C18:2 and C18:3 in *toc1* and WT seedlings and seeds

Lipidomic analyses performed in mature seeds showed similar glycerolipid profiles in both *toc1* mutants. The content of the total C18:2 moieties TAG was significantly increased in WT seeds **(Table 5)**, while the contents of the total C18:3 moieties TAG were significantly higher in both *toc1* mutants **(Table 5)**. Our results revealed that the glycerolipid profiles obtained in both *toc1* mutant seeds **(Figure 35 and 36)** were the consequences of the

FA modifications observed in both *toc1* mature seeds **(Figure 29A and 30A)**.

In the case of a potential participation of TOC1 in the control of C18:3-producing desaturases in developing seedlings, the contents of C18:2 and C18:3 moieties glycerolipids should be significantly modified between C24 and *toc1-1*. Unlike mature seeds, lipidomic analysis performed in seedlings did not show significant changes in the mole percents of C18:2 moieties glycerolipids between C24 and *toc1-1*, except for nine C18:2 species **(Figure 42)**. The increase observed in WT seedlings for five C18:2 species may explain the increase of the diunsaturated C18:2 FA content in WT seedlings **(Figure 32A)**. In order to validate this hypothesis, the mole percents of the total C18:2 moieties glycerolipids were calculated in C24 and *toc1-1* seedlings and then statistically compared between the loss-of-function mutant and its respective WT **(Table 5)**. The total C18:2 species were not significantly modified between C24 and *toc1-1* seedlings in contrast to mature seeds where differences of total C18:2 species were estimated to 6.2 % between C24 and *toc1-1* and 5.1 % between Col-0 and *toc1-2* **(Table 5)**. Thereby, results obtained in seedlings for C18:2 species did not reflect the C18:2 modification observed in WT seedlings **(Figure 32A)**.

Significant differences were observed for 24 C18:3 species between both *toc1* and their respective WT mature seeds **(Supplementary Table 12a)**. In contrast to mature seeds, C18:3 moieties glycerolipids were not significantly modified between C24 and *toc1-1* seedlings except for 17 C18:3 species **(Figure 43)**. Our results suggested that the significant increase observed in C24 seedlings for six C18:3 species combined with the decrease of eleven C18:3 species in the WT seedlings may explain the non-statistical significance obtained between C24 and *toc1-1* seedlings for the triunsaturated C18:3 FA content. In order to validate this hypothesis, the mole percents of the total C18:3 moieties glycerolipids were calculated in C24 and *toc1-1* seedlings and then statistically compared between C24 and *toc1-1*. The total C18:3 species were not significantly modified between C24 and *toc1-1* seedlings in contrast to mature seeds where differences in the mole percents of the total C18:3 species between both *toc1* mutants and respective WT were evaluated to 2.7 % in the case of *toc1-1* and 2.3 % in the case of *toc1-2* **(Table 5).** Results obtained in seedlings for C18:3 species reflect the non-statistical significance observed between C24 and *toc1-1* seedlings regarding the C18:3 content **(Figure 32A)**.

Table 5. Differences in glycerolipid composition between WT and clock mutants. *FA and glycerolipids were analyzed by GC-FID and HPLC-QTOF, respectively. Lipidomic data were acquired in positive (+) and negative (-) modes from mature seeds (n =9) and seedlings (n = 6). Values are expressed in mol % ± standard deviation. p-value > 0.05: NS; p-value < 0.05: *; p-value < 0.01: **; p-value < 0.001: ***.*

Mature seeds						
	FA (mol%)		Total glycerolipid containing (mol%)			
	C18:2	**C18:3**	**C18:2**		**C18:3**	
C24	29.0 ± 0.3	17.1 ± 0.7	57.2 ± 0.2 (+)		27.5 ± 0.4 (-)	
toc1-1	23.9 ± 0.2	19.1 ± 0.5	51.0 ± 1.3 (+)		30.2 ± 1.3 (-)	
p-value	***	***	***		***	
Col-0	29.1 ± 0.4	17.7 ± 0.6	56.9 ± 0.5 (+)		27.6 ± 0.4 (-)	
toc1-2	24.4 ± 0.2	20.0 ± 0.4	51.8 ± 1.3 (+)		29.9 ± 0.9 (-)	
p-value	***	***	***		***	
Col-0	28.3 ± 0.1	18.4 ± 0.3	56.9 ± 0.5 (+)		27.6 ± 0.4 (-)	
TOC1-ox	29.3 ± 0.4	18.8 ± 0.4	57.3 ± 1.1 (+)		27.6 ± 1.3 (-)	
p-value	***	***	NS		NS	
Seedlings						
	FA (mol%)		Total glycerolipid containing (mol%)			
	C18:2	**C18:3**	**C18:2**		**C18:3**	
C24	13.1 ± 1.3	49.4 ± 2.5	29.6 ± 2.5 (+)	9.9 ± 1.1 (-)	67.3 ± 2.8 (+)	84.3 ± 1.7 (-)
toc1-1	11.1 ± 0.9	49.6 ± 3.2	27.5 ± 1.5 (+)	9.0 ± 0.2 (-)	67.9 ± 1.8 (+)	85.7 ± 0.3 (-)
p-value	***	NS	NS	NS	NS	NS

3. Identification of FA-related genes under TOC1 control

The analysis of the FA profile suggested a potential role of TOC1 in the regulation of *FAD2*, *FAD3*, *bZIP67*, *FAE1* and *WRI1*. In *Arabidopsis thaliana*, these genes were expressed during seed maturation from 6 to 18 DAF (Ruuska *et al.*, 2002; Baud *et al.*, 2009a; 2009b). The expression of these genes was higher at 16 DAF and earlier seed developmental stage than at 17-18 DAF and later seed developmental stage (18-30 DAF). In addition, an active FA accumulation was observed from 10 to 18 DAF (Baud *et al.*, 2002). Indeed, the FA total amount increased from 2 µg/seed at 10 DAF to 7 µg/seed at 16 DAF and reached a maximum of 9 µg/seed at 18 DAF (Baud *et al.*, 2002). This active FA accumulation was the consequence of the positive controls of FA-related genes by master (LEC1, LEC2, ABI3 and FUS3) and secondary (WRI1 and L1L) regulators **(Figure 14)** (Baud *et al.*, 2007b; Kumar *et al.*, 2020). The potential regulation of FA-related genes by TOC1 may be observed from 10 to 18 DAF during seed maturation. It was proposed evaluating the expression of genes related to FA synthesis, elongation and desaturation from 10 to 16 DAF when FA-related genes and FA were expressed and actively accumulated in developing seeds, respectively.

In this part of the PhD project, the expression of FA-related genes was evaluated at 12 and 16 DAF in siliques and developing seeds collected from *toc1-1*, TOC1-ox and WT plants. The expression of FA-related genes was, however, not evaluated in *toc1-2*. Indeed, like in the first section (Results and discussion, 1.2.1), the expression of FA-related genes must have been altered in comparison to its respective WT because of a more important global phenotype in *toc1-2* than in its respective WT plants **(Figure 21)**.

3.1. Investigation of the role of TOC1 in the control of FA-related genes in developing seeds

3.1.1. Determination of the FA profiles in 16 DAF developing *toc1-1* seeds

Before the evaluation of the expression of target genes by RT-qPCR, FA were qualitatively and quantitatively analyzed in *toc1-1* and C24 developing seeds. The FA qualitative analysis were represented in **Figure 44A** and the FA quantitative analyses were illustrated in **Figure 44B**.

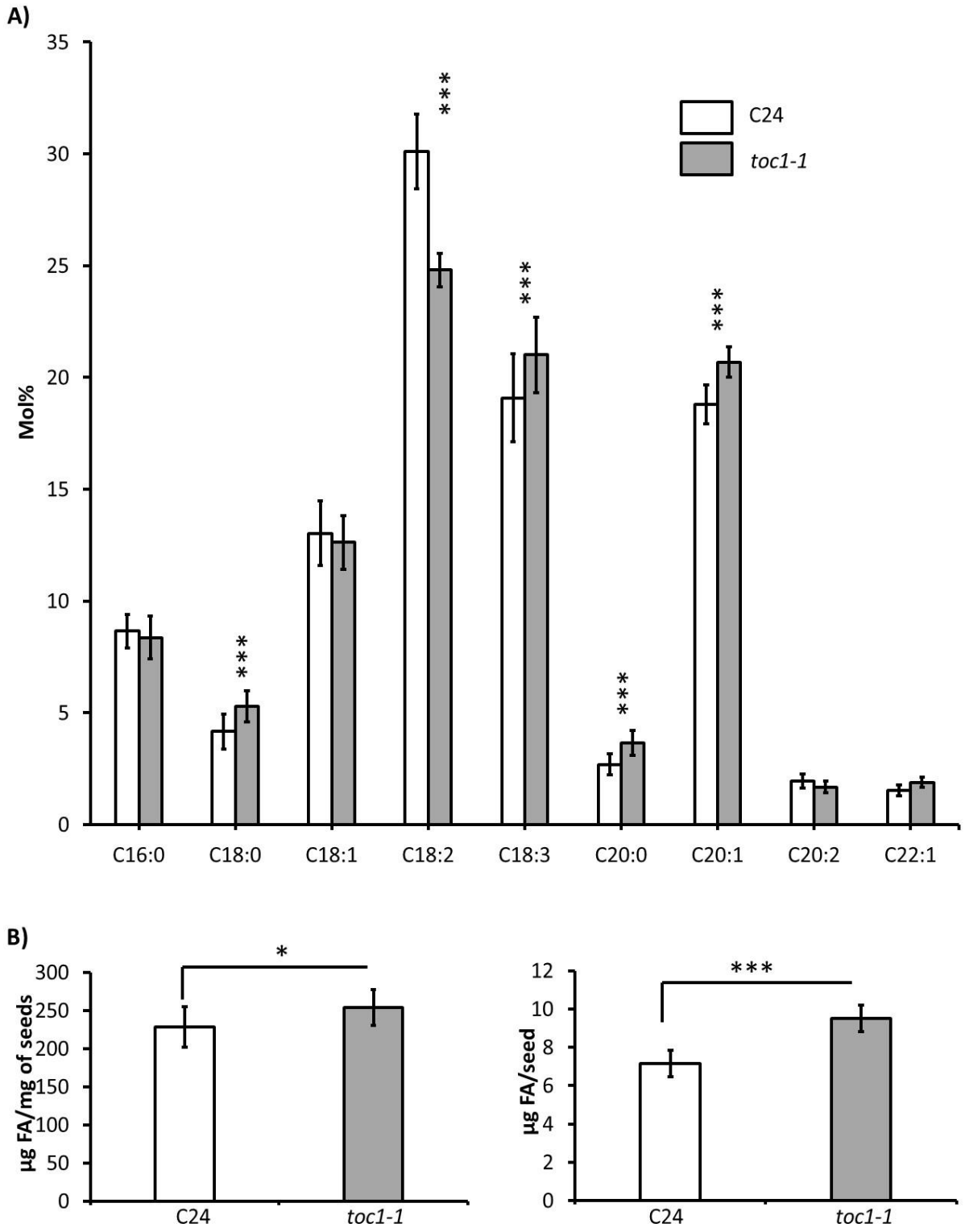

Figure 44. Differences in FA composition between 16 DAF developing C24 and *toc1-1* seeds. *A) The qualitative analysis of FA (mol %) and B) the quantitative analyses of FA (µg/seed and µg/mg) were performed using GC-FID data acquired from 16 DAF developing C24 and toc1-1* seeds*. The statistical significance was evaluated with a bilateral student test using unpaired samples (n = 15; p < 0.05: *, p < 0.01: ** and p < 0.001: ***). Numerical data were indicated in the Supplementary Table 16.*

FA qualitative analysis showed significant differences in the case of five FA (p-value < 0.001) between 16 DAF C24 and *toc1-1* seeds. C18:0, C18:3, C20:0 and C20:1 were

significantly higher in 16 DAF seeds collected from *toc1-1* plants, while C18:2 was significantly increased in 16 DAF seeds collected from C24 plants **(Figure 44A)**. Differences observed between 16 DAF C24 and *toc1-1* seeds represent 5.3 % for C18:2, 1.9 % for C18:3 and C20:1, 1.1 % for C18:0 and 1 % for C20:0. Modifications observed in 16 DAF developing seeds were similar to changes obtained in mature seeds except for C18:1. This monounsaturated FA was significantly higher in C24 than in *toc1-1* mature seeds but not significantly modified between 16 DAF developing C24 and *toc1-1* seeds **(Figure 29A and 44A)**.

Results generated in mature seeds allowed hypothesizing that *FAD3* and *bZIP67* may be potentially under TOC1 control since C18:2 was accumulated in WT mature seeds and C18:3 was increased in *toc1-1* **(Figure 29A)**. Like in mature seeds, C18:2 was significantly increased in 16 DAF developing WT seeds, while C18:3 was significantly higher in 16 DAF developing *toc1-1* seeds **(Figure 44A)**. The expression of *FAD3* and *bZIP67* were, therefore, evaluated by RT-qPCR in 16 DAF developing C24 and *toc1-1* seeds in order to study the potential role of TOC1 in the regulation of both target genes. The FA qualitative analysis performed in mature seeds showed that C18:1 was decreased in *toc1-1* mature seeds, while C20:0 and C20:1 were increased in *toc1-1* mature seeds **(Figure 29A)**. It was suggested that *FAE1* may be potentially regulated by TOC1. Unlike mature seeds, results generated from 16 DAF developing seeds showed no significant modification between C24 and *toc1-1* in the case of C18:1 **(Figure 44A)**. However, like in mature seeds, significant increase was observed in *toc1-1* for C20:0 and C20:1 **(Figure 44A)**. The expression of *FAE1* were, therefore, evaluated by RT-qPCR in 16 DAF developing C24 and *toc1-1* seeds in order to study the potential involvement of TOC1 in the control of this target gene. Results generated from mature seeds and 16 DAF developing seeds revealed that C18:2 was accumulated in C24 **(Figure 29A and 44A)**. These results suggested that the expression of *FAD2* may be under TOC1 control. The expression of this target gene was also evaluated in 16 DAF developing seeds in order to study the potential role of TOC1 in the regulation of this target gene.

The FA quantitative analyses showed significant differences (p-value < 0.05) in the total amount of FA per mg of seeds and total amount of FA per seed between 16 DAF developing *toc1-1* and C24 seeds, 1.1 and 1.3 folds increase in 16 DAF developing *toc1-1* seeds respectively **(Figure 44B)**. Results generated from mature seeds also revealed significant

increase of the FA total amount in *toc1-1* **(Figure 29B)**. Therefore, the development of *toc1-1* seeds was not delayed in comparison to the C24 seeds.

3.1.2. Evaluation of the expression of genes potentially under TOC1 control in seeds

The expression of *TOC1* oscillates in a 24h period. Like the other clock component, the expression of TOC1 were expressed in ZT, a unit of time based on a specific moment within a 12h light/12h dark cycle. The expression of *TOC1* increases from ZT0 to ZT12, reaching a maximum of expression at ZT12 (Huang and Nusinow, 2016). In a 12h light/12h dark, ZT0 corresponded to the time of light on and ZT12 represented the time of light off.

In this part of the PhD project, the expression of FA-related genes was evaluated in 16 DAF developing C24 and *toc1-1* seeds collected at the end of the day periods (ZT11) since FA were well accumulated at 16 DAF than at earlier seed developmental stage (Baud *et al.*, 2002). *TOC1* expression increases between ZT0 and ZT12, therefore reaching high expression level at ZT11 (Huang and Nusinow, 2016). The production of TOC1 increases from ZT0 to ZT12, therefore reaching high level of the functional and altered TOC1 protein at ZT11 in C24 and *toc1-1* respectively. The expression of FA-related genes potentially under TOC1 control should be significantly modified between C24 and *toc1-1* at ZT11.

The expression of *TOC1* was evaluated in 16 DAF developing C24 and *toc1-1* seeds at ZT11. The expression of TOC1 was normalized by the reference gene *EF1α* (AT5G60390). Our results revealed that *TOC1* expression was not affected at transcriptional level in *toc1-1* developing seeds collected at ZT11 **(Figure 45)**. Indeed, the *toc1-1* mutation affects the ability of TOC1 to interact with its target DNA sequence (Strayer *et al.*, 2000; Gendron *et al.*, 2012).

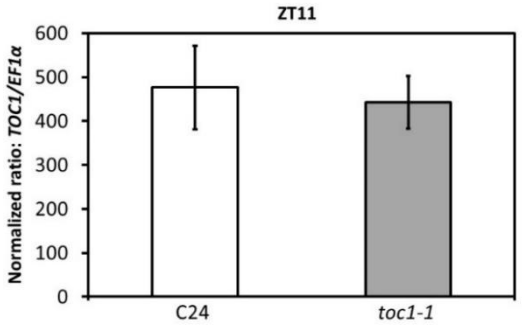

Figure 45. Evaluation of the expression of *TOC1*. *The expression of TOC1 was evaluated in 16 DAF C24 and toc1-1 seeds at ZT11 (1h before light off). The expression of TOC1 was normalized by EF1α. The comparison in the expression of TOC1 between C24 and toc1-1 was performed by a bilateral t-test using unpaired sample (n= 4; p < 0.05: *, p < 0.01: ** and p < 0.001: ***).*

3.1.2.1. Potential role of TOC1 in the regulation of *FAD2* expression

FAD2 is involved in the conversion of C18:1 into C18:2 within the ER (Okuley *et al.*, 1994). FA qualitative analysis showed that C18:2 was decreased in *toc1-1* seeds **(Figure 29A)**, suggesting that *FAD2* expression (AT3G12120) was altered in the loss-of-function mutant seeds. In order to validate this hypothesis, the expression of *FAD2* was evaluated in 16 DAF C24 and *toc1-1* seeds collected at ZT11. Surprisingly, the expression of this target gene was significantly increased (p-value < 0.001) in 16 DAF developing *toc1-1* seeds collected at ZT11 and not decreased in the loss-of-function mutant seeds as suggested **(Figure 46)**. The alteration of the TOC1 protein function in *toc1-1* developing seeds may strongly deregulate the expression of several other FA-related genes including *FAD3* and *bZIP67*, therefore promoting the accumulation of C18:2 in the WT and the synthesis of C18:3 in *toc1-1*.

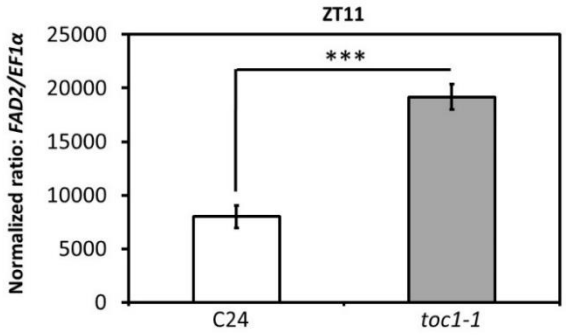

Figure 46. Evaluation of the expression of *FAD2*. *The expression of FAD2 was evaluated in 16 DAF C24 and toc1-1 seeds at ZT11 (1h before light off). The expression of TOC1 was normalized by EF1α. The comparison in the expression of FAD2 between C24 and toc1-1 was performed by a bilateral t-test using unpaired sample (n= 4; p < 0.05: *, p < 0.01: ** and p < 0.001: ***).*

3.1.2.2. Potential role of TOC1 in the regulation of *FAD3* and *bZIP67* expression

FAD3 is a microsomal C18:3-producing desaturase involved in the conversion of C18:2 into C18:3 within the ER (Browse *et al.*, 1993). The transcription factor bZIP67 positively regulates the expression of *FAD3* (Mendes *et al.*, 2013). FA qualitative analysis showed that C18:2 was decreased in *toc1-1* seeds, while C18:3 content was increased in the loss-of-function seeds **(Figure 29A)**. It was suggested that the expression of *FAD3* and *bZIP67* was increased in the loss-of-function mutant seeds. In order to validate this hypothesis, the expressions of *FAD3* and *bZIP67* were evaluated in 16 DAF C24 and *toc1-1* seeds collected at ZT11. *FAD3* (AT2G29980) and *bZIP67* (AT3G44460) expressions were, indeed, significantly increased (p-value < 0.001) in 16 DAF *toc1-1* seeds collected at ZT11 **(Figure 47A and 47B)**.

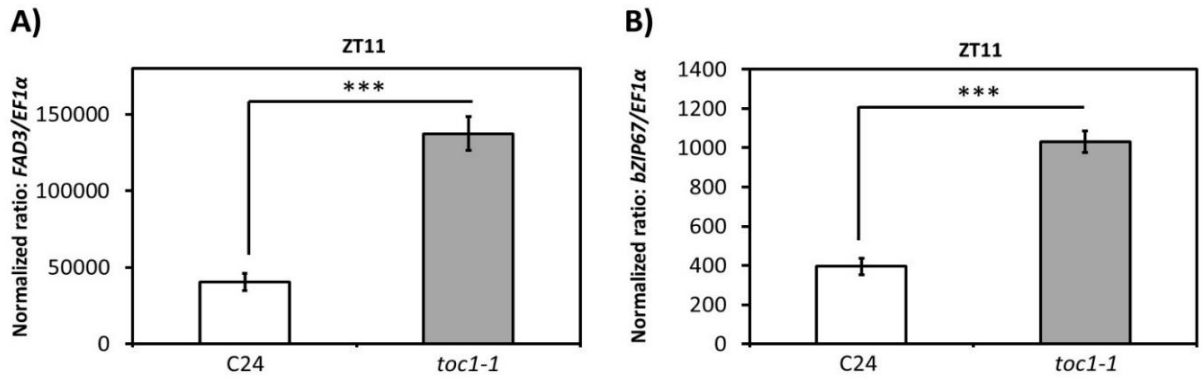

Figure 47. Evaluation of the expression of *FAD3* and *bZIP67*. *The expression of A) FAD3 and B) bZIP67 was evaluated in 16 DAF C24 and toc1-1 seeds at ZT11 (1h before light off). The expression of target genes was normalized by EF1α. The comparison in the expression of target genes between C24 and toc1-1 was performed by a bilateral t-test using unpaired sample (n= 4; p < 0.05: *, p < 0.01: ** and p < 0.001: ***).*

3.1.2.3. Potential role of TOC1 in the regulation of *FAE1* expression

FAE1 (AT4G34520) encodes for the β-ketoacyl-CoA synthase, one of the enzymes involved in the synthesis of VLCFA within the ER (James *et al.*, 1995; Millar and Kunst, 1997). FA qualitative analysis performed in mature seeds showed that C18:1 content was decreased in *toc1-1*, while C20:0 and C20:1 were increased in *toc1-1* **(Figure 29A)**. It was suggested that the expression of *FAE1* may be increased in the loss-of-function mutant seeds. In order to validate this hypothesis, the expression of *FAE1* was evaluated in 16 DAF C24 and *toc1-1* seeds collected at ZT11. The expression of *FAE1* was significantly modified (p-value < 0.001) between 16 DAF developing C24 and *toc1-1* seeds collected at ZT11. The expression of this target gene was significantly increased (p-value < 0.001) in 16 DAF developing *toc1-1* seeds **(Figure 48)**.

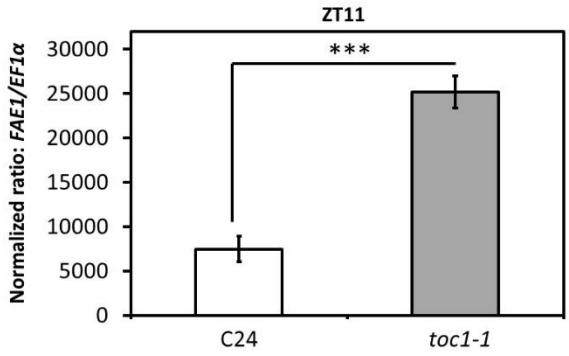

Figure 48. Evaluation of the expression of *FAE1*. *The expression of FAE1 was evaluated in 16 DAF C24 and toc1-1 seeds at ZT11 (1h before light off). The expression of FAE1 was normalized by EF1α. The comparison in the expression of FAE1 between C24 and toc1-1 was performed by a bilateral t-test using unpaired bilateral sample (n = 4; p < 0.05: *, p < 0.01: ** and p < 0.001: ***).*

3.1.2.4. Potential role of TOC1 in the regulation of *WRI1* expression

WRI1 positively regulates the expression of certain glycolytic genes and FA-related genes (Focks and Benning, 1998). FA quantitative analyses showed significant increase of the FA total amount in *toc1-1* seeds **(Figure 29B)**, suggesting an increase of *WRI1* expression in the loss-of-function mutant seeds. In order to validate this hypothesis, the expression of *WRI1* (AT3G54320) was evaluated in 16 DAF C24 and *toc1-1* seeds collected at ZT11. The expression of *FAE1* was, indeed, increased (p-value < 0.001) in 16 DAF *toc1-1* seeds at ZT11 **(Figure 49).**

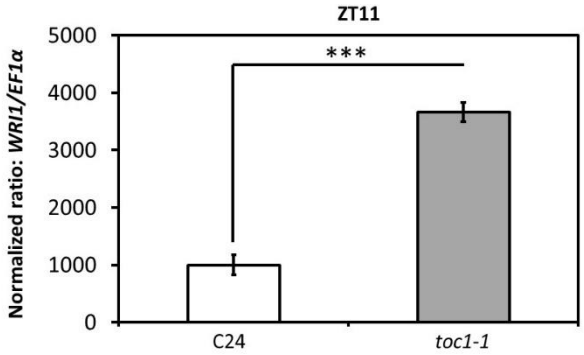

Figure 49. Evaluation of the expression of *WRI1*. *The expression of WRI1 was evaluated in 16 DAF C24 and toc1-1 seeds at ZT11 (1h before light off). The expression of WRI1 was normalized by EF1α. The comparison in the expression of WRI1 between C24 and toc1-1 was performed by a bilateral t-test using unpaired sample (n = 4; p < 0.05: *, p < 0.01: ** and p < 0.001: ***).*

3.2. Investigation of the role of TOC1 in the control of FA-related genes in siliques

In plants, siliques are structures derived from the female reproductive systems. These structures are composed of silique walls and seeds. Genes expressed in developing seeds can, therefore, be evaluated by RT-qPCR using siliques (Huang *et al.*, 2022). Previous studies showed that *FAD2*, *FAD3*, *bZIP67*, *FAE1* and *WRI1* reached a maximum of expression at 12 DAF in developing seeds (Ruuska *et al.*, 2002; Baud *et al.*, 2009a; 2009b). The expressions of *FAD2*, *FAD3*, *bZIP67*, *FAE1* and *WRI1* were, therefore, evaluated in siliques collected at 12 DAF in order to reduce the dilution of the target RNA (*FAD2*, *FAD3*, *bZIP67*, *FAE1* and *WRI1* RNA) extracted from developing seeds with the target RNA extracted from the silique wall.

Our results showed that the FA and glycerolipid profiles in TOC1-ox were close to the profiles obtained in its respective WT, suggesting that the expression of FA-related genes may not be significantly modified between Col-0 and TOC1-ox. In order to validate this hypothesis, the expressions of *FAD2*, *FAD3*, *bZIP67*, *FAE1* and *WRI1* were evaluated in 12 DAF developing siliques collected from TOC1-ox and its respective WT plants at ZT11.

TOC1 expression was first evaluated in the overexpressing *TOC1* mutant (TOC1-ox) and its respective WT. The overexpression of *TOC1* gene was performed by the insertion of the amplified *TOC1* cDNA fragment in a plasmid containing the *Cauliflower mosaic virus* 35S promoter (Makino *et al.*, 2002). Our results showed that the expression of *TOC1* was, indeed, increased in the overexpressing mutant (TOC1-ox) **(Figure 50)**.

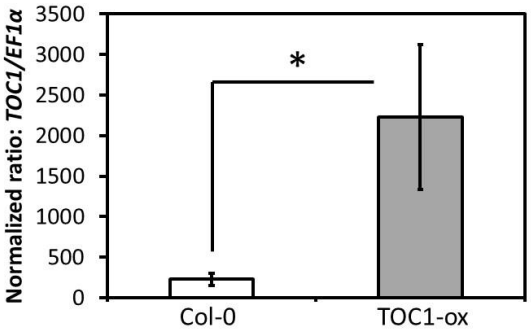

Figure 50. Evaluation of the expression of *TOC1*. *The expression of TOC1 was evaluated in 12 DAF Col-0 and TOC1-ox siliques collected at ZT11 (1h before light off). The expression of TOC1 was then normalized by EF1α. The comparison in the expression of TOC1 between Col-0 and TOC1-ox was performed by a bilateral t-test using unpaired sample (n= 4; p < 0.05: *, p < 0.01: ** and p < 0.001: ***).*

The expressions of *FAD2*, *FAD3*, *bZIP67*, *FAE1* and *WRI1* were then evaluated in 12 DAF developing Col-0 and TOC1-ox siliques. The expressions of these five target genes were not significantly modified between 12 DAF Col-0 and TOC1-ox siliques collected at ZT11 (p-value > 0.05) **(Figure 51)**.

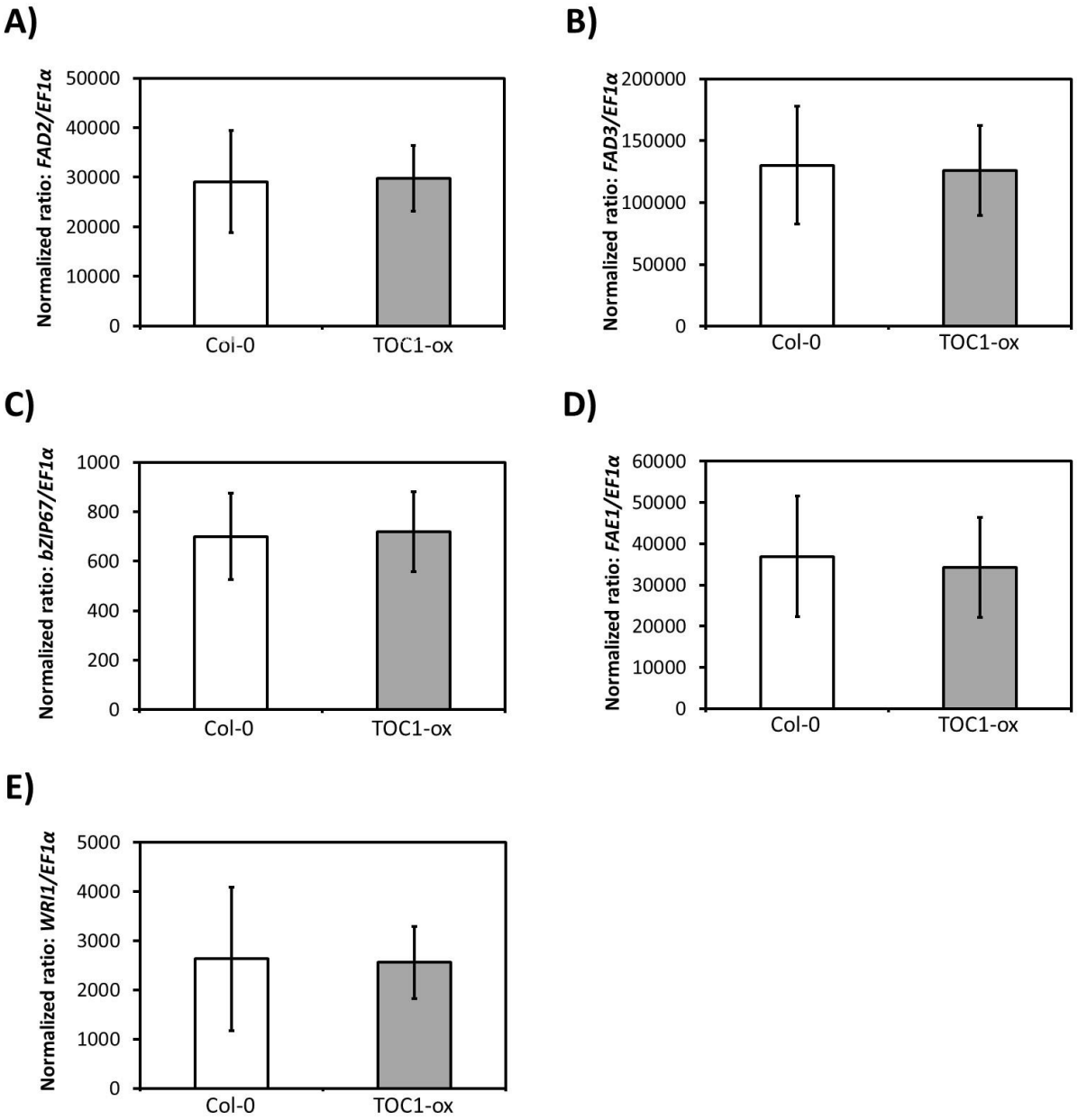

Figure 51. Evaluation of the expression of FA-related genes. *The expression of A) FAD2, B) FAD3, C) bZIP67, D) FAE1 and E) WRI1 was evaluated in 12 DAF Col-0 and TOC1-ox siliques collected at ZT11 (1h before light off). The expressions of these five target genes were normalized by EF1α. The comparison in the expression of target genes between Col-0 and TOC1-ox was performed by a bilateral t-test using unpaired sample (n = 4; p < 0.05: *, p < 0.01: ** and p < 0.001: ***).*

3.3. Involvement of TOC1 in the regulation of FA-related genes

Our results showed that the expression of *FAD2*, *FAD3*, *bZIP67*, *FAE1* and *WRI1* were not significantly modified between 12 DAF Col-0 and TOC1-ox siliques **(Figure 51)**. These results were consistent with the FA and glycerolipid qualitative analyses revealing that the FA and glycerolipid profiles in TOC1-ox were close to the profiles observed in its respective WT **(Figure 31, 38 and 39)**. On the contrary, the expression of *FAD2*, *FAD3*, *bZIP67*, *FAE1* and *WRI1*

were increased in 16 DAF developing *toc1-1* seeds **(Figure 46, 47, 48 and 49)**. The increase of *FAD3*, *bZIP67* and *FAE1* expressions in 16 DAF developing *toc1-1* seeds were consistent with the FA qualitative analysis showing an increase of C18:3, C20:0 and C20:1 in the loss-of-function mutant mature seeds **(Figure 29A)**. The increase of *WRI1* expression in 16 DAF *toc1-1* developing seeds **(Figure 49)** was consistent with the FA quantitative analyses revealing that the FA total amount was increased in the loss-of-function mutant mature seeds **(Figure 29B)**. In addition, Gendron *et al.* (2012) showed that TOC1 is a general transcriptional repressor. The expression of genes potentially under TOC1 control should be increased in the loss-of-function *toc1-1* mutant. Our results showed higher expression of *FAD3, bZIP67, FAD2, FAE1* and *WRI1* in 16 DAF developing *toc1-1* seeds than in C24 seeds. Thereby, results generated from 16 DAF developing C24 and *toc1-1* seeds revealed that TOC1 negatively regulates the expression of *FAD2*, *FAD3*, *bZIP67*, *FAE1* and *WRI1* during seed maturation.

SECTION 5: CONCLUSIONS AND PERSPECTIVES

CONCLUSIONS AND PERSPECTIVES

1. Conclusions

The objective of this PhD project was studying the role exerted by components of the circadian system on FA and glycerolipid metabolism in Arabidopsis developing seeds. This research work was divided into three main steps.

The first step consisted in the identification of clock components involved in the control of FA metabolism during seed maturation. FA composition was characterized in several circadian clock mutant mature seeds (*toc1-1*, *toc1-2*, TOC1-ox, *prr5-1*, *prr7-3*, *prr9-1* and *cca1-11 lhy*-21) and compared to their respective WT (C24, Col-0 and WS). Results showed that differences in the mole percents of six FA (C18:0, C18:1, C18:2, C18:3, C20:0 and C20:1) observed between both loss-of-function *toc1* mutants (*toc1-1* and *toc1-2*) and their respective WT (C24 and Col-0) mature seeds reached up to 5 %, while changes observed between the other clock mutants (TOC1-ox, *prr5-1*, *prr7-3*, *prr9-1* and *cca1-11 lhy*-21) and their respective WT (Col-0 and WS) were lower than 2 %. In addition, similar FA profiles were obtained in both *toc1* mutants in spite of *TOC1* expression and TOC1 protein function were deeper altered in *toc1-2* than in *toc1-1*. These findings support the potential participation of TOC1 in the regulation of FA metabolism during seed maturation. The alteration of the TOC1 protein function in both loss-of-function *toc1* mutants resulted in the increase of C18:0, C18:3, C20:0 and C20:1, while C18:1 and C18:2 contents were higher in WT. FA profiles obtained in both *toc1* mutant mature seeds were, therefore, similar to the profiles generated in *ela1* (*enhanced linolenate accumulation*), a mutant line characterized by the accumulation of C18:3 in mature seeds (Lemieux *et al.*, 1990). During the second step of the PhD project, lipidomic studies showed that TAG containing C18:0, C18:3, C20:0 and C20:1 were increased in both *toc1* mutants, while TAG containing C18:1 and C18:2 were higher in their respective WT. Differences in glycerolipid composition between both *toc1* mutants and their respective WT reflect the FA profiles observed in both loss-of-function mutants. FA qualitative analyses and lipidomic studies performed in both *toc1* mutant mature seeds allowed hypothesizing about the potential role of TOC1 in the regulation of *FAD3*, *bZIP67* and *FAE1* expressions during seed maturation. In addition, the decrease of the diunsaturated C18:2 FA and C18:2 species in both *toc1* mutant mature seeds support the hypothesis that TOC1 may potentially regulate *FAD2* expression. FA quantitative analyses revealed a 1.1-1.2 folds increase of the FA total amount

in both loss-of-function *toc1* mutant mature seeds, suggesting that the expression of *WRI1*, a transcription factor regulating FA synthesis during seed maturation, may be partially under TOC1 control.

During the first and second step of the PhD project, FA and glycerolipid were analyzed in *toc1-1* seedlings and leaves. Results showed that the triunsaturated C18:3 FA were significantly increased in both *toc1* mutant mature seeds, while the triunsaturated C18:3 FA were not significantly modified between C24 and *toc1-1* seedlings and leaves. Lipidomic studies performed in seedlings revealed that the total C18:3 glycerolipid species were significantly increased in *toc1-1* mature seeds, while the total C18:3 glycerolipid species were not significantly modified between C24 and *toc1-1* seedlings. FA and glycerolipid profile observed in mature seeds were not found in seedlings and leaves. Indeed, results showed that FA and glycerolipid phenotype were almost identical in both *toc1-1* and *toc1-2* mutant mature seeds, while FA profiles obtained in seedlings and leaves were not similar in both *toc1* mutants. These findings support the hypothesis that TOC1 may potentially control the expression of *FAD2* and *FAD3*, the main desaturases in seeds (Browse *et al.*, 1993; Okuley *et al.*, 1994)

During the third step of the PhD project, the objective was identifying FA-related genes partially under TOC1 control during seed maturation. The expression of candidate genes, including *FAD2*, *FAD3*, *bZIP67*, *FAE1* and *WRI1*, were therefore evaluated in C24 and *toc1-1* developing seeds, as well as in Col-0 and TOC1-ox siliques. Results showed that the expression of *FAD2*, *FAD3*, *bZIP67*, *FAE1* and *WRI1* were not significantly modified between Col-0 and TOC1-ox, while the expression of these genes were significantly increased in *toc1-1* developing seeds. Results generated during the PhD project allowed concluding that TOC1 negatively regulate the expression of *FAD2*, *FAD3*, *bZIP67*, *FAE1* and *WRI1* during seed maturation **(Figure 52)**.

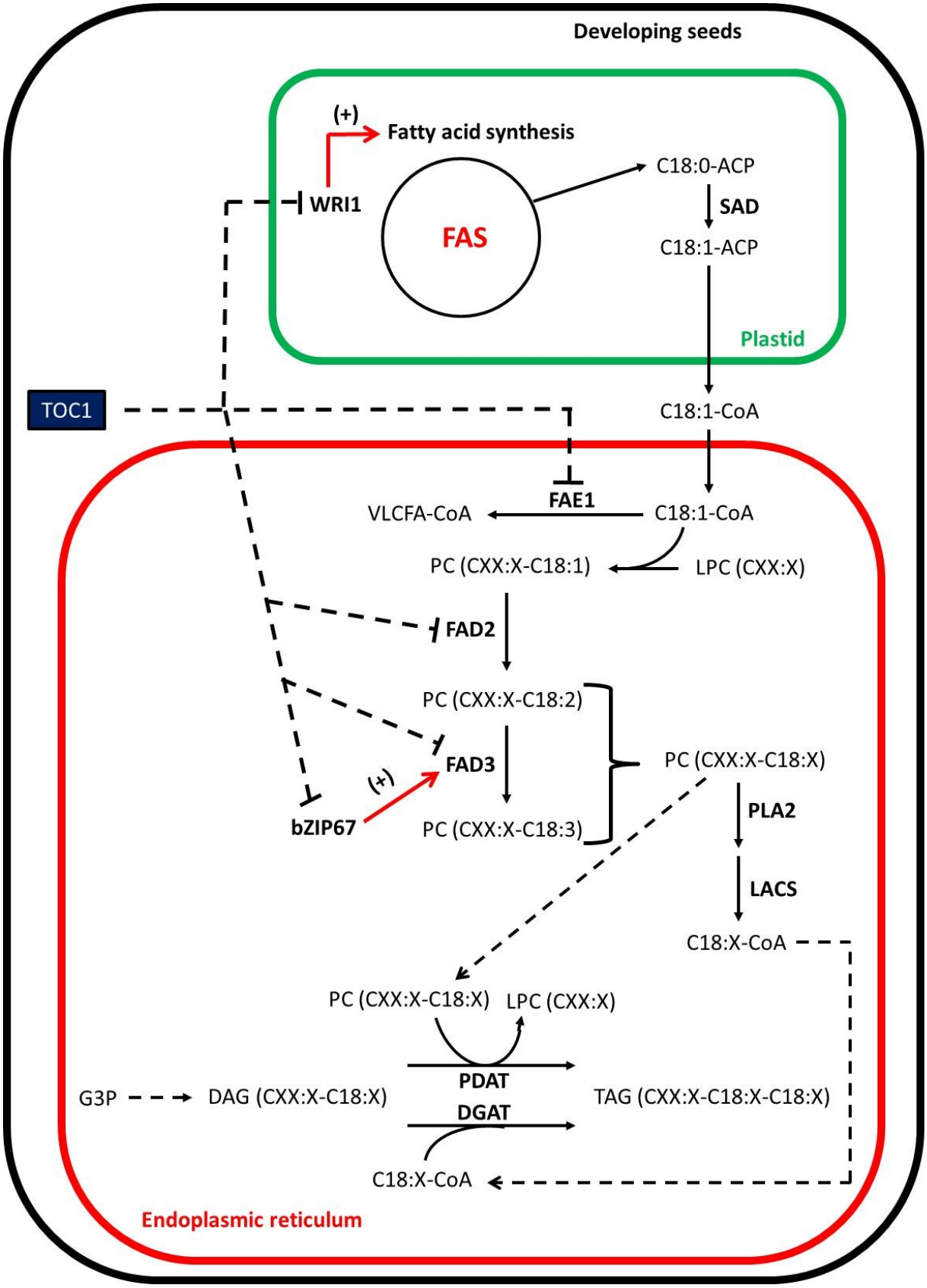

Figure 52. Regulation of FA-related genes by TOC1. *This figure showed enzymatic reactions from the intraplastidial de novo FA synthesis to the production of polyunsaturated TAG. The expression of FAD2, FAD3, bZIP67, FAE1 and WRI1 are inhibited by TOC1, therefore limiting the synthesis of polyunsaturated TAG in seeds. The control of the expression of target genes by TOC1 were represented by dotted inhibitory arrows.*

2. Perspectives

2.1. Short-term perspectives

Other experiments can be performed for further confirmation of the role of TOC1 in the inhibition of *FAD2*, *FAD3*, *bZIP67*, *WRI1* and *FAE1* during seed maturation. One of the experiments consists in evaluating the expression of these five FA-related genes in developing seeds collected at different moment of the light (ZT0, ZT3, ZT6 and ZT9) and dark (ZT12, ZT15, ZT18 and ZT21) periods. From this experiment, it was expected seeing a correlation between the oscillatory expression profile of *TOC1* and the expression of these five FA-related genes. The reconstitution of an oscillatory expression profile for *FAD2*, *FAD3*, *bZIP67*, *WRI1* and *FAE1* in continuous light conditions could further prove that these five FA-related genes are under the control of the circadian clock during seed maturation. Another experiment consists in studying the role of TOC1 in the regulation of *FAD2, FAD3, bZIP67, WRI1* and *FAE1* during the active accumulation of FA from 10 to 16 DAF.

Gendron *et al.* (2012) revealed that TOC1 is a general transcriptional repressor, therefore suggesting that the expression of many other FA-related genes, in addition to *FAD2*, *FAD3*, *bZIP67*, *WRI1* and *FAE1*, may be inhibited through the action of this clock component. The potential repression of the anabolic pathway involved in FA synthesis by TOC1 may be helpful in limiting the accumulation of FA and rather using carbohydrate in the production of energy during seed maturation. In the case of the inhibition of FA metabolism by TOC1, pyruvate may be rather converted into acetyl-CoA within mitochondria in order to be involved in the Krebs Cycle, an energy-producing catabolic pathway crucial for ensuring a correct seed maturation. In order to confirm this hypothesis, the expression of genes involved in FA metabolism, as well as in lipid metabolism, glycolysis, PPP and Krebs Cycle, should be evaluated in developing C24 and *toc1-1* seeds using untargeted transcriptomic approaches (RNAseq, microarray, etc). In addition, the evaluation of metabolic fluxes can be performed in developing C24 and *toc1-1* seeds using fluxomic approaches.

Although our results showed that TOC1 negatively regulates the expression of *FAD2, FAD3, bZIP67, WRI1* and *FAE1*, it was not yet confirmed that this clock component inhibits the expression of these five FA-related genes by directly interacting with their promoters. Gendron *et al.* (2012) revealed that TOC1 interacts with the G-box sequence

(CACGTG) of CCA1 and LHY promoters, suggesting that this evening expressed clock components may also recognize G-box sequences of many other target genes. The presence of G-box sequences within the promotor of *FAD3* (Mendes *et al.*, 2013), *FAD2* (Kim *et al.*, 2006) and *FAE1* (Du *et al.*, 2011) support the hypothesis that TOC1 may directly interact with *FAD3, FAD2* and *FAE1* promoters. Electrophoresis Mobility Shift Assay and Chromatin ImmunoPrecipitation experiments can be performed in order to confirm this hypothesis.

2.2. Long-term perspectives

One of the challenges in plant research is promoting the nutritional quality of vegetable oils. Results generated during this PhD project showed that the clock component TOC1, directly or indirectly, participates in the regulation of the expression of FA-related genes during seed maturation. C18:3, an essential FA for human health, was accumulated in Arabidopsis *toc1-1* seed oils. The role of TOC1 in C18:3 biosynthesis can be studied in other oilseed plants (e.g.: *Brassica napus*, *Camelina sativa*), therefore promoting the accumulation of this triunsaturated FA in seed oils intended for human consumption.

Another challenge consists in the redistribution of agricultural crops over new latitudes without affecting plant development and survival. The next step would be studying the role exerted by the circadian clock on FA and glycerolipid synthesis during the whole life of the plant model *Arabidopsis thaliana*. Indeed, as mentioned in the introduction section, the understanding of the involvement of the circadian clock in the regulation of FA and glycerolipid synthesis could help adapting oilseed crops plants to new rhythmic environmental fluctuations and fostering these cultivations over new latitudes.

BIBLIOGRAPHY

Adams S., Manfield I., Stockley P., and Carré I.A. (2015). Revised Morning Loops of the Arabidopsis Circadian Clock Based on Analyses of Direct Regulatory Interactions. *PLoS ONE* 10 (12): e0143943. https://doi.org/10.1371/journal.pone. 0143943.

Alabadi D., Oyama T., Yanovsky M.J., and Kay S.A. (2001). Reciprocal Regulation Between TOC1 and LHY/CCA1 Within the Arabidopsis Circadian Clock. *Science* 293 (5531): 880–883. https://doi.org/10.1126/science.1061320.

Allen D.K., Bates P.D., and Tjellström H. (2015). Tracking the Metabolic Pulse of Plant Lipid Production with Isotopic Labeling and Flux Analyses: Past, Present and Future. *Progress in Lipid Research* 58: 97–120. https://doi.org/10.1016/j.plipres. 2015.02.002.

Allen D.K., Ohlrogge J.B., and Shachar-Hill Y. (2009). The Role of Light in Soybean Seed Filling Metabolism. *Plant Journal* 58: 220–234. https://doi.org/10.1111/j.1365-313X.2008. 03771.x.

Andre C., Froehlich J.E., Moll M.R., and Benning C. (2007). A Heteromeric Plastidic Pyruvate Kinase Complex Involved in Seed Oil Biosynthesis in Arabidopsis. *Plant Cell* 19 (6): 2006–2022. https://doi.org/10.1105/tpc.106.048629.

Andriotis V.M.E., Kruger N.J., Pike M.J., and Smith A.M. (2010). Plastidial Glycolysis in Developing Arabidopsis Embryos. *New Phytologist* 185 (3): 649–662. https://doi.org/ 10.1111/j.1469-8137.2009.03113.x.

Andriotis V.M.E., and Smith A.M. (2019). The Plastidial Pentose Phosphate Pathway Is Essential for Postglobular Embryo Development in Arabidopsis. *PNAS* 116 (30): 15297–15306. https://doi.org/10.1073/pnas.1908556116.

Barthole G., To A., Marchive C., Brunaud V., Soubigou-Taconnat L., Berger N., Bertrand D., Lepiniec L., and Baud S. (2014). MYB118 Represses Endosperm Maturation in Seeds of Arabidopsis. *Plant Cell* 26 (9): 3519–3537. https://doi.org/10.1105/tpc.114.130021.

Bates P.D., Durrett T.P., Ohlrogge J.B., and Pollard M. (2009). Analysis of Acyl Fluxes through Multiple Pathways of Triacylglycerol Synthesis in Developing. *Plant Physiology* 150: 55–72. https://doi.org/10.1104/pp.109.137737.

Bates P.D., Fatihi A., Snapp A.R., Carlsson A.S., Browse J., and Lu C. (2012). Acyl Editing and Headgroup Exchange Are the Major Mechanisms That Direct Polyunsaturated Fatty Acid Flux into Triacylglycerols. *Plant Physiology* 160: 1530–1539. https://doi.org/10.1104/pp.112.204438.

Baud S., Boutin J.P., Miquel M., Lepiniec L., and Rochat C. (2002). An Integrated Overview of Seed Development in *Arabidopsis thaliana* Ecotype WS. *Plant Physiology and Biochemistry* 40 (2): 151–160. https://doi.org/10.1016/S0981-9428(01)01350-X.

Baud S., Dubreucq B., Miquel M., Rochat C., and Lepiniec L. (2008). Storage Reserve Accumulation in Arabidopsis: Metabolic and Developmental Control of Seed Filling. *American Society of Plant Biologists* 6: e0113. https://doi.org/ 10.1199/tab.0113.

Baud S., Guyon V., Kronenberger J., Wuillème S., Miquel M., Caboche M., Lepiniec L., and Rochat C. (2003). Multifunctional Acetyl-CoA Carboxylase 1 Is Essential for Very Long Chain Fatty Acid Elongation and Embryo Development in Arabidopsis. *Plant Journal* 33 (1): 75–86. https://doi.org/10.1046/ j.1365-313x.2003.016010.x.

Baud S., Kelemen Z., Thévenin J., Boulard C., Blanchet S., To A., Payre M., *et al*. (2016). Deciphering the Molecular Mechanisms Underpinning the Transcriptional Control of Gene Expression by Master Transcriptional Regulators in Arabidopsis Seed. *Plant Physiology* 171 (2): 1099–1112. https://doi.org/ 10.1104/pp.16.00034.

Baud S., and Lepiniec L. (2009a). Regulation of de Novo Fatty Acid Synthesis in Maturing Oilseeds of Arabidopsis. *Plant Physiology and Biochemistry* 47 (6): 448–455. https://doi.org/10.1016/j.plaphy.2008.12.006.

Baud S., and Lepiniec L. (2010). Physiological and Developmental Regulation of Seed Oil Production. *Progress in Lipid Research* 49 (3): 235–249. https://doi.org/10.1016/ j.plipres.2010.01.001.

Baud S., Santos-Mendoza M., To A., Harscoët E., Lepiniec L., and Dubreucq B. (2007b). WRINKLED1 Specifies the Regulatory Action of LEAFY COTYLEDON2 towards Fatty Acid Metabolism during Seed Maturation in Arabidopsis. *Plant Journal* 50 (5): 825–838. https://doi.org/10.1111/j.1365-313X.2007.03092.x.

Baud S., Wuillème S., Dubreucq B., De Almeida A., Vuagnat C., Lepiniec L., Miquel M., and

Rochat C. (2007a). Function of Plastidial Pyruvate Kinases in Seeds of *Arabidopsis thaliana. Plant Journal* 52: 405–419. https://doi.org/ 10.1111/j.1365-313X.2007.03232.x.

Baud S., Wuillème S., To A., Rochat C., and Lepiniec L.. 2009b. Role of WRINKLED1 in the Transcriptional Regulation of Glycolytic and Fatty Acid Biosynthetic Genes in Arabidopsis. *Plant Journal* 60 (6): 933–947. https://doi.org/ 10.1111/j.1365-313X.2009.04011.x.

Beeckman T., De Rycke R., Viane R., and Inzé D. (2000). Histological Study of Seed Coat Development in *Arabidopsis thaliana*. *Journal of Plant Research* 113 (2): 139–148. https://doi.org/10.1007/pl00013924.

Bewley J.D. (1997). Seed Germination and Dormancy. *Plant Cell.* 9 (7): 1055–1066. https://doi.org/10.1105/tpc.9.7.1055.

Bhat S.R. (2010). Transgenics for Increasing Productivity of Crops. *Journal of Plant Biochemistry and Biotechnology.* 19 (1): 1–7. https://doi.org/10.1007/BF03323430.

Blacklock B.J., and Jaworski J.G. (2006). Substrate Specificity of Arabidopsis 3-Ketoacyl-CoA Synthases. *Biochemical and Biophysical Research Communication* 346 (2): 583–590. https://doi.org/10.1016/j.bbrc.2006.05.162.

Boavida L.C., Becker J.D., and Feijó J.A. (2005). The Making of Gametes in Higher Plants. *International Journal of Developmental Biology.* 49: 595–614. https://doi.org/ 10.1387/ijdb.052019lb.

Boscá S., Knauer S., and Laux T. (2011). Embryonic Development in *Arabidopsis thaliana*: From the Zygote Division to the Shoot Meristem. *Frontiers in Plant Science.* 2: 1–6. https://doi.org/10.3389/fpls.2011.00093.

Braybrook S.A., and Harada J.J. (2008). LECs Go Crazy in Embryo Development. *Trends in Plant Science* 13 (12): 624–630. https://doi.org/10.1016/j.tplants.2008.09.008.

Braybrook S.A., Stone S.L., Park S., Bui A.Q., Le B.H., Fischer R.L., Goldberg R.B., and Harada J.J. (2006). Genes Directly Regulated by LEAFY COTYLEDON2 Provide Insight into the Control of Embryo Maturation and Somatic Embryogenesis. *PNAS* 103 (9): 3468–3473. https://doi.org/10.1073/pnas.0511331103.

Brown A.P., Affleck V., Fawcett T., and Slabas A.R. (2006). Tandem Affinity Purification Tagging

of Fatty Acid Biosynthetic Enzymes in Synechocystis Sp. PCC6803 and *Arabidopsis thaliana*. *Journal of Experimental Botany* 57 (7): 1563–1571. https://doi.org/10.1093/jxb/erj150.

Brown E., and Jacobson M.F. (2005). Cruel Oil: How Palm Oil Harms Health, Rainforest and Wildlife. *Center for Science in the Public Interest* 1-39.

Brown R.C., Lemmon B.E., Nguyen H., and Olsen O.A. (1999). Development of Endosperm in *Arabidopsis thaliana. Sexual Plant Reproduction.* 12 (1): 32–42. https://doi.org/10.1007/s004970050169.

Browse J., Kunst L., Anderson S., Hugly S., and Somerville C. (1989). A Mutant of Arabidopsis Deficient in the Chloroplast 16:1/18:1 Desaturase. *Plant Physiology* 90 (2): 522–529. https://doi.org/10.1104/pp.90.2.522.

Browse J., McConn M., James D., and Miquel M. (1993). Mutants of Arabidopsis Deficient in the Synthesis of α-Linolenate. Biochemical and Genetic Characterization of the Endoplasmic Reticulum Linoleoyl Desaturase. *Journal of Biological Chemistry* 268 (22): 16345–16351. https://doi.org/10.1016/s0021-9258(19)85427-3.

Browse J., McCourt P., and Somerville C. (1986). A Mutant of Arabidopsis Deficient in C18:3 and C16:3 Leaf Lipids. *Plant Physiology* 81 (3): 859–864. https://doi.org/10.1104/pp.81.3.859.

Browse J., Roughan P.G., and Slack C.R. (1981). Light Control of Fatty Acid Synthesis and Diurnal Fluctuations of Fatty Acid Composition in Leaves. *Biochemistry Journal* 196 (1): 347–354. https://doi.org/https://doi.org/10.1042/bj1960347.

Bullen H.E., and Soldati-Favre D. (2016). A Central Role for Phosphatidic Acid as a Lipid Mediator of Regulated Exocytosis in Apicomplexa. *FEBS Letters* 590 (15): 2469–2481. https://doi.org/10.1002/1873-3468.12296.

Capron A., Chatfield S., Provart N., and Berleth T. (2009). Embryogenesis: Pattern Formation from a Single Cell. *American Society of Plant Biologists* 7: e0126. https://doi.org/10.1199/tab.0126.

Casson S.A., and Lindsey K. (2006). The Turnip Mutant of Arabidopsis Reveals That LEAFY COTYLEDON1 Expression Mediates the Effects of Auxin and Sugars to Promote Embryonic

Cell Identity. *Plant Physiology* 142 (2): 526–541. https://doi.org/10.1104/ pp.106.080895.

Cernac A., and Benning C. (2004). WRINKLED1 Encodes an AP2/ EREB Domain Protein Involved in the Control of Storage Compound Biosynthesis in Arabidopsis. *Plant Journal* 40 (4): 575–585. https://doi.org/10.1111/j.1365-313X.2004.02235.x.

Chase M.W., Christenhusz M.J.M., Fay M.F., Byng J.W., Judd W.S., Soltis D.E., Mabberley D.J., *et al*. (2016). An Update of the Angiosperm Phylogeny Group Classification for the Orders and Families of Flowering Plants: APG IV. *Botanical Journal of the Linnean Society.* 181 (1): 1–20. https://doi.org/10.1111/boj.12385.

Chen L., Lee J.H., Weber H., Tohge T., Witt S., Roje S., Fernie A.R., and Hellmann H. (2013). Arabidopsis BPM Proteins Function as Substrate Adaptors to a CULLIN3-Based E3 Ligase to Affect Fatty Acid Metabolism in Plants. *Plant Cell* 25 (6): 2253–2264. https://doi.org/ 10.1105/tpc.112.107292.

Chen M., Brian P.M., Hajduch M., Joshi T., Zhou M., Xu D., and Thelen J.J. (2009). System Analysis of an Arabidopsis Mutant Altered in de Novo Fatty Acid Synthesis Reveals Diverse Changes in Seed Composition and Metabolism. *Plant Physiology* 150 (1): 27–41. https://doi.org/10.1104/pp.108.134882.

Chen M., Xuan L., Wang Z., Zhou L., Li Z., Du X., Ali E., Zhang G., and Jiang L. (2014). TRANSPARENT TESTA8 Inhibits Seed Fatty Acid Accumulation by Targeting Several Seed Development Regulators in Arabidopsis. *Plant Physiology* 165 (2): 905–916. https:// doi.org/10.1104/pp.114.235507.

Chen M., Zhang B., Li C., Kulaveerasingam H., Chew F.T., and Yu H. (2015). TRANSPARENT TESTA GLABRA1 Regulates the Accumulation of Seed Storage Reserves in Arabidopsis. *Plant Physiology* 169 (1): 391–402. https://doi.org/ 10.1104/pp.15.00943.

Christensen C.A., King E.J., John R.J., and Drews G.N. (1997). Megagametogenesis in Arabidopsis Wild Type and the Gf Mutant 10: 49–64. https://doi.org/10.1007/ s004970050067.

Citerne H., Jabbour F., Nadot S., and Damerval C. (2010). The Evolution of Floral Symmetry. *Advances in Botanical Research.* 54: 85–137. https://doi.org/10.1016/S0065-2296(10)54003-5.

Cramer W.P., and Allen M. (1993). Climatic Classification and Future Global Redistribution of Agricultural Land. *Climate Research* 3: 97–110. https://doi.org/ 10.3354/cr003097.

Cutler S., Ghassemian M., Bonetta D., Cooney S., and McCourt P. (1996). A Protein Farnesyl Transferase Involved in Abscisic Acid Signal Transduction in Arabidopsis. *Science* 273 (5279): 1239–1241. https://doi.org/10.1126/science.273.5279. 1239.

Dahlqvist A., Stahl U., Lenman M., Banas A., Lee M., Sandager L., Ronne H., and Stymne S. (2000). Phospholipid: Diacylglycerol Acyltransferase: An Enzyme That Catalyzes the Acyl-CoA-Independent Formation of Triacylglycerol in Yeast and Plants. *PNAS* 97 (12): 6487–6492. https://doi.org/10.1073/pnas.120067297.

Daie J. (1993). Cytosolic Fructose-1,6 Bisphosphatase : A Key Enzyme in the Sucrose Biosynthetic Pathway. *Photosnthesis Research* 38 (1): 5–14. https://doi.org/10.1007/ BF00015056.

Debeaujon I., Lepiniec L., Pourcel L., and Routaboul J. (2007). Seed Coat Development and Dormancy. *Annual Plant Reviews* 27: 25–49. https://doi.org/10.1002/9780470988848. ch2.

Debeaujon I., Nesi N., Perez P., Devic M., Grandjean O., Caboche M., and Lepiniec L. (2003). Proanthocyanidin-Accumulating Cells in Arabidopsis Testa: Regulation of Differentiation and Role in Seed Development. *Plant Cell* 15 (11): 2514–2531. https://doi.org/ 10.1105/tpc.014043.

Delmas F., Sankaranarayanan S., Deb S., Widdup E., and Bournonville C. (2013). ABI3 Controls Embryo Degreening through Mendel ' s/ Locus. *PNAS* 3 (7): 1–7. https://doi.org/10.1073/ pnas.1308114110.

Desjardins P., and Conklin D. (2010). NanoDrop Microvolume Quantitation of Nucleic Acids. *Journal of Visualized Experiments* 45: 2565. https://doi.org/10.3791/ 2565.

Dodd A.N., Salathia N., Hall A., Kévei E., Tóth R., Nagy F., Hibberd J.M., Millar A.J., and Webb A.A.R. (2005). Cell Biology: Plant Circadian Clocks Increase Photosynthesis, Growth, Survival, and Competitive Advantage. *Science.* 309 (5734): 630–633. https://doi.org/ 10.1126/science.1115581.

Drea S.C., Mould R.M., Julian M Hibberd J.M., Gray J.C., and Kavanagh T.A. (2001). Tissue-

Specific and Developmental-Specific Expression of an *Arabidopsis thaliana* Gene Encoding the Lipoamide Dehydrogenase Component of the Plastid Pyruvate Dehydrogenase Complex. *Plant Molecular Biology* 46 (6): 705–715. https://doi.org/ 10.1023/a:1011612921144.

Dresselhaus T., and Franklin-Tong N. (2013). Male-Female Crosstalk during Pollen Germination, Tube Growth and Guidance, and Double Fertilization. *Molecular Plant.* 6 (4): 1018–1036. https://doi.org/10.1093/mp/sst061.

Drews G.N., Lee D., and Christensen C.A. (1998). Genetic Analysis of Female Gametophyte Development and Function. *Plant Cell* 10 (1): 5–17. https://doi.org/ 10.1105/tpc.10.1.5.

Duan S., Jin C., Li D., Gao C., Qi S., Liu K., Hai J., Ma H., and Chen M. (2017). MYB76 Inhibits Seed Fatty Acid Accumulation in Arabidopsis. *Frontiers in Plant Science* 8: 226. https://doi.org/10.3389/fpls.2017.00226.

Du H., Yang X., Yan J., and Li J. (2011). Fatty Acid Elongase 1 (FAE1) Promoter as a Candidate for Genetic Engineering of Fatty Acids to Improve Seed Oil Composition. *African Journal of Biotechnology*. 10 (84): 19615–19622. https://doi.org/10.5897/AJB11.2207.

Durrett T.P., Benning C., and Ohlrogge J. (2008). Plant Triacylglycerols as Feedstocks for the Production of Biofuels. *Plant Journal*. 54 (4): 593–607. https://doi.org/10.1111/j.1365-313X.2008.03442.x.

Eady C., Lindsey K., and Twell D. (1995). The Significance of Microspore Division and Division Symmetry for Vegetative Cell-Specific Transcription and Generative Cell Differentiation. *Plant Cell.* 7 (1): 65–74. https://doi.org/10.2307/3869838.

Eastmond P.J. (2006). Sugar-Dependent1 Encodes a Patatin Domain Triacylglycerol Lipase That Initiates Storage Oil Breakdown in Germinating Arabidopsis Seeds. *Plant Cell* 18 (3): 665–675. https://doi.org/10.1105/tpc.105.040543.

Eckstein A., and Zie P. (2012). Sugar and Light Effects on the Condition of the Photosynthetic Apparatus of *Arabidopsis thaliana* Cultured in Vitro. *Journal of Plant Growth Regulation* 31 (1): 90–101. https://doi.org/10.1007/s00344-011-9222-z.

Ekman A., Bülow L., and Stymne S. (2007). Elevated Atmospheric CO_2 Concentration and Diurnal Cycle Induce Changes in Lipid Composition in *Arabidopsis thaliana*. *New*

Phytologist 174 (3): 591–599. https://doi.org/https://doi.org/10.1111/j.1469-8137.2007.02027.x.

Fallahi H., Scofield G.N., Badger M.R., Chow W.S., Furbank R.T., and Ruan Y.L. (2008). Localization of Sucrose Synthase in Developing Seed and Siliques of *Arabidopsis thaliana* Reveals Diverse Roles for SUS during Development. *Journal of Experimental Botany* 59 (12): 3283–3295. https://doi.org/ 10.1093/jxb/ ern180.

Fan J., Yan C., Zhang X., and Xu C. (2013). Dual Role for Phospholipid: Diacylglycerol Acyltransferase: Enhancing Fatty Acid Synthesis and Diverting Fatty Acids from Membrane Lipids to Triacylglycerol in Arabidopsis Leaves. *Plant Cell* 25 (9): 1–14. https://doi.org/10.1105/tpc.113.117358.

Focks N., and Benning C. (1998). wrinkled1: A Novel, Low-Seed-Oil Mutant of Arabidopsis with a Deficiency in the Seed-Specific Regulation of Carbohydrate Metabolism. *Plant Physiology* 118: 91–101. https://doi.org/10.1104/pp.118.1.91.

Folch J., Lees M., J. A. Meath J.A., and LeBaron N. (1951). Preparation of Lipide Extracts from Brain Tissue. *The Journal of Biological Chemistry* 191 (2): 833–841. https://doi.org/ 10.1016/s0021-9258(18)55987-1.

Footitt S., Slocombe S.P., Larner V., Kurup S., Wu Y., Larson T., Graham I., Baker A., and Holdsworth M. (2002). Control of Germination and Lipid Mobilization by COMATOSE, the Arabidopsis Homologue of Human ALDP. *EMBO Journal* 21 (12): 2912–2922. https://doi.org/10.1093/emboj/cdf300.

Franklin-Tong V.E. (2002). The Difficult Question of Sex: The Mating Game. *Current Opinion in Plant Biology* 5 (1): 14–18. https://doi.org/10.1016/S1369-5266(01)00217-5.

Franzke A., Koch M.A., and Mummenhoff K. (2016). Turnip Time Travels: Age Estimates in Brassicaceae. *Trends in Plant Science.* 21 (7): 554–561. https://doi.org/10.1016/j.tplants.2016.01.024.

Fulda M., Schnurr J., Abbadi A., Heinz E., and Browse J. (2004). Peroxisomal Acyl-CoA Synthetase Activity Is Essential for Seedling Development in *Arabidopsis thaliana*. *Plant Cell* 16 (2): 394–405. https://doi.org/10.1105/tpc.019646.

Gao J., Ajjawi I., Manoli A., Sawin A., Xu C., Froehlich J.E., Last R.L., and Benning C. (2009).

"FATTY ACID DESATURASE4 of Arabidopsis Encodes a Protein Distinct from Characterized Fatty Acid Desaturases." *Plant Journal* 60 (5): 832–839. https://doi.org/10.1111/j.1365-313X.2009.04001.x.

Gendron J.M., Pruneda-Paz J.L., Doherty C.J., Gross A.M., Kang S.E., and Kay S.A. (2012). Arabidopsis Circadian Clock Protein, TOC1,Is a DNA-Binding Transcription Factor. *PNAS* 109 (8): 3167–3172. https://doi.org/10.1073/pnas. 1200355109.

Gibon Y., Pyl E.T., Sulpice R., Lunn J.E., Höhne M., Günther M., and Stitt M. (2009). Adjustment of Growth, Starch Turnover, Protein Content and Central Metabolism to a Decrease of the Carbon Supply When Arabidopsis Is Grown in Very Short Photoperiods. *Plant, Cell and Environment* 32 (7): 859–874. https://doi.org/ 10.1111/j.1365-3040.2009.01965.x.

Glick N.R., and Fischer M.H. (2013). The Role of Essential Fatty Acids in Human Health. *Journal of Evidence-based Complementary and alternative Medicine.* 18 (4): 268–289. https://doi.org/10.1177/2156587213488788.

Goode J.H., and Dewey R.E. (1999). Characterization of aminoalcoholphosphotransferases from *Arabidopsis thaliana* and soybean. *Plant Physiology and Biochemistry* 37 (6): 445-457. https://doi.org/10.1016/S0981-9428(99)80049-7.

Graf A., Schlereth A., Stitt M., and Smith A.M. (2010). Circadian Control of Carbohydrate Availability for Growth in Arabidopsis Plants at Night. *PNAS* 107 (20): 9458–9463. https://doi.org/10.1073/pnas.0914299107.

Graham I.A. 2008. "Seed Storage Oil Mobilization." *Annual Review of Plant Biology* 59: 115–142. https://doi.org/10.1146/annurev.arplant.59.032607.092938.

Granot D., and Stein O. (2019). An Overview of Sucrose Synthases in Plants. *Frontiers in Plant Science* 10: 95. https://doi.org/10.3389/fpls.2019.00095.

Gui M.M., Lee K.T.Ã., and Bhatia S. (2008). Feasibility of Edible Oil vs . Non-Edible Oil vs . Waste Edible Oil as Biodiesel Feedstock. *Energy. Elsevier*. 33: 1646–1653. https:// doi.org/ 10.1016/j.energy.2008.06.002.

Hajduch M., Casteel J.E., Tang S., Hearne L.B., Knapp S., and Thelen J.J. (2007). Proteomic Analysis of Near-Isogenic Sunflower Varieties Differing in Seed Oil Traits. *Journal of*

Proteome Research 6 (8): 3232–3241. https://doi.org/ 10.1021/pr070149a.

Hall A., Bastow R.M., Davis S.J., Hanano S., McWatters H.G., Hibberd V., Doyle M.R., *et al.* (2003). The TIME FOR COFFEE Gene Maintains the Amplitude and Timing of Arabidopsis Circadian Clocks. *Plant Cell* 15 (11): 2719–2729. https://doi.org/10.1105/tpc.013730.

Hamamura Y., Nagahara S., and Higashiyama T. (2012). Double Fertilization on the Move. *Current Opinion in Plant Biology* 15: 70–77. https://doi.org/10.1016/ j.pbi.2011.11.001.

Harshfield E.L., Koulman A., Ziemek D., Marney L., Fauman E.B., Paul D.S., Stacey D., *et al.* (2019). An Unbiased Lipid Phenotyping Approach To Study the Genetic Determinants of Lipids and Their Association with Coronary Heart Disease Risk Factors. *Journal of Proteome Research* 18 (6): 2397–2410. https://doi.org/10.1021/acs.jproteome. 8b00786.

Harwood J.L. (1996). Recent Advances in the Biosynthesis of Plant Fatty Acids. *Biochimica et Biophysica Acta* 1301 (1–2): 7–56. https://doi.org/10.1016/0005-2760(95)00242-1.

Harwood J.L., Ramli U.S., Tang M., Quant P.A., Weselake R.J., Fawcett T., and Guschina I.A. (2013). Regulation and Enhancement of Lipid Accumulation in Oil Crops: The Use of Metabolic Control Analysis for Informed Genetic Manipulation. *European Journal of Lipid Science and Technology*. 115 (11): 1239–1246. https://doi.org/10.1002/ejlt.201300257.

Haughn G., and Chaudhury A. (2005). Genetic Analysis of Seed Coat Development in Arabidopsis. *Trends in Plant Science* 10 (10): 472–477. https://doi.org/10.1016/j. tplants. 2005.08.005.

Heilmann I., Mekhedov S., King B., Browse J., and Shanklin J. (2004). Identification of the Arabidopsis Palmitoyl-Monogalactosyldiacylglycerol Delta7-Desaturase Gene FAD5, and Effects of Plastidial Retargeting of Arabidopsis Desaturases on the *fad5* Mutant Phenotype. *Plant Physiology* 136 (4): 4237–4245. https:// doi.org/10.1104/ pp.104.052951.

Horvitz H.R., and Herskowitz I. (1992). Mechanisms of Asymmetric Cell Division: Two Bs or Not Two Bs, That Is the Question. *Cell.* 68 (2): 237–255. https://doi.org/10. 1016/0092-8674(92)90468-R.

Hsiao A., Haslam R.P., Michaelson L.V., Liao P., Napier J.A., and Chye M. (2014). Gene

Expression in Plant Lipid Metabolism in Arabidopsis Seedlings. *PLoS ONE.* 9 (9): e107372. https://doi.org/10.1371/journal.pone.0107372.

Huang H., and Nusinow D.A. (2016). Into the Evening : Complex Interactions in the Arabidopsis Circadian Clock. *Trends in Genetics* 32 (10): 674–686. https://doi.org/10.1016/j.tig. 2016.08.002.

Huang R., Liu M., Gong G., Wu P., Bai M., Qin H., Wang G., *et al*. (2022). BLISTER Promotes Seed Maturation and Fatty Acid Biosynthesis by Interacting with WRINKLED1 to Regulate Chromatin Dynamics in Arabidopsis. *Plant Cell* 34 (6): 2242–2265. https://doi.org/ 10.1093/plcell/koac083.

Hudson K.A. (2010). The Circadian Clock-controlled Transcriptome of Developing Soybean Seeds. *The Plant Genome* 3 (1): 3–13. https://doi.org/10.3835/plantgenome 2009. 08.0025.

Hunter S.C, and Ohlrogge J.B. (1998). Regulation of Spinach Chloroplast Acetyl-CoA Carboxylase. *Archives of Biochemistry and Biophysics* 359 (2): 170–178. https://doi.org/ https://doi.org/10.1006/abbi.1998.0900.

Hutchings D., Rawsthorne S., and Emes M.J. (2005). Fatty Acid Synthesis and the Oxidative Pentose Phosphate Pathway in Developing Embryos of Oilseed Rape (*Brassica Napus* L .). *Journal of Experimental Botany* 56 (412): 577–585. https://doi.org/10.1093/ jxb/eri046.

Ingram G., and Nawrath C. (2017). The Roles of the Cuticle in Plant Development: Organ Adhesions and Beyond. *Journal of Experimental Botany* 68 (19): 5307–5321. https:// doi.org/10.1093/jxb/erx313.

James D.W., Lim E., Keller J., Ralston E., and Dooner H.K. (1995). Directed Tagging of the Arabidopsis FATTY ACID ELONGATION 1 (FAE1) Gene with the Maize Transposon Activator. *Plant Cell* 7 (3): 309–319. https://doi.org/10.1105/tpc.7.3.309.

Jaworski J.G., Clough R.C., and Barnum S.R. (1989). A Cerulenin Insensitive Short Chain 3-Ketoacyl-Acyl Carrier Protein Synthase in Spinacia Oleracea Leaves. *Plant Physiology* 90 (1): 41–44. https://doi.org/10.1104/pp.90.1.41.

Jaworski J.G., and Stumpf P.K. (1974). Properties of a Soluble Stearyl-Acyl Carrier Protein Desaturase from Maturing *Carthamus tinctorius*. *Archives of Biochemistry and Biophysics*

162 (1): 158–165. https://doi.org/10.1016/0003-9861(74)90114-3.

Johnson M.P. (2016). Photosynthesis. *Essays in Biochemistry* 60: 255–273. https:// doi.org/10.1042/EBC20160016.

Johnston M.L., Luethy M.H., Miernyk J.A., and Randall D.D. (1997). Cloning and Molecular Analyses of the *Arabidopsis thaliana* Plastid Pyruvate Dehydrogenase Subunits. *Biochimica et Biophysica Acta* 1321 (3): 200–206. https://doi.org/10.1016/ s0005-2728(97)00059-5.

Jo L., Pelletier J.M., and Harada J.J. (2019). Central Role of the LEAFY COTYLEDON1 Transcription Factor in Seed Development. *Journal of Integrative Plant Biology.* 61 (5): 564–580. https://doi.org/10.1111/jipb.12806.

Karve A., Rauh B.L., Xia X., Kandasamy M., Meagher R.B., Sheen J., and Moore B. (2008). Expression and Evolutionary Features of the Hexokinase Gene Family in Arabidopsis. *Planta* 228: 411–425. https://doi.org/10.1007/ s00425-008-0746-9.

Katavic V., Reed D.W., Taylor D.C., Giblin E.M., Barton D.L., Zou J., Mackenzie S., Covello P.S., and Kunst L. (1995). Alteration of Seed Fatty Acid Composition by an Ethyl Methanesulfonate-Lnduced Mutation in *Arabidopsis thaliana* Affecting Diacylglycerol Acyltransferase Activity. *Plant Physiology* 108 (1): 399–409. https://doi.org/10.1104/ pp.108.1.399.

Kelly A.A., and Dörmann P. (2004). Green Light for Galactolipid Trafficking. *Current Opinion in Plant Biology* 7 (3): 262–269. https://doi.org/10.1016/j.pbi.2004.03.009.

Kim H.U., Lee K., Jung S., Shin H.A., Go Y.S., Suh M.C., and Kim J.B. (2015). Senescence-Inducible LEC2 Enhances Triacylglycerol Accumulation in Leaves without Negatively Affecting Plant Growth. *Plant Biotechnology Journal* 13 (9): 1346–1359. https://doi.org/ 10.1111/pbi.12354.

Kim. M.J., Kim H., Shin J.S., Chung H.C., Ohlrogge J.B. and Suh M.C. (2006). Seed-Specific Expression of Sesame Microsomal Oleic Acid Desaturase Is Controlled by Combinatorial Properties between Negative Cis-Regulatory Elements in the SeFAD2 Promoter and Enhancers in the 5'-UTR Intron. *Molecular Genetics and Genomics.* 276 (4): 351–68. https://doi.org/10.1007/s00438-006-0148-2.

Kim S., Nusinow D.A., Sorkin M.L., Pruneda-Paz J., and Wang X. (2019). Interaction and Regulation Between Lipid Mediator Phosphatidic Acid and Circadian Clock Regulators. *Plant Cell* 31 (2): 399–416. https://doi.org/10.1105/tpc.18.00675.

Kobayashi K., Endo K., and Wada H. (2016a). Roles of Lipids in Photosynthesis. *Subcellular Biochemistry.* 21–49. https://doi.org/10.1007/978-3-319-25979-6.

Kobayashi K., Endo K., and Wada H. (2016b). Multiple Impacts of Loss of Plastidic Phosphatidylglycerol Biosynthesis on Photosynthesis during Seedling Growth of Arabidopsis. *Frontiers in Plant Science* 7: 336. https://doi.org/10.3389/fpls.2016.00336.

Kong Q., Singh S.K., Mantyla J.J., Pattanaik S., Guo L., Yuan L., Benning C., and Ma W. (2020b). TEOSINTE BRANCHED1/CYCLOIDEA/ PROLIFERATING CELL FACTOR4 Interacts with WRINKLED1 to Mediate Seed Oil Biosynthesis. *Plant Physiology* 184 (2): 658–665. https://doi.org/ 10.1104/pp.20.00547.

Kong Q., Yang Y., Low P.M., Guo L., Yuan L., and Ma W. (2020a). The Function of the WRI1-TCP4 Regulatory Module in Lipid Biosynthesis. *Plant Signaling and Behavior* 15 (11): 1812878. https://doi.org/10.1080/15592324.2020.1812878.

Kruger N.J., and Von Schaewen A. (2003). The Oxidative Pentose Phosphate Pathway : Structure and Organisation. *Current Opinion in Plant Biology* 6: 236–246. https://doi.org/ 10.1016/S1369-5266(03)00039-6.

Kumar N., Chaudhary A., Singh D., Teotia S. (2020). Transcriptional Regulation of Seed Oil Accumulation in *Arabidopsis thaliana* : Role of Transcription Factors and Chromatin Remodelers. *Journal of Plant Biochemistry and Biotechnology* 29 (4). https://doi.org/ 10.1007/s13562-020-00616-2.

Lee H.G., Kim H., Suh M.C., Kim H.U., and Seo P.J. 2018. The MYB96 Transcription Factor Regulates Triacylglycerol Accumulation by Activating DGAT1 and PDAT1 Expression in Arabidopsis Seeds. *Plant and Cell Physiology* 59 (7): 1432–1442. https://doi.org/ 10.1093/pcp/pcy073.

Lessire R., and Stumpf P.K. (1983). Nature of the Fatty Acid Synthetase Systems in Parenchymal and Epidermal Cells of Allium Porrum L. Leaves. *Plant Physiology* 73 (3): 614–618. https://doi.org/10.1104/pp.73.3.614.

Lemieux B., Miquel M., Somerville C., and Browse J. 1990. Mutants of Arabidopsis with Alterations in Seed Lipid Fatty Acid Composition. *Theoretical and Applied Genetics* 80 (2): 234–240. https://doi.org/10.1007/BF00224392.

Li-Beisson Y., Shorrosh B., Beisson F., Andersson M.X., Arondel V., Bates P.D., Bird D., DeBono A., Durrett T.P., Franke R.B., Graham I.A., Katayama K., Kelly A.A., Larson T., Markham J.E., Miquel M., Molina I., Nishida I., Rowland O., Samuels L., Schmid K.M., Wada H., Welti R., Xu C., Zallot R., and Ohlrogge J.B. (2013). Acyl-Lipid Metabolism. *American Society of Plant Biologists* 11: e0161. https://doi.org/ 10.1199/tab.0161.

Li D., Jin C., Duan S., Zhu Y., Qi S., Liu K., Gao C., *et al.* (2017). MYB89 Transcription Factor Represses Seed Oil Accumulation. *Plant Physiology* 173 (2): 1211–1225. https://doi.org/ 10.1104/pp.16.01634.

Lindsey B.E., Rivero L., Calhoun C.S., Grotewold E., and Brkljacic J. (2017). Standardized Method for High-Throughput Sterilization of Arabidopsis Seeds. *Journal of Visualized Experiments* 128: 56587. https://doi.org/10.3791/56587.

Lin M., Behal R., and Oliver D.J. (2003). Disruption of PlE2 , the Gene for the E2 Subunit of the Plastid Pyruvate Dehydrogenase Complex , in Arabidopsis Causes an Early Embryo Lethal Phenotype. *Plant Molecular Biology* 52 (4): 865–872. https://doi.org/10.1023/ a:1025076805902.

Liu H., Zhai Z., Kuczynski K., Keereetaweep J., Schwender J., and Shanklin J. (2019). WRINKLED1 Regulates BIOTIN ATTACHMENT DOMAIN-CONTAINING Proteins That Inhibit Fatty Acid Synthesis. *Plant Physiology* 181 (1): 55–62. https://doi.org/10.1104/ pp.19.00587.

Li Y., Beisson F., Pollard M., and Ohlrogge J.B. (2006). Oil Content of Arabidopsis Seeds : The Influence of Seed Anatomy, Light and Plant-to-Plant Variation. *Phytochemistry.* 67: 904–915. https://doi.org/10.1016/j.phytochem.2006.02.015.

Locke J.C.W., Kozma-Bognar L., Gould P.D., Feher B., Kevei E., Nagy F., Turner M.S., Hall A., and Millar A.J. (2006). Experimental Validation of a Predicted Feedback Loop in the Multi-Oscillator Clock of *Arabidopsis thaliana*. *Molecular Systems Biology* 2: 59. https:// doi.org/ 10.1038/msb4100102.

Lora J., Laux T., and Hormaza J.I. (2018). The Role of the Integuments in Pollen Tube Guidance

in Flowering Plants. *New Phytologist.* 221 (2): 1074–1089. https://doi.org/10.1111/nph.15420.

Lu S.X., Knowles S.M., Andronis C., Ong M.S., and Tobin E.M. (2009). CIRCADIAN CLOCK ASSOCIATED1 and LATE ELONGATED HYPOCOTYL Function Synergistically in the Circadian Clock of Arabidopsis. *Plant Physiology* 150 (2): 834–843. https://doi.org/10.1104/pp.108.133272.

Maatta S., Scheu B., Roth M.R, Tamura P., Li M., Williams T.D., Wang X., and Welti R. (2012). Levels of *Arabidopsis thaliana* Leaf Phosphatidic Acids , Phosphatidylserines , and Most Trienoate-Containing Polar Lipid Molecular Species Increase during the Dark Period of the Diurnal Cycle. *Frontiers in Plant Science* 3: 49. https://doi.org/10.3389/ fpls.2012.00049.

Maeo K., Tokuda T., Ayame A., Mitsui N., Kawai T., Tsukagoshi H., Sumie I., and Kenzo N.. (2009). An AP2-Type Transcription Factor , WRINKLED1 , of *Arabidopsis thaliana* Binds to the AW-Box Sequence Conserved among Proximal Upstream Regions of Genes Involved in Fatty Acid Synthesis. *Plant Journal* 60 (3): 476–487. https://doi.org/10.1111/j.1365-313X.2009.03967.x.

Makino S., Matsushika A., Kojima M., Yamashino T., and Mizuno T. (2002). The APRR1/TOC1 Quintet Implicated in Circadian Rhythms of *Arabidopsis thaliana* : I. Characterization with APRR1-Overexpressing Plants. *Plant Cell Physiology* 43 (1): 58–69. https://doi.org/10.1093/pcp/pcf005.

Mansfield S.G., and Briarty L.G. (1991). Early Embryogenesis in *Arabidopsis thaliana*. II. The Developing Embryo. *Canadian Journal of Botany.* 69: 461–476. https://doi.org/10.1139/b91-063.

Martin C., and Smith A.M. (1995). Starch Biosynthesis. *Plant Cell* 7: 971–985. https://doi.org/10.1105/tpc.7.7.971.

Más P. (2005). Circadian Clock Signaling in *Arabidopsis thaliana* : From Gene Expression to Physiology and Development. *The International Journal of Developmental Biology.* 500: 491–500. https://doi.org/10.1387/ijdb.041968pm.

McConn M., Hugly S., Browse J., and Somerville C. (1994). A Mutation at the *fad8* Locus of Arabidopsis Identifies a Second Chloroplast ω-3 Desaturase. *Plant Physiology* 106 (4):

1609–1614. https://doi.org/10.1104/pp.106.4.1609.

Menard G.N., Bryant F.M., Kelly A.A., Craddock C.P., Lavagi I., Hassani-Pak K., Kurup S., and Eastmond P.J. (2018). Natural Variation in Acyl Editing Is a Determinant of Seed Storage Oil Composition. *Scientific Reports* 8: 17346. https://doi.org/10.1038/s41598-018-35136-6.

Mendes A., Kelly A.A., Van Erp H., Shaw E., Powers S.J., Kurup S., and Eastmond P.J. (2013). bZIP67 Regulates the Omega-3 Fatty Acid Content of Arabidopsis Seed Oil by Activating FATTY ACID DESATURASE3. *Plant Cell* 25 (8): 3104–3116. https://doi.org/10.1105/tpc.113.116343.

Merlier F., Octave S., Tse Sum Bui B., and Thomasset B. (2019). Evaluation of Performance and Validity Limits of Gas Chromatography Electron Ionisation with Orbitrap Detection for Fatty Acid Methyl Ester Analyses. *Rapid Communications in Mass Spectrometry* e8609. https://doi.org/10.1002/rcm.8609.

Mhaske V., Beldjilali K., Ohlrogge J.B., and Pollard M. (2005). Isolation and Characterization of an *Arabidopsis thaliana* Knockout Line for Phospholipid: Diacylglycerol Transacylase Gene (At5g13640). *Plant Physiology et Biochemistry* 43 (4): 413–417. https://doi.org/10.1016/j.plaphy.2005.01.013.

Michael T.P., Salomé P.A., Yu H.J., Spencer T.R., Sharp E.L., McPeek M.A., Alonso J.M., Ecker J.R., and McClung C.R. (2003). Enhanced Fitness Conferred by Naturally Occurring Variation in the Circadian Clock. *Science* 302 (5647): 1049–1053. https://doi.org/10.1126/science.1082971.

Millar A.A., and Kunst L. (1997). Very-Long-Chain Fatty Acid Biosynthesis Is Controlled through the Expression and Specificity of the Condensing Enzyme. *Plant Journal* 12 (1): 121–131. https://doi.org/10.1046/j.1365-313x.1997.12010121.x.

Millar A.J., Carre I.A., Strayer C.A., Chua N., and Kay S.A. (1994). Circadian Clock Mutants in Arabidopsis Identified by Luciferase Imaging. *Science* 267 (5201): 1161–1163. https://doi.org/10.1126/science.7855595.

Miquel M., and Browse J. (1992). Arabidopsis Mutants Deficient in Polyunsaturated Fatty Acid Synthesis: Biochemical and Genetic Characterization of a Plant Oleoyl-

Phosphatidylcholine Desaturase. *Journal of Biological Chemistry* 267 (3): 1502–1509. https://doi.org/10.1016/s0021-9258(18)45974-1.

Mizoguchi T., Wright L., Fujiwara S., Frédéric C., Lee K., Onouchi H., Mouradov A., *et al.* (2005). Distinct Roles of GIGANTEA in Promoting Flowering and Regulating Circadian Rhythms in Arabidopsis. *Plant Cell* 17 (8): 2255–2270. https://doi.org/10.1105/tpc.105.033464.

Mizoi J., Nakamura M., and Nishida I. (2006). Defects in CTP: PHOSPHORYLETHANOLAMINE CYTIDYLYLTRANSFERASE Affect Embryonic and Postembryonic Development in Arabidopsis. *Plant Cell* 18 (12): 3370–3385. https:// doi.org/10.1105/tpc.106.040840.

Mou Z., He Y., Dai Y., Liu X., and Li J. (2000). Deficiency in Fatty Acid Synthase Leads to Premature Cell Death and Dramatic Alterations in Plant Morphology. *Plant Cell* 12 (3): 405–417. https://doi.org/10.1105/tpc.12.3.405.

Mou Z., Wang X., Fu Z., Dai Y., Han C., Ouyang J., Bao F., Hu Y., and Li J. (2002). Silencing of Phosphoethanolamine N -Methyltransferase Results in Temperature-Sensitive Male Sterility and Salt Hypersensitivity in Arabidopsis. *Plant Cell* 14: 2031–2043. https://doi.org/10.1105/tpc.001701.2.

Mu J., Tan H., Zheng Q., Fu F., Liang Y., Zhang J., Yang X., *et al.* (2008). LEAFY COTYLEDON1 Is a Key Regulator of Fatty Acid Biosynthesis in Arabidopsis. *Plant Physiology* 148 (2): 1042–1054. https://doi.org/10.1104/pp.108.126342.

Nakamura Y. (2013). Phosphate Starvation and Membrane Lipid Remodeling in Seed Plants. *Progress in Lipid Research* 52 (1): 43–50. https://doi.org/10.1016/j.plipres. 2012.07.002.

Nakamura Y. (2018). Membrane Lipid Oscillation: An Emerging System of Molecular Dynamics in the Plant Membrane. *Plant and Cell Physiology* 59 (3): 441–447. https:// doi.org/10.1093/pcp/pcy023.

Nakamura Y., Andrés F., Kanehara K., Liu Y., Coupland G., and Dörmann P. (2014b). Diurnal and Circadian Expression Profiles of Glycerolipid Biosynthetic Genes in Arabidopsis. *Plant Signaling and Behavior* 9 (9): 29715. https://doi.org/ 10.4161/psb.29715.

Nakamura Y., Andrés F., Kanehara K., Liu Y., Dörmann P., and Coupland G. (2014a). Arabidopsis Florigen FT Binds to Diurnally Oscillating Phospholipids That Accelerate Flowering. *Nature Communications* 5: 3553. https://doi.org/10.1038/ ncomms4553.

Nerlich A., Von Orlow M., Rontein D., Hanson A.D., and Dormann P. (2007). Deficiency in Phosphatidylserine Decarboxylase Activity in the Psd1 Psd2 Psd3 Triple Mutant of Arabidopsis Affects Phosphatidylethanolamine Accumulation in Mitochondria. *Plant Physiology* 144 (2): 904–914. https://doi.org/10.1104/pp.107. 095414.

O'Neill J.P., Colon K.T., and Jenik P.D. (2019). The Onset of Embryo Maturation in Arabidopsis Is Determined by Its Developmental Stage and Does Not Depend on Endosperm Cellularization. *Plant Journal* 99 (2): 286–301. https://doi.org/10.1111/ tpj.14324.

Oakenfull R.J., and Davis S.J. (2017). Shining a Light on the Arabidopsis Circadian Clock. *Plant, Cell and Environment.* 40: 2571–2585. https://doi.org/10.1111/pce.13033.

Ohlrogge J.B., and Browse J. (1995). Lipid Biosynthesis. *Plant Cell* 7: 957–970. https:// doi.org/10.1105/tpc.7.7.957.

Okuley J., Lightner J., Feldmann K., Yadav N., Lark E., and Browse J. (1994). Arabidopsis *FAD2* Gene Encodes the Enzyme That Is Essential for Polyunsaturated Lipid Synthesis. *Plant Cell* 6: 147–158. https://doi.org/10.1105/ tpc.6.1.147.

Oliveira R.R.D., Viana A.J.C., and Vincentz M. (2015). An Efficient Method for Simultaneous Extraction of High-Quality RNA and DNA from Various Plant Tissues. *Genetics and Molecular Research* 14 (4): 18828–18838. https://doi.org/10.4238/2015.December. 28.32.

Oliver D.J., Nikolau B.J., and Wurtele E.S. (2009). Acetyl-CoA — Life at the Metabolic Nexus. *Plant Science* 176 (5): 597–601. https://doi.org/10.1016/j.plantsci. 2009.02.005.

Olsen O.A. (2004). Nuclear Endosperm Development in Cereals and *Arabidopsis thaliana*. *Plant Cell.* 16: 214–228. https://doi.org/10.1105/tpc.017111.

Pang Z., Zhou G., Ewald J., Basu N., and Xia J. (2022). Using MetaboAnalyst 5.0 for LC-HRMS Spectra Processing, Multi-Omics Integration and Covariate Adjustment of Global Metabolomics Data. *Nature Protocols* 17 (8): 1735–1761. https://doi.org/ 10.1038/s41596-022-00710-w.

Pan W.J., Wang X., Deng Y.R., Li J.H., Chen W., Chiang J.Y., Yang J.B., and Zheng L. (2015). Nondestructive and Intuitive Determination of Circadian Chlorophyll Rhythms in Soybean Leaves Using Multispectral Imaging. *Scientific Reports.* 5: 1–13. https://doi.org/

10.1038/srep11108.

Pelletier J.M., Kwong R.W., Park S., Le B.H., Baden R., Cagliari A., Hashimoto M., *et al.* (2017). LEC1 Sequentially Regulates the Transcription of Genes Involved in Diverse Developmental Processes during Seed Development. *PNAS* 114 (32): 6710–6719. https://doi.org/10.1073/pnas.1707957114.

Penfield S., Pinfield-Wells H.M., and Graham I.A. (2006). Storage Reserve Mobilisation and Seedling Establishment in Arabidopsis. *Arabidopsis Book*, 4: 0100. https://doi.org/ 10.1199/tab.0100.

Periappuram C., Steinhauer L., Barton D.L., Taylor D.C., Chatson B., and Zou J. (2000). The plastidic Phosphoglucomutase from Arabidopsis. A Reversible Enzyme Reaction with an Important Role in Metabolic Control. *Plant Physiology* 122: 1193–1199. https://doi.org/10.1104/pp.122.4.1193.

Pidkowich M.S., Nguyen H.T., Heilmann I., Ischebeck T., and Shanklin J. (2007). Modulating Seed β-Ketoacyl-Acyl Carrier Protein Synthase II Level Converts the Composition of a Temperate Seed Oil to That of a Palm-like Tropical Oil. *PNAS* 104 (11): 4742–4747. https://doi.org/10.1073/pnas.0611141104.

Pinfield-Wells H., Rylott E.L., Gilday A.D., Graham S., Job K., Larson T.R., and Graham I.A. (2005). Sucrose Rescues Seedling Establishment but Not Germination of Arabidopsis Mutants Disrupted in Peroxisomal Fatty Acid Catabolism. *The Plant Journal* 43 (6): 861–872. https://doi.org/10.1111/j.1365-313X.2005.02498.x.

Piskurewicz U., and Lopez-Molina L. (2011). Isolation of Genetic Material from Arabidopsis Seeds. *Methods in Molecular Biology* 773: 151–164. https://doi.org/ 10.1007/ 978-1-61779-231-1_10.

Pokhilko A., Mas P., and Millar A.J. (2013). Modelling the Widespread Effects of TOC1 Signalling on the Plant Circadian Clock and Its Outputs. *BMC Systems Biology* 7 (1): 23. https://doi.org/10.1186/1752-0509-7-23.

Prabhakar V., Löttgert T., Gigolashvili T., Bell K., Flügge U.I., and Häusler R.E. (2009). "Molecular and Functional Characterization of the Plastid-Localized Phosphoenolpyruvate Enolase (ENO1) from *Arabidopsis thaliana*." *FEBS Letters* 583 (6):

983–991. https://doi.org/10.1016/j.febslet.2009.02.017.

Riggs J.W., Cavales P.C., Chapiro S.M., and Callis J. (2017). Identification and Biochemical Characterization of the Fructokinase Gene Family in *Arabidopsis thaliana*. *BMC Plant Biology* 17: 83. https://doi.org/10.1186/s12870-017-1031-5.

Robert S.S., Singh S.P., Zhou X.R., Petrie J.R., Blackburn S.I., Mansour P.M., Nichols P.D, Liu Q., and Green A.G. 2005. Metabolic Engineering of Arabidopsis to Produce Nutritionally Important DHA in Seed Oil. *Functional Plant Biology* 32 (6): 473–479. https://doi.org/10.1071/FP05084.

Roden L.C., Song H., Jackson S., Morris K., and Carre I.A. (2002). Floral Responses to Photoperiod Are Correlated with the Timing of Rhythmic Expression Relative to Dawn and Dusk in Arabidopsis. *PNAS* 99 (20): 13313–13318. https://doi.org/10.1073/pnas.192365599.

Román Á., Hernández M.L., Soria-García A, López-Gomollón S., Lagunas B., Picorel R., Martínez-Rivas J.M., and Alfonso M. (2015). *Non-Redundant Contribution of the Plastidial FAD8 ω-3 Desaturase to Glycerolipid Unsaturation at Different Temperatures in Arabidopsis*. *Molecular Plant* 8 (11): 1599-1611. https://doi.org/10.1016/j.molp.2015.06.004.

Roscoe T.T., Guilleminot J., Bessoule J.J., Berger F., and Devic M. (2015). Complementation of Seed Maturation Phenotypes by Ectopic Expression of ABSCISIC ACID INSENSITIVE3, FUSCA3 and LEAFY COTYLEDON2 in Arabidopsis. *Plant and Cell Physiology* 56 (6): 1215–1228. https://doi.org/10.1093/pcp/pcv049.

Ruuska S.A., Girke T., Benning C., and Ohlrogge J.B. (2002). Contrapuntal Networks of Gene Expression during Arabidopsis Seed Filling. *Plant Cell* 14 (6): 1191–1206. https://doi.org/10.1105/tpc.000877.

Russell S.D. (1993). The Egg Cell: Development and Role in Fertilization and Early Embryogenesis. *Plant Cell*. 5 (10): 1349–1359. https://doi.org/10.2307/3869787.

Salie M.J., and Thelen J.J. (2016). Regulation and Structure of the Heteromeric Acetyl-CoA Carboxylase. *Biochimica et Biophysica Acta* 1861 (9): 1207–1213. https://doi.org/10.1016/j.bbalip.2016.04.004.

Sanchez A., Shin J., and Davis S.J. (2011). Abiotic Stress and the Plant Circadian Clock. *Plant Signaling and Behavior* 6 (2): 223–231. https://doi.org/10.4161/psb. 6.2.14893.

Sanda S., Leustek T., Theisen M.J., Garavito R.M., and Benning C. (2001). Recombinant Arabidopsis SQD1 Converts UDP-Glucose and Sulfite to the Sulfolipid Head Group Precursor UDP-Sulfoquinovose in Vitro. *Journal of Biological Chemistry* 276 (6): 3941–3946. https://doi.org/10.1074/jbc.M008200200.

Santos-Mendoza M., Dubreucq B., Baud S., Parcy F., Caboche M., and Lepiniec L. (2008). Deciphering Gene Regulatory Networks That Control Seed Development and Maturation in Arabidopsis. *The Plant Journal* 54 (4): 608–620. https://doi.org/10.1111/j.1365-313X.2008.03461.x.

Santos-Mendoza M., Dubreucq B., Miquel M., Caboche M., and Lepiniec L. (2005). LEAFY COTYLEDON 2 Activation Is Sufficient to Trigger the Accumulation of Oil and Seed Specific MRNAs in Arabidopsis Leaves. *FEBS Letters* 579 (21): 4666–4670. https://doi.org/ 10.1016/j.febslet.2005.07.037.

Sasnauskas G., Manakova E., Lapėnas K., Kauneckaitė K., and Siksnys V. (2018). DNA Recognition by Arabidopsis Transcription Factors ABI3 and NGA1. *FEBS Journal* 285 (21): 4041–4059. https://doi.org/10.1111/febs.14649.

Sauter M. (2000). Rice in Deep Water : ‘ How to Take Heed against a Sea of Troubles .’ *Naturwissenschaften* 87: 289–303. https://doi.org/10.1007/s001140050725.

Savadi S., Lambani N., Kashyap P.L., and Bisht D.S. (2017). Genetic Engineering Approaches to Enhance Oil Content in Oilseed Crops. *Plant Growth Regulation* 83 (2): 207–222. https://doi.org/10.1007/s10725-016-0236-1.

Scheres B., and Benfey P.N. (1999). Asymmetric Cell Division in Plants. *Annual Review of Plant Biology.* 50: 505–537. https://doi.org/10.1146/annurev.arplant.50.1.505.

Schwender J., Ohlrogge J.B., and Shachar-Hill Y. (2003). A Flux Model of Glycolysis and the Oxidative Pentosephosphate Pathway in Developing Brassica Napus Embryos. *Journal of Biological Chemistry* 278 (32): 29442–29453. https://doi.org/10.1074/ jbc.M303432200.

Sheldon P.S., Kekwick R.G.O., Sidebottom C., Smith C.G., and Slabas A.R. (1990). 3-Oxoacyl-(Acyl-Carrier Protein) Reductase from Avocado (Persea Americana) Fruit Mesocarp.

Biochemical Journal 271 (3): 713–720. https://doi.org/ 10.1042/bj2710713.

Shimakata T., and Stumpf P.K. (1982). Isolation and Function of Spinach Leaf β-Ketoacyl-[Acyl-Carrier- Protein] Synthases. *Proceedings of the National Academy of Sciences of the United States of America* 79 (19): 5808–5812. https://doi.org/ 10.1073/pnas.79.19.5808.

Shockey J.M., Fulda M.S., and Browse J. (2002). Arabidopsis Contains Nine Long-Chain Acyl-Coenzyme A Synthetase Genes That Participate in Fatty Acid and Glycerolipid Metabolism. *Plant Molecular Biology* 129 (4): 1710–1722. https://doi.org/10.1104/pp.003269.

Shrestha P., Callahan D.L., Singh S.P., Petrie J.R., and Zhou X.R. (2016). Reduced Triacylglycerol Mobilization during Seed Germination and Early Seedling Growth in Arabidopsis Containing Nutritionally Important Polyunsaturated Fatty Acids. *Frontiers in Plant Science* 7: 1402. https://doi.org/10.3389/fpls.2016.01402.

Simpson M.G. (2019). Diversity and Classification of Flowering Plants: Eudicots. *Plant Systematics.* 366: 285–466. https://doi.org/10.1016/b978-0-12-812628-8.50008-0.

Smith J., and Hitz S. (2003). Estimating Global Impacts from Climate Change. *OECD.*

Snell P., Grimberg A., Carlsson A.S., and Hofvander P. (2019). WRINKLED1 Is Subject to Evolutionary Conserved Negative Autoregulation. *Frontiers in Plant Science* 10: 387. https://doi.org/10.3389/fpls.2019.00387.

Song G., Li X., Munir R., Khan A.R., Azhar W., Yasin M.U., Jiang Q., Bancroft I., and Gan Y. (2020). The WRKY6 Transcription Factor Affects Seed Oil Accumulation and Alters Fatty Acid Compositions in *Arabidopsis thaliana*. *Plant Physiology* 169 (4): 612–624. https://doi.org/10.1111/ppl.13082.

Song J., Xie X, Chen C., Shu J., Thapa R.K., Nguyen V., Bian S., *et al*. (2021). LEAFY COTYLEDON1 Expression in the Endosperm Enables Embryo Maturation in Arabidopsis. *Nature Communications* 12 (1): 3963. https://doi.org/10.1038/s41467-021-24234-1.

Sorensen M.B., Mayer U., Lukowitz W., Robert H., Chambrier P., Jürgens G., Somerville C., Lepiniec L., and Berger F. (2002). Cellularisation in the Endosperm of *Arabidopsis thaliana* Is Coupled to Mitosis and Shares Multiple Components with Cytokinesis. *Development.* 129 (24): 5567–5576. https://doi.org/ 10.1242/dev.00152.

Stein O., Avin-Wittenberg T., Krahnert I., Zemach H., Bogol V., Daron O., Aloni R., Fernie A.R., and Granot D. (2017). Arabidopsis Fructokinases Are Important for Seed Oil Accumulation and Vascular Development. *Frontiers in Plant Science* 7: 2047. https://doi.org/ 10.3389/fpls.2016.02047.

Strayer C., Oyama T., Schultz T.F., Raman R., Somers D.E., Mas P., Panda S., Kreps J.A., and Kay S.A. (2000). Cloning of the Arabidopsis Clock Gene TOC1, an Autoregulatory Response Regulator Homolog. *Science* 289 (5480): 768–771. https://doi.org/10.1126/ science.289.5480.768.

Sun M., Folk R.A., Gitzendanner M.A., Soltis P.S., Chen Z., Soltis D.E., and Guralnick R.P. (2020). Recent Accelerated Diversification in Rosids Occurred Outside the Tropics. *Nature Communications.* 11 (1): 1–12. https://doi.org/ 10.1038/s41467-020-17116-5.

Ten Hove C.A., Lu K.J., and Weijers D. (2015). Building a Plant: Cell Fate Specification in the Early Arabidopsis Embryo. *Development.* 142 (3): 420–430. https://doi.org/ 10.1242/dev.111500.

Testerink C., and Munnik T. (2011). Molecular , Cellular, and Physiological Responses to Phosphatidic Acid Formation in Plants. *Journal of Experimental Botany* 62 (7): 2349–2361. https://doi.org/10.1093/jxb/err079.

Thelen J.J., and Ohlrogge J.B. (2002). Both Antisense and Sense Expression of Biotin Carboxyl Carrier Protein Isoform 2 Inactivates the Plastid Acetyl-Coenzyme A Carboxylase in *Arabidopsis thaliana*. *Plant Journal* 32 (4): 419–431. https://doi.org/ 10.1046/j.1365-313x.2002.01435.x.

Tian R., Wang F., Zheng Q. *et al.* (2020). Direct and indirect targets of the arabidopsis seed transcription factor ABSCISIC ACID INSENSITIVE 3. *The Plant Journal* 103 (5). https://doi.org/10.1111/tpj.14854.

To A., Valon C., Savino G., Guilleminot J., Devic M., Giraudat J., and Parcy F. (2006). A Network of Local and Redundant Gene Regulation Governs Arabidopsis Seed Maturation. *Plant Cell* 18 (7): 1642–1651. https://doi.org/ 10.1105/tpc.105.039925.

Troncoso-Ponce M.A., Barthole G., Tremblais G., To A., Miquel M., Lepiniec L., and Baud S. (2016). Transcriptional Activation of Two Delta-9 Palmitoyl-ACP Desaturase Genes by

MYB115 and MYB118 Is Critical for Biosynthesis of Omega-7 Monounsaturated Fatty Acids in the Endosperm of Arabidopsis Seeds. *Plant Cell* 28 (10): 2666–2682. https://doi.org/10.1105/tpc.16.00612.

Troncoso-Ponce M.A., Kilaru A., Cao X., Durrett T.P., Fan J., Jensen J.K., Thrower N.A., Pauly M., Wilkerson C., and Ohlrogge J.B. (2011). Comparative Deep Transcriptional Profiling of Four Developing Oilseeds. *Plant Journal* 68 (6): 1014–1027. https://doi.org/ 10.1111/j.1365-313X.2011.04751.x.

Tsugawa H., Ikeda K., Takahashi M., Satoh A., Mori Y., Uchino H., Okahashi N., *et al.* (2020). A Lipidome Atlas in MS-DIAL 4. *Nature Biotechnology* 38 (10): 1159–1163. https://doi.org/10.1038/s41587-020-0531-2.

Verma S., Attuluri V.P.S., and Robert H.S. (2022). Transcriptional Control of Arabidopsis Seed Development. *Planta* 255 (4): 90. https://doi.org/10.1007/ s00425-022-03870-x.

Wada H., Shintani D., and Ohlrogge J.B. (1997). Why Do Mitochondria Synthesize Fatty Acids? Evidence for Involvement in Lipoic Acid Production. *Proceedings of the National Academy of Sciences of the United States of America* 94 (4): 1591–1596. https://doi.org/ 10.1073/pnas.94.4.1591.

Wang X., Devaiah S.P., Zhang W., and Welti R. (2006). Signaling Functions of Phosphatidic Acid. *Progress in Lipid Research* 45 (3): 250–278. https://doi.org/10.1016/j.plipres. 2006.01.005.

Wang Z., Chen M., Chen T., Xuan L., Li Z., Du X., Zhou L., Zhang G., and Jiang L. (2014). TRANSPARENT TESTA2 Regulates Embryonic Fatty Acid Biosynthesis by Targeting FUSCA3 during the Early Developmental Stage of Arabidopsis Seeds. *Plant Journal* 77 (5): 757–769. https://doi.org/10.1111/tpj.12426.

Yamamoto A., Kagaya Y., Toyoshima R., Kagaya M., Takeda S., and Hattori T. (2009). Arabidopsis NF-YB Subunits LEC1 and LEC1-LIKE Activate Transcription by Interacting with Seed-Specific ABRE-Binding Factors. *Plant Journal* 58 (5): 843–856. https://doi.org/ 10.1111/j.1365-313X.2009.03817.x.

Yamamoto A., Kagaya Y., Usui H., Hobo T., Takeda S., and Hattori T. (2010). Diverse Roles and Mechanisms of Gene Regulation by the Arabidopsis Seed Maturation Master Regulator

FUS3 Revealed by Microarray Analysis. *Plant and Cell Physiology* 51 (12): 2031–2046. https://doi.org/10.1093/pcp/pcq162.

Yamaoka Y., Yu Y., Mizoi J., Fujiki Y., Saito K., Nishijima M., Lee Y., and Nishida I. (2011). PHOSPHATIDYLSERINE SYNTHASE1 Is Required for Microspore Development in *Arabidopsis thaliana*. *Plant Journal* 67 (4): 648–661. https://doi.org/10.1111/j.1365-313X.2011.04624.x.

Yan D., Duermeyer L., Leoveanu C., and Nambara E. (2014). The Functions of the Endosperm during Seed Germination. *Plant and Cell Physiology.* 55 (9): 1521–1533. https://doi.org/ 10.1093/pcp/pcu089.

Ye Y., Nikovics K., To A., Lepiniec L., Fedosejevs E.T., Van Doren S.R., Baud S., and Thelen J.J. (2020). Docking of Acetyl-CoA Carboxylase to the Plastid Envelope Membrane Attenuates Fatty Acid Production in Plants. *Nature Communications* 11 (1): 6191. https://doi.org/10.1038/s41467-020-20014-5.

Yu B., and Benning C. (2003). Anionic Lipids Are Required for Chloroplast Structure and Function in Arabidopsis. *Plant Journal* 36 (6): 762–770. https://doi.org/10.1046/ j.1365-313X.2003.01918.x.

Yu B., Xu C., and Benning C. (2002). Arabidopsis Disrupted in SQD2 Encoding Sulfolipid Synthase Is Impaired in Phosphate-Limited Growth. *PNAS* 99 (8): 5732–5737. https:// doi.org/10.1073/pnas.082696499.

Yu X., Li A., and Li W. (2015). How Membranes Organize during Seed Germination: Three Patterns of Dynamic Lipid Remodelling Define Chilling Resistance and Affect Plastid Biogenesis. *Plant Cell Environment* 38 (7): 1391–1403. https://doi.org/10.1111/ pce.12494.

Zabel F., Putzenlechner B., and Mauser W. (2014). Global Agricultural Land Resources - A High Resolution Suitability Evaluation and Its Perspectives until 2100 under Climate Change Conditions. *PLoS ONE* 9 (9): 107522. https://doi.org/10.1371/ journal.pone.0107522.

Zafar S. Li Y., Li N., Zhu K., and Tan X. (2019). Recent Advances in Enhancement of Oil Content in Oilseed Crops. *Journal of Biotechnology* 301: 35–44. https://doi.org/10.1016/ j.jbiotec.2019.05.307.

Zhai Z., Keereetaweep J., Liu H., Feil R., Lunn J.E., and Shanklin J. (2018). Trehalose 6-Phosphate Positively Regulates Fatty Acid Synthesis by Stabilizing WRINKLED1. *Plant Cell* 30 (10): 2616–2627. https://doi.org/10.1105/tpc.18.00521.

Zhai Z., Liu H., and Shanklin J. (2017). "Phosphorylation of WRINKLED1 by KIN10 Results in Its Proteasomal Degradation, Providing a Link between Energy Homeostasis and Lipid Biosynthesis." *Plant Cell* 29 (4): 871–889. https://doi.org/10.1105/tpc.17.00019.

Zhang M., Fan J., Taylor D.C., and Ohlrogge J.B. (2009). DGAT1 and PDAT1 Acyltransferases Have Overlapping Functions in Arabidopsis Triacylglycerol Biosynthesis and Are Essential for Normal Pollen and Seed Development. *Plant Cell* 21 (12): 3885–3901. https://doi.org/10.1105/tpc.109.071795.

Zhang W., Qin C., Zhao J., and Wang X. (2004). Phospholipase Dα1-Derived Phosphatidic Acid Interacts with ABI1 Phosphatase 2C and Regulates Abscisic Acid Signaling. *PNAS* 101 (25): 9508–9513. https://doi.org/10.1073/pnas.0402112101.

Zhao X., Xiang X., Huang J., Sun J., and Zhu D. (2021). Studying the Evaluation Model of the Nutritional Quality of Edible Vegetable Oil Based on Dietary Nutrient Reference Intake. *ACS Omega* 0–7. https://doi.org/10.1021/acsomega.0c05544.

Zinkl G.M., Zwiebel B.I., Grier D.G., and Preuss D. (1999). Pollen-Stigma Adhesion in Arabidopsis: A Species-Specific Interaction Mediated by Lipophilic Molecules in the Pollen Exine. *Development* 126 (23): 5431–5440. https://doi.org/10.1242/dev.126.23.5431.

Zolman B.K., Silva I.D., and Bartel B. (2001). The Arabidopsis Pxa1 Mutant Is Defective in an ATP-Binding Cassette Transporter-like Protein Required for Peroxisomal Fatty Acid β-Oxidation. *Plant Physiology* 127 (3): 1266–1278. https://doi.org/10.1104/pp.010550.

Zonia L., Tupý J., and Staiger C.J. (1999). Unique Actin and Microtubule Arrays Co-Ordinate the Differentiation of Microspores to Mature Pollen in Nicotiana Tabacum. *Journal of Experimental Botany.* 50 (334): 581–594. https://doi.org/10.1093/jxb/50.334.581.

SUPPLEMENTARY FIGURES

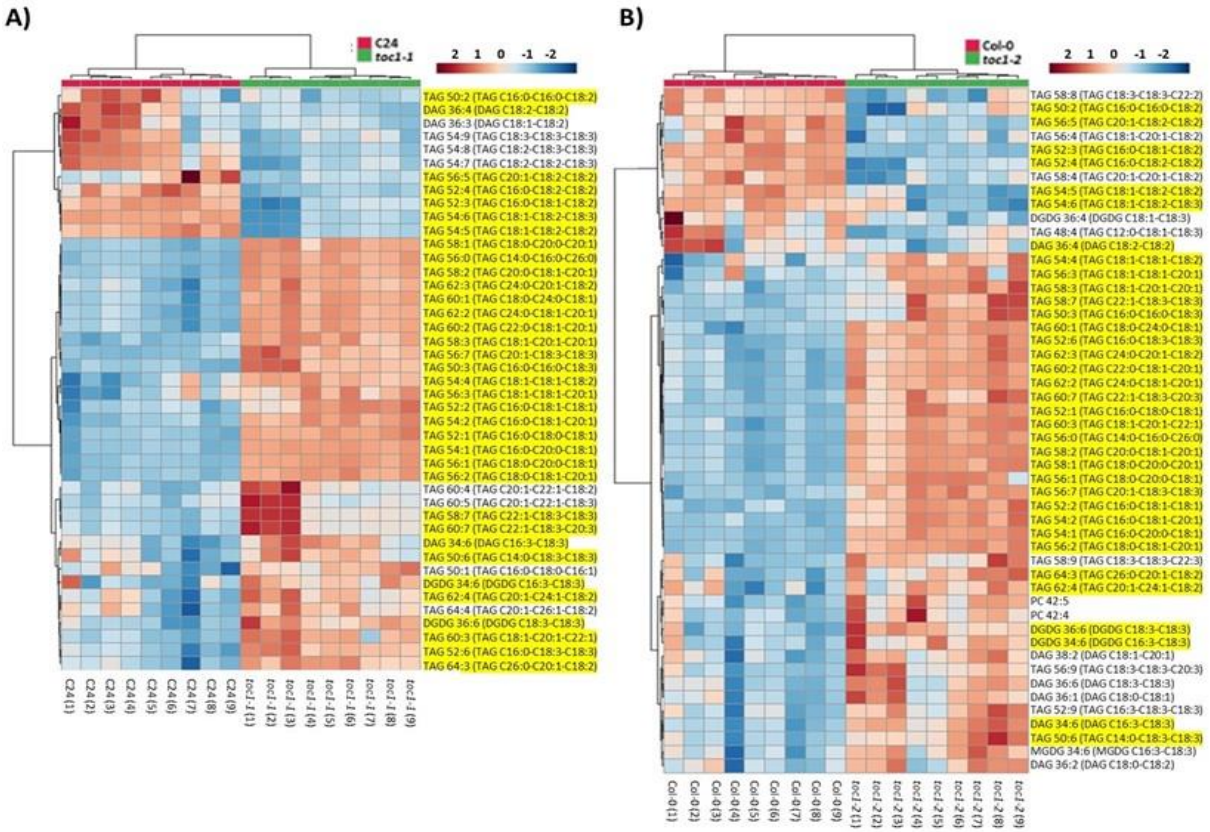

Supplementary Figure 1. Differences in glycerolipid composition between *toc1* and WT mature seeds observed by heatmaps. *Heatmaps were performed using lipidomic data generated from A) C24 (red group) and toc1-1 (green group) mature seeds and B) Col-0 (red group) and toc1-2 (green group) mature seeds. In A), the heatmap was carried out by focusing on the 43 glycerolipid species significantly modified between C24 and toc1-1. In B), the heatmap was performed on the 50 glycerolipid species significantly changed between Col-0 and toc1-2. Glycerolipid species with significantly lower and higher levels in a group were represented by blue and red bars, respectively. Glycerolipid species highlighted in yellow were discriminated in both toc1 mutants.*

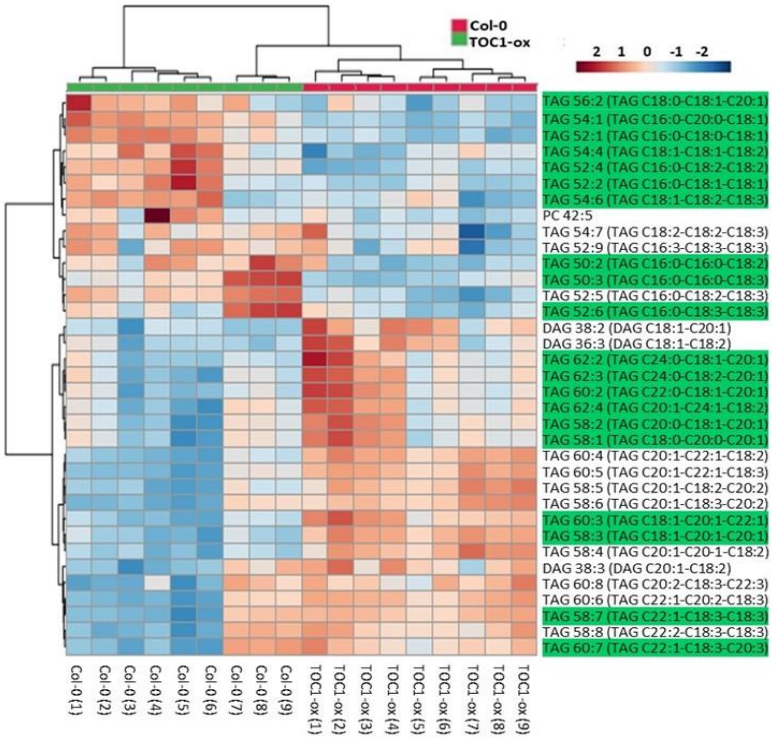

Supplementary Figure 2. Differences in glycerolipid composition between TOC1-ox and Col-0 observed by heatmap. *The heatmap was performed using lipidomic data generated from Col-0 (red group) and TOC1-ox (green group) mature seeds. The heatmap was carried out by focusing on the glycerolipid species significantly modified between Col-0 and TOC1-ox. Species highlighted in green were also significantly modified between both toc1 mutants and their respective WT. Glycerolipid species with significantly lower and higher levels in a group were represented by blue and red bars, respectively.*

SUPPLEMENTARY TABLES

Supplementary Table 1. Differences in FA composition between Col-0 and *prr9-1* mature seeds. *Values are expressed in mol% ± standard deviation. These numerical values are represented in form of histogram in Figure 24A. Plant culture and FA analysis were performed in same conditions for all prr mutants and their respective WT (Col-0). p-value > 0.05: NS; p-value < 0.05: *; p-value < 0.01: **; p-value < 0.001: ***; (n = 9).*

FA	Col-0	*prr9-1*	p-value
C16:0	7.2 ± 0.2	7.3 ± 0.1	NS
C18:0	3.0 ± 0.1	2.9 ± 0.1	*
C18:1	17.6 ± 0.7	16.0 ± 0.2	***
C18:2	29.5 ± 0.3	28.6 ± 0.1	***
C18:3	16.5 ± 0.7	18.1 ± 0.2	***
C20:0	1.9 ± 0.1	1.8 ± 0.1	NS
C20:1	20.8 ± 0.4	21.7 ± 0.1	***
C20:2	1.8 ± 0.1	1.8 ± 0.1	NS
C22:1	1.7 ± 0.1	1.8 ± 0.1	*

Supplementary Table 2. Differences in FA composition between Col-0 and *prr7-3* mature seeds. *Values are expressed in mol% ± standard deviation. These numerical values are represented in form of histogram in Figure 25A. Plant culture and FA analysis were performed in same conditions for all prr mutants and their respective WT (Col-0). p-value > 0.05: NS; p-value < 0.05: *; p-value < 0.01: **; p-value < 0.001: ***; (n = 9).*

FA	Col-0	*prr7-3*	p-value
C16:0	7.2 ± 0.2	7.0 ± 0.1	**
C18:0	3.0 ± 0.1	3.1 ± 0.1	*
C18:1	17.6 ± 0.7	18.0 ± 0.4	NS
C18:2	29.5 ± 0.3	30.1 ± 0.4	**
C18:3	16.5 ± 0.7	15.5 ± 0.2	***
C20:0	1.9 ± 0.1	2.0 ± 0.1	**
C20:1	20.8 ± 0.4	20.9 ± 0.4	NS
C20:2	1.8 ± 0.1	1.7 ± 0.1	NS
C22:1	1.7 ± 0.1	1.7 ± 0.1	NS

Supplementary Table 3. Differences in FA composition between Col-0 and *prr5-1* mature seeds. *Values are expressed in mol% ± standard deviation. These numerical values are represented in form of histogram in Figure 26A. Plant culture and FA analysis were performed in same conditions for all prr mutants and their respective WT (Col-0). p-value > 0.05: NS; p-value < 0.05: *; p-value < 0.01: **; p-value < 0.001: ***; (n = 9).*

FA	Col-0	*prr5-1*	p-value
C16:0	7.2 ± 0.2	6.9 ± 0.4	*
C18:0	3.0 ± 0.1	3.5 ± 0.5	*
C18:1	17.6 ± 0.7	17.7 ± 0.9	NS
C18:2	29.5 ± 0.3	29.7 ± 0.2	NS
C18:3	16.5 ± 0.7	16.0 ± 0.5	NS
C20:0	1.9 ± 0.1	2.1 ± 0.1	***
C20:1	20.8 ± 0.4	20.7 ± 0.8	NS
C20:2	1.8 ± 0.1	1.7 ± 0.2	NS
C22:1	1.7 ± 0.1	1.7 ± 0.3	NS

Supplementary Table 4. Differences in FA composition between Ws and *cca1-11 lhy-21* mature seeds. *Values are expressed in mol% ± standard deviation. These numerical values are represented in form of histogram in Figure 27A. Plant culture and FA analysis were performed in same conditions for Ws and cca1-11 lhy-21. p-value > 0.05: NS; p-value < 0.05: *; p-value < 0.01: **; p-value < 0.001: ***; (n = 18).*

FA	Ws	*cca1-11 lhy-21*	p-value
C16:0	7.0 ± 0.1	6.9 ± 0.2	NS
C18:0	3.9 ± 0.1	4.5 ± 0.2	***
C18:1	15.3 ± 0.2	14.5 ± 0.3	***
C18:2	28.1 ± 0.3	28.1 ± 0.1	NS
C18:3	17.3 ± 0.3	17.0 ± 0.3	NS
C20:0	2.4 ± 0.1	2.8 ± 0.1	***
C20:1	22.2 ± 0.2	22.2 ± 0.3	NS
C20:2	2.0 ± 0.1	2.0 ± 0.1	NS
C22:1	1.8 ± 0.1	1.9 ± 0.1	NS

Supplementary Table 5. Differences in FA composition between C24 and Col-0 mature seeds. *Values are expressed in mol% ± standard deviation. These numerical values are represented in form of histogram in Figure 28A. Plant culture and FA analysis were performed in the same conditions for Col-0 and C24. p-value > 0.05: NS; p-value < 0.05: *; p-value < 0.01: **; p-value < 0.001: ***, (n = 17).*

FA	C24	Col-0	p-value
C16:0	7.3 ± 0.2	7.2 ± 0.2	NS
C18:0	3.4 ± 0.1	3.4 ± 0.2	NS
C18:1	16.3 ± 0.6	15.6 ± 1.0	*
C18:2	29.0 ± 0.3	29.1 ± 0.4	NS
C18:3	17.1 ± 0.7	17.7 ± 0.6	**
C20:0	2.0 ± 0.1	2.0 ± 0.1	NS
C20:1	21.2 ± 0.3	21.2 ± 0.6	NS
C20:2	1.9 ± 0.1	2.0 ± 0.2	NS
C22:1	1.8 ± 0.1	1.8 ± 0.1	NS

Supplementary Table 6. Differences in FA composition between *toc1* mutants and WT mature seeds. *Values are expressed in mol% ± standard deviation. These numerical values are represented in form of histogram in Figure 29A and 30A. Plant culture and FA analysis were performed in same conditions for both toc1 and respective WT. p-value > 0.05: NS; p-value < 0.05: *; p-value < 0.01: **; p-value < 0.001: ***; (n = 17).*

FA	C24	*toc1-1*	p-value
C16:0	7.3 ± 0.2	7.5 ± 0.2	NS
C18:0	3.4 ± 0.1	4.6 ± 0.1	***
C18:1	16.3 ± 0.6	15.2 ± 0.8	***
C18:2	29.0 ± 0.3	23.9 ± 0.2	***
C18:3	17.1 ± 0.7	19.1 ± 0.5	***
C20:0	2.0 ± 0.1	2.9 ± 0.1	***
C20:1	21.2 ± 0.3	23.0 ± 0.3	***
C20:2	1.9 ± 0.1	1.7 ± 0.1	NS
C22:1	1.8 ± 0.1	2.0 ± 0.1	NS
FA	Col-0	*toc1-2*	p-value
C16:0	7.2 ± 0.2	7.4 ± 0.4	NS
C18:0	3.4 ± 0.2	4.8 ± 0.1	***
C18:1	15.6 ± 1.0	14.5 ± 0.4	***
C18:2	29.1 ± 0.4	24.4 ± 0.2	***
C18:3	17.7 ± 0.6	20.0 ± 0.4	***
C20:0	2.0 ± 0.1	2.8 ± 0.1	***
C20:1	21.2 ± 0.6	22.5 ± 0.3	***
C20:2	2.0 ± 0.2	1.8 ± 0.1	NS
C22:1	1.8 ± 0.1	1.9 ± 0.1	NS

Supplementary Table 7. Differences in FA composition between Col-0 and TOC1-ox mature seeds. *Values are expressed in mol% ± standard deviation. These numerical data were represented in form of histogram in Figure 31A. Plant culture and FA analysis were performed in same conditions for Col-0 and TOC1-ox. p-value > 0.05: NS; p-value < 0.05: *; p-value < 0.01: **; p-value < 0.001: ***, (n = 18).*

FA	Col-0	TOC1-ox	p-value
C16:0	7.3 ± 0.1	7.9 ± 0.6	***
C18:0	3.6 ± 0.1	4.1 ± 0.1	***
C18:1	14.5 ± 0.2	14.5 ± 0.5	NS
C18:2	28.3 ± 0.1	29.3 ± 0.4	***
C18:3	18.4 ± 0.3	18.8 ± 0.4	***
C20:0	2.2 ± 0.1	2.1 ± 0.1	NS
C20:1	21.7 ± 0.2	20.0 ± 0.3	***
C20:2	2.1 ± 0.1	2.0 ± 0.1	***
C22:1	1.9 ± 0.1	1.3 ± 0.1	***

Supplementary Table 8. Summary of results generated using different mutants and their respective WT mature seeds. *FA significantly decreased and increased in mutants were represented by blue and red stars, respectively. Stars were highlighted in grey when statistical significance reflects differences in mol% observed between WT and mutants (or between WT1 and WT2). p-value > 0.05: NS; p-value < 0.05: *; p-value < 0.01: **; p-value < 0.001: ***.*

Mature seeds		Circadian rhythm	p-value								
WT1	Mutant or WT2	Mutant or WT2	C16:0	C18:0	C18:1	C18:2	C18:3	C20:0	C20:1	C20:2	C22:1
Col-0	*prr9-1*	24h	NS	*	***	***	***	NS	***	NS	*
Col-0	*prr7-3*	26h	**	*	NS	**	***	**	NS	NS	NS
Col-0	*prr5-1*	23h	*	*	NS	NS	NS	***	NS	NS	NS
Ws	*cca1-11 lhy-21*	17h	NS	***	***	NS	NS	***	NS	NS	NS
C24	Col-0	24h	NS	NS	*	NS	**	NS	NS	NS	NS
C24	*toc1-1*	20h	NS	***	***	***	***	***	***	NS	NS
Col-0	*toc1-2*	20h	NS	***	***	***	***	***	***	NS	NS
Col-0	TOC1-ox	30h	***	***	NS	***	***	NS	***	***	***

Supplementary Table 9. Differences in FA profiles between *toc1* and WT seedlings. *Values are expressed in mol% ± standard deviation. These numerical data were represented in form of histogram in Figure 32. Both toc1 and WT seedlings were grown in the same light, temperature and hygrometry conditions. Seedlings were collected from medium in same light condition. Three batches of FA extraction and analysis were performed for WT and toc1. In each batch (n = 9), FA extraction and analysis were performed in same conditions for WT and toc1. p-value > 0.05: NS; p-value < 0.05: *; p-value < 0.01: **; p-value < 0.001: ***; (n = 27).*

FA	C24	*toc1-1*	p-value
C16:0	23.3 ± 3.5	24.1 ± 4.35	*
C16:1	2.5 ± 0.4	2.2 ± 0.29	NS
C16:2	0.4 ± 0.0	0.4 ± 0.0	NS
C16:3	7.5 ± 1.0	8.8 ± 0.8	***
C18:0	2.0 ± 0.3	2.0 ± 0.6	NS
C18:1	1.8 ± 0.3	1.6 ± 0.2	*
C18:2	13.1 ± 1.3	11.1 ± 0.9	***
C18:3	49.4 ± 2.5	49.6 ± 3.2	NS
FA	Col-0	*toc1-2*	p-value
C16:0	21.0 ± 3.5	24.3 ± 3.4	**
C16:1	2.2 ± 0.3	2.1 ± 0.3	NS
C16:2	0.4 ± 0.0	0.4 ± 0.1	NS
C16:3	8.4 ± 0.5	8.0 ± 0.5	**
C18:0	1.7 ± 0.4	2.3 ± 0.3	***
C18:1	1.5 ± 0.1	1.4 ± 0.1	**
C18:2	13.7 ± 0.6	11.7 ± 0.7	***
C18:3	51.0 ± 3.0	49.7 ± 2.7	NS

Supplementary Table 10. Differences in FA composition between *toc1* and WT leaves. *Values are expressed in mol% ± standard deviation. These numerical data were represented in form of histogram in Figure 33. Both toc1 and WT leaves were grown in the same light, temperature and hygrometry conditions. Leaves were collected from plants in same light conditions. Three batches of FA extraction and analysis were performed for WT and toc1. In each batch (n = 9), FA extraction and analysis were performed in same conditions for WT and toc1. p-value > 0.05: NS; p-value < 0.05: *; p-value < 0.01: **; p-value < 0.001: ***; (n = 27).*

FA	C24	*toc1-1*	p-value
C16:0	17.0 ± 3.2	17.2 ± 1.0	NS
C16:1	2.2 ± 0.3	1.9 ± 0.2	*
C16:2	0.4 ± 0.1	0.4 ± 0.0	NS
C16:3	9.3 ± 2.5	10.5 ± 0.9	NS
C18:0	2.9 ± 1.2	2.1 ± 0.8	NS
C18:1	4.4 ± 2.2	5.7 ± 1.5	NS
C18:2	21.0 ± 2.2	17.4 ± 1.6	**
C18:3	42.8 ± 4.0	44.6 ± 2.9	NS
FA	Col-0	*toc1-2*	p-value
C16:0	15.2 ± 0.2	21.8 ± 0.6	***
C16:1	2.0 ± 0.1	1.5 ± 0.1	***
C16:2	0.5 ± 0.0	0.4 ± 0.1	***
C16:3	13.0 ± 1.0	7.1 ± 0.3	***
C18:0	1.6 ± 0.2	1.9 ± 0.1	***
C18:1	4.7 ± 0.8	5.9 ± 0.2	***
C18:2	19.1 ± 0.7	20.1 ± 0.8	**
C18:3	43.8 ± 0.7	41.3 ± 1.0	***

Supplementary Table 11. Differences in glycerolipid composition between Col-0 and C24 mature seeds. *Data were acquired in positive mode. Values are expressed in mol% ± standard deviation. p-value > 0.05: NS; p-value < 0.05: *; p-value < 0.01: **; p-value < 0.001: ***; (n = 9).*

Glycerolipids	Species	C24	Col-0	p-value
DAG 34:0	DAG 16:0-18:0	0.012 ± 0.002	0.012 ± 0.003	NS
DAG 34:1	DAG 16:0-18:1	0.015 ± 0.004	0.016 ± 0.004	NS
DAG 34:2	DAG 16:0-18:2	0.085 ± 0.021	0.083 ± 0.018	NS
DAG 34:3	DAG 16:0-18:3	0.023 ± 0.005	0.025 ± 0.005	NS
DAG 34:5	DAG 18:2-16:3	0.006 ± 0.002	0.005 ± 0.001	NS
DAG 34:6	DAG 16:3-18:3	0.010 ± 0.003	0.010 ± 0.002	NS
DAG 36:0	DAG 18:0-18:0	0.014 ± 0.005	0.015 ± 0.005	NS
DAG 36:1	DAG 18:0-18:1	0.008 ± 0.002	0.008 ± 0.001	NS
DAG 36:2	DAG 18:0-18:2	0.040 ± 0.012	0.035 ± 0.006	NS
DAG 36:3	DAG 18:1-18:2	0.144 ± 0.038	0.129 ± 0.022	NS
DAG 36:4	DAG 18:2-18:2	0.375 ± 0.097	0.312 ± 0.047	NS
DAG 36:5	DAG 18:2-18:3	0.186 ± 0.052	0.164 ± 0.031	NS
DAG 36:6	DAG 18:3-18:3	0.032 ± 0.009	0.029 ± 0.005	NS
DAG 38:2	DAG 18:1-20:1	0.016 ± 0.005	0.016 ± 0.002	NS
DAG 38:3	DAG 20:1-18:2	0.087 ± 0.027	0.079 ± 0.013	NS
DAG 38:4	DAG 18:2-20:2	0.035 ± 0.009	0.032 ± 0.005	NS
DAG 38:5	DAG 20:2-18:3	0.013 ± 0.004	0.013 ± 0.002	NS
DAG 44:6	DAG 22:0-22:6	0.006 ± 0.003	0.006 ± 0.004	NS
DGDG 34:6	DGDG 16:3-18:3	0.003 ± 0.001	0.002 ± 0.001	NS
DGDG 36:4	DGDG 18:1-18:3	0.002 ± 0.000	0.002 ± 0.000	NS
DGDG 36:5	DGDG 18:2-18:3	0.002 ± 0.000	0.002 ± 0.000	NS
DGDG 36:6	DGDG 18:3-18:3	0.003 ± 0.001	0.003 ± 0.001	NS
LPC 16:0	LPC 16:0-0:0	0.002 ± 0.001	0.003 ± 0.002	NS
LPC 18:1	LPC 18:1-0:0	0.002 ± 0.001	0.002 ± 0.001	NS
LPC 18:2	LPC 18:2-0:0	0.006 ± 0.003	0.005 ± 0.002	NS
LPC 18:3	LPC 18:3-0:0	0.002 ± 0.001	0.002 ± 0.001	NS
MGDG 34:6	MGDG 16:3-18:3	0.012 ± 0.004	0.011 ± 0.002	NS
PC 32:1	PC 32:1	0.007 ± 0.002	0.006 ± 0.002	NS
PC 34:1	PC 16:0-18:1	0.018 ± 0.012	0.018 ± 0.012	NS
PC 34:2	PC 16:0-18:2	0.097 ± 0.068	0.079 ± 0.056	NS
PC 34:3	PC 16:0-18:3	0.032 ± 0.020	0.026 ± 0.017	NS
PC 34:4	PC 16:1-18:3	0.008 ± 0.004	0.007 ± 0.003	NS
PC 34:5	PC 16:2-18:3	0.004 ± 0.003	0.003 ± 0.002	NS
PC 34:6	PC 16:3-18:3	0.004 ± 0.003	0.003 ± 0.002	NS
PC 36:1	PC 16:0-20:1	0.006 ± 0.004	0.006 ± 0.004	NS
PC 36:2	PC 18:0-18:2	0.039 ± 0.026	0.034 ± 0.025	NS
PC 36:3	PC 18:1-18:2	0.098 ± 0.071	0.080 ± 0.062	NS
PC 36:4	PC 18:2-18:2	0.262 ± 0.192	0.190 ± 0.153	NS
PC 36:5	PC 18:2-18:3	0.100 ± 0.073	0.074 ± 0.060	NS
PC 36:6	PC 18:3-18:3	0.011 ± 0.007	0.009 ± 0.006	NS

Supplementary Table 11. Continued

Glycerolipids	Species	C24	Col-0	p-value
PC 38:2	PC 38:2	0.006 ± 0.004	0.006 ± 0.004	NS
PC 38:3	PC 20:1-18:2	0.044 ± 0.031	0.040 ± 0.030	NS
PC 38:4	PC 20:1-18:3	0.023 ± 0.016	0.019 ± 0.014	NS
PC 38:5	PC 38:5	0.006 ± 0.004	0.005 ± 0.004	NS
PC 42:4	PC 42:4	0.003 ± 0.000	0.003 ± 0.001	NS
PC 42:5	PC 42:5	0.003 ± 0.000	0.003 ± 0.000	NS
PE 34:1	PE 16:0-18:1	0.002 ± 0.001	0.002 ± 0.001	NS
PE 34:2	PE 16:0-18:2	0.031 ± 0.020	0.025 ± 0.017	NS
PE 34:3	PE 16:0-18:3	0.008 ± 0.005	0.006 ± 0.004	NS
PE 36:2	PE 18:0-18:2	0.006 ± 0.003	0.004 ± 0.003	NS
PE 36:3	PE 18:1-18:2	0.014 ± 0.009	0.011 ± 0.007	NS
PE 36:4	PE 18:2-18:2	0.044 ± 0.031	0.033 ± 0.024	NS
PE 36:5	PE 18:2-18:3	0.013 ± 0.009	0.010 ± 0.008	NS
PE 36:6	PE 18:3-18:3	0.001 ± 0.000	0.001 ± 0.000	NS
PE 38:3	PE 20:1-18:2	0.004 ± 0.002	0.004 ± 0.002	NS
PE 38:4	PE 38:4	0.002 ± 0.001	0.001 ± 0.000	NS
PE 38:5	PE 38:5	0.001 ± 0.000	0.001 ± 0.000	NS
TAG 48:4	TAG 12:0-18:1-18:3	0.014 ± 0.004	0.013 ± 0.001	NS
TAG 48:5	TAG 12:0-18:2-18:3	0.011 ± 0.003	0.010 ± 0.001	NS
TAG 50:1	TAG 16:0-18:0-16:1	0.355 ± 0.024	0.364 ± 0.020	NS
TAG 50:2	TAG 16:0-16:0-18:2	1.445 ± 0.090	1.475 ± 0.040	NS
TAG 50:3	TAG 16:0-16:0-18:3	0.548 ± 0.026	0.579 ± 0.018	**
TAG 50:4	TAG 16:0-16:1-18:3	0.172 ± 0.035	0.164 ± 0.026	NS
TAG 50:5	TAG 14:0-18:2-18:3	0.079 ± 0.021	0.072 ± 0.012	NS
TAG 50:6	TAG 14:0-18:3-18:3	0.029 ± 0.008	0.025 ± 0.004	NS
TAG 52:1	TAG 16:0-18:0-18:1	0.264 ± 0.012	0.265 ± 0.008	NS
TAG 52:2	TAG 16:0-18:1-18:1	1.633 ± 0.055	1.638 ± 0.030	NS
TAG 52:3	TAG 16:0-18:1-18:2	3.529 ± 0.061	3.551 ± 0.058	NS
TAG 52:4	TAG 16:0-18:2-18:2	5.105 ± 0.123	5.151 ± 0.096	NS
TAG 52:5	TAG 16:0-18:2-18:3	4.640 ± 0.230	4.546 ± 0.119	NS
TAG 52:6	TAG 16:0-18:3-18:3	2.109 ± 0.248	2.033 ± 0.130	NS
TAG 52:7	TAG 16:1-18:3-18:3	0.102 ± 0.027	0.092 ± 0.017	NS
TAG 52:8	TAG 18:2-16:3-18:3	0.038 ± 0.012	0.035 ± 0.008	NS
TAG 52:9	TAG 16:3-18:3-18:3	0.011 ± 0.004	0.010 ± 0.003	NS
TAG 54:1	TAG 16:0-20:0-18:1	0.264 ± 0.015	0.272 ± 0.005	NS
TAG 54:2	TAG 16:0-18:1-20:1	1.785 ± 0.066	1.823 ± 0.040	NS
TAG 54:3	TAG 16:0-20:1-18:2	4.504 ± 0.238	4.630 ± 0.158	NS
TAG 54:4	TAG 18:1-18:1-18:2	3.749 ± 0.252	3.851 ± 0.183	NS
TAG 54:5	TAG 18:1-18:2-18:2	5.255 ± 0.184	5.150 ± 0.147	NS
TAG 54:6	TAG 18:1-18:2-18:3	6.511 ± 0.077	6.285 ± 0.197	**
TAG 54:7	TAG 18:2-18:2-18:3	5.195 ± 0.472	4.863 ± 0.393	NS
TAG 54:8	TAG 18:2-18:3-18:3	2.292 ± 0.428	2.103 ± 0357	NS

Supplementary Table 11. Continued

Glycerolipids	Species	C24	Col-0	p-value
TAG 54:9	TAG 18:3-18:3-18:3	0.672 ± 0.170	0.607 ± 0.131	NS
TAG 56:0	TAG 14:0-16:0-26:0	0.039 ± 0.003	0.040 ± 0.003	NS
TAG 56:1	TAG 18:0-20:0-18:1	0.341 ± 0.011	0.339 ± 0.009	NS
TAG 56:2	TAG 18:0-18:1-20:1	1.593 ± 0.058	1.587 ± 0.039	NS
TAG 56:3	TAG 18:1-18:1-20:1	3.912 ± 0.184	3.906 ± 0.104	NS
TAG 56:4	TAG 18:1-20:1-18:2	4.115 ± 0.211	4.135 ± 0.119	NS
TAG 56:5	TAG 20:1-18:2-18:2	6.673 ± 0.481	6.780 ± 0.351	NS
TAG 56:6	TAG 20:1-18:2-18:3	7.815 ± 0.500	7.936 ± 0.440	NS
TAG 56:7	TAG 20:1-18:3-18:3	6.766 ± 0.136	6.752 ± 0.151	NS
TAG 56:8	TAG 20:2-18:3-18:3	0.531 ± 0.077	0.509 ± 0.052	NS
TAG 56:9	TAG 18:3-18:3-20:3	0.132 ± 0.032	0.125 ± 0.022	NS
TAG 58:1	TAG 18:0-20:0-20:1	0.190 ± 0.013	0.194 ± 0.017	NS
TAG 58:2	TAG 20:0-18:1-20:1	0.849 ± 0.056	0.873 ± 0.066	NS
TAG 58:3	TAG 18:1-20:1-20:1	2.961 ± 0.087	3.062 ± 0.067	*
TAG 58:4	TAG 20:1-20:1-18:2	3.169 ± 0.171	3.328 ± 0.114	*
TAG 58:5	TAG 20:1-18:2-20:2	2.803 ± 0.133	2.963 ± 0.110	*
TAG 58:6	TAG 20:1-20:2-18:3	1.806 ± 0.069	1.939 ± 0.089	**
TAG 58:7	TAG 22:1-18:3-18:3	0.924 ± 0.044	0.980 ± 0.039	*
TAG 58:8	TAG 18:3-18:3-22:2	0.061 ± 0.003	0.067 ± 0.002	***
TAG 58:9	TAG 18:3-18:3-22:3	0.037 ± 0.007	0.037 ± 0.005	NS
TAG 60:1	TAG 18:0-24:0-18:1	0.051 ± 0.006	0.047 ± 0.007	NS
TAG 60:2	TAG 22:0-18:1-20:1	0.224 ± 0.027	0.224 ± 0.022	NS
TAG 60:3	TAG 18:1-20:1-22:1	0.661 ± 0.048	0.694 ± 0.053	NS
TAG 60:4	TAG 20:1-22:1-18:2	0.690 ± 0.023	0.746 ± 0.031	***
TAG 60:5	TAG 20:1-22:1-18:3	0.470 ± 0.018	0.515 ± 0.022	***
TAG 60:6	TAG 22:1-20:2-18:3	0.202 ± 0.010	0.222 ± 0.010	***
TAG 60:7	TAG 22:1-18:3-20:3	0.068 ± 0.006	0.072 ± 0.005	NS
TAG 60:8	TAG 20:2-18:3-22:3	0.006 ± 0.001	0.007 ± 0.000	***
TAG 62:2	TAG 24:0-18:1-20:1	0.057 ± 0.007	0.058 ± 0.007	NS
TAG 62:3	TAG 24:0-20:1-18:2	0.163 ± 0.018	0.167 ± 0.015	NS
TAG 62:4	TAG 20:1-24:1-18:2	0.171 ± 0.016	0.175 ± 0.014	NS
TAG 62:5	TAG 24:1-18:2-20:2	0.088 ± 0.006	0.091 ± 0.004	NS
TAG 62:6	TAG 26:1-18:2-18:3	0.027 ± 0.002	0.028 ± 0.002	NS
TAG 64:3	TAG 26:0-20:1-18:2	0.019 ± 0.002	0.019 ± 0.002	NS
TAG 64:4	TAG 20:1-26:1-18:2	0.022 ± 0.003	0.023 ± 0.002	NS
TAG 64:5	TAG 28:0-18:2-18:3	0.013 ± 0.001	0.014 ± 0.001	NS

Supplementary Table 12. Differences in glycerolipid composition between WT and clock mutant seeds. *Data were acquired in positive mode from mature seeds (n =9). Values are expressed in mol% ± standard deviation. p-value > 0.05: NS; p-value < 0.05: *; p-value < 0.01: **; p-value < 0.001: ***.*

Mature seeds (a)						
Glycerolipids	Mol % of 24 over the 35 species discriminated between *toc1* and WT				p-value	
C18:0, C18:3, C20:0 and C20:1 species	C24	*toc1-1*	Col-0	*toc1-2*	C24/*toc1-1*	Col-0/toc1-2
DAG 34:6	0.010 ± 0.003	0.017 ± 0.003	0.010 ± 0.002	0.019 ± 0.003	***	***
DGDG 34:6	0.003 ± 0.001	0.004 ± 0.000	0.002 ± 0.001	0.003 ± 0.000	**	***
DGDG 36:6	0.003 ± 0.001	0.005 ± 0.001	0.003 ± 0.001	0.006 ± 0.001	***	***
TAG 50:3	0.548 ± 0.026	0.769 ± 0.058	0.579 ± 0.018	0.741 ± 0.006	***	***
TAG 50:6	0.029 ± 0.008	0.039 ± 0.006	0.025 ± 0.004	0.037 ± 0.006	*	***
TAG 52:6	2.109 ± 0.248	2.895 ± 0.181	2.033 ± 0.130	2.955 ± 0.155	***	***
TAG 54:1	0.264 ± 0.015	0.390 ± 0.005	0.272 ± 0.005	0.387 ± 0.014	***	***
TAG 54:2	1.785 ± 0.066	2.192 ± 0.049	1.824 ± 0.040	2.144 ± 0.079	***	***
TAG 56:0	0.039 ± 0.003	0.072 ± 0.003	0.040 ± 0.003	0.071 ± 0.004	***	***
TAG 56:1	0.341 ± 0.011	0.462 ± 0.007	0.339 ± 0.009	0.428 ± 0.027	***	***
TAG 56:2	1.593 ± 0.057	2.139 ± 0.047	1.587 ± 0.039	2.056 ± 0.061	***	***
TAG 56:7	6.766 ± 0.136	8.055 ± 0.309	6.752 ± 0.151	7.803 ± 0.231	***	***
TAG 58:1	0.190 ± 0.013	0.305 ± 0.018	0.194 ± 0.017	0.298 ± 0.018	***	***
TAG 58:2	0.849 ± 0.056	1.357 ± 0.047	0.873 ± 0.066	1.320 ± 0.072	***	***
TAG 58:3	2.960 ± 0.087	3.488 ± 0.081	3.062 ± 0.067	3.342 ± 0.138	***	***
TAG 58:7	0.924 ± 0.044	1.198 ± 0.185	0.980 ± 0.039	1.239 ± 0.132	**	***
TAG 60:1	0.051 ± 0.006	0.082 ± 0.004	0.047 ± 0.007	0.081 ± 0.005	***	***
TAG 60:2	0.224 ± 0.027	0.361 ± 0.014	0.224 ± 0.022	0.354 ± 0.018	***	***
TAG 60:3	0.661 ± 0.047	0.917 ± 0.105	0.694 ± 0.053	0.936 ± 0.052	***	***
TAG 60:7	0.067 ± 0.006	0.094 ± 0.019	0.072 ± 0.005	0.103 ± 0.010	**	***
TAG 62:2	0.057 ± 0.007	0.095 ± 0.004	0.058 ± 0.007	0.092 ± 0.006	***	***
TAG 62:3	0.163 ± 0.019	0.228 ± 0.011	0.167 ± 0.015	0.222 ± 0.014	***	***
TAG 62:4	0.171 ± 0.016	0.197 ± 0.012	0.175 ± 0.014	0.190 ± 0.009	**	*
TAG 64:3	0.019 ± 0.002	0.024 ± 0.001	0.019 ± 0.002	0.023 ± 0.002	***	***

(a) These data were represented in form of histograms in Figure 35 and 36

Supplementary Table 12. Continued

Mature seeds (a)						
Glycerolipids	Mol % of 11 over the 35 species discriminated between *toc1* and WT				p-value	
C18:1 and C18:2 species	C24	*toc1-1*	Col-0	*toc1-2*	C24/*toc1-1*	Col-0/toc1-2
DAG 36:4	0.374 ± 0.097	0.234 ± 0.026	0.312 ± 0.047	0.265 ± 0.026	**	*
TAG 50:2	1.445 ± 0.089	1.355 ± 0.033	1.475 ± 0.038	1.326 ± 0.147	*	*
TAG 52:1	0.264 ± 0.012	0.367 ± 0.010	0.265 ± 0.008	0.361 ± 0.021	***	***
TAG 52:2	1.633 ± 0.055	1.837 ± 0.066	1.638 ± 0.030	1.811 ± 0.035	***	***
TAG 52:3	3.529 ± 0.061	3.080 ± 0.171	3.551 ± 0.058	3.092 ± 0.034	***	***
TAG 52:4	5.106 ± 0.123	4.703 ± 0.054	5.151 ± 0.096	4.516 ± 0.223	***	***
TAG 54:4	3.749 ± 0.252	4.230 ± 0.068	3.851 ± 0.183	4.105 ± 0.126	***	**
TAG 54:5	5.255 ± 0.185	4.052 ± 0.296	5.149 ± 0.147	4.223 ± 0.334	***	***
TAG 54:6	6.511 ± 0.077	4.895 ± 0.413	6.285 ± 0.198	5.388 ± 0.564	***	**
TAG 56:3	3.912 ± 0.184	4.217 ± 0.100	3.906 ± 0.104	4.062 ± 0.089	***	**
TAG 56:5	6.673 ± 0.482	6.184 ± 0.113	6.780 ± 0.352	5.850 ± 0.157	*	***

(a) These data were represented in form of histograms in Figure 35 and 36

Supplementary Table 12. Continued

Mature seeds (b)					
Glycerolipids	Mol % of 20 over 35 glycerolipids discriminated between *toc1* and WT			p-value	
	Col-0	TOC1-ox	*toc1-2*	Col-0/TOC1-ox	Col-0/toc1-2
TAG 50:3	0.579 ± 0.018	0.643 ± 0.042	0.741 ± 0.006	**	***
TAG 52:6	2.033 ± 0.130	2.276 ± 0.258	2.955 ± 0.155	*	***
TAG 54:1	0.272 ± 0.005	0.309 ± 0.012	0.387 ± 0.014	***	***
TAG 56:2	1.587 ± 0.039	1.663 ± 0.056	2.056 ± 0.061	**	***
TAG 58:1	0.194 ± 0.017	0.174 ± 0.015	0.298 ± 0.018	*	***
TAG 58:2	0.873 ± 0.066	0.775 ± 0.063	1.320 ± 0.072	**	***
TAG 58:3	3.062 ± 0.067	2.659 ± 0.105	3.342 ± 0.138	***	***
TAG 58:7	0.980 ± 0.039	0.765 ± 0.159	1.239 ± 0.132	**	***
TAG 60:2	0.224 ± 0.022	0.195 ± 0.014	0.354 ± 0.018	**	***
TAG 60:3	0.694 ± 0.053	0.536 ± 0.043	0.936 ± 0.052	***	***
TAG 60:7	0.072 ± 0.005	0.061 ± 0.013	0.103 ± 0.010	*	***
TAG 62:2	0.058 ± 0.007	0.050 ± 0.003	0.092 ± 0.006	**	***
TAG 62:3	0.167 ± 0.015	0.144 ± 0.013	0.222 ± 0.014	**	***
TAG 62:4	0.175 ± 0.014	0.156 ± 0.013	0.190 ± 0.009	**	*
TAG 50:2	1.475 ± 0.038	1.561 ± 0.048	1.326 ± 0.147	***	*
TAG 52:1	0.265 ± 0.008	0.303 ± 0.014	0.361 ± 0.021	***	***
TAG 52:2	1.638 ± 0.030	1.752 ± 0.081	1.811 ± 0.035	**	***
TAG 52:4	5.151 ± 0.096	5.485 ± 0.143	4.516 ± 0.223	***	***
TAG 54:4	3.851 ± 0.183	4.169 ± 0.209	4.105 ± 0.126	**	**
TAG 54:6	6.285 ± 0.198	6.572 ± 0.279	5.388 ± 0.564	*	**

(b) These data were represented in form of histograms in Figure 35 and 36 for the comparison between Col-0 and toc1-2 and Figure 37 for the comparison between Col-0 and TOC1-ox. The 15 other species discriminated between toc1 and WT were not significantly modified between Col-0 and TOC1-ox.

Supplementary Table 12. Continued

Mature seeds (c)									
Glycerolipids	Mol % of 24 over the 35 species discriminated between *toc1* and WT					p-value			
C18:0, C18:3, C20:0 and C20:1 species	C24	*toc1-1*	Col-0	*toc1-2*	TOC1-ox	C24/ *toc1-1*	Col-0/ *toc1-2*	Col-0/ TOC1-ox	TOC1-ox/ *toc1-2*
DAG 34:6	0.010 ± 0.003	0.017 ± 0.003	0.010 ± 0.002	0.019 ± 0.003	0.010 ± 0.003	***	***	NS	***
DGDG 34:6	0.003 ± 0.001	0.004 ± 0.000	0.002 ± 0.001	0.003 ± 0.000	0.002 ± 0.000	**	***	NS	**
DGDG 36:6	0.003 ± 0.001	0.005 ± 0.001	0.003 ± 0.001	0.006 ± 0.001	0.004 ± 0.001	***	***	NS	**
TAG 50:3	0.548 ± 0.026	0.769 ± 0.058	0.579 ± 0.018	0.741 ± 0.006	0.643 ± 0.042	***	***	**	*
TAG 50:6	0.029 ± 0.008	0.039 ± 0.006	0.025 ± 0.004	0.037 ± 0.006	0.029 ± 0.004	*	***	NS	**
TAG 52:6	2.109 ± 0.248	2.895 ± 0.181	2.033 ± 0.130	2.955 ± 0.155	2.276 ± 0.258	***	***	*	***
TAG 54:1	0.264 ± 0.015	0.390 ± 0.005	0.272 ± 0.005	0.387 ± 0.014	0.309 ± 0.012	***	***	***	***
TAG 54:2	1.785 ± 0.066	2.192 ± 0.049	1.824 ± 0.040	2.144 ± 0.079	1.870 ± 0.084	***	***	NS	***
TAG 56:0	0.039 ± 0.003	0.072 ± 0.003	0.040 ± 0.003	0.071 ± 0.004	0.042 ± 0.002	***	***	NS	***
TAG 56:1	0.341 ± 0.011	0.462 ± 0.007	0.339 ± 0.009	0.428 ± 0.027	0.344 ± 0.037	***	***	NS	***
TAG 56:2	1.593 ± 0.057	2.139 ± 0.047	1.587 ± 0.039	2.056 ± 0.061	1.663 ± 0.056	***	***	**	***
TAG 56:7	6.766 ± 0.136	8.055 ± 0.309	6.752 ± 0.151	7.803 ± 0.231	6.703 ± 0.371	***	***	NS	***
TAG 58:1	0.190 ± 0.013	0.305 ± 0.018	0.194 ± 0.017	0.298 ± 0.018	0.174 ± 0.015	***	***	*	***
TAG 58:2	0.849 ± 0.056	1.357 ± 0.047	0.873 ± 0.066	1.320 ± 0.072	0.775 ± 0.063	***	***	**	***
TAG 58:3	2.960 ± 0.087	3.488 ± 0.081	3.062 ± 0.067	3.342 ± 0.138	2.659 ± 0.105	***	***	***	***
TAG 58:7	0.924 ± 0.044	1.198 ± 0.185	0.980 ± 0.039	1.239 ± 0.132	0.765 ± 0.159	**	***	**	***
TAG 60:1	0.051 ± 0.006	0.082 ± 0.004	0.047 ± 0.007	0.081 ± 0.005	0.045 ± 0.003	***	***	NS	***
TAG 60:2	0.224 ± 0.027	0.361 ± 0.014	0.224 ± 0.022	0.354 ± 0.018	0.195 ± 0.014	***	***	**	***
TAG 60:3	0.661 ± 0.047	0.917 ± 0.105	0.694 ± 0.053	0.936 ± 0.052	0.536 ± 0.043	***	***	***	***
TAG 60:7	0.067 ± 0.006	0.094 ± 0.019	0.072 ± 0.005	0.103 ± 0.010	0.061 ± 0.013	**	***	*	***
TAG 62:2	0.057 ± 0.007	0.095 ± 0.004	0.058 ± 0.007	0.092 ± 0.006	0.050 ± 0.003	***	***	**	***
TAG 62:3	0.163 ± 0.019	0.228 ± 0.011	0.167 ± 0.015	0.222 ± 0.014	0.144 ± 0.013	***	***	**	***
TAG 62:4	0.171 ± 0.016	0.197 ± 0.012	0.175 ± 0.014	0.190 ± 0.009	0.156 ± 0.013	**	*	**	***
TAG 64:3	0.019 ± 0.002	0.024 ± 0.001	0.019 ± 0.002	0.023 ± 0.002	0.018 ± 0.001	***	***	NS	***

(c) These data were represented in form of histograms in Figure 38 and 39

Supplementary Table 12. Continued

Mature seeds (c)									
Glycerolipids	Mole percents of 11 over the 35 species discriminated between *toc1* and WT					p-value			
C18:1 and C18:2 species	C24	*toc1-1*	Col-0	*toc1-2*	TOC1-ox	C24/ *toc1-1*	Col-0/ *toc1-2*	Col-0/ TOC1-ox	TOC1-ox/ *toc1-2*
DAG 36:4	0.374 ± 0.097	0.234 ± 0.026	0.312 ± 0.047	0.265 ± 0.026	0.278 ± 0.096	**	*	NS	NS
TAG 50:2	1.445 ± 0.089	1.355 ± 0.033	1.475 ± 0.038	1.326 ± 0.147	1.561 ± 0.048	*	*	***	**
TAG 52:1	0.264 ± 0.012	0.367 ± 0.010	0.265 ± 0.008	0.361 ± 0.021	0.303 ± 0.014	***	***	***	***
TAG 52:2	1.633 ± 0.055	1.837 ± 0.066	1.638 ± 0.030	1.811 ± 0.035	1.752 ± 0.081	***	***	**	NS
TAG 52:3	3.529 ± 0.061	3.080 ± 0.171	3.551 ± 0.058	3.092 ± 0.034	3.646 ± 0.155	***	***	NS	***
TAG 52:4	5.106 ± 0.123	4.703 ± 0.054	5.151 ± 0.096	4.516 ± 0.223	5.485 ± 0.143	***	***	***	***
TAG 54:4	3.749 ± 0.252	4.230 ± 0.068	3.851 ± 0.183	4.105 ± 0.126	4.169 ± 0.209	***	**	**	NS
TAG 54:5	5.255 ± 0.185	4.052 ± 0.296	5.149 ± 0.147	4.223 ± 0.334	5.295 ± 0.379	***	***	NS	***
TAG 54:6	6.511 ± 0.077	4.895 ± 0.413	6.285 ± 0.198	5.388 ± 0.564	6.572 ± 0.279	***	**	*	***
TAG 56:3	3.912 ± 0.184	4.217 ± 0.100	3.906 ± 0.104	4.062 ± 0.089	3.852 ± 0.150	***	**	NS	**
TAG 56:5	6.673 ± 0.482	6.184 ± 0.113	6.780 ± 0.352	5.850 ± 0.157	6.674 ± 0.299	*	***	NS	***

(c) These data were represented in form of histograms in Figure 38 and 39

Supplementary Table 13. Differences in the mole percents of 49 glycerolipid species between C24 and *toc1-1* seedlings. *Lipidomic data were acquired in positive mode. Values are expressed in in mol% ± standard deviation. p-value > 0.05: NS; p-value < 0.05: *; p-value < 0.01: **; p-value < 0.001: ***; (n = 6).*

Glycerolipids	Species	C24	*toc1-1*	p-value
DAG 34:2	DAG 16:0-18:2	1.020 ± 0.213	1.124 ± 0.366	NS
DAG 34:3	DAG 16:0-18:3	1.884 ± 0.478	2.882 ± 0.288	**
DAG 36:3	DAG 18:1-18:2	0.047 ± 0.021	0.112 ± 0.011	***
DAG 36:4	DAG 18:2-18:2	0.193 ± 0.075	0.336 ± 0.053	**
DAG 36:5	DAG 18:2-18:3	0.462 ± 0.234	0.693 ± 0.385	NS
DAG 36:6	DAG 18:3-18:3	0.602 ± 0.441	1.084 ± 0.314	NS
DGDG 34:1	DGDG 16:0-18:1	0.044 ± 0.025	0.098 ± 0.036	*
DGDG 34:2	DGDG 16:0-18:2	0.312 ± 0.132	0.427 ± 0.161	NS
DGDG 34:3	DGDG 16:0-18:3	0.843 ± 0.242	1.299 ± 0.416	NS
DGDG 36:4	DGDG 18:1-18:3	0.062 ± 0.045	0.134 ± 0.066	NS
MGDG 34:2	MGDG 16:1-18:1	0.237 ± 0.022	0.389 ± 0.127	*
MGDG 34:3	MGDG 16:0-18:3	1.067 ± 0.131	1.324 ± 0.226	NS
MGDG 34:4	MGDG 16:2-18:2	1.017 ± 0.180	1.166 ± 0.076	NS
MGDG 34:5	MGDG 16:2-18:3	1.902 ± 0.641	1.737 ± 0.280	NS
MGDG 34:6	MGDG 16:3-18:3	12.322 ± 2.001	14.446 ± 1.519	NS
MGDG 36:4	MGDG 18:1-18:3	0.323 ± 0.047	0.368 ± 0.076	NS
MGDG 36:5	MGDG 18:2-18:3	1.349 ± 0.188	1.276 ± 0.203	NS
PC 32:1	PC 16:0-16:1	0.181 ± 0.015	0.215 ± 0.029	NS
PC 32:3	PC 14:0-18:3	0.473 ± 0.120	1.205 ± 0.280	**
PC 32:4	PC 16:0-16:4	0.604 ± 0.151	1.610 ± 0.403	**
PC 34:1	PC 16:0-18:1	1.795 ± 0.341	2.101 ± 0.341	NS
PC 34:2	PC 16:0-18:2	11.630 ± 0.978	9.634 ± 0.557	**
PC 34:3	PC 16:0-18:3	15.432 ± 0.767	13.589 ± 1.081	**
PC 34:4	PC 16:1-18:3	0.372 ± 0.021	0.405 ± 0.064	NS
PC 34:5	PC 18:2-16:3	0.089 ± 0.011	0.046 ± 0.032	*
PC 36:1	PC 18:0-18:1	0.189 ± 0.120	0.153 ± 0.043	NS
PC 36:2	PC 18:0-18:2	1.228 ± 0.420	1.059 ± 0.264	NS
PC 36:3	PC 18:1-18:2	4.368 ± 0.861	3.969 ± 0.450	NS
PC 36:4	PC 18:2-18:2	5.537 ± 0.876	6.011 ± 0.317	NS
PC 36:5	PC 18:2-18:3	9.859 ± 1.054	9.727 ± 1.148	NS
PC 36:6	PC 18:3-18:3	13.289 ± 1.308	11.472 ± 0.716	*
PC 38:2	PC 20:0-18:2	0.309 ± 0.042	0.235 ± 0.023	**
PC 38:3	PC 20:0-18:3	0.109 ± 0.015	0.040 ± 0.025	***
PC 38:4	PC 20:1-18:3	0.094 ± 0.019	0.093 ± 0.012	NS
PE 34:2	PE 16:0-18:2	2.077 ± 0.367	1.330 ± 0.314	**
PE 34:3	PE 16:0-18:3	3.442 ± 0.282	2.797 ± 0.308	**
PE 36:2	PE 18:0-18:2	0.213 ± 0.047	0.194 ± 0.047	NS
PE 36:3	PE 18:0-18:3	0.405 ± 0.069	0.396 ± 0.052	NS
PE 36:4	PE 18:2-18:2	0.543 ± 0.357	0.706 ± 0.041	NS

Supplementary Table 13. Continued

Glycerolipids	Species	C24	*toc1-1*	p-value
PE 36:5	PE 18:2-18:3	1.324 ± 0.397	1.405 ± 0.306	NS
PE 36:6	PE 18:3-18:3	0.685 ± 0.193	0.665 ± 0.263	NS
PE 40:2	PE 22:0-18:2	0.068 ± 0.044	0.046 ± 0.010	NS
PE 42:2	PE 24:0-18:2	0.156 ± 0.076	0.130 ± 0.064	NS
PE 42:3	PE 24:0-18:3	0.147 ± 0.090	0.098 ± 0.050	NS
PG 34:4	PG 16:1-18:3	0.822 ± 0.094	0.757 ± 0.094	NS
TAG 52:3	TAG 16:0-18:1-18:2	0.134 ± 0.018	0.128 ± 0.038	NS
TAG 54:4	TAG 18:1-18:1-18:2	0.516 ± 0.268	0.517 ± 0.185	NS
TAG 54:5	TAG 18:1-18:2-18:2	0.179 ± 0.098	0.224 ± 0.063	NS
TAG 54:6	TAG 18:1-18:2-18:3	0.044 ± 0.144	0.144 ± 0.064	*

Supplementary Table 14. Differences in the mole percents of 51 glycerolipid species between C24 and *toc1-1* seedlings. *Lipidomic data were acquired in negative mode. Values are expressed in in mol% ± standard deviation. p-value > 0.05: NS; p-value < 0.05: *; p-value < 0.01: **; p-value < 0.001: ***; (n = 6).*

Glycerolipids	Species	C24	*toc1-1*	p-value
MGDG 32:3	MGDG 16:0-16:3	0.062 ± 0.018	0.071 ± 0.008	NS
MGDG 32:6	MGDG 16:3-16:3	0.199 ± 0.041	0.289 ± 0.070	*
MGDG 34:1	MGDG 16:0-18:1	0.058 ± 0.019	0.114 ± 0.018	***
MGDG 34:2	MGDG 16:1-18:1	0.194 ± 0.035	0.230 ± 0.034	NS
MGDG 34:3	MGDG 16:0-18:3	0.563 ± 0.073	0.664 ± 0.164	NS
MGDG 34:4	MGDG 16:1-18:3	0.539 ± 0.043	0.512 ± 0.024	NS
MGDG 34:5	MGDG 16:2-18:3	1.499 ± 0.184	0.823 ± 0.085	***
MGDG 34:6	MGDG 16:3-18:3	26.537 ± 3.420	31.955 ± 1.595	**
MGDG 36:4	MGDG 18:1-18:3	0.176 ± 0.041	0.184 ± 0.033	NS
MGDG 36:5	MGDG 18:2-18:3	1.109 ± 0.408	0.600 ± 0.106	*
MGDG 36:6	MGDG 18:3-18:3	20.085 ± 2.732	20.764 ± 3.051	NS
PA 34:2	PA 16:0-18:2	0.084 ± 0.032	0.113 ± 0.026	NS
PA 34:3	PA 16:0-18:3	0.0629 ± 0.022	0.109 ± 0.021	**
PA 36:6	PA 18:3-18:3	0.091 ± 0.031	0.024 ± 0.010	**
PC 34:1	PC 16:0-18:1	0.199 ± 0.070	0.154 ± 0.033	NS
PC 34:2	PC 16:0-18:2	0.748 ± 0.201	0.492 ± 0.102	*
PC 34:3	PC 16:0-18:3	1.306 ± 0.338	0.973 ± 0.217	NS
PC 36:2	PC 18:0-18:2	0.152 ± 0.046	0.106 ± 0.014	NS
PC 36:3	PC 18:0-18:3	0.208 ± 0.072	0.165 ± 0.039	NS
PC 36:4	PC 18:2-18:2	0.409 ± 0.134	0.341 ± 0.054	NS
PC 36:5	PC 18:2-18:3	0.718 ± 0.430	0.584 ± 0.303	NS
PC 36:6	PC 18:3-18:3	0.623 ± 0.188	0.435 ± 0.075	NS
PE 34:1	PE 16:0-18:1	0.155 ± 0.071	0.109 ± 0.016	NS
PE 34:2	PE 16:0-18:2	2.967 ± 0.748	1.896 ± 0.157	*
PE 34:3	PE 16:0-18:3	4.003 ± 0.939	2.810 ± 0.376	*
PE 36:2	PE 18:0-18:2	0.383 ± 0.147	0.236 ± 0.036	NS
PE 36:3	PE 18:0-18:3	0.550 ± 0.247	0.325 ± 0.063	NS
PE 36:4	PE 18:2-18:2	0.941 ± 0.296	0.772 ± 0.153	NS
PE 36:5	PE 18:2-18:3	1.315 ± 0.568	0.872 ± 0.254	NS
PE 36:6	PE 18:3-18:3	0.689 ± 0.441	1.391 ± 0.907	NS
PE 42:2	PE 24:0-18:2	0.380 ± 0.142	0.145 ± 0.020	**
PG 32:0	PG 16:0-16:0	0.407 ± 0.100	0.400 ± 0.080	NS
PG 32:1	PG 16:0-16:1	3.275 ± 0.235	2.419 ± 0.290	***
PG 32:2	PG 16:1-16:1	0.090 ± 0.010	0.0798 ± 0.024	NS
PG 34:1	PG 16:0-18:1	0.998 ± 0.302	1.249 ± 0.430	NS
PG 34:2	PG 16:0-18:2	2.809 ± 0.285	3.110 ± 0.081	NS
PG 34:3	PG 16:0-18:3	3.488 ± 0.570	3.516 ± 0.238	NS
PG 34:4	PG 16:1-18:3	9.990 ± 0.477	9.010 ± 0.813	*
PG 34:5	PG 16:2-18:3	0.055 ± 0.003	0.048 ± 0.008	NS

Supplementary Table 14. Continued

Glycerolipids	Species	C24	*toc1-1*	p-value
PG 36:6	PG 18:3-18:3	0.089 ± 0.030	0.130 ± 0.049	NS
PI 34:3	PI 16:0-18:3	2.485 ± 0.480	1.516 ± 0.347	**
PI 36:5	PI 18:2-18:3	0.111 ± 0.021	0.050 ± 0.011	***
PI 36:6	PI 18:3-18:3	0.154 ± 0.045	0.098 ± 0.009	*
SQDG 32:3	SQDG 16:0-16:3	0.099 ± 0.028	0.085 ± 0.020	NS
SQDG 34:2	SQDG 16:0-18:2	0.962 ± 0.297	1.697 ± 0.461	*
SQDG 34:3	SQDG 16:0-18:3	5.843 ± 0.602	5.648 ± 0.207	NS
SQDG 34:4	SQDG 16:1-18:3	0.084 ± 0.013	0.083 ± 0.014	NS
SQDG 36:3	SQDG 18:0-18:3	0.103 ± 0.037	0.155 ± 0.027	*
SQDG 36:4	SQDG 18:2-18:2	0.126 ± 0.015	0.134 ± 0.035	NS
SQDG 36:5	SQDG 18:2-18:3	0.315 ± 0.056	0.478 ± 0.086	**
SQDG 36:6	SQDG 18:3-18:3	1.513 ± 0.456	1.837 ± 0.533	NS

Supplementary Table 15. Differences in glycerolipid composition between C24 and *toc1-1* seedlings. *Data were acquired in positive and negative modes from seedlings (n = 6). Values are expressed in mol% ± standard deviation. p-value > 0.05: NS; p-value < 0.05: *; p-value < 0.01: **; p-value < 0.001: ***, (n = 6).*

Seedlings (positive mode)			
Glycerolipids	Molar percents		p-value
C18:2 species	C24	*toc1-1*	C24/*toc1-1*
DAG 34:2	1.020 ± 0.213	1.124 ± 0.366	NS
DAG 36:3	0.047 ± 0.021	0.112 ± 0.011	***
DAG 36:4	0.193 ± 0.075	0.336 ± 0.053	**
DGDG 34:2	0.312 ± 0.132	0.427 ± 0.161	NS
MGDG 34:4	1.017 ± 0.180	1.166 ± 0.076	NS
PC 34:2	11.630 ± 0.978	9.634 ± 0.557	**
PC 34:5	0.089 ± 0.011	0.046 ± 0.032	*
PC 36:2	1.228 ± 0.420	1.059 ± 0.264	NS
PC 36:3	4.368 ± 0.861	3.969 ± 0.450	NS
PC 36:4	5.537 ± 0.876	6.011 ± 0.317	NS
PC 38:2	0.309 ± 0.042	0.235 ± 0.023	**
PE 34:2	2.077 ± 0.367	1.330 ± 0.314	**
PE 36:2	0.213 ± 0.047	0.194 ± 0.047	NS
PE 36:4	0.543 ± 0.357	0.706 ± 0.041	NS
PE 40:2	0.068 ± 0.044	0.046 ± 0.010	NS
PE 42:2	0.156 ± 0.076	0.130 ± 0.064	NS
TAG 52:3	0.134 ± 0.018	0.128 ± 0.038	NS
TAG 54:4	0.516 ± 0.268	0.517 ± 0.185	NS
TAG 54:5	0.179 ± 0.098	0.224 ± 0.063	NS
TAG 54:6	0.044 ± 0.144	0.144 ± 0.064	*

Seedlings (negative mode)			
Glycerolipids	Molar percents		p-value
C18:2 species	C24	*toc1-1*	C24/*toc1-1*
PA 34:2	0.084 ± 0.032	0.113 ± 0.026	NS
PC 34:2	0.748 ± 0.201	0.492 ± 0.102	*
PC 36:2	0.152 ± 0.046	0.106 ± 0.014	NS
PC 36:4	0.409 ± 0.134	0.341 ± 0.054	NS
PE 34:2	2.967 ± 0.748	1.896 ± 0.157	*
PE 36:2	0.383 ± 0.147	0.236 ± 0.036	NS
PE 36:4	0.941 ± 0.296	0.772 ± 0.153	NS
PE 42:2	0.380 ± 0.142	0.145 ± 0.020	**
PG 34:2	2.809 ± 0.285	3.110 ± 0.081	NS
SQDG 34:2	0.962 ± 0.297	1.697 ± 0.461	*
SQDG 36:4	0.126 ± 0.015	0.134 ± 0.035	NS

These data were represented in form of histogram in Figure 42.

Supplementary Table 15. Continued

Seedlings (positive mode)			
Glycerolipids	Molar percents		p-value
C18:3 species	C24	*toc1-1*	C24/*toc1-1*
DAG 34:3	1.884 ± 0.478	2.882 ± 0.288	**
DAG 36:5	0.462 ± 0.234	0.693 ± 0.385	NS
DAG 36:6	0.602 ± 0.441	1.084 ± 0.314	NS
DGDG 34:3	0.843 ± 0.242	1.299 ± 0.416	NS
DGDG 36:4	0.062 ± 0.045	0.134 ± 0.066	NS
MGDG 34:3	1.067 ± 0.131	1.324 ± 0.226	NS
MGDG 34:5	1.902 ± 0.641	1.737 ± 0.280	NS
MGDG 34:6	12.322 ± 2.001	14.446 ± 1.519	NS
MGDG 36:4	0.323 ± 0.047	0.368 ± 0.076	NS
MGDG 36:5	1.349 ± 0.188	1.276 ± 0.203	NS
PC 32:3	0.473 ± 0.120	1.205 ± 0.280	**
PC 34:3	15.432 ± 0.767	13.589 ± 1.081	**
PC 34:4	0.372 ± 0.021	0.405 ± 0.064	NS
PC 36:5	9.859 ± 1.054	9.727 ± 1.148	NS
PC 36:6	13.289 ± 1.308	11.472 ± 0.716	*
PC 38:3	0.109 ± 0.015	0.040 ± 0.025	***
PC 38:4	0.094 ± 0.019	0.093 ± 0.012	NS
PE 34:3	3.442 ± 0.282	2.797 ± 0.308	**
PE 36:3	0.405 ± 0.069	0.396 ± 0.052	NS
PE 36:5	1.324 ± 0.397	1.405 ± 0.306	NS
PE 36:6	0.685 ± 0.193	0.665 ± 0.263	NS
PE 42:3	0.147 ± 0.090	0.098 ± 0.050	NS
PG 34:4	0.822 ± 0.094	0.757 ± 0.094	NS

These data were represented in form of histogram in Figure 43.

Supplementary Table 15. Continued

Seedlings (negative mode)							
Glycerolipids	Molar percents		p-value	Glycerolipids	Molar percents		p-value
C18:3 species	C24	*toc1-1*	C24/*toc1-1*	**C18:3 species**	C24	*toc1-1*	C24/*toc1-1*
MGDG 34:3	0.563 ± 0.073	0.664 ± 0.164	NS	PI 36:6	0.154 ± 0.045	0.098 ± 0.009	*
MGDG 34:4	0.539 ± 0.043	0.512 ± 0.024	NS	SQDG 34:3	5.843 ± 0.602	5.648 ± 0.207	NS
MGDG 34:5	1.499 ± 0.184	0.823 ± 0.085	***	SQDG 34:4	0.084 ± 0.013	0.083 ± 0.014	NS
MGDG 34:6	26.537 ± 3.420	31.955 ± 1.595	**	SQDG 36:3	0.103 ± 0.037	0.155 ± 0.027	*
MGDG 36:4	0.176 ± 0.041	0.184 ± 0.033	NS	SQDG 36:5	0.315 ± 0.056	0.478 ± 0.086	**
MGDG 36:5	1.109 ± 0.408	0.600 ± 0.106	*	SQDG 36:6	1.513 ± 0.456	1.837 ± 0.533	NS
MGDG 36:6	20.085 ± 2.732	20.764 ± 3.051	NS				
PA 34:3	0.0629 ± 0.022	0.109 ± 0.021	**				
PA 36:6	0.091 ± 0.031	0.024 ± 0.010	**				
PC 34:3	1.306 ± 0.338	0.973 ± 0.217	NS				
PC 36:3	0.208 ± 0.072	0.165 ± 0.039	NS				
PC 36:5	0.718 ± 0.430	0.584 ± 0.303	NS				
PC 36:6	0.623 ± 0.188	0.435 ± 0.075	NS				
PE 34:3	4.003 ± 0.939	2.810 ± 0.376	*				
PE 36:3	0.550 ± 0.247	0.325 ± 0.063	NS				
PE 36:5	1.315 ± 0.568	0.872 ± 0.254	NS				
PE 36:6	0.689 ± 0.441	1.391 ± 0.907	NS				
PG 34:3	3.488 ± 0.570	3.516 ± 0.238	NS				
PG 34:4	9.990 ± 0.477	9.010 ± 0.813	*				
PG 34:5	0.055 ± 0.003	0.048 ± 0.008	NS				
PG 36:6	0.089 ± 0.030	0.130 ± 0.049	NS				
PI 34:3	2.485 ± 0.480	1.516 ± 0.347	**				
PI 36:5	0.111 ± 0.021	0.050 ± 0.011	***				

These data were represented in form of histogram in Figure 43.

Supplementary Table 16. Differences in FA composition between C24 and *toc1-1* in 16 DAF developing seeds. *Values are expressed in mol% ± standard deviation. These data were represented in form of histogram in Figure 44. Plant culture and FA analysis were performed in the same conditions for toc1-1 and C24. p-value > 0.05: NS; p-value < 0.05: *; p-value < 0.01: **; p-value < 0.001: ***; (n = 15).*

FA	C24	*toc1-1*	p-value
C16:0	8.7 ± 0.8	8.4 ± 1.0	NS
C18:0	4.2 ± 0.8	5.3 ± 0.7	***
C18:1	13.0 ± 1.5	12.6 ± 1.2	NS
C18:2	30.1 ± 1.7	24.8 ± 0.8	***
C18:3	19.1 ± 1.8	21.0 ± 1.7	***
C20:0	2.7 ± 0.5	3.7 ± 0.6	***
C20:1	18.8 ± 0.9	20.7 ± 0.7	***
C20:2	1.9 ± 0.3	1.7 ± 0.3	NS
C22:1	1.5 ± 0.3	1.9 ± 0.2	NS

COMPLEMENTARY ACTIVITIES PERFORMED DURING THE PhD

1. Formation

I attended a total of 103 hours of formations divided into linguistic (43 hours) and scientific (60 hours) training sessions. I was able to improve my knowledge in English at the beginning of the PhD experience thanks to a 43-hour formation. All advises given during this 43-hour training was helpful for the writing of my thesis dissertation and the upcoming publication related to this PhD project. A part of the 60-hour scientific training sessions enabled to learning about biological risks encountered during the achievement of experiments related to the biological researches. In addition, I was able to improve my theoretical knowledge in molecular biology (RT-qPCR and CRISPR-Cas9: 7 hours) and my understanding in the use several tools related to metabolomics/lipidomics (39 hours), including statistical software (metaboanalyst, Workflow4metabolomics and R) and data processing software (MS-DIAL, Mzmine, MetGem and OptFlux). Among these 60-hour scientific training sessions, a small part (7 hours) was also devoted to the understanding of risk related to the use of the autoclave. I was able to improve my experimental skills in the use of autoclave with this seven-hour formation, which was helpful for the sterilization of culture medium (MS medium), water and many other reagent and tools. Below is listed all the formations I was attended during my PhD in “Génie Enzymatique et Cellulaire” unit research (UMR CNRS 7025):

Name of the formation	Number of hours
English	43 hours
Biological risks	7 hours
CRISPR-Cas9	7 hours
Metabolomic/metabolomics (RFMF)	17 hours
Use of statistical software	22 hours
Autoclave	7 hours
Total	103 hours

2. Ethics in research and scientific integrity

During my PhD, I was attended to the formation related to the ethics in research and scientific integrity. Thereby, I certify on my honor that all results presented in my thesis dissertation were not illegally taken from “already published studies” and have been meticulously generated by experiments carried out several times during my experience as PhD student in “Génie Enzymatique et Cellulaire” unit research.

3. Congresses

During my experience as a PhD student, some of my results was presented in three international scientific congresses. During these experiences, I had the opportunity to meet several famous researches in the field of plant biology, as well as discovering many other topics related to plant biology. Below is listed all congresses I was attended during my PhD:

- **Makni S.**, Acket S., Rossez Y., Thomasset B., Haupt K., and Troncoso-Ponce M. A., Involvement of circadian clock in the production of lipids in *Arabidopsis thaliana*. 9th European Symposium on Plant Lipids, Marseille, France, 2019 (Poster).

- **Makni S.**, Acket S., Rossez Y., Thomasset B., Haupt K., and Troncoso-Ponce M. A., Involvement of circadian clock in the production of lipids in *Arabidopsis thaliana*. 9th European Symposium on Plant Lipids, Marseille, France, 2019 (Poster).

- **Makni S.**, Acket S., Rossez Y., Thomasset B., Haupt K., and Troncoso-Ponce M. A., Involvement of circadian clock in the production of lipids in *Arabidopsis thaliana*. 15th International GERLI Lipidomics Meeting, Compiègne, France, 2019 (Poster)

4. Publications

During my experience as a PhD student, I had the opportunity to collaborate with Professor Martinez-Force from the “Instituto de la Grasa" (Sevilla, Spain) in order to study the fatty acid and lipid profile of *Camelina sativa* and *Arabidopsis thaliana* in different mutants and transgenic lines. I also had the privilege to work with Dr. Enrico Magnani from INRA Versaille (Versaille, France) for studying the accumulation of squalene in Amaranthus seeds. Thanks to these collaborations, my name is currently associated as co-author in two articles.

The publication of the key findings of the main research work lead during my PhD is expected after the achievement of the defense. Below is listed all publications associating my name:

- Martins-Noguerol R, Moreno-Pérez AJ, Acket S, **Makni S.**, Garcés R, Troncoso-Ponce A, Salas JJ, Thomasset B & Martínez-Force E (2019) Lipidomic analysis of plastidial octanoyltransferase mutants of *Arabidopsis thaliana*. *Metabolites* **9:** 1–16.

- Rodriguez-Rodriguez M.F., Moreno-Pérez A.J., **Makni S.**, Troncoso-Ponce M.A., Acket S. et al. (2021). Lipid profiling and oil properties of Camelina sativa seeds engineered to enhance the production of saturated and omega-7 fatty acids. 170: 113765.

5. Teaching and supervision

During my PhD, I supervised a total of eight students, including five 2-week visitor interns, one BTS intern (Charlotte Henocq) and two master's students (Maxime Sommer and Sana Afensiss), during their internship in the "Génie Enzymatique et Cellulaire" unit research.

For a total of 68 hours, I was also in charge of accompanying students in the achievement of their experiments during their practical work (TP3 and TP5 of BL20) class sessions. During the TP3 of BL20 (total of 48 hours including 4h through zoom), the aim was studying the transport of ions through a semi-permeable membrane. During the TP5 of BL20 (total of 20 hours), the objective was studying the regulation of the glycolysis.

6. Future research interest

The objective in my future professional career will be working as research professor specialized in omics approaches, including metabolomics, lipidomics and fluxomics. Following my experience at the University of Technology of Compiègne (Compiègne, France), I found a postdoctoral position at the University of North Texas (Denton, Texas, United States), therefore giving me the privilege to work with the Professor Ana Alonso from the "Department of Biological Science". My research at the University of North Texas will be focused on mechanisms allowing the infection of human macrophages by *Histoplasma capsulatum*. *Histoplasma capsulatum* is a fungal pathogen capable of inhibiting the human immune system and causing respiratory disease. One of the challenges would be identifying molecules of the

host cells that are consumed by this pathogen during infection processes which could help in the development of potential therapeutic treatment.